Metabolomics study of human embryonic stem cell culture media

Antonio Alejandro Alfaro Alfonzo

Thesis submitted to the University of Nottingham for the degree of Doctor of Philosophy

July 2015

Abstract

Self-renewal and pluripotency, the hallmarks of human embryonic stem cells (hESC), confer these cells with the capacity to expand indefinitely while maintaining the ability to differentiate into any cell type of the human body; thus, making hESC a valuable source of functional differentiated cells suitable for applications in regenerative medicine, drug discovery, biotechnology, biopharmaceuticals and developmental biology. However, the large-scale production of clinical-grade hESC, required for such applications, has been hampered by the current culture conditions in which hESC still depend on the use of mouse embryonic fibroblast-conditioned medium (MEF-CM) for their efficient growth. Therefore, investigation of the factors provided by MEFs is of the utmost importance to discover which components of MEF-CM allow the long-term expansion of undifferentiated hESC.

While considerable progress has been made on the identification of the protein components of MEF-CM, very little is known about the small molecules (metabolites) secreted by MEFs. In this context, an untargeted metabolomics method was developed for the investigation of potential bioactive metabolites present in MEF-CM implicated in the proliferation and/or maintenance of pluripotency of hESC *in vitro*.

A metabolomics method was applied and successfully identified a number of metabolites which were later confirmed in their identities with the use of authentic standards, to be further investigated for their effect on hESC culture. Interestingly, the addition of PGE_2, 6-keto-PGF1α, 9, 12, 13-TriHOME, 7-Ketocholesterol and stearidonic acid (the metabolites found in MEF-CM) to the unconditioned medium (UM), a medium incapable of the maintenance of hESC, showed a delay in apoptosis when compared to the negative control UM; thus, suggesting that these metabolites could help with the proliferation of hESC.

Increasing evidence that hESC secrete factors into their microenvironment that can also help them to proliferate or to maintain an undifferentiated state prompted the application of the same

metabolomics method to the analysis of hESC spent culture media. The results identified lysophospholipids (LPLs) as potential molecules mediating some biological activities; however, the precise role of these LPLs still remains to be determined.

Overall, the results of this thesis are expected to impact and add knowledge to the field of stem cell biology providing useful information for the creation and development of more efficient and defined culture conditions for the propagation of hESC with the appropriate quality to realise their widespread application in clinic and other research areas.

Acknowledgements

I would like to thank sincerely my supervisors Professor David Barrett and Professor Morgan Alexander for their advice, guidance and support throughout this work. Also many thanks to Dr Cath Ortori for her help at the beginning of method development and for sorting out problems with the instruments when they were misbehaving. Likewise, I want to thank Dr James Smith for his advice and support with cell culture and for supplying the samples.

I want to thank greatly to the Consejo Nacional de Ciencia y Technología (CONACYT, Mexico) and the School of Pharmacy (The University of Nottingham, UK) for their financial support which made this research project possible.

Many thanks to my family: my parents, Consuelo and Germán and my brothers, Victor Hugo and José Carlos who always supported and encouraged me through the whole PhD in spite of the geographical distance.

I also want to say thanks to my Colombian friends: Jorge, Camilo, Manuel, Juan Camilo and Alicia for all those moments of fun which made the intense work easier.

Finally, I would like to acknowledge that this thesis has also been carried out with the support of the complementary scholarship awarded by the Secretariat of Public Education and the Mexican government.

Table of contents

List of abbreviations

6-keto-PGF1α	6-keto-prostaglandin F1α
7-KC	7-ketocholesterol
AA-d8	Deuterated arachidonic acid
ANOVA	Analysis of variance
bFGF	Basic fibroblast growth factor
BMP	Bone morphogenetic protein
BSA	Bovine serum albumin
CHO	Chinese hamster ovary
CV	Coefficient of variation
CV-ANOVA	Cross-validation-Analysis of variance
ECM	Extracellular matrix
EIC	Extracted ion chromatogram
ESI	Electrospray ionisation
FBS	Foetal bovine serum
FT-ICR	Fourier transformed-ion cyclotron resonance
FWHM	Full width at half maximum
GC-MS	Gas chromatography-mass spectrometry
GDF	Growth differentiation factor
GPCR	G-protein coupled receptors
hESC	Human embryonic stem cells
HFF	Human foreskin fibroblast
HILIC	Hydrophilic liquid chromatography
HPLC	High performance liquid chromatography
HRMS	High resolution mass spectrometry
ICM	Inner cell mass
ICAM-1	Intracellular adhesion molecule-1
IGFBP	Insulin-like growth factor binding protein
KEGG	Kyoto Encyclopaedia of Genes and Genomes
KOSR	Knock-Out serum replacement
LC-MS	Liquid chromatography-mass spectrometry
LPA	Lysophosphatidic acid
LPC	Lysophosphatidylcholine
LPE	Lysophosphatidylethanolamine
LPL	Lysophospholipids
MEF-CM	Mouse embryonic fibroblast-conditioned medium
MEFs	Mouse embryonic fibroblasts
mESC	Mouse embryonic stem cells
MS/MS	Tandem mass spectrometry
NMR	Nuclear magnetic resonance
OPLS-DA	Orthogonal partial least squares-discriminant analysis

PCA	Principal components analysis
PDGF	Platelet-derived growth factor
PDH	Pyruvate dehydrogenase
PGD_2	Prostaglandin D_2
PGE_2	Prostaglandin E_2
PGH_2	Prostaglandin H_2
PUFA	Polyunsaturated fatty acid
QC	Quality control
QqQ	Triple quadrupole
ROS	Reactive oxygen species
RPLC	Reversed-phase liquid chromatography
S1P	Sphingosine-1-phosphate
SSEA	Stage specific embryonic antigen
TGF-β	Transforming growth factor-β
TOF	Time of flight
TriHOME	Trihydroxyoctadecenoic acid
UM	Unconditioned medium
UPLC	Ultra performance liquid chromatography
VCAM-1	Vascular cell adhesion molecule-1
VIP	Variable importance to the projection

List of figures

List of tables

CHAPTER 1

General Introduction

1 General introduction

1.1 Human embryonic stem cells

Approximately 5 to 6 days after fertilisation, the early human embryo develops into a hollow sphere of cells known as the blastocyst. The blastocyst is formed by an outer layer of cells (the trophoblasts) which contains inside a cluster of cells called the inner cell mass (ICM) (Figure 1-1). Human embryonic stem cells (hESC) are derived from the ICM of the blastocyst and have the ability to self-renew *in vitro* for extensive periods of time while retaining their pluripotency (Thomson et al., 1998, Amit et al., 2000, Odorico et al., 2001).

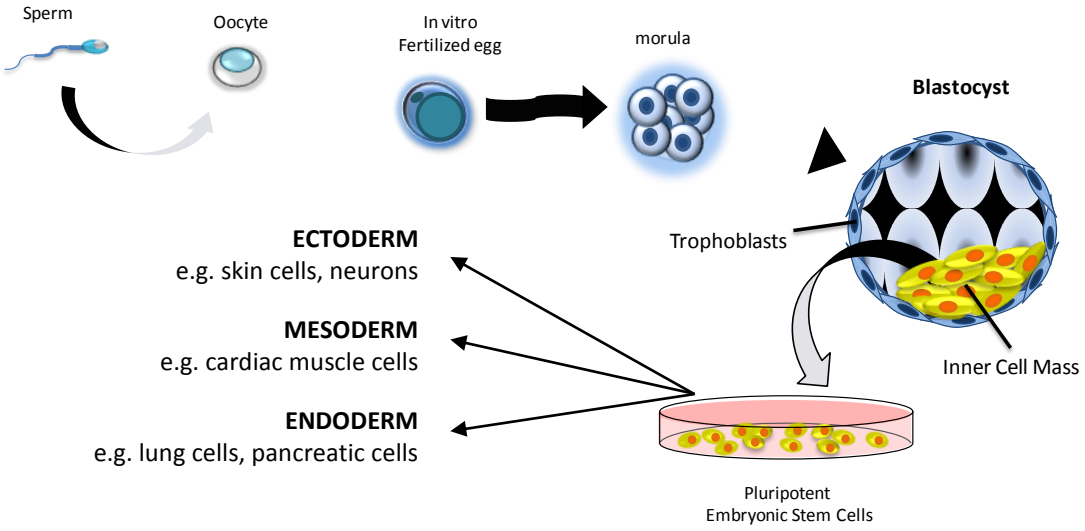

Figure 1-1 Derivation of human embryonic stem cells.

Self-renewal (the process by which stem cells divide to produce more stem cells) and pluripotency (the ability to differentiate into tissues from all three germ layers of the body: ectoderm, mesoderm and endoderm) are the two fundamental characteristics that make hESC so attractive for their application in drug discovery, drug testing, human developmental biology studies as well as in regenerative medicine because they represent a valuable source of numerous functional differentiated cells including neurons (Guan et al., 2001), cardiomyocytes (Gallo and Condorelli, 2006), endothelial cells (Levenberg et al., 2002) and pancreatic cells (Zhang et al., 2009a). However, the widespread

application of hESC has been limited by 1) the undefined conditions in which they are grown, making difficult the expansion of the cells in a reproducible manner, and 2) the reliance on non-human culture components, raising issues regarding animal-pathogen transmission.

1.2 Stem cell culture

When hESC were derived for the first time from the ICM of the human blastocysts, they were cultured over mouse embryonic fibroblasts (MEFs) feeder layers using a culture medium supplemented with foetal bovine serum (FBS) (Thomson et al., 1998). Under such undefined conditions, the large-scale production of hESC, required for their clinical applications, becomes difficult to control as the culture components vary from batch to batch. Furthermore, the reliance on animal-derived products increases the risk of pathogen transmission such as retroviruses and xenoepitopes (for example, non-human sialic acid and N-glycolneuraminic acid (Neu5GC)) from the culture system to hESC (Martin et al., 2005). Therefore, to realize the potential of hESC in clinic, it will be necessary to find more defined and animal product-free conditions where hESC can proliferate while maintaining their self-renewal and pluripotency properties. In culture, hESC require a substrate (supportive matrix), to which they will attach and grow, and an environment (culture medium) that will provide the correct growth factors and nutrients to keep them in an undifferentiated state (Figure 1-2). Thus, in order to obtain a more defined culture system, both substrate and culture medium have to be optimised.

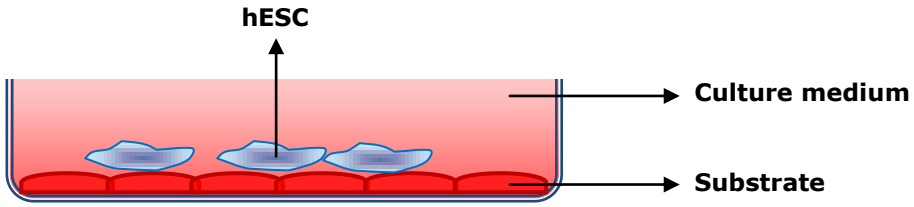

Figure 1-2 *In vitro* culture requirements of hESC.

1.2.1 Towards definition of the culture system

As shown in Figure 1-2, the substrate and the culture medium are the essential requirements for *in vitro* hESC growth. Thus, they have been the target in the optimisation and definition of the culture system. Since the derivation of hESC in 1998, a large number of publications have arisen addressing the issue of a more defined culture system. Table 1-1 summarises the advances made in the field while the major breakthroughs are explained in the text below.

1.2.1.1 Optimisation of the substrate

Human feeder cells

Alternative to MEFs, the use of human feeder layers as substrate was introduced by Richards et al. (Richards et al., 2002). They successfully cultured and maintained the undifferentiated growth of hESC on human foetal muscle, foetal skin and adult fallopian tubal epithelial cells (Richards et al., 2002). Additionally, they derived a new hESC line under complete animal-free conditions using human serum instead of FBS in the medium. Subsequently, other research groups reported the use of other human feeders such as human foreskin fibroblasts (Amit et al., 2003, Hovatta et al., 2003). The main benefit in the use of human feeders is the elimination of animal contamination; however, the culture system still remains with an undefined and complex composition and subject to lot-to-lot variation.

Extracellular matrix and protein-based substrates

A significant progress in the definition of the substrate was the culture of hESC in feeder-free systems. Xu et al were the first to report the use of Matrigel, an extracellular matrix (ECM) derived from mouse Engelbreth-Holm-Swarm sarcoma cells, which supported the cultivation of hESC for more than 130 population doublings (Xu et al., 2001). However, the system still required the use of medium conditioned by MEFs. This conditioned medium (CM) consists in the incubation of hES medium,

known as unconditioned medium (UM), with mitotically inactivated MEFs for 24 h, after which it is collected and ready to use for feeder-free culture, in this case with Matrigel (Figure 1-3), although other feeder-free matrices can be used.

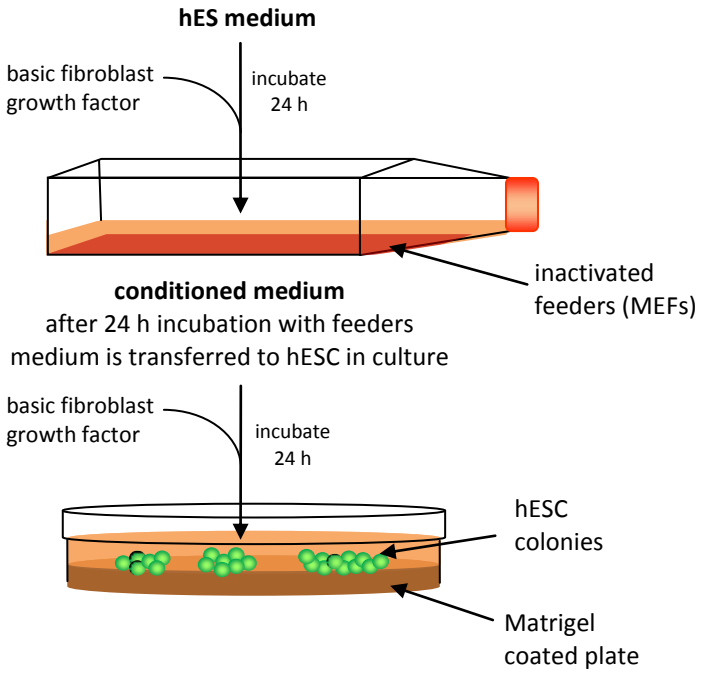

Figure 1-3 Feeder-free culture system of hESC.

Individual Matrigel components such as laminin and collagen IV (Kleinman and Martin, 2005) as well as other purified proteins like fibronectin and vitronectin have also been shown to support the feeder-free growth of hESC; and as with Matrigel, these protein-based substrates also rely on mouse embryonic fibroblast-conditioned medium (MEF-CM) (Xu et al., 2001, Amit et al., 2004). However, there have also been reports of their successful use (either alone or in combination) with more defined culture media (Liu et al., 2006, Lu et al., 2006, Ludwig et al., 2006b, Wang et al., 2007). In spite of being relatively more defined and with a more consistent composition than the use of feeder cells, these feeder-free substrates still lack a complete chemical definition, show chemical variability and their relatively high production costs make them unsuitable for the large-scale expansion of hESC (Villa-Diaz et al., 2013, Celiz et al., 2014).

Table 1-1 Summary of the optimisation of the hESC culture system.

Substrate	Basal medium	Supplements	Cell lines	Reference
Mouse embryonic fibroblasts	DMEM, Gln, BME, NEAA	20% FBS	H1, H7, H9, H13 & H14	(Thomson et al., 1998)
Mouse embryonic fibroblasts	KO-DMEM, Gln, BME, NEAA	20% KOSR, bFGF	H9.1 & H9.2	(Amit et al., 2000)
Matrigel & laminin	MEF-CM: KO-DMEM, Gln, BME, NEAA	20% KOSR, bFGF	H1, H7, H9 & H14	(Xu et al., 2001)
Human fetal muscle, fetal skin, AFT epithelial cells	DMEM, Gln, Penicillin-Streptomycin, BME, NEAA	20% HS, hITS	HS-3 & HS-4	(Richards et al., 2002)
Human foreskin fibroblasts	KO-DMEM, Gln, BME, NEAA	15% SR, bFGF	H9, I6 & I3	(Amit et al., 2003)
Human foreskin fibroblasts	KO-DMEM, Gln, BME, NEAA	20% FCS, hLIF	Isolation from ICM	(Hovatta et al., 2003)
Fibronectin	KO-DMEM, Gln, BME, NEAA	15% SR, TGFβ1, LIF, bFGF	H9, I6 & I3	(Amit et al., 2004)
Human foreskin fibroblasts	KO-DEME, Gln, Penicillin-Streptomycin, BME, NEAA,	20% SR, ITS, bFGF	HS293, HS306 & 10 new lines	(Inzunza et al., 2005)
Matrigel & fibronectin	DMEM/F12	bFGF, Wnt3a, April/BAFF, albumin, cholesterol, insulin, transferrin	H9 & BG01	(Lu et al., 2006)
Matrigel, fibronectin, laminin, vitronectin & collagen IV	DMEM/F12, Gln, BME, NEAA	N2: ITS, progesterone, putrescine. B27 supplement, bFGF	H1 & H9	(Liu et al., 2006)

Table 1-1 continued

Substrate	Basal medium	Supplements	Cell lines	Reference
Matrigel	DMEM/F12, Gln, BME, NEAA	N2 or N2/B27 supplement	H1 & HSF6	(Yao et al., 2006)
Matrigel & combination of collagen IV, fibronectin, vitronectin and laminin	mTeSR1™: DMEM/F12	BSA, human insulin, human holo transferring, bFGF, LiCl, TGFβ1, GABA, pipecolic acid	H1, H7, H9 & H14	(Ludwig et al., 2006a)
Matrigel	StemPro™: DMEM/F12, penicillin, streptomycin, BME, NEAA	BSA, transferrin, ascorbic acid, heregulin 1β, bFGF, Activin A, LR3-IGF1	BG01 & BG02	(Wang et al., 2007)
Laminin-derived peptide	MEF-CM		H1 & H9	(Derda et al., 2007)
Plastic	hEL-CM: KO-DMEM, Gln, BME, NEAA	20% KOSR	SA167 & AS034	(Bigdeli et al., 2008)
PE-TCPS	MEF-CM: DMEM/F12, BME, NEAA, GlutaMAX	15% KOSR, bFGF	HUES7 & NOTT1	(Mahlstedt et al., 2010)
PMEDSAH	MEF-CM, mTESR1™ & StemPro™		BG01 & H9	(Villa-Diaz et al., 2010)
Conjugated heparin-binding peptide GKKQRFRHRNRKG	mTeSR1™	ROCK inhibitor	H1, H7, H9, H13, H14 & IMR-90-1	(Klim et al., 2010)
APMAAm	mTeSR1™		H1 & H9	(Irwin et al., 2011)

Table 1-1 continued

Substrate	Basal medium	Supplements	Cell lines	Reference
Vitronectin-NC	E8™: DMEM/F12	ITS, L-ascorbic acid, bFGF, $NaHCO_3$, TGFβ1 or NODAL	hESC lines: H1 & H9; iPSC lines: iPS-imr90, iPS-foreskin & iPS-DF19	(Chen et al., 2011)
HG21	mTeSR1™		RH1 & H9	(Zhang et al., 2013)

DMEM, Dulbecco's Modified Eagle Medium; Gln, L-glutamine; BME, β-mercaptoethanol; NEAA, non-essential amino acids; FBS, foetal bovine serum; KOSR, Knock Out Serum Replacement; bFGF, basic fibroblast growth factor; MEF-CM, mouse embryonic fibroblast-conditioned medium; KO-DMEM, Knock Out DMEM; HS, human serum; AFT, adult fallopian tubes; hITS, human insulin-transferrin-selenium; SR, serum replacement; FCS, fetal calf serum; hLIF, human leukemia inhibitory factor; TGFβ1, transforming growth factor β1; April, a proliferation-inducing ligand; BAFF, B cell-activating factor belonging to TNF; BSA, bovine serum albumin; LiCl, lithium chloride; GABA, gamma aminobutyric acid; hEL-CM, human embryonic lung fibroblast conditioned medium; LR3-IGF1, Long R3-insulin-like growth factor 1; PE-TCPS, plasma etched tissue culture polystyrene; PMEDSAH, poly[2-(methacryloyloxy)ethyl dimethyl-(3-sulfopropyl)ammonium hydroxide]; iPSC, induced-pluripotent SC; ROCK, rho-associated kinase; APMAAm, aminopropylmethacrylamide; HG, hydrogel.

N2 supplements contain 1 mM human transferrin (Holo), 8.61 μM recombinant human insulin, 1 mM progesterone, 1 mM putrescine, and 1 mM selenite. The B27 supplements contain D-biotin, BSA (fatty acid-free, fraction V), catalase, L-carnitine HCl, corticosterone, ethanolamine HCl, D-galactose (anhydrous), glutathione (reduced), insulin (human, recombinant), linoleic acid, linolenic acid, progesterone, putrescine, sodium selenite, superoxide dismutase, T-3_albumin complex, DL-α-tocopherol, DL-α-tocopherol acetate, and transferrin (human, iron-poor).

Peptide-based substrates

Following the use of protein-based substrates, polymers functionalized with biomolecules (i.e. peptides) have also been shown to support hESC. For example, Klim et al conjugated the heparin-binding peptide GKKQRFRHRNRKG to an alkanethiol self-assembled monolayer and found that hESC cultured on this substrate showed comparable growth rates with the Matrigel controls (Klim et al., 2010). Similarly, Derda and colleagues employed arrays of laminin-derived peptides which allowed hESC to attach and proliferate (Derda et al., 2007); however, the medium used in this case was MEF-CM thus resulting in a poorly defined system.

Polymer-based substrates

More recently, a huge improvement in substrate definition has been achieved with the use of synthetic polymers. Plasma etched tissue culture polystyrene (PE-TCPS) (Mahlstedt et al., 2010), poly[2-(methacryloyloxy)ethyl dimethyl-(3-sulfopropyl) ammonium hydroxide] (PMEDSAH) (Villa-Diaz et al., 2010) and aminopropylmethacrylamide (APMAAm) (Irwin et al., 2011) were all able to maintain the pluripotency and the long-term growth of hESC. Furthermore, their culture performance (growth rates and expression of pluripotency markers) was similar to those achieved with Matrigel controls. Although some of these substrates (PMEDSAH and APMAAm) demonstrated their utility with chemically defined culture media (StemPro and mTeSR1, respectively), some others like PMEDSAH and PE-TCPS showed better efficiencies when MEF-CM was used (Villa-Diaz et al., 2010, Mahlstedt et al., 2010). Nevertheless, synthetic substrates hold the most promising results as they are chemically defined, can be synthesised reproducibly, have longer stability than biological matrices and are more easily scalable for the large-scale production of hESC (Celiz et al., 2014).

1.2.1.2 Optimisation of the culture medium

Serum-free medium

A couple of years after the derivation of hESC using FBS supplementation in the medium (Thomson et al., 1998), Amit et al successfully cultivated clonally derived hESC cell lines with a substitute of serum commercially known as Knock-Out Serum Replacement (KOSR) (Price et al., (1998), Amit et al., 2000). This was the first serum-free hESC culture conditions reported in the literature. Further, a comparative study demonstrated that cells cultured in the presence of KOSR showed better proliferation rates when compared with FBS- and human serum-containing media (Koivisto et al., 2004). Subsequently, the use KOSR was adopted by other research groups as well (Xu et al., 2001, Amit et al., 2003, Amit et al., 2004, Inzunza et al., 2005). However, in spite of a relatively more defined and with a more consistent composition than FBS, KOSR still lacks a complete chemical definition. Furthermore, its animal-derived source (bovine plasma) (Price et al., (1998)) makes it incompatible with the clinical-grade hESC required in regenerative medicine.

Chemically defined medium

The development of chemically defined medium (CDM), as this group of culture media is called, represented a milestone in the definition of the hESC culture medium as they eliminated the use of KOSR and their components were chemically known and of high purity. The underlying success of CDM was the supplementation of a basal culture medium (Dulbecco's Modified Eagle Medium, DMEM) with recently identified factors that promoted self-renewal and/or pluripotency. These factors included basic fibroblast growth factor (bFGF) (Xu et al., 2005a), transforming growth factor-β (TGF-β) (Amit et al., 2004, Beattie et al., 2005) and Wnt3a (Sato et al., 2004). In this context several CDM media were developed (Lu et al., 2006, Liu et al., 2006, Ludwig et al., 2006b, Wang et al., 2007, Yao et al., 2006). However, when tested for their ability to maintain a set of 10 different hESC cell lines, only mTeSR1™

(Ludwig et al., 2006a) and StemPro™ (Wang et al., 2007) supported the maintenance of most cell lines and produced comparable results with the positive control (bFGF- and KOSR-containing medium on MEFs feeder cells) (Akopian et al., 2010). For comparison, Table 1-2 provides a list of the known components of mTeSR1, StemPro and MEF-CM.

BSA-free medium

Common to all CDMs listed in Table 1-1 was the use of bovine serum albumin (BSA) which, amongst the rest of components, is the only one whose composition is not fully defined. Furthermore, its animal origin also impedes the use of hESC (cultured with BSA-containing CDM) in transplantation therapies. In 2011, the same group that developed mTeSR1 medium, by a systematic pairwise re-examination of its components, discovered that BSA was no longer necessary when β-mercaptoethanol (BME), another component of the medium, was also excluded (Chen et al., 2011). The resulting BSA-free medium, named E8™, supported the undifferentiated proliferation of hESC at comparable levels to its predecessor mTeSR1. However, the applicability of E8 was only demonstrated with vitronectin VTN-NC variant (Chen et al., 2011) which being a biological matrix, makes it prone to batch-to-batch variability, less stable than synthetic surfaces and expensive for large-scale hESC expansion (Villa-Diaz et al., 2013). Nevertheless, E8 is the most and truly defined medium of its kind and holds promising results for the transfer of hESC from basic research to the clinic.

Table 1-2 List of known components of MEF-CM and the two most widely used chemically defined media, mTeSR1 and StemPro.

	mTeSR1™	StemPro™	MEF-CM
Amino acids			
Glycine	✓	✓	✓
L-Alanine	✓	✓	✓
L-Alanyl-L-glutamine		✓	✓
L-Arginine	✓	✓	✓
L-Asparagine	✓	✓	✓
L-Aspartic acid	✓	✓	✓
L-Cysteine	✓	✓	✓
L-Cystine	✓	✓	✓
L-Glutamic Acid	✓	✓	✓
L-Histidine	✓	✓	✓
L-Hydroxyproline			✓
L-Isoleucine	✓	✓	✓
L-Leucine	✓	✓	✓
L-Lysine	✓	✓	✓
L-Methionine	✓	✓	✓
L-Phenylalanine	✓	✓	✓
L-Proline	✓	✓	✓
L-Serine	✓	✓	✓
L-Threonine	✓	✓	✓
L-Tryptophan	✓	✓	✓
L-Tyrosine	✓	✓	✓
L-Valine	✓	✓	✓

	mTeSR1™	StemPro™	MEF-CM
Vitamins			
Ascorbic acid	✓	✓	✓
Biotin	✓	✓	✓
Choline chloride	✓	✓	✓
D-Ca pantothenate	✓	✓	✓
Folic Acid	✓	✓	✓
i-Inositol	✓	✓	✓
Niacinamide	✓	✓	✓
Pyridoxal		✓	
Pyridoxine	✓	✓	✓
Riboflavin	✓	✓	✓
Thiamine	✓	✓	✓
Vitamin B12	✓	✓	✓
Lipids			
Arachidonic acid	✓		
Cholesterol	✓		
DL-alpha tocopherol acetate	✓		
Linolenic acid	✓		
Myristic acid	✓		
Oleic acid	✓		
Palmitic acid	✓		
Palmitoleic acid	✓		
Stearic acid	✓		
Linoleic Acid	✓	✓	✓
Lipoic Acid	✓	✓	✓

Table 1-2 *continued*

	mTeSR1™	StemPro™	MEF-CM		mTeSR1™	StemPro™	MEF-CM
Growth Factors				**Other Components**			
Heregulin-1b EGF domain		✓		D-Glucose (Dextrose)	✓	✓	✓
Activin A		✓		Hypoxanthine Na	✓	✓	✓
LR3-IGF1		✓		Phenol Red	✓	✓	✓
FGF2	✓	✓		Putrescine 2HCl	✓	✓	✓
Bovine or Human Transferrin	✓	✓	✓	Sodium Pyruvate	✓	✓	✓
BSA: fatty acid free Cohn's fraction V		✓		Thymidine	✓	✓	✓
GABA	✓			2-Mecaptoethanol	✓	✓	✓
Lithium chloride	✓			Penicillin		✓	
Pipecolic acid	✓			Streptomycin		✓	
TGF-B	✓			HEPES	✓		
BSA	✓			Pluronic F-68	✓		
Insulin	✓		✓	Tween 80	✓		
AlbuMAX			✓	Reduced glutathione	✓		✓

In spite of the significant progress made in defining the culture conditions, a complete chemically defined culture system (comprising both substrate and culture medium) has not been attained. On the one hand, the most defined substrates still depend on the use of MEF-CM. On the other hand, the most defined culture media still require extracellular matrices subject to batch-to-batch variability. Both scenarios indicate a lack of understanding of the molecular mechanisms regulating cell adhesion, proliferation, self-renewal and differentiation. Furthermore, the intracellular and extracellular factors that activate such mechanisms remain largely unknown. Therefore, identification of the factors that influence hESC behaviour will be pivotal to the development of the appropriate combination of substrate and culture medium, with known chemistries, that will enable the massive propagation of clinical-grade hESC as well as the controlled differentiation of hESC into specified lineages, thus providing sufficient functional differentiated cells suitable for therapeutics and other applications.

1.3 Identification of the factors involved in hESC regulation

Under feeder-free conditions, hESC depend largely on the use of medium conditioned by the feeders; otherwise, they readily undergo differentiation (Xu et al., 2001). This indicates that feeders (either murine or human) secrete a plethora of factors to the conditioned medium that are essential for the long-term expansion of undifferentiated hESC. Therefore, investigation of these factors is of utmost importance to understanding stem cell biology which ultimately will lead to the creation of more defined and controlled conditions for the culture of hESC.

Several studies have reported the identification of the factors released by the feeders; however, most of them have focused on the protein components of the CM, as it will be detailed below, while very little attention has been paid to the low-molecular weight factors. Because small molecules can also activate signalling pathways in hESC (Pebay et al., 2005, Kumagai et al., 2013), it will be of equal importance to

investigate which small-molecule components are also present in the conditioned medium.

1.3.1 Investigation of protein components in CM

The first MS-based analysis pursuing the discovery of the factors secreted by the feeders was carried out by Lim and Bodnar. Conditioned medium from MEFs (STO cell line) was analysed by sodium dodecyl sulfate polyacrylamide gel electrophoresis (SDS-PAGE) and matrix-assisted laser desorption/ionisation-time of flight mass spectrometry (MALDI-ToF-MS). Of the 828 proteins that were subjected to mass spectrometry analysis, 136 were successfully identified and from these only three were associated to differentiation and cell growth. The 3 relevant proteins identified were insulin-like growth factor binding protein 4 (IGFBP-4), pigment epithelium derived factor (PEDF) and secreted protein, acidic and rich in cysteine (SPARC) (Lim and Bodnar, 2002).

A few years later, Buhr et al in addition to analysing the CM from CD1 MEFs, also investigated the proteome profiles of the MEFs and gelatine, the basement on which MEFs were grown (Buhr et al., 2007). By two-dimensional (2D) SDS-PAGE followed by MALDI-ToF-MS and nano-liquid chromatography-tandem mass spectrometry (LC-MS/MS), they identified 110 unique proteins in MEFs, 23 in the CM and none in gelatine due to technical problems. Of the 110 proteins identified in MEFs, only 1% was related to signal transduction and another 1% with cell adhesion. The rest of the proteins were related to other kind of functions. Comparison of the 2D gel patterns of unconditioned and conditioned medium did not present any significant differences; therefore, it was not possible to distinguish protein candidates that may be able to regulate self-renewal or pluripotency.

Another study analysing the proteins of CM was that of Chin and co-workers. They compared the serum-free conditioned medium obtained from primary MEFs with that from ΔE-MEFs, an immortalised MEF line that did not support the undifferentiated growth of hESC (Chin et al., 2007). Six growth factors (monocyte chemoattractant protein-1, interleukine-6, plasminogen activator inhibitor, pigment epithelium

derived factor, insulin-like growth factor binding protein (IGFBP)-2, and IGFBP-7) were identified in the CM of the supporting feeder cells (primary MEFs) which were further tested to investigate their relevance in hESC culture. It was found that the addition of the six growth factors to the UM delayed the loss of pluripotency; however, they were insufficient to maintain the long-term hESC expansion when compared with the positive control MEF-CM (Chin et al., 2007). This indicated that other secreted factors or components present in the serum supplement were also necessary.

In 2005 Prowse et al published the protein analysis of the medium conditioned by human neonatal fibroblasts (Prowse et al., 2005) which they further expanded in 2007 with the additional analysis of the CM from human foreskin fibroblasts and MEFs (Prowse et al., 2007). The comparative study of the CM from the three feeder cell lines identified 34 proteins in common and significantly increased the number of proteins associated with cell growth, differentiation and pluripotency. Some of the proteins identified included IGFBP-3, -6 and -7, inhibin *β* A/activin A, follistatin-related protein-1, and SPARC. Amongst these, activin A had already documented information of its implication in the maintenance of hESC pluripotency (Beattie et al., 2005).

Bendall and colleagues, by employing an enhanced mass-spectrometry approach, increased 10-12 fold the number of proteins previously detected in MEF-CM (Bendall et al., 2009). Their iterative exclusion methodology which consisted in the repetitive analysis of individual samples using successive mass (*m/z*) and retention time-directed exclusion, so that the same peptide ion was not sampled twice for MS/MS analysis, allowed the identification of low abundant proteins that were usually masked by the high abundant ones and that used to go unidentified. As a result, they found 29 growth factor-like proteins in MEF-CM which represented approximately 10 times more proteins than the 3 previously identified by Lim and Bodnar (Lim and Bodnar, 2002). Platelet derived growth factor (PDGF)-α, basic fibroblast growth factor (bFGF), hepatoma derived growth factor, glia maturation factor β and thymic stromal lymphopoietin were some of the newly identified

differentiation and growth factors that had not been previously reported by Lim and Bodnar (Lim and Bodnar, 2002) or by Prowse et al (Prowse et al., 2007).

Unlike the proteomics studies discussed thus far that employed mass spectrometry for the identification of the proteins in MEF-CM, Talbot et al performed a quantitative and semiquantitative immunoassay of the growth factors and cytokines produced by STO and CF1 mouse feeder cells (Talbot et al., 2012). In pure terms, this immunoassay could not be considered a discovery study since Talbot et al targeted proteins that had been previously described in the literature (Xu et al., 2005b, Greber et al., 2007, Eiselleova et al., 2008). However, the quantitative aspect added a deeper understanding of the medium conditioning process and provided possible explanations to the varying culture efficiencies observed when hESC are grown with CM of different mouse strains (Xu et al., 2001). The quantitative antibody-based analysis of Talbot et al found that CF1 cells expressed 10 times more activin A than STO cells and also produced larger quantities of interleukin-6, IGFBP-2, -3, -4 and -5. On the contrary, STO produced more hepatocyte growth factor and stem cell factor than CF1 cells (Talbot et al., 2012). These results demonstrated that each strain of mouse feeders had different capabilities to condition the medium which might be critical for the efficient growth of hESC (Xu et al., 2001).

1.3.2 Investigation of small-molecule components in CM

While the previously described studies have contributed to the identification of the protein components of CM, very few reports have addressed the identification of the small molecules (metabolites) secreted by the feeders which could also be involved in the maintenance of hESC. In fact, many of the feeder-secreted metabolites remain largely unknown, likely because of the lack of methods focused on their analysis. In the current literature only two publications have aimed at the identification of the metabolites secreted by mouse and/or human fibroblasts during the medium conditioning process. The first one, published in 2011, aimed to characterise the metabolites in a medium

conditioned by human foreskin fibroblasts (HFFs) (MacIntyre et al., 2011). The authors in that publication employed a ^{1}H-nuclear magnetic resonance (^{1}H-NMR) method to compare the metabolite profile of the chemically defined TeSR1™ medium (Ludwig et al., 2006b) before and after incubation with HFFs. They found that HFF-CM contained higher levels of lactate, pyruvate and alanine than the TeSR1™ medium without conditioning (MacIntyre et al., 2011). These increased metabolites secreted by HFFs are by-products of glycolysis but their effects on hESC proliferation or pluripotency are still unknown. Interestingly, these and other less significantly increased metabolites found in HFF-CM were mostly those present at higher concentrations, this is one of the limitations of NMR methods which lack enough sensitivity to detect low abundant analytes. It might be possible that other known bioactive compounds are present in CM at levels below the detection limits of NMR; therefore, more sensitive analytical methods like mass spectrometry may be required.

The second study that investigated the metabolites secreted by feeders was that carried out by Gupta et al. In their report the authors analysed the consumption of glucose and the production of lactate by mouse embryonic fibroblasts over a period of 72 h (Gupta et al., 2012). At regular intervals they measured the concentrations of glucose and lactate present in MEF-CM and fitted mathematical models to the data in order to predict the trends of glucose consumption and lactate production beyond the 72 h experimental time. Given the specific analysis of glucose and lactate, information regarding other secreted metabolites was neglected; therefore, making this method unsuitable for identification of unknown metabolites.

Other methods analysing the culture medium of hESC have targeted their investigations to the discovery of drugs' toxicity biomarkers (Cezar et al., 2007, West et al., 2010). As these protocols have perturbed the system with the addition of drugs to the hESC culture, the investigation of the factors secreted by MEFs or any other feeder cells cannot directly be assessed. As a consequence, there is still a lack of protocols pointing to the investigation and identification of the metabolites present in the

conditioned medium. Furthermore, in spite of its widespread use as feeder cells, at present, there is no report of the comprehensive analysis of the metabolites secreted by MEFs. Metabolomics methods offer the appropriate tool for such kind of studies and will be described in more detail in the following sections.

1.4 Metabolomics

Metabolomics comprise the identification as well as the qualitative and quantitative measurement of all the metabolites (compounds with molecular mass lower than 1000 Da) present in a biological system (Fiehn, 2002). The related term, *metabonomics*, was coined by Nicholson et al and defined as the quantitative measurement of the dynamic multiparametric response of a living system to pathophysiological stimuli or genetic modification (Nicholson et al., 1999). Because in practice both terms overlap by a large degree, they are frequently used interchangeably; however, throughout this thesis the term metabolomics will be used. The whole set of intracellular and extracellular metabolites produced by a living cell is known as the *metabolome* (Oliver et al., 1998). As metabolites are the downstream products of other '-omics' such as transcriptomics and proteomics, metabolomics provide complementary information for a better understanding of the cellular processes occurring in the biological system under study (Villas-Boas et al., 2005).

Metabolomics analyses are mainly undertaken by two major approaches: *targeted* and *untargeted* methods. A targeted metabolomics approach aims to quantify a pre-determined number of metabolites belonging to a certain class of compounds (e.g. lipids, amino acids, carbohydrates) or to a specific metabolic pathway (e.g. glycolysis) (Roberts et al., 2012). This targeted approach is usually hypothesis-driven and requires a priori knowledge of the biological system under study. An example of this approach was the analysis of 22 amino acids in *Pichia pastoris* cell extracts (Guerrasio et al., 2014). Because investigators focused on the measurement of the amino acids, other metabolites present in the cell

extracts were neglected. The advantage of targeted methods is that they provide quantitative information; however, because they are biased towards a selected number (or group) of metabolites, information about other components remains unknown.

On the other hand, untargeted metabolomics methods (also known as global metabolomics or metabolite profiling) aim to detect all the metabolites in a biological sample, including the unknowns. Untargeted approaches usually compare the metabolite profile of a control group with that of an altered group allowing the identification of the metabolites of interest which could be further quantified with a targeted approach (Leon et al., 2013). Therefore, targeted and untargeted metabolomics are complementary approaches that if used in combination can provide more in-depth insights of the metabolic events occurring in the biological system. Untargeted metabolomics has found application in the discovery of potential biomarkers in cancer (Lin et al., 2011, Xie et al., 2012), Alzheimer's disease (Li et al., 2010), onchocerciasis (Denery et al., 2010) and metabolic disorders such as diabetes and obesity (Zhang et al., 2009b, Kim et al., 2010), amongst other conditions. However, this type of approach risks the identification of artefacts as markers; thus, the results should be properly validated. For this, it is recommended that metabolomics analyses are repeated with different sample sets to verify the legitimacy of the potential biomarkers; and finally, carry out absolute quantification using validated methods to confirm that test and control samples show concentrations significantly different. Other limitations in the application of untargeted metabolomics methods include the lack of standardised protocols in analytical performance, data mining and data reporting which, so far, have not been completely established yet.

Given the complexity of untargeted methods, they can be sub-divided into: a) *metabolomics fingerprinting* (Fiehn, 2001), if the aim is to analyse all the intracellular metabolites (endo-metabolome) and b) *metabolomics footprinting* (Allen et al., 2003), if the aim is to analyse all the extracellular metabolites (exo-metabolome) (Figure 1-4).

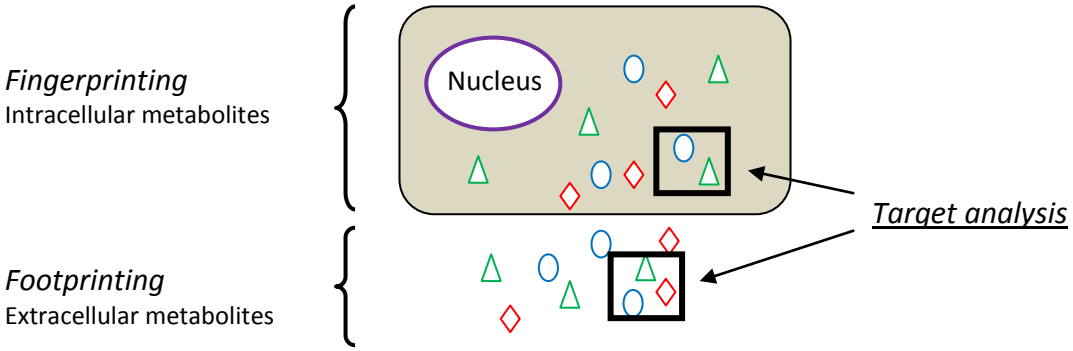

Figure 1-4 Metabolomics strategies for the analysis of the metabolome. Untargeted metabolomics comprising fingerprinting and footprinting aim to identify all the intracellular and extracellular metabolites, respectively, whereas targeted approaches focus only on a selected number of metabolites that can be intracellular or extracellular. Diamond, circle and triangle shapes represent metabolites.

Footprinting analyses are relatively straightforward when compared to metabolomics fingerprinting. Metabolomics footprinting requires minimal sample preparation, usually filtration or centrifugation to separate the cells from the culture medium. In contrast, metabolomics fingerprinting requires more elaborate procedures to extract the metabolites from the cells and the protocols are also extensively optimised in order to obtain good metabolite recoveries (Leon et al., 2013). An example of these metabolic strategies is the study of the intracellular and extracellular metabolites of Chinese hamster ovary (CHO) cells (Dietmair et al., 2012). Dietmair et al compared the metabolome of CHO cells cultivated in three different media and identified metabolites that correlated with differences observed in growth rate and cell viability. They centrifuged the culture medium to analyse the extracellular metabolites but employed a series of solvent addition, centrifugation, freeze-drying and reconstitution steps to extract the intracellular metabolites (Dietmair et al., 2012).

Because untargeted methods (more specifically metabolomics footprinting) suit better the objective of identifying the metabolites secreted by MEFs, the following sections will focus on the instrumentation and data processes required by untargeted metabolomics.

1.4.1 Analytical platforms for metabolomics

Amongst the analytical platforms applied in metabolomics, the most commonly used are nuclear magnetic resonance (NMR) spectroscopy and mass spectrometry (MS) (Dunn et al., 2005). The latter usually coupled to a separation technique such as liquid chromatography (LC), gas chromatography (GC) and, less often, with capillary electrophoresis.

NMR has been extensively used in metabolomics (Smolinska et al., 2012) and is particularly an advantageous technique since it requires minimal sample preparation, produces signals that correlate with the concentrations of the analytes in the samples and its non-destructive nature allows the recovery of the samples after analysis (Sotelo and Slupsky, 2013). However, NMR faces some limitations in terms of sensitivity; only the most abundant analytes in a given sample are detected. This limitation is overcome by MS which provides greater sensitivity than NMR and therefore enables the detection of low abundant metabolites that usually go undetected with NMR methods.

Direct infusion MS (DIMS) offers a rapid way to analyse hundreds of samples per day due to its short analysis times, usually 1–2 min long. However, because all the analytes enter simultaneously to the mass spectrometer, DIMS can suffer from extensive ion suppression, a type of matrix effect where the signal of a particular ion can be suppressed or enhanced due to the presence of another co-eluting ion. Another limitation of DIMS is that it cannot distinguish between isobaric and isomeric compounds. Nevertheless, DIMS has proven to be successful in metabolomics, for example, it was able to identify biomarkers in a serum metabolomics study of kidney cancer (Lin et al., 2010).

Hyphenated MS approaches (e.g. LC-MS, GC-MS) have several advantages over DIMS although at the expense of longer analysis times. For example, chromatographic separation of the analytes prior to detection reduces ion suppression effects, creates a retention-time identifier that will support the investigator at the time of metabolite identification and also produces better MS data quality due to reduced background noise (Patti, 2011).

The use of GC-MS in metabolomics is restricted to the analysis of volatile and semi-volatile compounds or to some extent it employs chemical derivatisation to make non-volatile analytes suitable for analysis. However, derivatisation requires extensive sample preparation times and not all sorts of molecules can be derivatised (Kopka et al., 2004). As a result, only a limited number of metabolites can be analysed by GC-MS. In contrast, LC-MS allows the separation of compounds of a wide range of polarity with little effort in sample preparation which makes it, probably, the most versatile separation method. LC-MS will be discussed in more detail in the next section.

1.4.2 LC-MS-based metabolomics

The highly complex samples used in metabolomics require that the tools/instruments used for the study of the metabolome perform at the highest resolution possible in order to increase metabolome coverage and facilitate metabolite identification.

1.4.2.1 Liquid chromatography

Although conventional high performance liquid chromatography (HPLC) is well suited to metabolomics analysis, the introduction of ultra performance liquid chromatography (UPLC), with its greatly enhanced chromatographic efficiency, has improved sensitivity, resolution and analysis time, resulting in the detection of an even greater number of metabolites (Swartz, 2005). Because of this, the use of UPLC is preferred over conventional HPLC as it increases metabolome coverage (Wilson et al., 2005).

Reversed-phase liquid chromatography (RPLC) is by far the most widely used separation mode in metabolomics because of the wide range of metabolites that can be analysed. Furthermore, RPLC provides the most reliable, robust and sophisticated stationary phases than any other separation mode (Gika et al., 2014). However, there are some limitations with the use of RPLC, polar and/or ionic compounds are poorly retained

and cannot be effectively analysed with RPLC (Theodoridis et al., 2011). Hydrophilic liquid chromatography (HILIC) is an alternative separation mode suitable for the analysis of polar compounds although it sacrifices the retention of hydrophobic molecules (the ones retained with RPLC). Therefore, RPLC and HILIC are complementary approaches that if used in combination, provide a greater coverage of the metabolome (Zhou et al., 2012). However, a compromise between metabolome coverage and high-throughput analysis has to be met as the use of both types of chromatography implies that samples are analysed twice therefore increasing analysis times. Some examples of LC-MS-based metabolomics in cell culture include the metabolite profiling of *Arabidopsis thaliana* plant leaves (t'Kindt et al., 2008), the RPLC analysis of the extracellular metabolites of CHO (Chong et al., 2009) and the HILIC analysis of *Escherichia coli* extracts (Bajad et al., 2006).

1.4.2.2 Mass spectrometry

Because untargeted metabolomics deals with samples of unknown composition, one of the objectives is to identify the metabolites of interest that distinguish the conditions under study (usually, altered vs. control group). Therefore, untargeted metabolomics requires the use of mass spectrometers with high mass accuracy in order to determine more precisely the elemental composition of the unknown metabolites and to reduce the number of candidate identities when searched against metabolomics databases. Time of flight (TOF) mass spectrometers have extensively been used in untargeted metabolomics mainly due to its excellent sensitivity, rapid data acquisition and high mass accuracy (typically < 5ppm) (Wikoff et al., 2007, Want et al., 2010, Loftus et al., 2011). Fourier transformed (FT) mass spectrometers such as ion cyclotron resonance (FT-ICR) and Orbitrap have also been used. Furthermore, they provide higher resolution and better mass accuracy than TOF instruments, although at lower scan rates. Therefore, with FT instruments there is usually a trade-off between high resolution and scan speed in order to obtain good resolution with enough data points per

chromatographic peak. The resolving power of FT-ICR is 1,000,000 full width at half maximum (FWHM) whereas that of Orbitrap is 140,000 FWHM, both values calculated at *m/z* 400. The mass accuracy of these instruments is sub-ppm for FT-ICR and 1–2 ppm for Orbitrap (Zhou et al., 2012).

Selection of the ionisation mode used in LC-MS also plays a major role in the metabolite profile that will be obtained (Theodoridis et al., 2012). Although various atmospheric pressure ionisation methods exist, the majority of experiments utilize electrospray ionisation (ESI) due to its soft ionisation and the capability of forming intact molecular ions that help in the identification process. Atmospheric pressure chemical ionisation (APCI) and atmospheric pressure photoionisation are complementary to ESI but they are preferred for the analysis of more non-polar and thermally stable analytes (Xiao et al., 2012).

1.4.3 Data analysis

LC-MS untargeted metabolomics analyses result in complex data sets of a large number of variables (ions) monitored simultaneously during the experiments. Therefore, data scrutiny requires the use of advanced statistical tools such as multivariate analysis (MVA) to extract information from the raw data files.

However, prior to MVA, a series of pre-processing steps including noise filtering, peak picking, alignment and normalisation (Katajamaa and Oresic, 2007, Hendriks et al., 2011) are required in order to reduce the three-dimensionality (mass-to-charge ratio (*m/z)*, retention time and signal intensity) of LC-MS data into a two dimensional data matrix that will be further manipulated with MVA software. Data pre-processing may be performed with the MS manufacturer's software (e.g. Markerlynx, Sieve) or with freely available software like MZmine (Pluskal et al., 2010), MetAlign (Lommen, 2009) or XCMS (Smith et al., 2006).

Once data pre-processing has been completed and the data matrix generated, then MVA analysis begins. Initial MVA analysis involves the

use of unsupervised methods such as hierarchical cluster analysis (HCA) or principal components analysis (PCA). These methods do not require a priori information about the samples class (Sumner et al., 2007b) and are used to reduce data dimensionality and to provide an overview of class separation, groupings and outliers.

Unsupervised methods are usually followed by supervised approaches such as partial least squares-discriminant analysis (PLS-DA) or orthogonal-PLS-DA (OPLS-DA). Supervised methods enhance the separation between classes and allow the identification of the variables (metabolites) responsible for the class separation. Sometimes the use of OPLS-DA is preferred to PLS-DA because it facilitates data interpretation. OPLS-DA, but not PLS-DA, can separate the between-class variation and the within-class variation which results in a more straightforward interpretation of the model and consequently of the data (Trygg et al., 2007). The discriminating metabolites that result from supervised methods are subjected to classical univariate statistics (e.g. Student's *t*-tests, analysis of variance (ANOVA)) to test their significance and the most significant ones are finally identified for biological interpretation.

1.4.4 Metabolite identification

Initial metabolite identification in LC-MS-based metabolomics starts by searching the accurate masses obtained in the experiments against in-house or web-based databases such as the Human Metabolome Database (www.hmdb.ca) (Wishart et al., 2009), Lipid Maps (www.lipidmaps.org) (Fahy et al., 2007) and/or METLIN Metabolomics Database (www.metlin.scripps.edu) (Smith et al., 2005) to obtain a list of possible candidates that can be further reduced by investigating the biological relevance of the putative identities. For a higher level of confidence in the identification of the metabolites MS/MS experiments can be performed and the MS/MS spectra likewise compared with spectral libraries. In the end, the unambiguous identification of the metabolites will only be achieved with the use of reference standards by comparing retention times, full scans and MS/MS spectra (Gika et al., 2014).

1.5 Aims and objectives

In this thesis, the low-molecular weight factors (metabolites) secreted by MEFs during the medium conditioning process will be investigated with the use of untargeted metabolomics methods. The methodology will also be extended to the analysis of hESC spent culture medium based on recent evidence that hESC also secrete factors that help them to maintain their self-renewal and pluripotency properties.

- To develop an untargeted LC-MS-based metabolomics method for the identification of the metabolites secreted by MEFs.

- To identify potential small-molecule factors released by MEFs that could be implicated in the pluripotency maintenance and/or proliferation of hESC.

- To investigate the effect on hESC in culture of potential small molecules identified in MEF-CM.

CHAPTER 2

Development of an LC-MS-based metabolomics approach for metabolite profiling of culture media used in hESC culture

2 Development of an LC-MS-based metabolomics approach for metabolite profiling of culture media used in hESC culture

2.1 Introduction

2.1.1 Metabolomics methods for the analysis of mammalian cell cultures

The application of metabolomics in the area of mammalian cell culture is relatively undeveloped as compared to the number of publications focused on the study of body fluids (e.g. serum, plasma, urine) (Cuperlovic-Culf et al., 2010). Nevertheless, there have been published a considerable number of reports applying cell culture metabolomics in several research fields including toxicology (Cezar et al., 2007, Palmer et al., 2013), drug testing (Croixmarie et al., 2009), cell-culture monitoring (Chong et al., 2009, Chong et al., 2010, Dietmair et al., 2012, McNamara et al., 2012), medium optimisation (Selvarasu et al., 2010), physiological cellular status monitoring (Chrysanthopoulos et al., 2010) and biopharmaceutical production (Fernandez et al., 2008, Mohmad-Saberi et al., 2013).

The metabolomics methods applied in cell culture can be divided in two groups: 1) those interested in the analysis of the intracellular metabolites (metabolomics fingerprinting) and 2) those focused on the profile of extracellular metabolites (metabolomics footprinting). Either type of methodology requires the immediate stop of all metabolic activity (quenching) to provide representative metabolic profiles of the physiological status of the cells at the time of sampling (Leon et al., 2013).

For metabolomics footprinting, separation of the culture medium from cells in suspension is achieved by cold centrifugation or by filtration. In the case of adherent cells, the medium is simply collected by pipetting and subsequently centrifuged to eliminate cell debris. For metabolomics fingerprinting, a metabolite extraction procedure is necessary in addition to the quenching step. After removal of the culture medium, cell quenching is generally performed by freezing in liquid nitrogen, acid

treatment or addition of cold buffered methanol (Sellick et al., 2010); however, these techniques are more suitable when working with cells in suspension. Adherent cells on the other hand have first to be detached from the flask, washed and finally quenched with liquid nitrogen or cold organic mixtures. Conventionally, cell detachment is achieved by using trypsin/ethylenediaminetetraacetic acid (EDTA) solutions or by cell scraping (Dettmer et al., 2011). This process is time consuming and requires multiple wash/centrifuge cycles; alternatively, quenching and extraction can be carried out at once by adding a solvent mixture directly to the culture dish (Ritter et al., 2008). The choice of the experimental protocol will depend on the study objective.

Because the objective of this thesis is to investigate the metabolites secreted by mouse embryonic fibroblasts to the conditioned medium, the methodology to be considered for method development will be metabolomics footprinting of the cultured medium (MEF-CM) used to grow hESC *in vitro*.

2.1.2 Metabolomics footprinting of hESC

Current LC-MS-based metabolomics methods analysing hESC culture media have been designed more properly to the discovery of toxicity biomarkers rather than characterising the medium itself. Furthermore, these methods have relied on long sample preparation times and long chromatographic analysis times making them unsuitable for high-throughput analysis. Typically, these protocols pass spent culture media through molecular weight cut-off (MWCO) filters by centrifuging the samples for approximately 180 min (Cezar et al., 2007) and then concentrating the filtrate for several hours to finally reconstitute them in a water/solvent mixture before analysis (West et al., 2010). Although initial methods required 90-min chromatographic runs per sample (Cezar et al., 2007), more recent protocols have significantly decreased the analysis time to approximately 20 min (Kleinstreuer et al., 2011, Palmer et al., 2013) (Table 2-1 and Table 2-2). Nevertheless, they still rely on long sample preparation times. With such long sample preparation methods the stability of the metabolites could be compromised and the

metabolite profile obtained might not be representative of the cellular status. Therefore, a method with reduced sample preparation times would be ideal. In this chapter, the development of a high-throughput LC-MS method will be pursued.

Table 2-1. Sample preparation protocols of methods analysing hESC culture media.

Culture medium	MWCO	Centrifugation time	Drying time	Reference
MEF-CM	3 KDa	180 min	0 min	(Cezar et al., 2007)
mTeSR1	3 KDa	200 min	Several hours	(West et al., 2010)
mTeSR1	10 KDa	240 min	Dried overnight	(Kleinstreuer et al., 2011)
mTeSR1	10 KDa	200 min	Dried overnight	(Palmer et al., 2013)

Table 2-2. Liquid chromatography conditions of methods analysing hESC culture media.

Type of column	Column dimensions	Organic modifier	Analysis time	Reference
C18	2.1x200 mm	0.1% formic acid	90 min	(Cezar et al., 2007)
HILIC	3x100 mm	0.1% formic acid	30 min	(West et al., 2010)
HILIC	3x100 mm	0.1% formic acid	22 min	(Kleinstreuer et al., 2011)
HILIC	3x100 mm	0.1% formic acid	17 min	(Palmer et al., 2013)

2.1.3 Analytical strategy adopted for method development

The LC-MS method development undertaken in this chapter will be based on the chromatographic and mass spectrometry response optimisation of the components of unconditioned medium (UM). UM was chosen because it is the medium used to obtain MEF-CM (as explained in chapter 1) whose mutual comparison will allow the identification of the small-molecule factors secreted by MEFs.

The known components of UM are listed in Table 2-3. Although it seems that UM is composed of polar molecules (amino acids and vitamins), it contains AlbuMAX® I, a lipid-rich bovine serum albumin, whose composition is not completely defined yet and that has been reported to contain different classes of lipids (Garcia-Gonzalo and Izpisua Belmonte, 2008), although these lipids have not been assigned a singular identity.

Table 2-3. Known composition of the ingredients of unconditioned medium.

DMEM/F12 (1:1)

Amino Acids

Glycine	L-Glutamic Acid	L-Phenylalanine
L-Alanine	L-Glutamine	L-Proline
L-Arginine	L-Histidine	L-Serine
L-Asparagine	L-Isoleucine	L-Threonine
L-Aspartic acid	L-Leucine	L-Tryptophan
L-Cysteine	L-Lysine	L-Tyrosine
L-Cystine	L-Methionine	L-Valine

Vitamins	**Other Components**	**Inorganic Salts**
Biotin	D-Glucose (Dextrose)	Calcium chloride
Choline chloride	Hypoxanthine Na	Cupric sulfate
D-Calcium pantothenate	Linoleic Acid	Ferric nitrate
Folic Acid	Lipoic Acid	Ferric sulfate
Niacinamide	Phenol Red	Magnesium chloride
Pyridoxine hydrochloride	Putrescine 2HCl	Magnesium sulfate
Riboflavin	Sodium Pyruvate	Potassium chloride
Thiamine hydrochloride	Thymidine	Sodium bicarbonate
Vitamin B12		Sodium chloride
i-Inositol		Sodium phosphate dibasic
		Sodium phosphate monobasic
		Zinc sulfate

KnockOut™ Serum Replacement

Glycine	L-Hydroxyproline	Thiamine
L-Histidine	L-Serine	Reduced glutathione
L-Isoleucine	L-Threonine	L-ascorbic acid-2-phosphate
L-Methionine	L-Tryptophan	Transferrin (iron saturated)
L-Phenylalanine	L-Tyrosine	Insulin
L-Proline	L-Valine	AlbuMAX® I

Non-essential amino acids

Glycine	L-Glutamic Acid
L-Alanine	L-Proline
L-Asparagine	L-Serine
L-Aspartic acid	

GlutaMAX™ Supplement

L-Alanyl-L-Glutamine

Note. Besides the ingredients stated here, β-mercaptoethanol and bFGF are added separately before incubation with mouse embryonic fibroblasts.

To optimise the chromatographic separation, the experiments carried out in this chapter will monitor the retention times of amino acids and fatty acids as representative polar and non-polar compounds contained in UM. As the lipidic part of UM is still unclear, the fatty acids monitored in these experiments were the known lipids present in mTeSR1™ medium (Ludwig et al., 2006a) (Table 1-2, chapter 1), assuming that to some extent these media share a certain number of components.

2.1.4 Aims and objectives

- Employ LC-MS technology to develop a comprehensive, high-throughput untargeted method for metabolite profiling of human embryonic stem cell culture media.

- Apply the developed method to characterise the components of unconditioned medium (the medium to be conditioned by mouse embryonic fibroblasts) used in hESC culture.

- Make use of metabolomics databases to assign putative identities to the unknown components of unconditioned medium.

2.2 Materials and methods

2.2.1 Chemicals

HPLC-grade acetonitrile (ACN) and methanol (MeOH) were obtained from Fischer Scientific (Loughborough, UK). Deionized water (18.2 MΩ) was prepared using an ELGA USF-Maxima water purification system (Marlow, UK). Ammonium acetate and ammonium carbonate were supplied by Merck (Darmstadt, Germany). MS-grade formic acid, DL-amino acid standards and leucine-enkephalin were purchased from Sigma-Aldrich (Gillingham, UK). Tissue culture reagents were purchased from Invitrogen.

2.2.2 Samples and sample preparation

100 mL of unconditioned medium (UM) were prepared using 83% v/v DMEM/F12 (1:1), 15% v/v KnockOut™ serum replacement, 1% v/v of GlutaMAX™, 1% v/v Non-essential amino acids, 10 µL of 1M β-mercaptoethanol and 100 µL of basic fibroblast growth factor at 4 ng/mL. Unconditioned medium was kept at -80^{0}C until analysis, and thawed over ice prior to sample preparation.

For each sample preparation method, samples were prepared three times and injected in triplicate to provide analytical replicates. Water blanks were prepared in exactly the same manner as the test samples.

2.2.2.1 Centrifugation method

In 1.5 mL Eppendorf tubes, 500 µL of UM were centrifuged at 17000 rpm for 10 min in a precooled (4^{0}C) centrifuge. Then, the supernatant was transferred into LC vials for analysis.

2.2.2.2 Ultrafiltration method

For the ultrafiltration method, 200 µL of sample were passed through Amicon Ultra filters (Millipore) with molecular weight cut-off (MWCO) of 10 kDa. Samples were dispensed into the filter device either alone or as a pre-mixed sample containing 10% of ACN. Afterwards, they were centrifuged at 14000 rpm for 15 min at 4^{0}C and the filtrate transferred into LC vials.

2.2.2.3 Solvent precipitation method

Based on a modification of (Pereira et al., 2010), aliquots of 250 µL of UM were mixed with 750 µL of cold solvent (MeOH or ACN kept at -20^{0}C), vortexed for 1 min to precipitate the proteins and stored at -20^{0}C for 20 min. After the cold storage period, samples were vortexed again for 15 s prior to centrifugation (17000 rpm, 10 min, 4^{0}C). The supernatants were transferred into LC vials for analysis.

2.2.3 Preparation of amino acids standards

A solution of 19 amino acids was prepared by weighing ~10 mg of each amino acid and transferring them into a 250 mL beaker, stirred with 80 mL of purified water and heated at ~70^{0}C to dissolve the amino acids thoroughly. The solution was let cool down and diluted to 100 mL in a 100-mL volumetric flask. The solution comprised the following amino acids: DL-alanine, DL-arginine, DL-asparagine, DL-aspartic acid, DL-cystine, DL-glutamic acid, glycine, DL-histidine, DL-isoleucine, DL-leucine, DL-lysine, DL-methionine, DL-phenylalanine, DL-proline, DL-serine, DL-threonine, DL-tryptophan, DL-tyrosine and DL-valine. The solution was further diluted 1:10 to obtain a working concentration of ~10 µg/mL for each amino acid.

2.2.4 Liquid chromatography

Unconditioned medium samples were analysed under each of the 12 different chromatography conditions listed in Table 2-4. Mobile phase composition comprised solvent A: aqueous buffer and solvent B: acetonitrile with the respective pH modifier: 0.1% v/v formic acid (pH 3.0), 10 mM ammonium acetate (pH 6.9) and 10 mM ammonium carbonate (pH 8.5).

Table 2-4. Chromatography columns and conditions tested.

Column name (supplier)	Column type	Dimensions, particle size	Chromatogra-phy mode	pH stability of column	pH tested
Hypersil Gold (ThermoScientific)	C18	2.1x50mm, 1.9 µm	RP	1 – 11	3.0
Hypersil Gold (ThermoScientific)	C18	2.1x150mm, 1.9 µm	RP	1 – 11	3.0
Zorbax Eclipse Plus (Agilent Technologies)	C18	2.1x100mm, 1.8 µm	RP	2 – 9	3.0
Zorbax Eclipse Plus (Agilent Technologies)	C18	2.1x150mm, 1.8 µm	RP	2 – 9	3.0; 6.9; 8.5
Synergi Polar-RP (Phenomenex)	Ether linked Phenyl (PH)	2.0x100mm, 2.5 µm	RP	1.5 – 7	3.0; 6.9
Acquity BEH Amide (Waters)	Ethylene Bridge Hybrid	2.1x150mm, 1.7 µm	HILIC	2 – 11	3.0; 6.9; 8.5
SeQuant ZIC-HILIC (Merck)	Zwitterion, Sulfobetaine	2.1x150mm, 5 µm	HILIC	3 – 8	6.9

For reversed-phase liquid chromatography (RPLC), the gradient used a linear increase from 10% B to 90% B in 10 min, held these conditions for 11 min, and returned to 10% B within 1 min. Then, three minutes of column re-equilibration were allowed. For hydrophilic interaction chromatography (HILIC), a 15-min gradient started with 80% B which was held for 1 min and then decreased to 50% B in 11 min. Initial mobile phase conditions were achieved again in 0.1 min, followed by 2.9 min of re-equilibration.

The chromatographic separations were performed on an Accela U-HPLC system (Thermo Fisher Scientific, USA) with a flow rate of 300 µL/min. The autosampler and column oven temperatures were set at 4^0C and 40^0C, respectively. The injection sample volume was 7 µL.

2.2.5 Mass spectrometry

The LC system was coupled online to an Exactive Orbitrap mass spectrometer (Thermo Fischer Scientific, USA) equipped with a heated

electrospray interface (HESI-II) operating in positive and negative ion modes to provide the most comprehensive MS profile possible. A 50 µg/mL solution of leucine-enkephalin (dissolved in 0.1% formic acid ACN/H_2O 50/50) was used to optimise MS parameters. The parameters at which the highest signal was achieved were: spray voltage, 3 kV; heated capillary temperature, 350^0C; heater temperature, 300^0C; sheath, auxiliary and sweep gas flow rates were 35, 10 and 5 arbitrary units, respectively. Data were acquired in full scan mode from *m/z* 70–1000 at 50,000 FWHM resolving power at 2 Hz.

2.2.6 Optimised LC-MS conditions for ZORBAX Eclipse Plus C18 column (2.1x100mm)

The final LC method that provided a good compromise between separation and analysis time is detailed next. The mobile phase consisted of A: 0.01% formic acid in water and B: 0.01% formic acid in acetonitrile. A step gradient programme was used, starting with 10% B, 0-0.3 min; 50% B, 5-6 min; 70% B, 7-8 min; 90% B, 9-10 min; 98% B, 11-16 min; and coming back to the re-equilibration mobile phase composition of 10% B, 16.5-18 min. The flow rate was kept at 300 µL/min with the exception of minute 9 to 11 which was increased to 400 µL/min. Before each sample injection of 7 µL in no-waste mode, the needle was washed with 400 µL of 75% methanol.

2.2.7 LC-MS/MS data dependent analysis

Experiments were carried out on an Accela U-HPLC system hyphenated with an LTQ Velos mass spectrometer (all from Thermo Fischer Scientific, USA) using the data dependent scanning mode with 35 eV collision energy. The LC conditions were the same as those described in section 2.2.6. The MS/MS method was fed with the list of parent ions –retrieved from the Exactive analyses– and the expected retention times of the analytes.

2.2.8 Data analysis

Positive and negative data sets were processed using Tox ID 2.1.1 Software to extract the retention times of the analytes, and QuanBrowser Xcalibur 2.2 software (both from Thermo Fischer Scientific, USA) to obtain the peak areas. When a compound was detected in +ve and –ve mode, the polarity at which it provided better sensitivity was chosen for quantification. Plots were created with GraphPad Prism version 6.03 (GraphPad Software Inc., California, USA).

Unknown compounds present in the UM were assigned a putative identity after searching their *m/z* values against web-based databases such as the Human Metabolome Database (www.hmdb.ca) (Wishart et al., 2009), Lipid Maps (www.lipidmaps.org) (Fahy et al., 2007) and METLIN Metabolomics Database (www.metlin.scripps.edu) (Smith et al., 2005). Confirmation of their identities was performed by means of tandem mass spectrometry (section 2.2.7). The MS/MS spectra of the possible compounds were compared with those in the databases aforementioned.

2.3 Results and discussion

2.3.1 Effect of pH and type of chromatography on separation

Initial scouting gradients were performed on the Hypersil Gold (2.1x50 mm) column, but polar compounds –amino acids, especially– were poorly retained (data not shown). Therefore, longer columns (2.1x150 mm) with the same stationary phase chemistry were tested. These longer columns included the Zorbax Eclipse Plus in addition to the Hypersil Gold. To keep the LC-MS method as simple as possible, the UM was injected directly into the LC columns using the centrifugation method (see materials and methods).

During HPLC method development, the mobile phase pH should be 1.5 units below or above the pK_a of the analyte of interest in order to have the analyte either in the ionized or non-ionized form which will produce a decent retention time and a good peak shape (Snyder et al., 1997). In metabolomics, however, with hundreds of metabolites, it is practically impossible to meet this criterion for all the analytes present in the

sample. As a result, a common practice is to explore different mobile phase pHs.

Retention times of amino acids and lipids run with mobile phase pH 3.0, 6.9 and 8.5 are shown in Figure 2-1. Amino acids represent a challenge in terms of chromatographic separation as this group of chemicals have at least two pK_a values, one for the carboxyl- and other for the amino-group; some amino acids even have a third pK_a. Consequently, a mobile phase with a single pH will not suit the best chromatographic conditions for all of them. Exploring an acidic, a basic and a neutral pH demonstrated that major separation is achieved when using pH 3.0 (0.1% v/v formic acid).

L-Tryptophan, L-isoleucine and L-phenylalanine seemed to be less affected by change in the pH. On the other hand, L-glutamic acid, L-cysteine, L-cystine, glycine and L-aspartic acid retention times dropped drastically while the mobile phase pH increased. The reason for this is that acidic amino acids lose their proton at higher pH, ionizing them and making them more polar; hence, eluting faster from the C_{18} column (Snyder et al., 1997).

a)

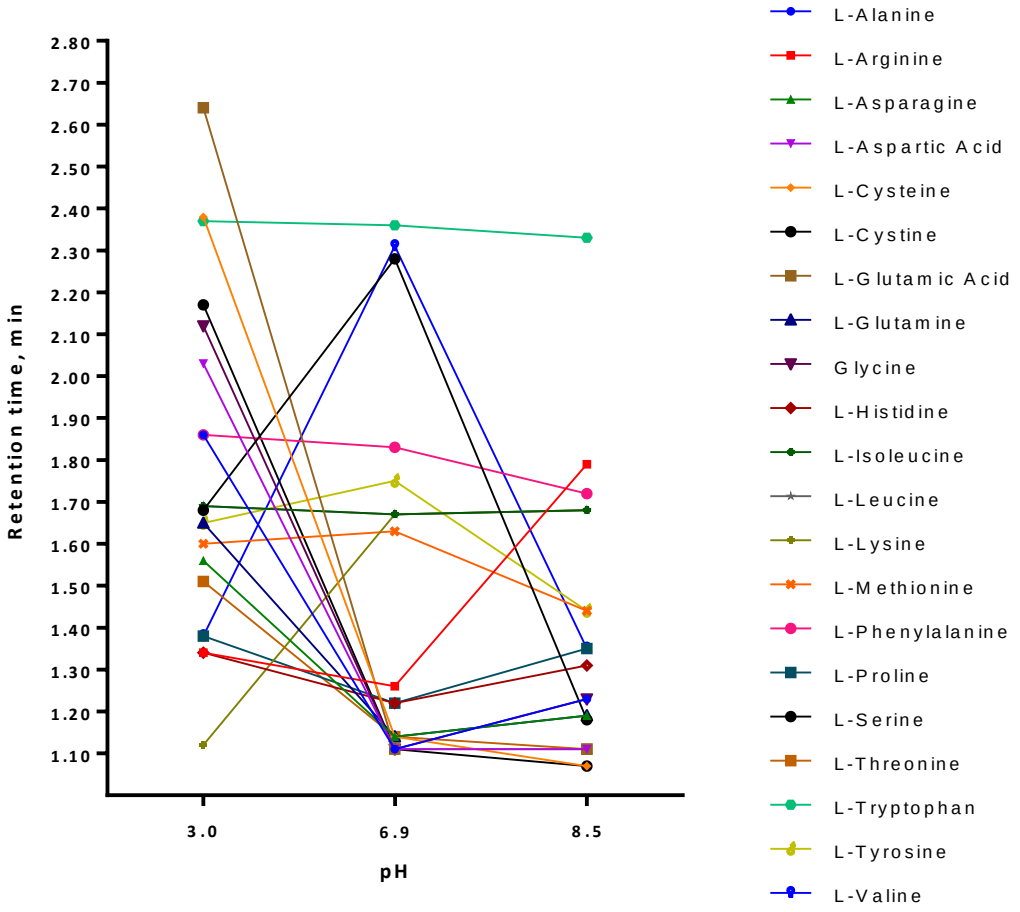

b)

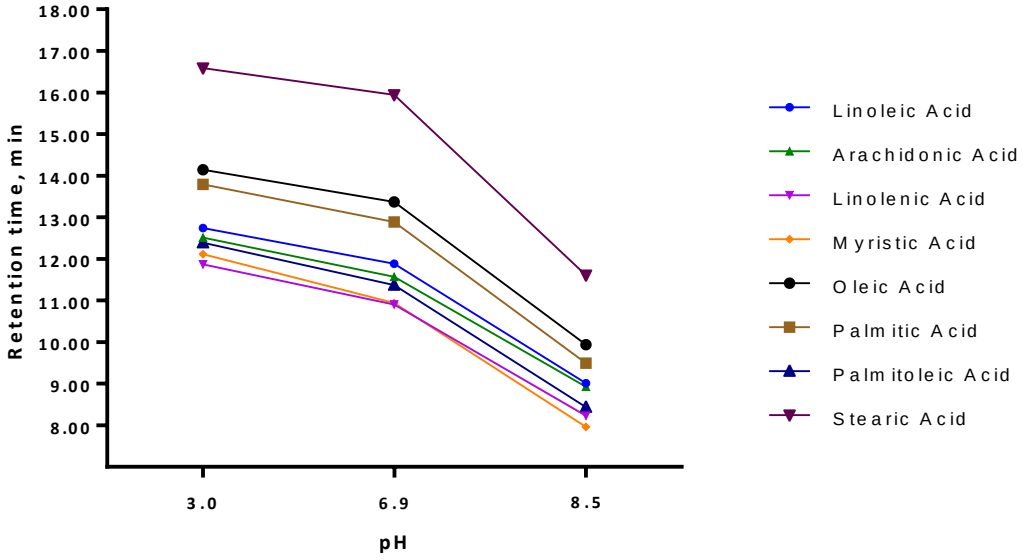

Figure 2-1 Retention times of a) amino acids and b) fatty acids with the Zorbax Eclipse Plus (2.1x150 mm) column under acidic (pH 3.0), neutral (pH 6.9) and basic (pH 8.5) conditions.

a)

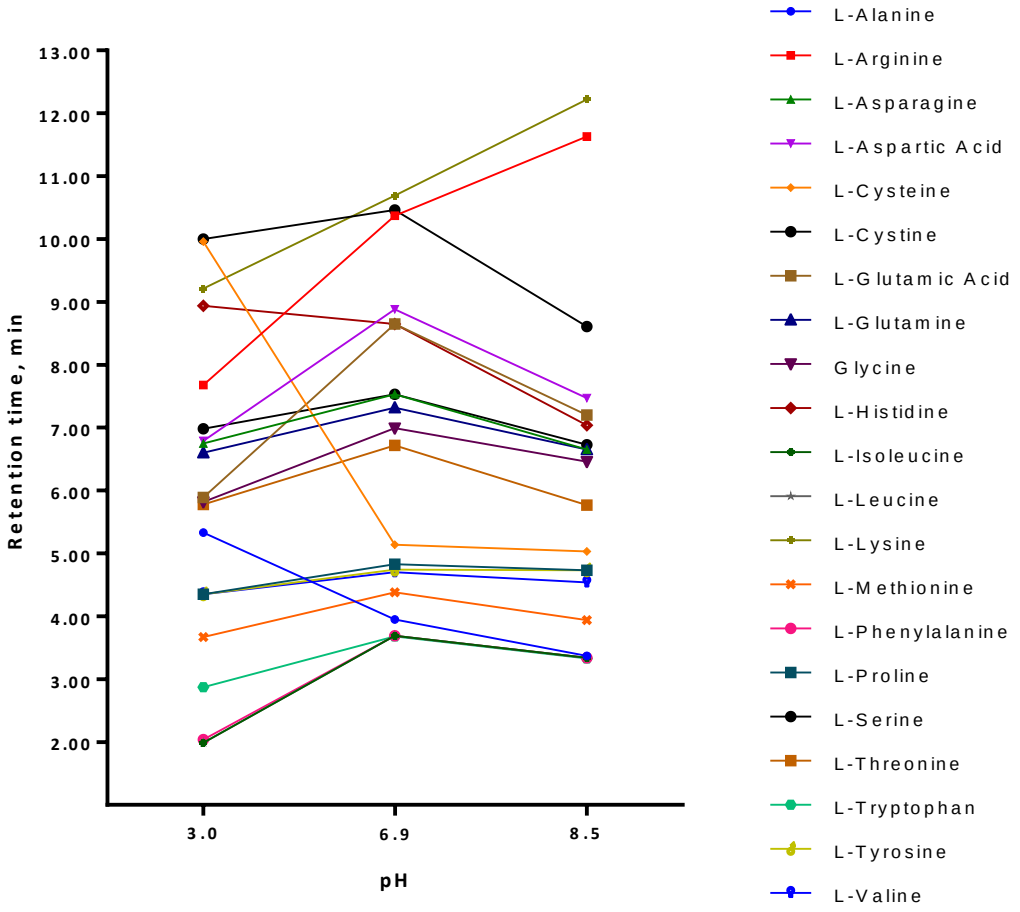

b

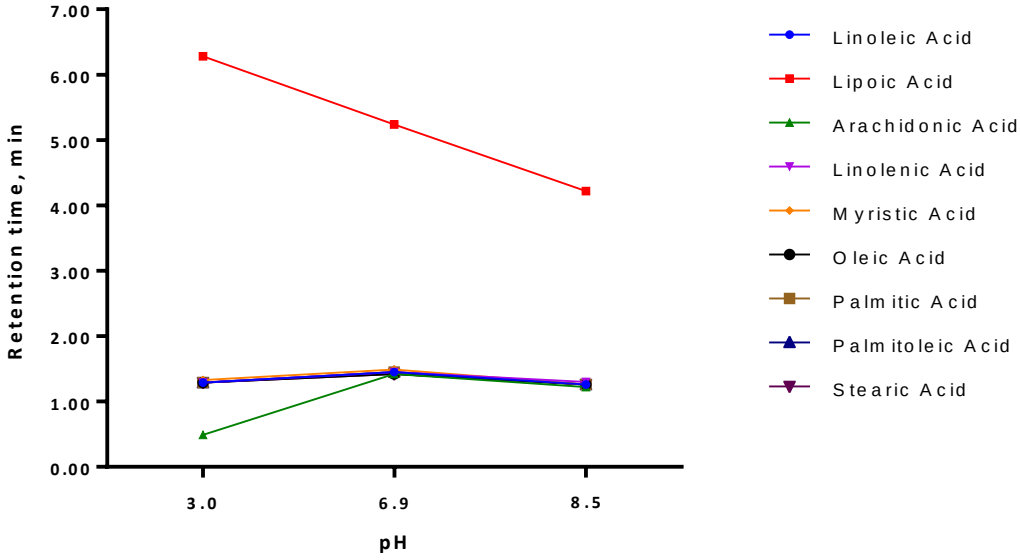

Figure 2-2 Retention times of a) amino acids and b) fatty acids with the Acquity BEH Amide column under acidic (pH 3.0), neutral (pH 6.9) and basic (pH 8.5) conditions.

In contrast to the amino acids, lipids (like the fatty acids shown in Figure 2-1b) were well retained and separated; again, mobile phase pH 3.0 provided better retention times. Short and unsaturated fatty acids eluted earlier than long and saturated fatty acids. This is explained by the fact that long and saturated fatty acids interact more with the stationary phase (octadodecylsilane also known as C_{18}) making them elute at the end of the gradient (Snyder et al., 1997). Similar results were obtained with the Hypersil Gold (2.1x150 mm) column.

In spite of the fact that increasing the length of the column increased the retention time of the polar compounds (amino acids and vitamins), some amino acids still eluted very closely at the void volume time. Derivatization (a chemical transformation process) (Sharma et al., 2014) or the use of ion-pairing agents (Piraud et al., 2005) could have enhanced the reversed-phase retention of these compounds; however, these strategies would complicate the already laborious analysis of metabolomics data, so they were not considered here. Instead, I decided to experiment with hydrophilic interaction chromatography (HILIC), a chromatography technique employed for retention of more polar compounds like sugars (Antonio et al., 2008), nucleosides (Guo et al., 2013), nucleotides (Inoue et al., 2010), etc., including amino acids (Guerrasio et al., 2014, Guo et al., 2013).

As with the Zorbax Eclipse Plus column, UM was injected into the Acquity BEH Amide column under the same conditions of mobile phase. Figure 2-2 shows the retention times of amino acids and lipids obtained with this column. In this case, amino acids presented superior retention times at pH 8.5, but lipids –except for lipoic acid– were practically unretained at all pHs.

Even though good retention was achieved for polar compounds with the HILIC column, some inconveniences were encountered with its usage. The column required longer equilibration times (Valette et al., 2004) and broad peaks were observed for certain amino acids in both Acquity BEH Amide and SeQuant ZIC-HILIC columns. The latter led to the decision of not taking further the analysis of UM with HILIC columns.

2.3.2 Optimising the chromatographic separation of amino acids

A second alternative to improve the chromatography of polar compounds in RPLC is by increasing the initial percentage of the aqueous buffer; in other words, reducing as much as possible the percentage of organic phase in the initial conditions of the RP-gradient (Snyder et al., 1997). To explore this route, a column (Synergi Polar) capable of supporting 100% aqueous was tested.

For this experiment, a solution containing 19 amino acid standards was injected into the Synergi Polar column. Series of injections from 0% to 50% organic (acetonitrile or methanol, as starting gradient composition) were performed to monitor the retention times of the amino acids (Figure 2-3). Notice that methanol was also used as mobile phase B as a way to change the selectivity and improve elution times, nonetheless, retention times did not change much, but column backpressure increased considerably; hence, methanol was discarded as an organic modifier. Mobile phase at pH 3.0 (0.1% v/v formic acid) and 6.9 (10 mM ammonium acetate) were also investigated. Consistently with experiments detailed so far, formic acid still accounted for longer retention times.

Amino acids started to elute faster while increasing the starting percentage of organic. It was at 20% organic when amino acids began to co-elute more significantly. In the case of methanol, this event occurred at 40%. Certainly, 100% aqueous (or 0% organic) conditions improved the chromatography for few amino acids, but for the rest, it had little or no benefit (Figure 2-3).

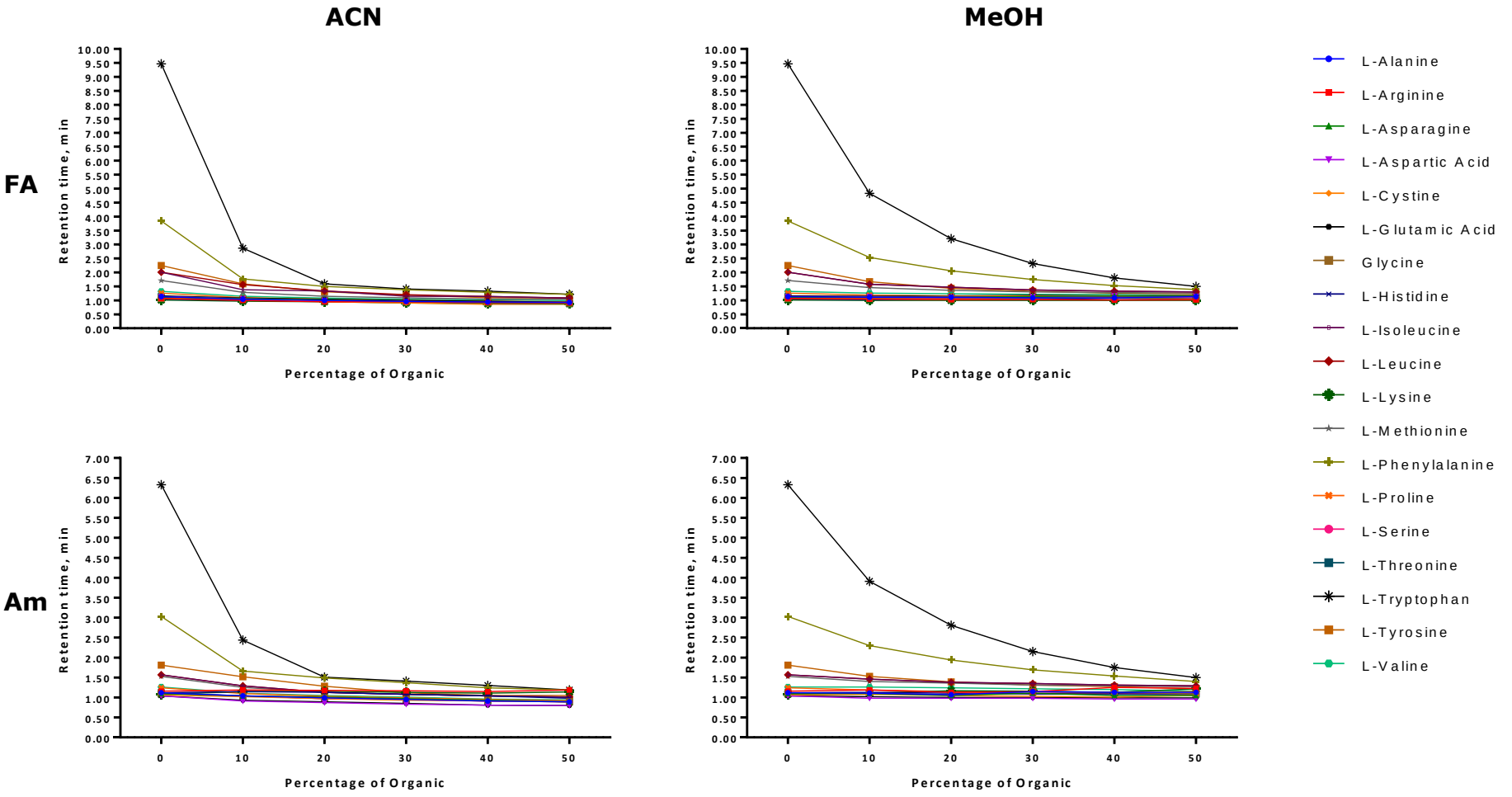

Figure 2-3 Retention maps of amino acid standards on the Synergi-Polar column with different initial percentages of organic solvent (ACN and MeOH), using both formic acid (FA) and ammonium acetate (Am) as pH buffers.

When comparing these results with those obtained with the Zorbax Eclipse Plus (2.1x150 mm) column at pH 3.0, the longer retention times observed with the Zorbax column could be explained by *a)* the length of the column, the longer the analytes travel, the slower the elution; *b)* the particle size, the smaller the particle size, the higher the number of theoretical plates, which means that the analytes interact more with the stationary phase (Swartz, 2005) and *c)* the stationary phase chemistry, Zorbax Eclipse Plus is a normal C_{18} column that has more affinity for carbon-chain compounds, while the Synergi Polar column possesses an ether-linked phenyl phase which explains the good retention of aromatic amino acids like L-Phenylalanine, L-Tryptophan and L-Tyrosine, and the insignificant retentivity of the others. Since not all RP columns can deal with high aqueous percentages, 10% starting organic was considered for optimising the method.

2.3.3 MS parameters optimisation

This section includes the optimisation of the MS acquisition parameters, but the ESI source parameters (see materials and methods) were kept the same throughout the experimental work.

In metabolomics experiments, high-resolution high mass accuracy MS data are required for the correct assignment of analyte masses and their identification/confirmation (Kellmann et al., 2009). The Thermo Exactive Orbitrap mass spectrometer has features to control the resolution and accuracy of the MS measurements: ion injection time, automatic gain control (AGC) target, microscans and resolution power. All these are interrelated for the final resolution outcome and will be explained shortly.

The AGC target regulates the amount of ions that enter into the C-trap whereas the injection time is the time in milliseconds that ions are allowed to accumulate in this trap. The AGC target settings in the Exactive are: ultimate mass accuracy ($5x10^5$ charges), balanced ($1x10^6$ charges) and high dynamic range ($3x10^6$ charges). If the ion population is small, the instrument sensitivity decreases (Wong et al., 2011). On the other hand, big ion populations can cause space-charge effects that induce mass measurement errors due to electrostatic interactions

(Makarov et al., 2006). Because of this, AGC target was set into balanced and injection time, 100 ms.

With respect to mass resolution, two settings were evaluated; enhanced (25,000 FWHM, 4Hz) and high (50,000 FWHM, 2Hz). Figure 2-4 illustrates the effect of increasing the resolution power. At 25,000 FWHM, the instrument was incapable of resolving the interference peak *m/z* 524.2996 from the true ion *m/z* 524.3357, a fact that could induce mass errors and unreliable peak assignment.

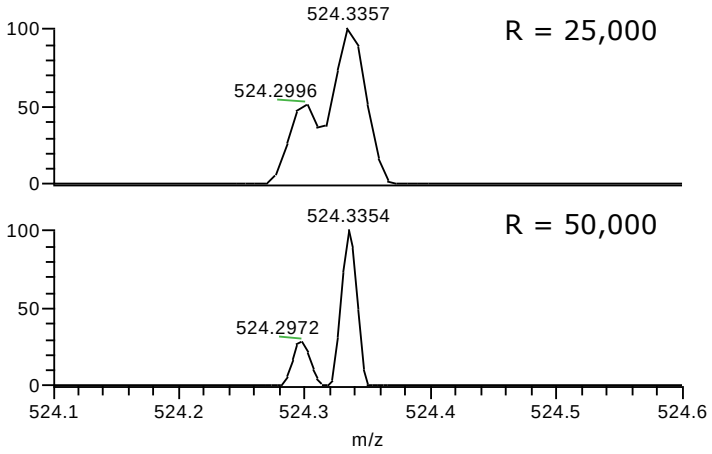

Figure 2-4 Effect of resolving power on separation of the analyte *m/z* 524.3357 from the interference *m/z* 524.2996. High-resolution mass spectra are a prerequisite for correct peak assignments.

It was found that high (50,000 FWHM) resolution power was necessary for separating analytes from interferences that could affect the mass accuracy and lead to false negatives. Experiments with different number of microscans were also assessed; in the end, microscans were set at 1 as increasing the number of them reduced the chromatographic sampling resulting in fewer data points per peak (data not shown).

50,000 FWHM resolution power and 1 microscan were chosen and finally adopted by the method as they provided a good compromise between resolution, mass accuracy and number of chromatographic points.

2.3.4 Sample preparation: comparison of centrifugation, ultrafiltration and protein precipitation methods

To keep the sample preparation methodology as simple as possible, UM was initially injected into the LC-MS system following centrifugation (as described in the materials and methods section). Although centrifuged samples provided valuable information during the development of the method, fast deterioration of the column was observed possibly as a result of proteinaceous material sticking to the stationary phase (Chambers et al., 2007). For this reason, and the likely existence of unwanted ion-suppression effects, other methods for preparing the samples were investigated (Figure 2-5).

Firstly, ultrafiltration (UF) of the unconditioned medium using a 10 kDa cut-off filter would allow small molecules (metabolites) to pass through the membrane whilst retaining proteins and high molecular weight compounds. Secondly, the same ultrafiltration method employing as sample a premixed solution of UM containing 10% ACN (UF-ACN) instead of UM alone. Finally, sample deproteinization carried out by solvent precipitation (PPT) with methanol and acetonitrile in a proportion 3:1 v/v solvent to sample (PPT-ACN and PPT-MeOH, respectively) (Lai et al., 2010). The samples were chromatographically separated with the Zorbax Eclipse Plus (2.1x150 mm) column and formic acid in the mobile phase.

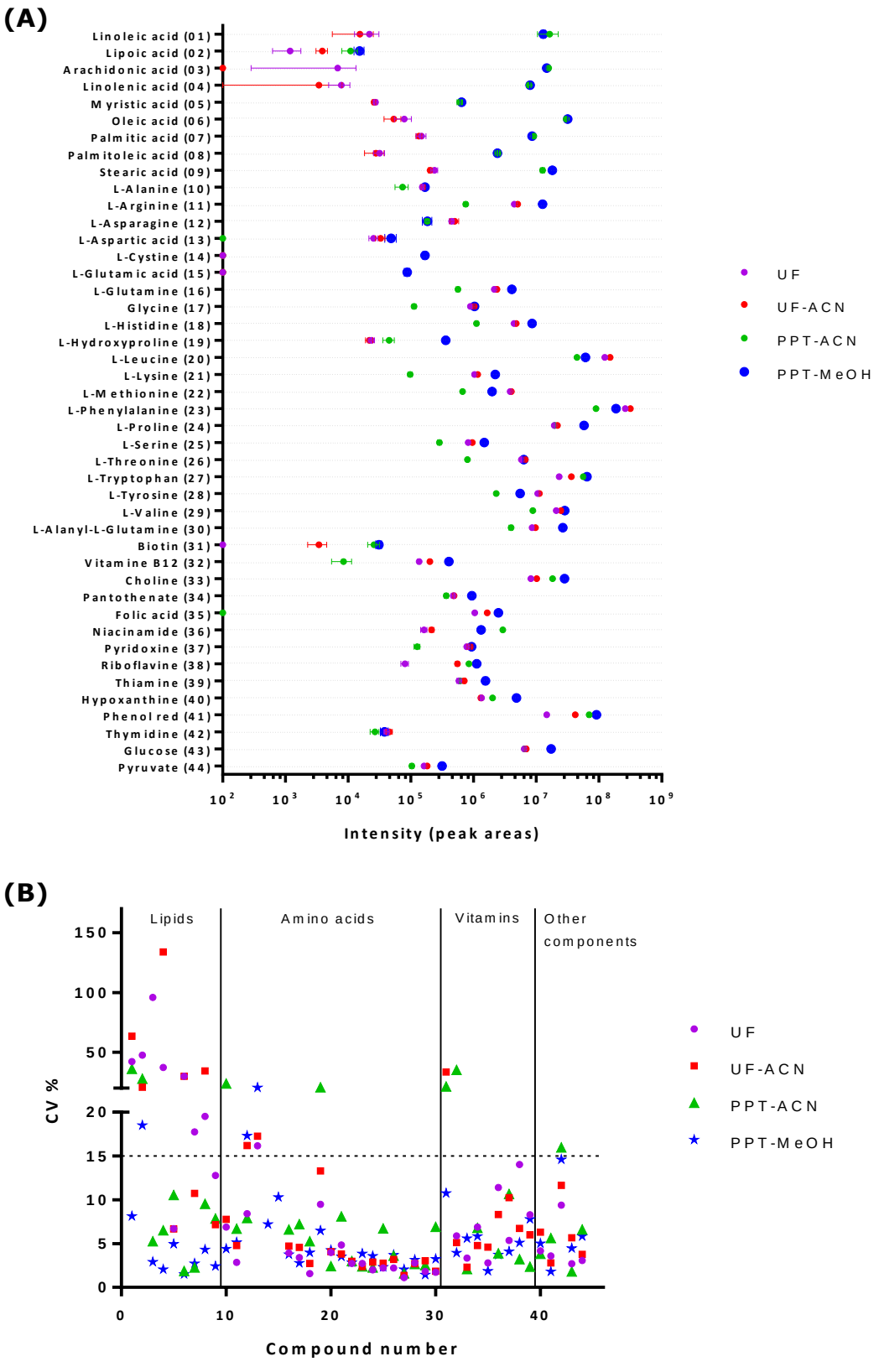

Figure 2-5 (A) Relative quantification of 44 identified metabolites in UM using four different preparation methods. Data points and error bars represent peak area means (n=9) and standard deviation. (B) Distribution of the coefficient of variation (CV) of the metabolites according to the methodology used. The dash line indicates the level of acceptance of reproducible results (<15%).

Ultrafiltration by molecular weight cut-off filters offers a rapid solution to remove proteins from samples; however, in these experiment, the cut-off filters not only retained the proteins, but also the non-polar (e.g. lipids) and semi-polar (i.e. phenol red) compounds present in the UM (Figure 2-6). Amino acids and vitamins passed freely through the membrane. Compare the intensity levels (peak areas) of these polar compounds with those of the fatty acids in Figure 2-5a.

In fact, permeation of phenol red served as an indicator of this phenomenon. The retentate fraction in the filter device remained red while the filtrate was almost clear. To overcome this issue, 900 µL of UM were mixed with 100 µL of ACN (UF-ACN) and then processed as it was done with the pure UM (UF). Other percentages of ACN were tried too, but did not make any significant difference (data not shown). In Figure 2-5a it is observed that while this trick worked well for some vitamins and phenol red, it did not improve the permeation of the fatty acids. Furthermore, this attempt produced larger CV (coefficient of variation) percentages (Figure 2-5b).

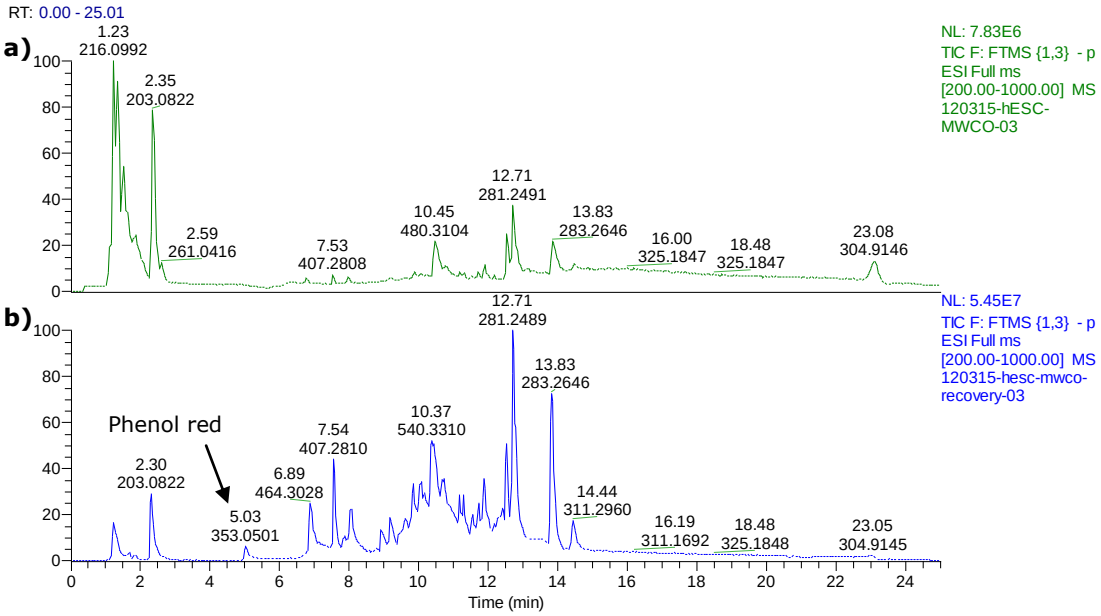

Figure 2-6 Total ion count (TIC) chromatograms of a) permeate and b) retentate fractions of unconditioned medium after ultrafiltration.

Because of the failure of UF as a sample preparation method in either of the two ways experimented here, the next step was to try solvent-induced protein precipitation in order to eliminate the proteins in the samples. MeOH- and ACN-precipitated samples provided similar results with regard to the response of fatty acids, but amino acids and vitamins gave higher intensities when MeOH was used. What is more, amino acids like L-cystine and L-glutamic acid were only detected with this method.

For the selection of the final sample preparation method, three important characteristics were taken into account: i) sensitivity, ii) number of compounds detected and iii) peak area reproducibility. Metabolites in the UM span a wide range of concentrations (Figure 2-5a), so it was desirable a method that could detect as many compounds as possible, including those at lower concentrations. Of the four sample preparation methods tested herein, MeOH-precipitated samples showed better sensitivity and the ability to detect more compounds than the other methods. Furthermore, MeOH-precipitated samples also generated more reproducible results. Figure 2-5b shows the distribution of the coefficients of variation of all the analytes monitored by the four sample preparation methods. While UF and UF-ACN had the highest number of metabolites with CV > 15%, PPT-MeOH had the fewest. Precipitation of proteins with methanol fulfilled the abovementioned criteria and it was decided to be the method of choice for the subsequent sample preparation of culture media in the next chapters.

2.3.5 Finalization of LC-MS method

After having identified the type of column (Zorbax Eclipse Plus), the mobile phase conditions (pH 3.0), MS parameters and the sample preparation method whereby the components of UM presented higher sensitivity and enhanced separation, there were two issues concerning the final LC-MS method. The first one was the length of the analytical run per sample. Metabolomics studies generally involve tens or even hundreds of samples, that if injected in a single analytical experiment, would create long analysis times and cause inconsistent results (retention time drifts and loss of sensitivity) as contaminants build up in the LC-MS

system over time (Zelena et al., 2009). The second issue was the known ability of higher concentrations of formic acid to cause ion suppression (Annesley, 2003) and thus reduce sensitivity. Reducing the concentration of formic acid in the mobile phase may further increase the sensitivity but possibly at the expense of a change in mobile phase pH which might affect separation.

To tackle these problems, the length of the column was reduced from 150 mm to 100 mm. Reducing the length of the column reduces the analysis time but also reduces the resolution of the peaks (Swartz, 2005). Thus, instead of a linear gradient, a step gradient was implemented and this maximised the separation of the components. The final LC parameters are provided in section 2.2.6 of this chapter.

For the ion suppression effect, the mobile phase concentration of formic acid was reduced from 0.1% to 0.01%. An increase in sensitivity was observed when 0.01% formic acid was used, noticed in the normalization level (NL) in the extracted ion chromatograms (EIC) of glucose and niacinamide (Figure 2-7). Reducing the concentration of formic acid increased slightly the pH of the mobile phase, so ionic compounds were more affected; in this example, basic compounds like niacinamide were less ionized and more retained (Snyder et al., 1997). Non-ionic analytes remained unaffected by the change of pH (i.e. glucose). These changes were beneficial overall so it was decided to implement the change to 0.01% formic acid in the mobile phase.

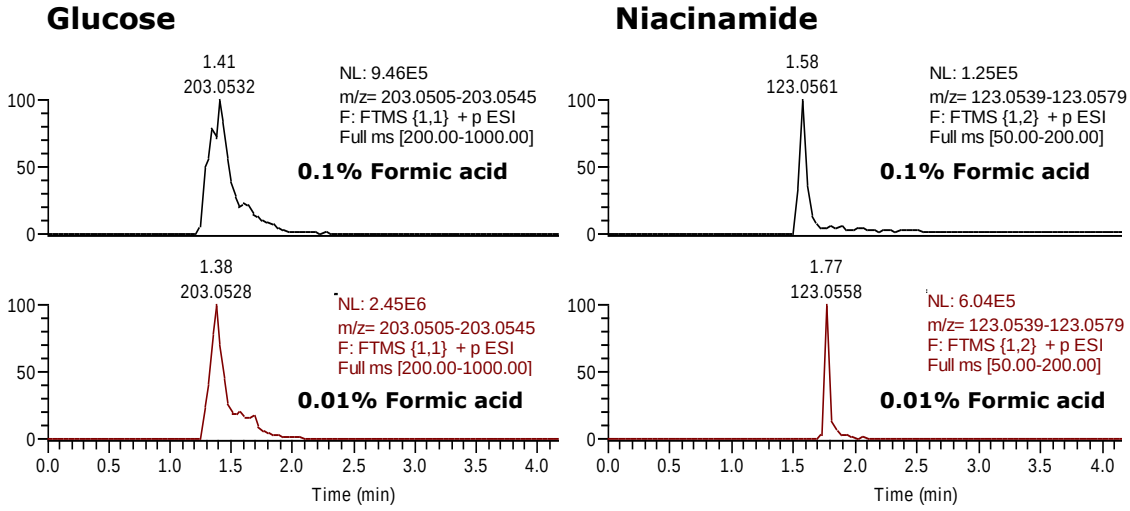

Figure 2-7 Extracted ion chromatograms (EIC) of glucose *m/z* 203.0532 ($[M+Na]^+$) and niacinamide *m/z* 123.0553 ($[M+H]^+$). The ion suppression effect of formic acid is reduced when lowered its concentration in the mobile phase.

2.3.6 Characterisation of the unknown lipid components of unconditioned medium

Once the final settings of the method were established, it was applied to characterise the components of the UM. Table 2-3 provides the composition of each of the known ingredients that constitute the UM; which are mainly amino acids and vitamins. Notice, however, that the KnockOut™ SR (Price et al., (1998)) contains AlbuMAX I (a lipid-rich bovine serum albumin) whose exact chemical composition is still unclear.

Analysis of AlbuMAX I by means of thin layer chromatography (Frankland et al., 2007) and HPLC (Garcia-Gonzalo and Izpisua Belmonte, 2008) identified different classes of lipids (Table 2-5), but as far as the thesis author is aware, no LC-MS analysis has been done to characterise more specifically the components of AlbuMAX I.

Table 2-5. HPLC analysis reveals the type of lipids present in AlbuMAX (Garcia-Gonzalo and Izpisua Belmonte, 2008)

Lipid species	mg/ml in 1% AlbuMAX
Free fatty acids (FFAs)	35.29
Lysophosphatidylcholine (LPC)	11.30
Triacylglycerides (TAGs)	9.79
Phosphatidylcholine (PC)	5.29
Phosphatidic acid (PA)	2.07
Cholesterol (CH)	0.88
Sphingomyelin (SM)	0.80

Herein, the final method demonstrates its potential to separate, identify, and ultimately, characterise the unknown components of UM. Figure 2-8 shows typical base peak chromatograms of UM and KnockOut™ SR (15% v/v) in negative electrospray ionisation mode. It is observed that the lipidic part –compounds eluting after minute 6, 50% organic– of UM is due to AlbuMAX I present in KOSR. This area of the chromatogram contains peaks which form the fraction of UM not listed in Table 2-3 and in this section these unknown peaks are identified and characterised with a putative identity.

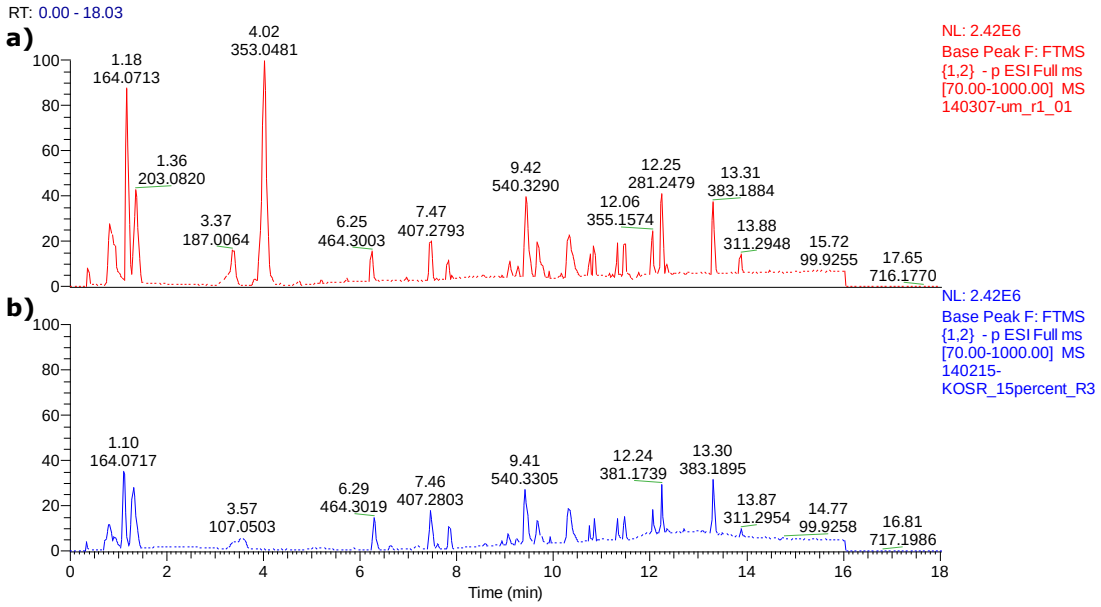

Figure 2-8 Typical base peak chromatograms of a) unconditioned medium and b) KOSR at 15% v/v. Albumax I is responsible for the lipidic part of UM.

To illustrate the identification process used, the ion at *m/z* 329.2487 ($[M-H]^-$) is taken as an example. First, the EIC of the ion was generated to confirm that it was derived from an authentic peak and the mass spectrum scrutinised to discern amongst possible adducts. Second, the exact mass was searched against the databases of HMDB, Lipid Maps and METLIN with a pre-specified mass tolerance (0.5 mDa). Assignment of the possible metabolite was based on isotope peak patterns, use of the nitrogen rule, charge state, retention time and biological relevance. In this case, docosapentaenoic acid was found to be the most likely identification, though accurate mass alone was not considered sufficient to confirm the identity. To further assist in identification, a mass fragmentation experiment was conducted for the quasi-molecular ion and the MS/MS spectrum was compared with that of the standard registered in the databases (Figure 2-9). Putative identity confirmation by means of MS/MS increases the level of reliability but it is not definitive until pure authentic standards are injected along with the sample and compared their retention times and MS/MS spectra (Gika et al., 2014). Table 2-6 summarises the compounds that were detected with this methodology. It is worth mentioning that metabolite assignments in this table remain tentative as no authentic standards were analysed.

According to the Chemical Analysis Working Group, a member of the Metabolomics Standard Initiative, the identity of the compounds shown in Table 2-6 corresponds to levels 2 and 4. Level 2 for those compounds which were assigned a putative identity and their MS/MS spectra matched those registered in the spectral libraries. And level 4 for those compounds which remain unidentified (unknowns) to which it was not possible to assign a putative identity but can still be differentiated and quantified based upon spectral data (Sumner et al., 2007a). In accordance with the proposed minimum reporting standards suggested by the Chemical Analysis Working Group, the MS/MS spectra of the level 2 compounds listed in Table 2-6 are shown in Appendix A.

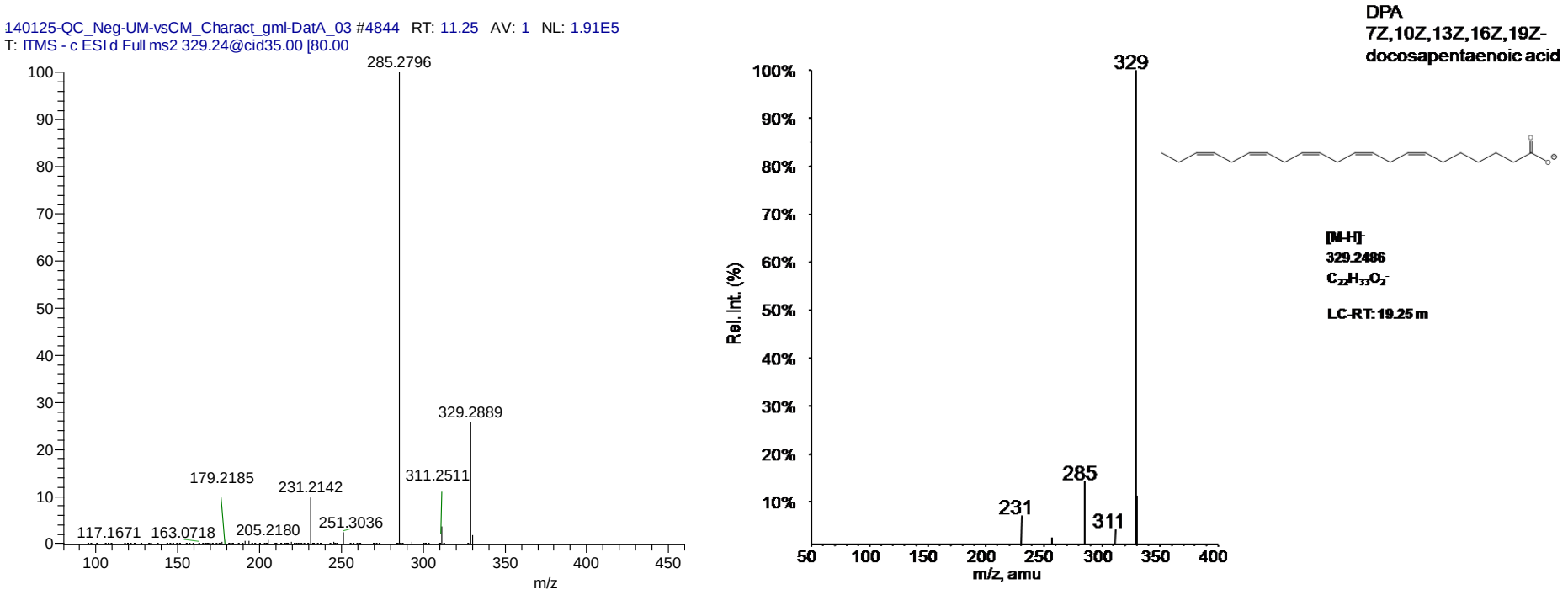

Figure 2-9 MS/MS spectrum comparison of ion *m/z* 329 in a) sample and b) standard registered in Lipid Maps database. Fragment ions in the sample (*m/z* 311, *m/z* 285 and *m/z* 231) match those present in the standard. MS/MS spectral matching increases the level of confidence in the confirmation of the putative identity of the ion at *m/z* 329.2487 (docosapentaenoic acid).

Table 2-6. Characterisation of UM by retention time, experimental monoisotopic mass and database accession numbers.

PUTATIVE IDENTITY	RT, min	$[M-H]^-$	$[M+H]^+$	Δ ppm	HMDB ID	Lipid Maps ID	METLIN ID
L-Histidine	0.80	154.0617		3.2	HMDB00177		21
L-Lysine	0.80	145.0978		2.8	HMDB00182		25
Glycine	0.83	74.0243		5.4	HMDB00123		20
L-Serine	0.83	104.0353		0.0	HMDB00187		30
L-Alanyl-L-glutamine	0.83	216.0983		3.2	HMDB28685		85601
Glucose	0.84		203.0527	2.5	HMDB00122		133
Choline chloride	0.87		104.1078	-2.9	HMDB00097		56
L-Threonine	0.89	118.0506		3.4	HMDB00167		32
Pyruvate	0.89	87.0085		3.4	HMDB00243		117
L-Arginine	0.93		175.1182	4.0	HMDB00517		13
L-Glutamine	0.93		147.0758	4.1	HMDB00641		18
L-Asparagine	0.95		133.0603	3.8	HMDB00168		14
L-Proline	0.95		116.0706	0.0	HMDB00162		29
Thiamine	0.95		265.1105	1.9	HMDB00235		229
L-Hydroxyproline	0.98		132.0649	4.5	HMDB00725		58354
L-Valine	0.98		118.0858	4.2	HMDB00883		35
L-Aspartic acid	1.06		134.0442	4.5	HMDB00191		15
L-Cystine	1.06		241.0300	4.6	HMDB00192		17
L-Glutamic acid	1.06		148.0598	4.1	HMDB00148		19
L-Methionine	1.17		150.0576	4.7	HMDB00696		26
L-Phenylalanine	1.17		166.0855	4.8	HMDB00159		28
Hypoxanthine	1.17		137.0452	4.4	HMDB00157		83
L-Tyrosine	1.18	180.0661		2.8	HMDB00158		34
Thymidine	1.18	241.0822		3.3	HMDB00273		3375
L-Alanine	1.19		90.0548	2.2	HMDB00161		11

PUTATIVE IDENTITY	RT, min	$[M-H]^-$	$[M+H]^+$	Δ ppm	HMDB ID	Lipid Maps ID	METLIN ID
L-Leucine/L-Isoleucine	1.19		132.1013	4.5	HMDB00687		24
Niacinamide	1.19		123.0547	4.9	HMDB01406		1497
Pyridoxine	1.19		170.0804	4.7	HMDB00239		2202
D-Calcium pantothenate	1.22		220.1169	4.5	HMDB00210		241
Folic acid	1.31	440.1314		2.3	HMDB00121		246
L-Tryptophan	1.37	203.0820		3.0	HMDB00929		33
Vitamin B12	1.70		678.2894[a]	2.2	HMDB02274		245
Unknown	1.78		267.0424				
Riboflavin	2.67		377.1437	5.0	HMDB00244		233
Unknown	2.80	277.0175					
4-Sulfobenzyl alcohol	3.54	187.0065		2.7			66489
Unknown	4.00	371.0597					
Biotin	4.03		245.0952	0.8	HMDB00030		243
Phenol red	4.24	353.0491	355.0632	-0.6			69460
Unknown	4.57	351.0333	353.0474				
Unknown	4.79	473.1453					
Unknown	4.92	213.0553					
Unknown	5.28	377.0702					
Taurocholic acid or possible isomer	5.85	514.2844	516.2987[b]	0.0	HMDB00036		
Unknown	5.93	462.2865					
Unknown	6.39	631.3494	633.3633				
Glycocholic acid or possible isomer	6.44	464.3021	466.3163[b]	-0.9	HMDB00138		
Unknown	6.50	509.2394					
Unknown	6.63	633.3650					
Unknown	6.74	243.0695					

PUTATIVE IDENTITY	RT, min	$[M-H]^-$	$[M+H]^+$	Δ ppm	HMDB ID	Lipid Maps ID	METLIN ID
3-Oxocholic acid or possible isomer	6.82	405.2648	389.2685[c]	-0.5	HMDB00502		
Taurodeoxycholic acid or possible isomer	6.96	498.2898	500.3038	-0.6	HMDB00896		
Unknown	7.06		601.2656				
Lysophosphatidylserine (20:1(11Z)/0:0)	7.15	550.3152	552.3292	-0.4		LMGP03050020	
Unknown	7.18	429.0801	431.0947				
Unknown	7.21	312.1816					
Unknown	7.26	433.2809					
C17 Sphinganine	7.52		288.2893	1.4		LMSP01040003	41558
Cholic acid	7.64	407.2805	391.2842[c]	-0.5	HMDB00619		206
Unknown	7.89	291.0698					
Deoxycholic acid glycine conjugate or possible isomer	8.02	448.3071	450.3214	-0.7	HMDB00631		
Unknown	8.18	293.1760					
Lithocholyltaurine	8.43	482.2945		0.0	HMDB00722	LMST05040003	
LysoPC(14:0)	8.65	452.2784*	468.3082	0.4	HMDB10379		
LysoPE(18:3(9Z,12Z,15Z)/0:0) or possible isomer	8.67	474.2626	476.2768	0.0	HMDB11509		
LysoPC(18:3(9Z,12Z,15Z))	8.73	502.2941*	518.3239	0.4	HMDB10388		
LysoPC(20:5(5Z,8Z,11Z,14Z,17Z))	8.76	526.2939*	542.3241	0.0	HMDB10397	LMGP01050050	
LysoPC(O-14:1(1E)/0:0) or possible isomer	8.84	436.2833*	452.3131	0.9		LMGP01070001	
LysoPC(16:1(9Z))	8.89	478.2939*	494.3238	0.6	HMDB10383		
LysoPC(15:0/0:0)	9.05	466.2938*	482.3237	0.8	HMDB10381	LMGP01050016	
LysoPC(20:4(5Z,8Z,11Z,14Z)) or possible isomer	9.05	528.3098*	544.3392	0.9	HMDB10395	LMGP01050048	
Deoxycholic acid	9.11	391.2854	375.2894[c]	0.0	HMDB00626		265
LysoPE(18:2(9Z,12Z)/0:0) or possible isomer	9.14	476.2785	478.2928	-0.6	HMDB11507	LMGP02050011	
LysoPE(20:4(5Z,8Z,11Z,14Z)/0:0) or possible isomer	9.14	500.2788	502.2927	-1.2	HMDB11517	LMGP02050009	
LysoPC(18:2(9Z,12Z)) or possible isomer	9.19	504.3101*	520.3397	0.0	HMDB10386	LMGP01050035	

PUTATIVE IDENTITY	RT, min	$[M-H]^-$	$[M+H]^+$	Δ ppm	HMDB ID	Lipid Maps ID	METLIN ID
LysoPC(P-15:0/0:0)	9.24	450.2993*	466.3289	0.6		LMGP01070003	
LysoPE(22:5(4Z,7Z,10Z,13Z,16Z)/0:0) or possible isomer	9.35	526.2939	528.3081	0.0	HMDB11524		
LysoPC(22:5(7Z,10Z,13Z,16Z,19Z)) or possible isomer	9.41	554.3252*	570.3549	0.9	HMDB10403		
LysoPE(16:0/0:0)	9.46	452.2784	454.2926	-0.4	HMDB11503	LMGP02050002	
LysoPC(16:0/0:0)	9.54	480.3094*	496.3393	0.8	HMDB10382	LMGP01050018	
LysoPC(20:3(8Z,11Z,14Z)) or possible isomer	9.57	530.3251*	546.3550	0.2	HMDB10394	LMGP01050133	
LysoPE(18:1(9Z)/0:0) or possible isomer	9.71	478.2939	480.3085	0.0	HMDB11506	LMGP02050004	
(4E,8E,10E-d18:3)sphingosine	9.75		296.2582	0.7		LMSP01080013	53913
LysoPE(P-16:0e/0:0)	9.76	436.2833	438.2977	0.0	HMDB11152		
LysoPC(18:1(9Z)/0:0) or possible isomer	9.79	506.3252*	522.3553	0.2	HMDB02815	LMGP01050032	
LysoPC(P-16:0/0:0) or possible isomer	9.87	464.3149*	480.3447	0.2	HMDB10407	LMGP01070006	
3R-hydroxypalmitic acid	9.90	271.2278		0.2	HMDB10734	LMFA01050366	
Octadecanedioic acid	9.95	313.2386	315.2527	-0.6	HMDB00782		
Unknown	9.99		440.4093				
LysoPC(17:0)	10.01	494.3253*	510.3550	0.8	HMDB12108	LMGP01050024	
Unknown	10.06	337.2385					
Halaminol A	10.35		228.2319	1.3		LMSP01080034	
LysoPE(18:0/0:0)	10.36	480.3094	482.3237	0.8	HMDB11130	LMGP02050001	
Hydroxy stearic acid or possible isomer	10.36	299.2591		0.3		LMFA02000120	35432
LysoPC(18:0) or possible isomer	10.50	508.3409*	524.3705	1.0	HMDB10384	LMGP01050026	
Palmitoleamide	10.54		254.2475	1.2		LMFA08010010	97431
2-hydroxy-nonadecanoic acid or possible isomer	10.70	313.2750		-0.6		LMFA01050071	
Linoleamide	10.81		280.2632	1.1		LMFA08010008	43435
LysoPC(20:0)	10.82	536.3726*	552.4021	0.4	HMDB10390	LMGP01050045	

PUTATIVE IDENTITY	RT, min	$[M-H]^-$	$[M+H]^+$	Δ ppm	HMDB ID	Lipid Maps ID	METLIN ID
Eicosapentaenoic acid	10.85	301.2174		-0.3	HMDB01999		
Alpha-Linolenic acid	10.96	277.2172		0.4	HMDB01388	LMFA01030152	192
Myristic acid	11.12	227.2012		1.8	HMDB00806	LMFA01010014	196
Docosahexaenoic acid	11.20	327.2328		0.3	HMDB02183	LMFA01030185	
Palmitamide	11.24		256.2633	0.8	HMDB12273	LMFA08010009	62905
Palmitoleic acid or possible isomer	11.31	253.2173		0.0	HMDB03229	LMFA01030056	188
Arachidonic acid	11.39	303.2331		-0.7	HMDB01043	LMFA01030001	
Pentadecanoic acid or possible isomer	11.47	241.2171		0.8	HMDB00826	LMFA01010015	4205
Oleamide	11.49		282.2789	0.7	HMDB02117	LMFA08010004	4115
Docosapentaenoic acid	11.53	329.2487		-0.3	HMDB06528	LMFA04000044	
Linoleic acid	11.56	279.2331		-0.7	HMDB00673	LMFA01030120	
(Z)-9-Heptadecenoic acid or possible isomer	11.83	267.2331		-0.7	HMDB31046	LMFA01030060	
Dihomo-γ-Linolenic Acid or possibly Mead acid	11.85	305.2485		0.3	HMDB02925	LMFA01030158	
Palmitic acid	12.15	255.2329	301.2112[d]	0.0	HMDB00220	LMFA01010001	
Oleic acid	12.32	281.2485	327.2266[d]	0.4	HMDB00207	LMFA01030002	
Stearamide	12.38		284.2943	1.8	HMDB34146	LMFA08010003	34494
Oleoyl Ethyl Amide	12.55		310.3100	1.3			44905
Heptadecanoic acid	12.75	269.2485		0.4	HMDB02259	LMFA01010017	4206
Stearic acid	13.49	283.2642	329.2422[d]	0.0	HMDB00827	LMFA01010018	
13Z-Docosenamide	14.07		338.3412	1.5			64926
Arachidic acid	14.08	311.2955		0.0	HMDB02212	LMFA01010020	401

* Loss of one methyl group from the choline moiety, $[M-CH_3-H]^-$

[a] $[M+2H]^{2+}$

[b] Preferentially observed as $[M-3H_2O+H]^+$

[c] $[M-H_2O+H]^+$

[d] $[M+2Na-H]^+$

RT, retention time

LysoPC, lysophosphatidylcholine

LysoPE, lysophosphatidylethanolamine

Δ ppm = mass error in parts per million

In general, UM lipids were better ionised in negative ESI mode. Depending on the class of lipids, some of them were observed in both polarities (e.g. phosphatidylcholines and phosphatidylethanolamines); others preferentially in negative mode (i.e. free fatty acids); while few species were only detected in positive mode (i.e. fatty acid amides).

Although most of the components were identified, some metabolites still remained unknown simply because they were not found in any of the databases or the candidates retrieved were biologically irrelevant. Also, compounds with multiple double bonds resulted in a less precise identification due to the diverse conformations that the molecule can adopt (isomers); nonetheless, it was possible to specify the type of compound and a molecular structure.

2.4 Conclusions

The present LC-MS method takes advantage of technological advances in chromatography and mass spectrometry. While UPLC increases peak capacity and enhances sensitivity, high resolution MS allows a more precise peak annotation. These analytical tools are of paramount importance in untargeted metabolomics for the discovery and identification of metabolites of interest in the biological systems under investigation.

Enhanced metabolome coverage was achieved by the optimisation of the sample preparation method, type of chromatography and the use of heated electrospray ionisation in both positive and negative modes. In the end, methanol-precipitated samples and reversed-phase LC provided the most sensitive and reproducible results.

As with any other LC-ESI-MS approach only ionisable molecules were observed. Nevertheless, the current method was capable of the detection and relative quantification of a wide range of small molecules present in the unconditioned medium. Additionally it allowed a more specific identification (albeit tentative) of the lipid classes contained in AlbuMAX I. This has made considerable advances compared with previous

methodologies (Frankland et al., 2007, Garcia-Gonzalo and Izpisua Belmonte, 2008), and contributed to an improved chemical definition of a widely used culture medium.

In summary, this is the first time that a method has been developed for the comprehensive characterisation of the small molecule inventory of human embryonic stem cell culture media. The novel method developed in this chapter has many potential applications in the field of metabolomics and stem cell biology. As shown in subsequent chapters of this thesis, the methodology has enabled the metabolomics analysis of not only the traditionally culture medium (mouse embryonic fibroblast-conditioned medium), but also of more defined media such as StemPro (Wang et al., 2007). Other applications also include metabolomics footprinting (analysis of extracellular metabolites) of different culture systems.

CHAPTER 3

Metabolite profiling of mouse embryonic fibroblast-conditioned medium for identification of potential low-molecular weight factors involved in hESC pluripotency

3 Metabolite profiling of mouse embryonic fibroblast-conditioned medium for identification of potential low-molecular weight factors involved in the maintenance of hESC

3.1 Introduction

As mentioned in chapter 1, progress in the definition of the human embryonic stem cell (hESC) culture system has allowed the cultivation of hESC in the absence of the initially required mouse embryonic fibroblasts (MEFs) feeder layers. However, under feeder-free conditions, using either Matrigel (Xu et al., 2001) or a synthetic polymer (Villa-Diaz et al., 2010) as substrate, hESC still require the use of mouse embryonic fibroblast-conditioned medium (MEF-CM) to retain their pluripotency; otherwise, in the presence of the unconditioned medium, hESC start to differentiate (Xu et al., 2001) (Figure 3-1).

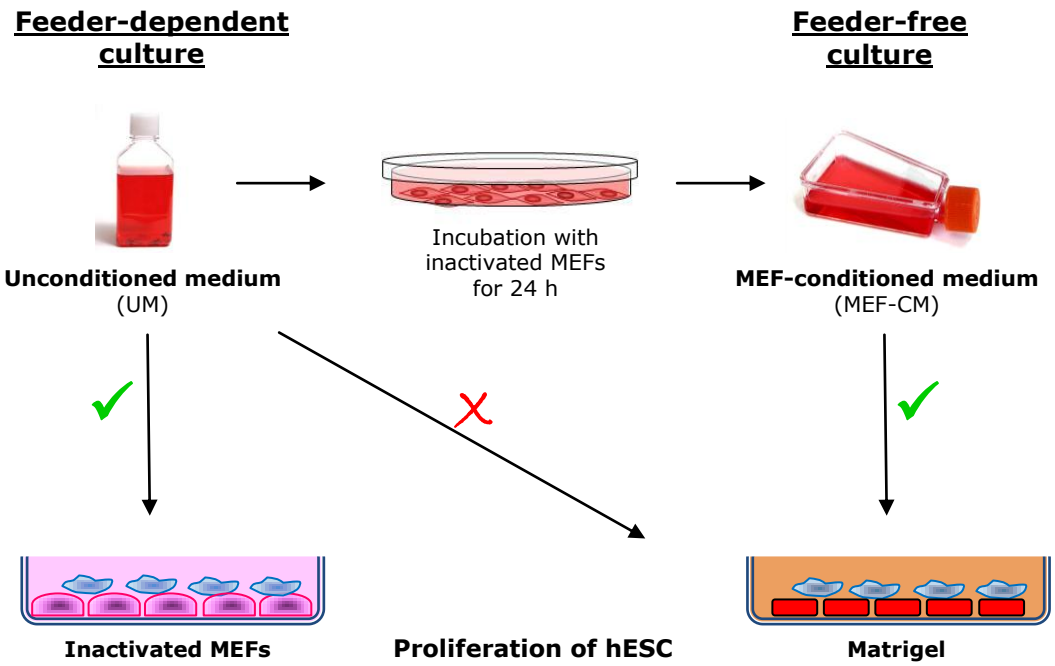

Figure 3-1 Dependence on the use of mouse embryonic fibroblasts (MEFs) either as feeder cells or as a means to produce conditioned medium (CM) for the successful proliferation of hESC. Under feeder-free conditions unconditioned medium is unable to maintain hESC in an undifferentiated state.

The strong dependence on the use of MEFs, either as feeder cells or as a means to produce CM, suggests that MEFs secret a number of factors that are critical for the maintenance of hESC in an undifferentiated state. Therefore, the study of the factors released by the feeders into the medium during the conditioning process would identify potential compounds responsible for maintaining hESC pluripotency which could subsequently be used in the formulation of more defined culture systems that ultimately will place hESC technology a step forward in realising potential clinical applications.

3.1.1 Investigation of the factors released into the medium conditioned by feeders

Over the last 12 years, most of the work done in the investigation of the factors secreted by feeders (mouse or human fibroblasts) has focused on the analysis of the protein components of the medium (Lim and Bodnar, 2002, Xie et al., 2004, Prowse et al., 2005, Prowse et al., 2007, Bendall et al., 2009, Talbot et al., 2012). Although many proteins have been detected, only a small fraction of them is known to be secreted or related with hESC growth, differentiation and pluripotency (Lim and Bodnar, 2002, Prowse et al., 2007). The rest of proteins identified were of intracellular origin (endoplasmic reticulum, nucleus and cytoplasm) (Lim and Bodnar, 2002, Bendall et al., 2009). Furthermore, the CM used for identification of the protein factors is typically obtained under conditions different from those normally used for its collection or hESC culture. For instance, the unconditioned medium incubated with MEFs is serum- or serum replacement-free (to ease identification of the proteins released by MEFs) and is required to be collected after 16 – 18 hours of incubation, instead of the usual 24 hour-conditioning time, as the lack of serum may introduce stress to the MEFs (Lim and Bodnar, 2002, Chin et al., 2007). Under these conditions cellular physiology might have been altered and as a consequence the measured protein profiles may not be representative of normal culture conditions; nonetheless, these experiments have provided a valuable insight into the secretome of MEFs.

With regards to the profiling of the small-molecule (non-protein) components of the CM, only one report has been published to date. In this report, the authors employed a nuclear magnetic resonance (NMR)-based metabolomics approach. They compared the metabolic profile of TeSR1™ medium (Ludwig et al., 2006b) before and after incubation with human foreskin fibroblasts (HFFs) (MacIntyre et al., 2011). The metabolites identified as secreted by the fibroblasts were lactate, pyruvate, formate and alanine which were found at higher concentrations in the medium conditioned by HFFs (MacIntyre et al., 2011). However, the effects of these metabolites on hESC proliferation or pluripotency remain unknown. Although this NMR method offered a rapid way of analysing CM samples, as it required minimal sample preparation, the compounds detected were mainly those present at higher concentrations in the medium. This highlights the need for a more sensitive method (like mass spectrometry) for the detection of more bioactive compounds secreted by feeders that may be found at lower concentrations in the CM.

3.1.2 Murine or human feeders?

Feeder cells from human origin are also able to support the growth of hESC (Richards et al., 2002, Amit et al., 2003, Hovatta et al., 2003); nonetheless, amongst feeder layers, mouse embryonic fibroblasts surprisingly proved to be more efficient in maintaining undifferentiated hESC than human feeders (Eiselleova et al., 2008). The capacity of conditioned media to support hESC growth relies on the ability of the feeders to secrete growth factors. Whereas human feeders secreted higher levels of basic fibroblast growth factor (bFGF), MEFs produced higher levels of Activin A. Although both factors have been shown to play an important role in the maintenance of hESC pluripotency (Vallier et al., 2005), comparison of the percentage of cells expressing pluripotency markers (i.e. stage specific embryonic antigen-3 (SSEA-3)) showed a higher proportion of undifferentiated cells when hESC were grown on MEFs than when human feeders were used (Eiselleova et al., 2008). Consequently, medium conditioned by MEFs offers a better model for the

study of the extracellular factors involved in the regulation of hESC pluripotency.

Metabolites secreted by MEFs feeder layers offer an important unexplored complementary approach for identification of potential low-molecular weight factors involved in the maintenance of hESC. However, at present, there is a lack of metabolomics methods for the identification of bioactive compounds in MEF-CM. In this study, a novel LC-MS-based metabolomics method has been applied to the analysis of the small-molecule components of MEF-CM and represents, to the best of the author's knowledge, the first LC-MS metabolomics study of the factors secreted by MEFs.

3.1.3 Aims and objectives

- Employ the LC-MS metabolomics method described in chapter 2 for the analysis of the metabolic differences between UM and MEF-CM.

- Identify potential small-molecule components in MEF-CM involved in hESC growth and pluripotency.

- Investigate metabolic variability between batches of MEF-CM as well as MEF-CM collected over a time course of ten days.

3.2 Materials and methods

3.2.1 Chemicals

HPLC-grade acetonitrile and methanol were obtained from Fischer Scientific (Loughborough, UK). Deionized water (18.2MΩ) was prepared using an ELGA USF-Maxima water purification system (Marlow, UK). Mass spectrometry-grade formic acid and dimethylsulfoxide (DMSO) were purchased from Sigma-Aldrich (Gillingham, UK) and tissue culture reagents were obtained from Invitrogen. Deuterated arachidonic acid [5, 6, 8, 9, 11, 12, 14, 15-$^{2}H_{8}$] (AA-d8) was purchased from Qmx Laboratories (Essex, UK).

3.2.2 Preparation of AA-d8 stock solutions

Under sterile conditions, stock solutions of AA-d8 were prepared with DMSO at concentrations of 0.032, 3.2 and 32 mM.

3.2.3 Preparation of conditioned media

Conditioned medium (CM) was prepared as described elsewhere (Burridge et al., 2007). Briefly, MEFs (strain CD1, 13.5 days post coitum) were mitotically inactivated with mitomycin C (10 µg/mL, 2.5 h) and seeded at $6x10^{4}$ cells/cm^{2} in T75 flasks. The next day, inactivated MEFs were washed with PBS and incubated with 25 mL of unconditioned medium (UM) for 24 h, at which time CM was collected and stored at –80ºC until analysis. Unconditioned medium composition consisted of DMEM-F12 supplemented with 15% KnockOut Serum Replacement, 100 mM β-mercaptoethanol, 1% non-essential amino acids (NEAA), 2mM GlutaMAX, and 4 ng/mL bFGF. MEF-conditioned media were prepared by Mrs Penny Howick, Mrs Katarzyna Lis-Slimak, Mrs Maria Barbadillo-Munoz and Dr James Smith, Wolfson Centre for Stem Cells, Tissue Engineering & Modelling, Centre for Biomolecular Sciences, University of Nottingham.

3.2.3.1 Time course experiment

For the time course experiment, MEF-CM was collected similarly for 10 consecutive days by adding fresh UM to the same flask of MEFs after each day of CM collection.

3.2.3.2 Isotope labelling flux experiment

25 mL of UM were supplemented with deuterated arachidonic acid at $1.29x10^{-5}$, $1.29x10^{-3}$ and $1.29x10^{-2}$ mM by addition of 10 µL of each AA-d8 stock solution. As a control, 10 µL of DMSO were added to 25 mL of UM too. All the media were incubated with or without MEFs and collected after 24 h.

3.2.4 Sample preparation

Unconditioned and MEF-conditioned media samples were prepared by solvent precipitation as described in chapter 2. Briefly, 250 µL of sample were mixed with 750 µL of cold MeOH (kept at -20^0C), vortexed for 1 min to precipitate the proteins and stored at -20^0C for 20 min. After the cold storage period, samples were vortexed again for 15 s and centrifuged at 17000 rpm for 10 min at 4^0C. The supernatants were transferred into LC vials for analysis.

The number of prepared samples and analytical replicates are detailed in section 3.2.5. As part of the system conditioning and quality control process, a pooled "quality control" (QC) sample was prepared by mixing equal volumes of the samples involved in each experiment (Gika et al., 2007, Want et al., 2010). These QC samples were also prepared in exactly the same manner as the test samples.

3.2.5 Sample analysis

Ten QC samples were injected at the beginning of each experiment to condition the LC system and then intermittently once every 6 test samples to assess the stability of the analysis. All test samples were injected in a randomised order to eliminate any bias.

To avoid problems related with long analysis times (retention time drifts, built-up contamination, loss of sensitivity, etc) (Zelena et al., 2009), the number of samples to prepare and number of injections were adjusted in order to keep analysis times to a minimum but still with enough analytical replicates to enable good statistics at the end of the experiment. For this, the number of sample conditions to be analysed were considered allowing at least three analytical replicates for each time each sample condition was prepared in order not to exceed 25 hours of LC-MS analysis.

3.2.5.1 Unconditioned medium versus MEF-conditioned medium experiment

For the comparison of UM vs MEF-CM, samples were prepared six times for each type of medium and injected in triplicate into the LC-MS system. To assess the reproducibility and robustness of the method (inter-day variability), the whole experiment was repeated three times with the same samples but on different days.

3.2.5.2 Analysis of CM obtained from different batches of MEFs

Samples of UM and MEF-CM batches 107, 115, 116, 117, 118, 120, 121 and 122 were prepared three times each and injected in triplicates into the column.

3.2.5.3 Time course experiment

UM and MEF-CM samples from day 1 to day 10 (CM-day1 to CM-day10) were prepared two times each and injected in triplicates into the LC-MS system.

3.2.6 Liquid chromatography conditions

The chromatographic separations were performed on an Accela U-HPLC system (Thermo Fisher Scientific, USA) using a ZORBAX Eclipse Plus C18 column 1.8 µm (i.d. 2.1x100 mm) attached to a guard column (2.1x5

mm) of the same chemistry and particle size (Agilent Technologies, Cheadle, UK). The oven temperature was maintained at 40^0C while the autosampler temperature set at 4^0C. The mobile phase consisted of solvent A: 0.01% formic acid in water and solvent B: 0.01% formic acid in acetonitrile. A step gradient programme was used starting with 10% B, 0-0.3 min; 50% B, 5-6 min; 70% B, 7-8 min; 90% B, 9-10 min; 98% B, 11-16 min; and coming back to the re-equilibration mobile phase composition of 10% B, 16.5-18 min. The flow rate was kept at 300 µL/min with the exception of minute 9 to 11 which was increased to 400 µL/min. Before each sample injection of 7 µL in no-waste mode, the needle was washed with 400 µL of 75% methanol.

3.2.7 Mass spectrometry instrumentation

The LC system was coupled online to an Exactive Orbitrap mass spectrometer (Thermo Fischer Scientific, USA) equipped with a heated electrospray interface (HESI-II) operating in positive and negative ion mode. The working parameters were: spray voltage, 3 kV; heated capillary temperature, 350^0C; heater temperature, 300^0C; sheath, auxiliary and sweep gas flow rates were 35, 10 and 5 arbitrary units, respectively. Data were acquired in full scan mode from *m/z* 70 – 1000 at 50,000 FWHM (2 Hz) resolving power.

To provide a higher degree of confidence for metabolite identification data dependent MS/MS experiments were carried out on an LTQ Velos mass spectrometer (Thermo Fischer Scientific, USA) as detailed in section 2.2.7. The collision energy used was adjustable from 35 to 45 eV.

3.2.8 Data processing and analysis

The LC-MS raw data files were imported to SIEVE software version 2.0 (Thermo Fisher Scientific, USA) and analysed in an unbiased manner, using the non-differential single class analysis option, in order not to specify classes or groups. The positive and negative electrospray ionisation data were analysed separately with the following settings: ion intensity threshold, 10000; peak width, 10 ppm; frame time width, 2.50

min and normalised to the total ion current. SIEVE analysis resulted in a data matrix containing the detected peaks characterised by their retention time, *m/z* value, and integrated intensity. This data matrix was exported in the form of a spreadsheet (Microsoft Excel) to be further manipulated for multivariate and univariate statistical analyses. For multivariate analysis (MVA), the data were processed with SIMCA version 13.0 (Umetrics AB, Umea, Sweden) to create PCA and OPLS-DA models using unit variance (UV)-scaling. Positive and negative data sets were merged together into one single file for MVA manipulation.

The ions responsible for the class separation were selected by means of the OPLS-DA loadings plots and VIP (Variable Importance to the Projection) plots. The metabolites that increased in one condition and reduced in the other were verified as true peaks using Xcalibur 2.2 software (Thermo Fischer Scientific, USA). After verification, the *m/z* values were searched against web-based databases such as the Human Metabolome Database (www.hmdb.ca) (Wishart et al., 2009), Lipid Maps (www.lipidmaps.org) (Fahy et al., 2007) and METLIN Metabolomics Database (www.metlin.scripps.edu) (Smith et al., 2005). The MS/MS spectra of the ions were also compared with those registered in the aforementioned databases.

For univariate statistics, data were exported to GraphPad Prism version 6.03 (GraphPad Software Inc., California, USA). One-way ANOVA (using Dunnett's *post hoc* test) and *t*-tests with Welch's correction were applied where appropriate. Prior to Student's t-test, D'Agostino-Pearson omnibus normality test was performed. Accounting for multiple comparisons Bonferroni correction was applied (maintaining a type I error probability of 0.05) before considering any statistically significant difference. Data are reported as the mean ± standard deviation (SD).

3.3 Results and discussion

3.3.1 Chromatography and mass spectrometry stability

Typical base peak chromatograms of MEF-CM in positive and negative ion electrospray are shown in Figure 3-2. Compounds previously identified in the UM (described in chapter 2) were also found in MEF-CM samples in addition to new compounds resulting from the MEF conditioning. The different classes of metabolites eluted at different retention time windows which are depicted in Figure 3-2 with capital letters. The elution order of typical small molecules detected in the MEF-CM was as follows: amino acids and vitamins, cholic-acid derivatives, lysophosphatidylcholines and lysophosphatidylethanolamines, fatty-acid amides (detected only in positive mode) and free fatty acids. Representative compounds for each class of metabolites are displayed in Table 3-1. In the analysis, 1178 and 846 individual ions were detected in positive and negative electrospray ion (ESI) modes, respectively.

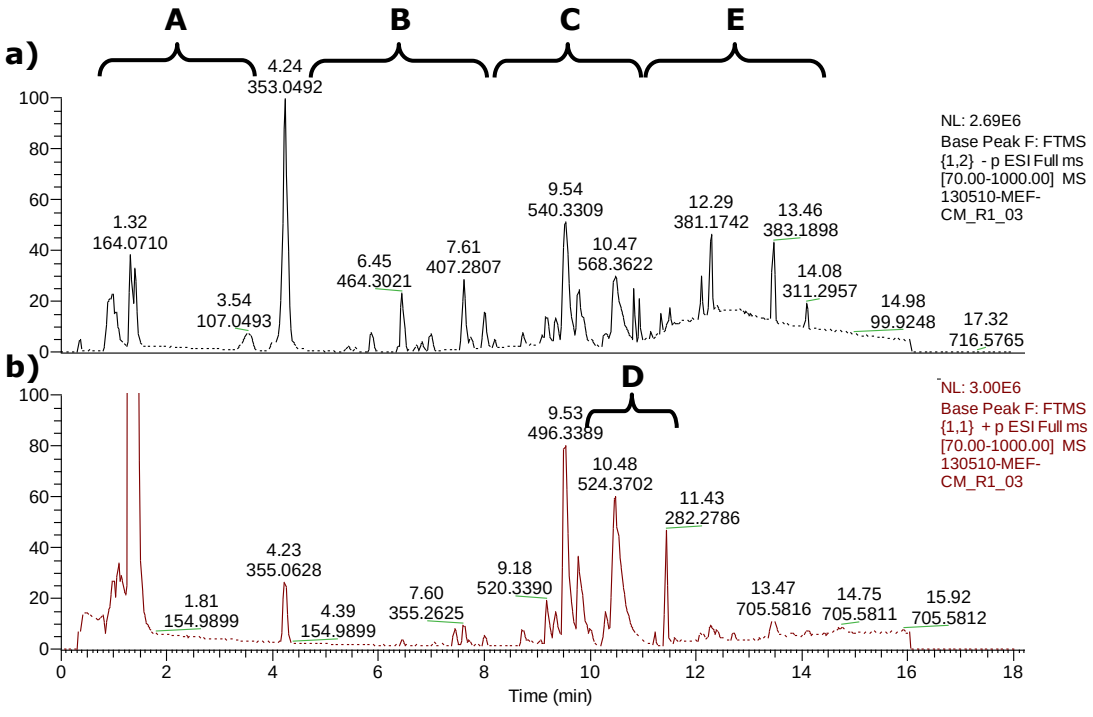

Figure 3-2 Base peak chromatograms of MEF-CM in a) negative and b) positive ionisation mode. The elution order of identified compounds was: A, amino acids and vitamins; B, cholic-acid derivatives; C, lysophosphatidylcholines and lysophosphatidylethanolamines; D, fatty-acid amides; and E, free fatty acids.

Table 3-1. Representative compounds for each class of metabolites found in MEF-CM. The capital letters represent the elution order of the metabolites depicted in Figure 3-2. From polar to non-polar compounds, A-E.

Polarity	Class	Subclass name	Examples
High	A	Amino acids	L-glutamine L-phenylalanine
		Vitamins	Niacinamide Folic acid
Intermediate	B	Cholic-acid derivatives	Taurocholic acid Glycocholic acid 3-Oxocholic acid
	C	Lysophosphatidyl-ethanolamines (LPE)	LPE(16:0) LPE(18:2(9Z,12Z))
		Lysophosphatidyl-cholines (LPC)	LPC (18:3(9Z,12Z,15Z)) LPC(20:4(5Z,8Z,11Z,14Z))
Low	D	Fatty-acid amides	Palmitoleamide Linoleamide Oleamide
	E	Polyunsaturated free fatty acids	Arachidonic acid Dihomo-gamma-linolenic acid
		Saturated free fatty acids	Palmitic acid Stearic acid

Data quality in metabolomics experiments is of paramount importance since these experiments will provide biological insights of the systems under study. Therefore, the use of quality control (QC) samples (Gika et al., 2007) was adopted as a way of assessing the quality of the data obtained from the analysis of UM and MEF-CM samples. A small subset of peaks (6 in +ESI and 6 in –ESI), covering a range of retention times and signal intensities, were selected to monitor their retention time (RT) and intensity variability in the QCs injected throughout the LC-MS analysis, discarding the first 10 QCs used for equilibration. Table 3-2 reports the percentage of coefficient of variation (%CV) of RT and intensity of the selected peaks. The acceptance criteria suggested by the Food and Drug Administration (FDA) for bioanalysis and biomarker validation are <2% variation for RT and <30% variation for signal intensity (FDA, 2013). Good mass accuracy for these ions was also observed with variability

lower than 5 mDa. The observed repeatability in RT and intensity of the QC samples indicated satisfactory analytical stability, well within the FDA acceptance criteria and demonstrated that the metabolomics analysis of the samples was valid.

Table 3-2. Variation in retention time and intensity for selected peaks in positive and negative ESI mode.

Negative ESI mode				
	Retention time, min		Intensity (arbitrary units)	
Peak (*m/z*)	mean ± SD	%CV	mean ± SD	%CV
164.0710	1.33 ± 0.01	**1.06**	5572088 ± 263062	**4.72**
277.0175	4.43 ± 0.02	**0.35**	96995 ± 5248	**5.41**
514.2845	5.88 ± 0.01	**0.25**	1022065 ± 14068	**1.38**
502.2944	8.75 ± 0.02	**0.18**	980682 ± 23755	**2.42**
327.2331	11.13 ± 0.01	**0.12**	660063 ± 16378	**2.48**
311.2957	14.03 ± 0.02	**0.16**	2834680 ± 43181	**1.52**

Positive ESI mode				
	Retention time, min		Intensity (arbitrary units)	
Peak (*m/z*)	mean ± SD	%CV	mean ± SD	%CV
146.0597	1.41 ± 0.01	**0.96**	22666244 ± 1303675	**5.75**
377.1450	2.45 ± 0.04	**1.68**	188756 ± 16912	**8.96**
218.2111	4.65 ± 0.01	**0.27**	78636 ± 2538	**3.23**
412.2841	6.46 ± 0.00	**0.00**	630859 ± 15216	**2.41**
522.3547	9.79 ± 0.01	**0.11**	11016529 ± 183850	**1.67**
284.2943	12.3 ± 0.01	**0.11**	750636 ± 8974	**1.20**

3.3.2 Multivariate analysis

Datasets obtained from positive and negative ion electrospray were combined to perform multivariate analysis. Initially, PCA was applied to generate an overview of the data as well as for detecting groups, outliers and/or trends within the samples. Figure 3-3 shows the PCA scores plot of UM and MEF-CM samples using unit variance (UV)-scaling. For clarity purposes, only one of the three experimental replicates is shown here, however, similar results were obtained on the other two days that the experiment was repeated. PCA with Pareto-scaled data was also

evaluated. However, stronger outliers in the principal component 2 were observed hence it was decided not to be used any further. The reason of the stronger outliers with Pareto scaling will be explain later with Figure 3-4a and b.

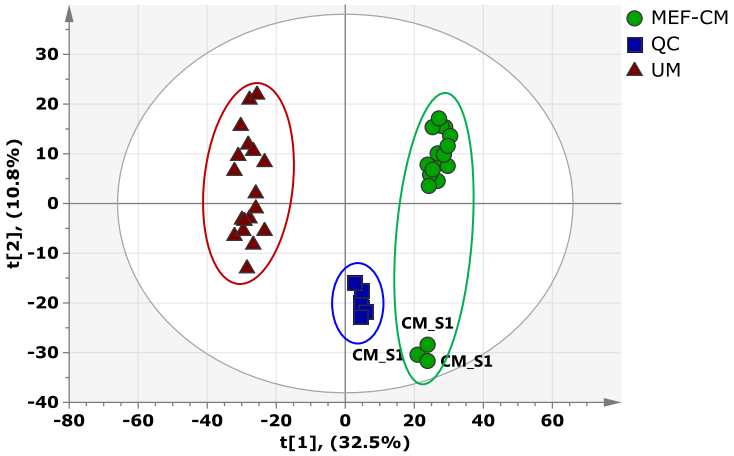

Figure 3-3 PCA scores plot of unconditioned medium (triangles) and mouse embryonic fibroblasts-conditioned medium (circles) samples. The separation between the two types of culture media indicates metabolic differences. Stability of the system is indicated by the tight cluster of QC samples (squares). CM_S1, analytical replicates of one of the prepared MEF-CM samples.

Whereas principal component 1 (t[1]) in Figure 3-3 showed a clear separation between unconditioned and MEF-conditioned media, indicating metabolic differences between the samples, principal component 2 (t[2]) displayed the analytical variability. It is observed that MEF-CM samples (circles) present better clustering on the right-hand side of the plot although three replicates appear apart from the group. As the deviated injections were all the replicates of one of the six MEF-CM prepared samples, the atypical behaviour was attributed to a bad manipulation during sample preparation; however, since they are still within the 95% confidence interval (indicated by the Hotelling's T2 ellipse) they were kept in the model. On the other hand, UM samples (triangles) were more scattered in t[2]. Nonetheless, the analytical run demonstrated sufficient stability as described previously and also indicated here by the tight cluster of QC samples (squares) injected throughout the analysis. 52.4% of the data variation was explained by the first three principal components of the PCA model.

When PCA with Pareto-scaled data was performed, stronger outliers in the direction of the principal component 2 were observed (data not shown). Figure 3-4 shows the p[2] loadings plot of the UV- and Pareto-scaled data. Notice that when Pareto scaling is used, the weight of particular variables (those depicted with an open red circle) in the p[2] loadings plot is increased (Figure 3-4b) when compared to the same variables in the UV-scaled data (Figure 3-4a). This signifies that these highlighted variables contribute largely to the scores (some of them outliers) in t[2] of the Pareto-scaled PCA (data not shown). Having examined these variables in more detail, it was noted that the outliers observed with the Pareto-scaled PCA showed lower levels of these variables which made them deviate from the rest of samples and appear outside of the Hotelling's T2 ellipse. As a consequence, for the experiments carried out in this thesis, UV-scaling was preferred as it provided all the variables with an equal opportunity to influence the data analysis.

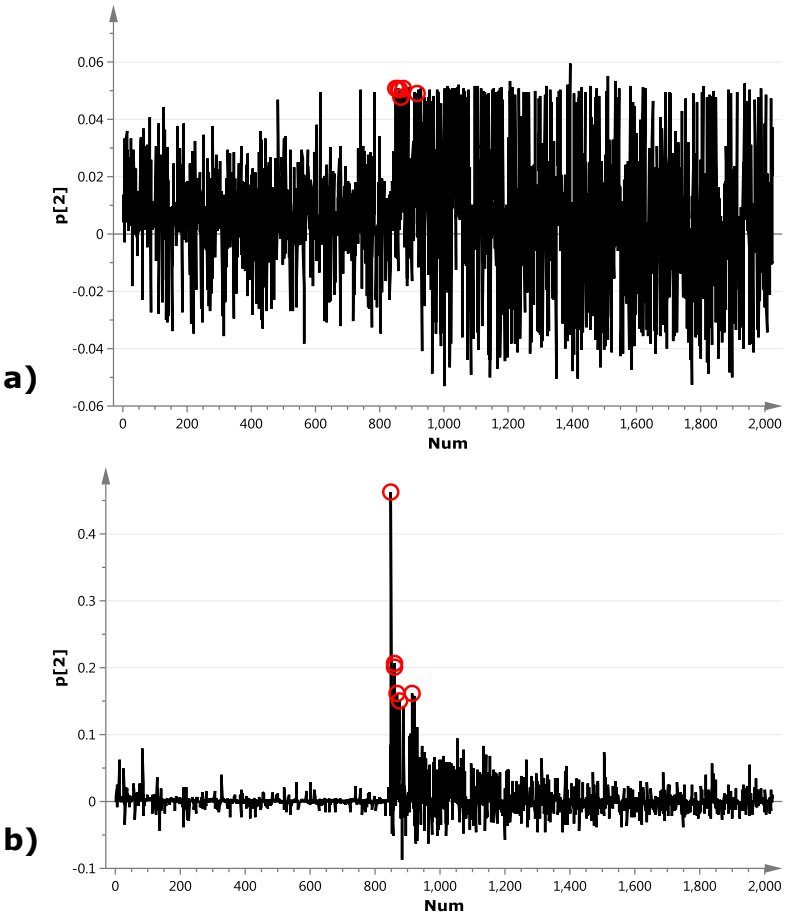

Figure 3-4 p[2] loadings plot of a) UV- and b) Pareto-scaled data. The open red circles highlight the variables that contributed to the observation of outliers when Pareto-scaling was used.

3.3.2.1 OPLS-DA and OPLS-DA model validation

To find out the metabolites that accounted for the difference between UM and MEF-CM, OPLS-DA was applied. Since OPLS-DA is a supervised method that maximises the separation between the groups and minimises within class variation (Bylesjo et al., 2006), it allows the identification of the important metabolites that contribute to the class separation. To build the model, 75% of the samples (n=27) were randomly selected and the 25% left (n=9) was used for model external validation (Figure 3-5). $R^2Y(cum)$ and $Q^2(cum)$ parameters were used for the evaluation of the model. R^2 is a measure of how well the model fits the data while Q^2 indicates how well the model predicts new data. Values above 0.4 are respectively indicative of good model fitting and good predictivity (Westerhuis et al., 2008). In this experiment, a good discriminating model was achieved. $R^2Y(cum)$ and $Q^2(cum)$ values were 0.997 and 0.992, respectively.

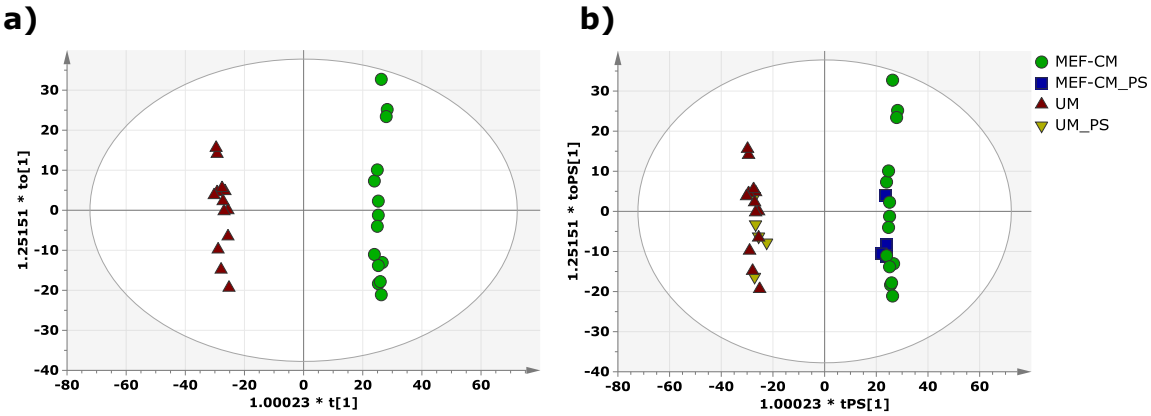

Figure 3-5 a) OPLS-DA model of UM versus MEF-CM. b) T-predicted plot as a result of the OPLS-DA model external validation. ▲ UM, ● MEF-CM, ▼ UM prediction set, and ■ MEF-CM prediction set. Q^2(cum) 0.992, R^2X(cum) 0.467, R^2Y(cum) 0.997.

Classification models like OPLS-DA require validation to assess their predictive ability (Westerhuis et al., 2008); thus, cross-validation and external validation were used to validate the model. Initially, a cross-validation-analysis of variance (CV-ANOVA) test ensured model validity with a resulting *p*-value of $2.56x10^{-33}$. This provided statistical verification that metabolites in MEF-CM were distinct from those found in UM. Additionally, external validation of the OPLS-DA model was

performed with an independent test set which consisted of 5 UM and 4 MEF-CM samples (the 25% of the samples initially excluded). None of these samples had been previously included during the supervised model building, therefore allowed the evaluation of the predictivity of the model. As shown in Figure 3-5b, the OPLS-DA model correctly predicted all the UM- and MEF-CM-prediction set samples, demonstrating its feasibility for classifying new data.

3.3.2.2 Discovery and identification of altered metabolites in MEF-CM

The small molecules responsible for the separation (metabolic difference) between UM and MEF-CM were selected according to pq values (loading weights of the X (p) and Y (q) variables combined in one vector) obtained from the loadings plot. Variables (ions) with the lowest and the highest loading weights were chosen as long as their VIP (variable importance for the projection) values were above 1.5. Ions that fulfilled the criteria were subjected to Student's *t*-tests. In metabolomics, the number of univariate-paralleled *t*-tests equals the number of ions detected. As the number of hypotheses tests increases so does the probability of rejecting a null hypothesis; that is, the chance of making a Type I error (false positive) (Vinaixa et al., 2012). Therefore, the *p*-value threshold at which a statistically significant difference is considered should be stricter. Bonferroni correction is applied to correct for multiple comparisons according to the following equation:

$$\alpha = FWER/k$$

Where:

α = pre-defined threshold of probability in each individual test.

FWER = family wise error, the probability (0.05) of yielding one or more false positives out of all hypotheses tested.

k = the number of hypothesis tests performed (number of ions detected).

Therefore, in this experiment, only those ions with *p*-values $\leq 2.47 \times 10^{-5}$ were considered statistically significant as $\alpha = 0.05/2024 = 2.47 \times 10^{-5}$.

Further, the ions that differed significantly were identified. The detailed method of compound identification has been described in section 2.3.6 and in the same way was applied here. The list of significant metabolic changes are summarised in Table 3-3. To provide a more intuitive comparison, box and whiskers plots of some representative metabolites are shown in Figure 3-6.

Owing to limitations of databases' repositories some ions remained unknown; however, they were listed in Table 3-3 due to their importance, as they were only detected in MEF-CM. Other ions like those at *m/z* 329.2336, 333.2074, 247.1703, 249.1859 and 251.2017, although identified, lacked a more precise identification because of the high chemical structure similarity of their isomers. Furthermore, MS/MS data could not provide specific information to distinguish amongst them. For example, the *m/z* 333.2074 ion matched the exact $[M–H_2O–H]^-$ ion mass of the prostaglandins PGE_2, PGD_2 and PGH_2. Then, when the MS/MS spectrum of the *m/z* 333.2074 ion in the samples was obtained and compared with the LipidMaps reference MS/MS spectra of PGE_2, PGD_2 and PGH_2 (Figure 3-7), it was difficult to assign a unique identity because the MS/MS pattern of the sample was similar to the MS/MS patterns of the three prostaglandins. Therefore, to discern between isomers, the use of authentic standards will be required so that retention time can be used as discriminator when the three prostaglandins are injected into the LC-MS system. In the particular case of the ion at *m/z* 333.2074, it is very likely that PGE_2 is the one present in the samples since it has been previously identified in MEF-CM (Jones et al., 2010). However, for the rest of ions, this is the first time that they have been reported in MEF-CM and their identity will be confirmed and described in more detail in chapter 4. In this chapter the metabolites will be discussed based on their putative identity (shown in Table 3-3) assigned with high degree of confidence after MS/MS analysis.

Table 3-3. Significant metabolic changes between unconditioned medium and MEF-conditioned medium.

Accurate mass (*m/z*)	Δ ppm	RT (min)	Ion	Formula	Putative Identification	Fold change	Database Reference	Supporting Information
147.0762	1.4	0.81	$[M+H]^+$	$C_5H_{10}N_2O_3$	L-Glutamine	-2.31	HMDB00641	MS2; 130; 101
216.0986	1.9	0.89	$[M-H]^-$	$C_8H_{15}N_3O_4$	L-Alanyl-L-glutamine	-2.66	HMDB28685	
308.8783		0.97	$[M+H]^+$		Unknown	Note 1		
89.0234	11.2	0.98	$[M-H]^-$	$C_3H_6O_3$	Lactic acid	39.51	HMDB00190	MS2; 71; 61
129.0548	7.0	1.71	$[M-H]^-$	$C_6H_{10}O_3$	4-methyl-2-oxovalerate	27.35	HMDB00695	MS2; 111; 101; 85
267.0422		1.71	$[M+H]^+$		Unknown	66.31		
642.3073	-1.1	5.41	$[M-H]^-$	$C_{30}H_{49}N_3O_{10}S$	S-(9 deoxy-delta12-PGD2)glutathione	Note 1	HMDB13057	
369.2284	-0.5	5.51	$[M-H]^-$	$C_{20}H_{34}O_6$	6-keto-PGF1α	Note 1	LMFA03010001	MS2; 351; 333; 315; 289
329.2336	-0.9	6.39	$[M-H]^-$	$C_{18}H_{34}O_5$	9,10,13-TriHOME or 9,12,13-TriHOME	14.86	HMDB04710, HMDB04708	MS2; 311; 285
333.2074	-0.9	6.59	$[M-H_2O-H]^-$	$C_{20}H_{32}O_5$	PGE_2 or PGD_2 or PGH_2	6.78	LMFA03010003, LMFA03010004, LMFA03010010	MS2; 333; 315; 271; 189
586.3154	-1.5	8.76	$[M+HCOO^-]^-$	$C_{28}H_{48}NO_7P$	LPC(20:5(5Z,8Z,11Z,14Z,17Z))	-1.53	LMGP01050050	MS2; 301; 257; 224
588.3309	-1.4	9.19	$[M+HCOO^-]^-$	$C_{28}H_{50}NO_7P$	LPC(20:4(5Z,8Z,11Z,14Z))	-1.69	LMGP01050048	MS2; 303; 259; 224
614.3467	-1.5	9.40	$[M+HCOO^-]^-$	$C_{30}H_{52}NO_7P$	LPC(22:5(7Z,10Z,13Z,16Z,19Z))	-1.41	HMDB10403	MS2; 329; 285; 242
590.3470	-2.0	9.55	$[M+HCOO^-]^-$	$C_{28}H_{52}NO_7P$	LPC(20:3(5Z,8Z,11Z)) or LPC(20:3(8Z,11Z,14Z))	-1.74	HMDB10393, LMGP01050133	MS2; 305; 242; 224
417.3357	1.4	9.90	$[M+H]^+$	$C_{27}H_{44}O_3$	1, 25-Dihydroxyvitamin D3	88.97	HMDB01903	MS2; 399; 381

Accurate mass (m/z)	Δ ppm	RT (min)	Ion	Formula	Putative Identification	Fold change	Database Reference	Supporting Information
464.3131		9.96	$[M+H]^+$		Unknown	2.49		
247.1703	0.0	10.05	$[M-H]^-$	$C_{16}H_{24}O_2$	Hexadecatetraenoic acid	122.19	LMFA01030163[a]	MS2; 229; 203; 149
249.1859	0.4	10.45	$[M-H]^-$	$C_{16}H_{26}O_2$	Hexadecatrienoic acid	24.66	LMFA01030134[a]	MS2; 231; 205; 151
345.2437	-0.6	10.51	$[M-H]^-$	$C_{22}H_{34}O_3$	1alpha,22-dihydroxy-23,24,25,26,27-pentanorvitamin D3	2.95	LMST03020011	
275.2019	-1.1	10.54	$[M-H]^-$	$C_{18}H_{28}O_2$	Stearidonic acid	4.70	LMFA01030357	MS2; 257; 231; 177
251.2017	-0.4	10.95	$[M-H]^-$	$C_{16}H_{28}O_2$	Hexadecadienoic acid	4.58	LMFA01030109[a]	
623.4171		11.06	$[M-H]^-$		Unknown	Note 1		
303.2331	-0.7	11.39	$[M-H]^-$	$C_{20}H_{32}O_2$	Arachidonic acid	-1.86	LMFA01030001	MS2; 285; 259; 205
305.2488	-0.7	11.83	$[M-H]^-$	$C_{20}H_{34}O_2$	Dihomo-gamma-linolenic acid	-2.52	LMFA01030158	MS2; 287; 261; 207
331.2645	-0.9	12.15	$[M-H]^-$	$C_{22}H_{36}O_2$	Adrenic acid	-2.09	LMFA01030178	MS2; 313; 287; 233
401.3407	1.7	13.78	$[M+H]^+$	$C_{27}H_{44}O_2$	7-Ketocholesterol	4.21	LMST01010049	MS2; 383; 365

Fold changes were calculated as the ratio of the average peak area (n=18) of MEF-CM and UM, for decreased metabolites the ratio is inverted and the sign changed to indicate such decrease. [a] Used here only as an example as LipidMaps database provides a list of similar isomers.

LPC, lysophosphatidylcholine; PGF1, prostaglandin F1; PGD_2, prostaglandin D2; PGE_2, prostaglandin E2; PGH_2, prostaglandin H2; TriHOME, trihydroxyoctadecenoic acid.

MS2 supporting information indicates the characteristic fragment ions of each molecule and whose MS/MS spectrum is shown in appendix B.

Note 1: the ion was only detected in MEF-CM.

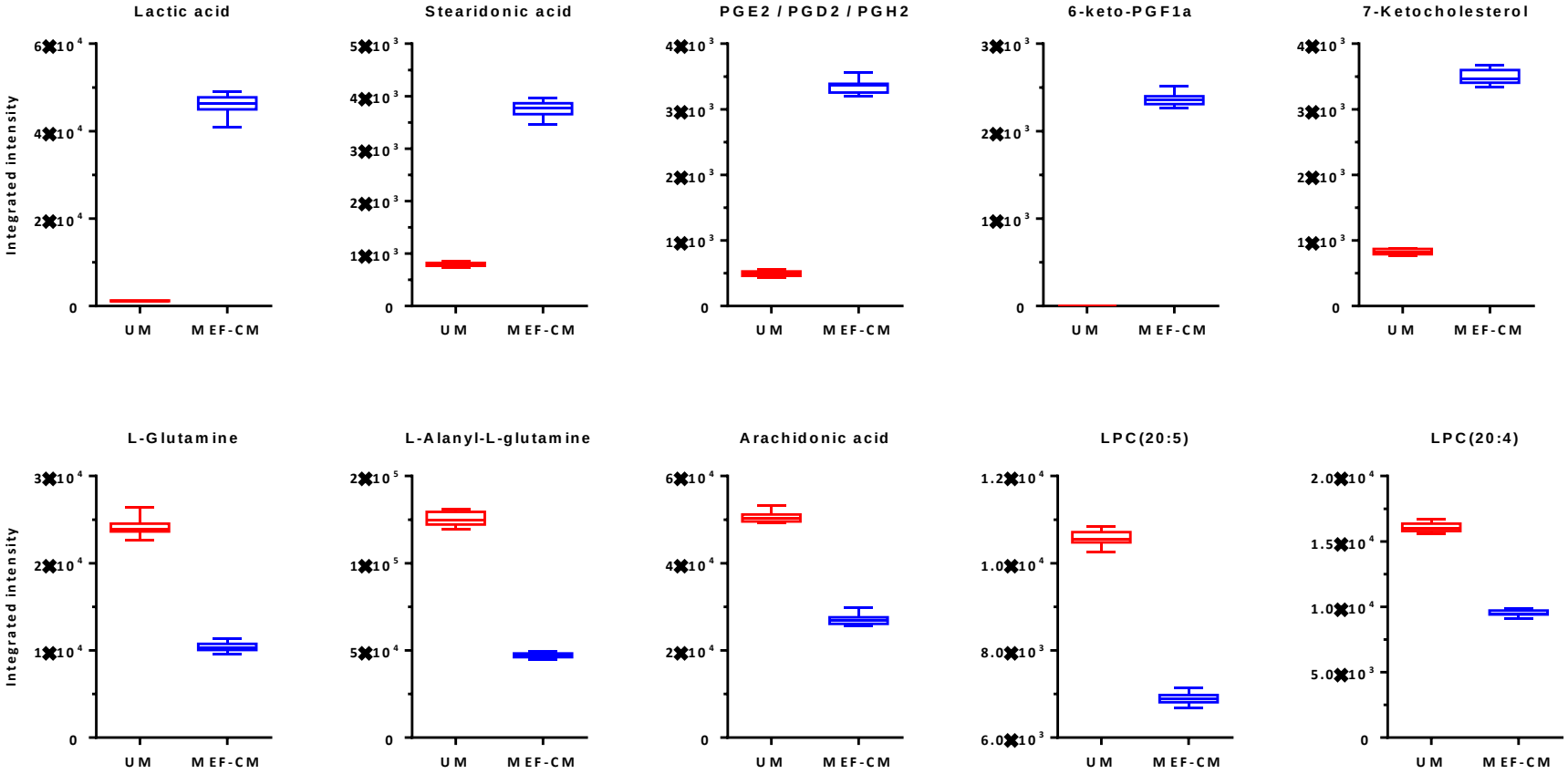

Figure 3-6 Upper panel, integrated intensities of representative metabolites whose concentrations increased in the CM after UM incubation with MEFs. Lower panel, integrated intensities of representative metabolites with decreased levels in CM. The boxes are drawn from the 25th to 75th percentiles in the intensity distribution. The median, or 50th percentile, is represented as a horizontal line inside the box.

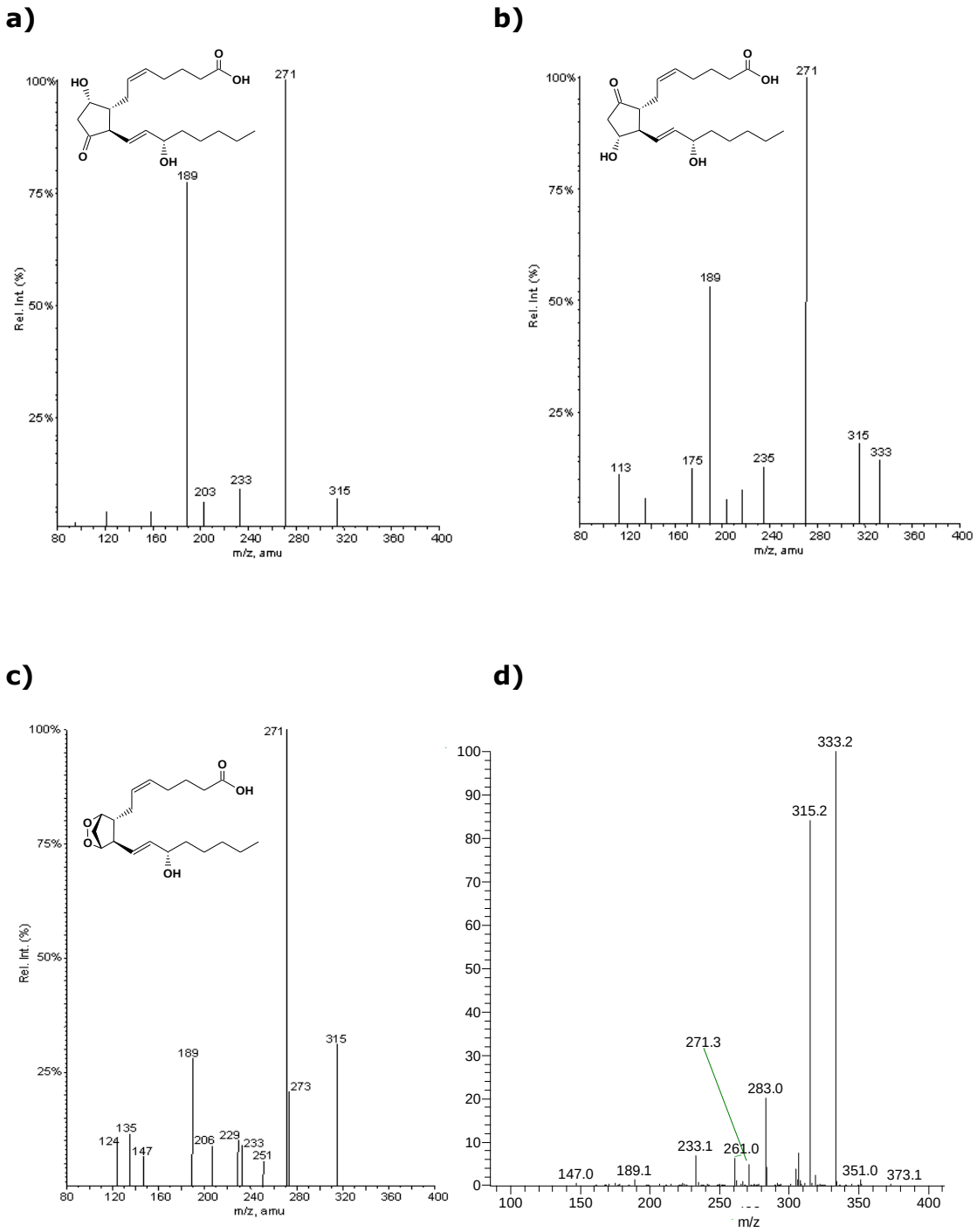

Figure 3-7 Example showing identification by reference to library MS/MS spectra. Reference MS/MS spectra of a) PGD2, b) PGE2 and c) PGH2 obtained from LipidMaps database. d) experimental MS/MS spectrum of ion m/z 333.2074 in MEF-CM samples. It is difficult to assign a more precise identification for this ion since the MS/MS data is insufficient to provide specific information to distinguish between isomers.

3.3.3 Identification of possible metabolic pathways occurring during the MEF-conditioning process

As shown in Table 3-3, the compounds that decreased their concentration in the MEF-CM were, amongst others, lysophosphatidylcholines and arachidonic acid, while those that increased (secreted by MEFs) were mostly polyunsaturated fatty acids, including prostaglandins (PGs). Searching into the Kyoto Encyclopaedia of Genes and Genomes (KEGG, www.genome.jp/kegg), it was possible to identify different metabolic pathways relating both the increased and decreased metabolites (Figure 3-8). Arachidonic acid (AA), linoleic acid (LA) and alpha-linolenic acid (ALA) metabolism pathways were found to be involved during the conditioning of the medium.

AA can be released from phospholipids (i.e. lysophosphatidylcholines) via phospholipase A_2 or formed by the elongation and desaturation of LA. Moreover, β-oxidation of adrenic acid can also lead to AA formation (Mann et al., 1986). Further, AA can be metabolised by a number of enzyme pathways including cyclooxygenase (COX), which gives rise to PGs; lipoxygenase (LOX), which forms leukotrienes, lipoxins and hydroxyeicosatetraenoic acids (HETEs); and cytochrome *P*-450 (CYP), which results in epoxyeicosatrienoic acids (EETs) (Wenzel, 1997). LA, on the other hand, can produce trihydroxyoctadecenoic acids (TriHOMEs) via 9S-lipoxygenase and lastly, stearidonic acid results from the action of Δ6-desaturase on alpha-linolenic acid (Guil-Guerrero, 2007). Due to the central importance of AA metabolism to produce bioactive oxylipins such as the observed here with increased levels of PGs, it was decided to investigate this area further as described below.

3.3.3.1 Arachidonic acid metabolism

To test the hypothesis that the prostaglandins observed in the CM are produced by MEFs using arachidonic acid as substrate, an isotope labelling flux experiment was carried out. UM was supplemented with AA-d8 at three different concentrations; $1.29x10^{-5}$, $1.29x10^{-3}$ and $1.29x10^{-2}$ mM. The UM+DMSO, used as a control, and the AA-d8-supplemented unconditioned media were incubated with and without MEFs for 24 h, after which the samples were analysed.

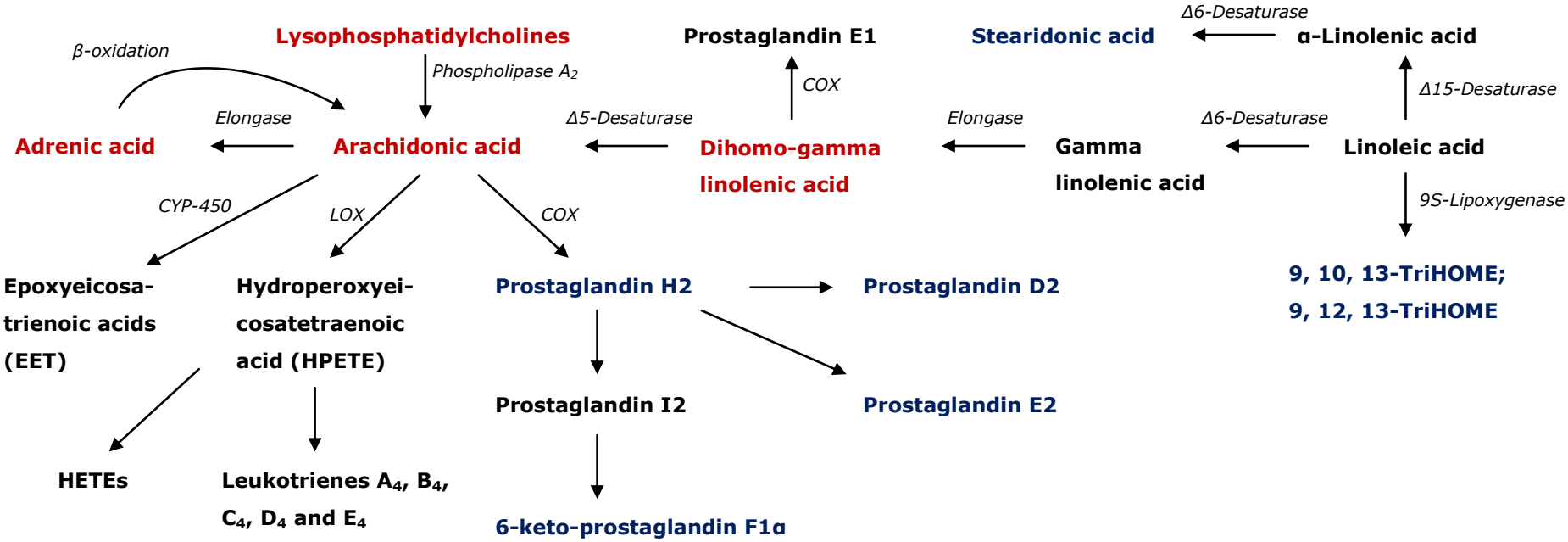

Figure 3-8 Metabolic pathways identified during the process of medium conditioning. One of the main pathways is arachidonic acid (AA) metabolism since it relates most of the decreased metabolites found in CM. Although AA can be metabolised by several enzyme pathways (cytochrome P-450 (CYP-450), lipoxygenase (LOX) and cyclooxygenase (COX)), only metabolites associated with COX activity (prostaglandins) were detected in the CM. Other increased metabolites can be explained by linoleic acid (LA) and α-linolenic acid (ALA) metabolism. LA oxidation by 9S-lipooxygenase leads to trihydroxyoctadecenoic acids (TriHOMEs), while desaturation of ALA produces stearidonic acid. Furthermore, LA and AA metabolism are interconnected as desaturation and elongation of LA can give rise to AA. Increased (blue) and decreased (red) metabolites of CM are coloured to ease interpretation. HETEs, hydroxyeicosa-tetraenoic acids.

The peak areas of AA-d8 and the deuterated forms of PGE_2 (or its isomers, PGD_2 or PGH_2) and 6-keto-PGF1a were taken from the extracted ion chromatograms of UM incubated with and without MEFs. Samples incubated without MEFs did not produce PGs (data not shown). On the contrary, those incubated with MEFs showed a decrease of AA-d8 and an increase of deuterated PGE_2 (or isomers), 6-keto-PGF1a and S-(9 deoxy-delta12-PGD_2) glutathione (Figure 3-9). It is worth noting that during the transformation of AA-d8 to prostaglandins, there is a loss of one deuterium atom, hence, producing prostaglandins (PGE_2-d7 and 6-keto-PGF1a-d7) seven mass units different from the non-labelled ones (Figure 3-9c, d). With this experiment, it was confirmed that arachidonic acid is used by mouse embryonic fibroblasts to produce prostaglandins; however, products from other enzymatic pathways (LOX or CYP-450) were not identified, suggesting a predominant COX activity in MEFs.

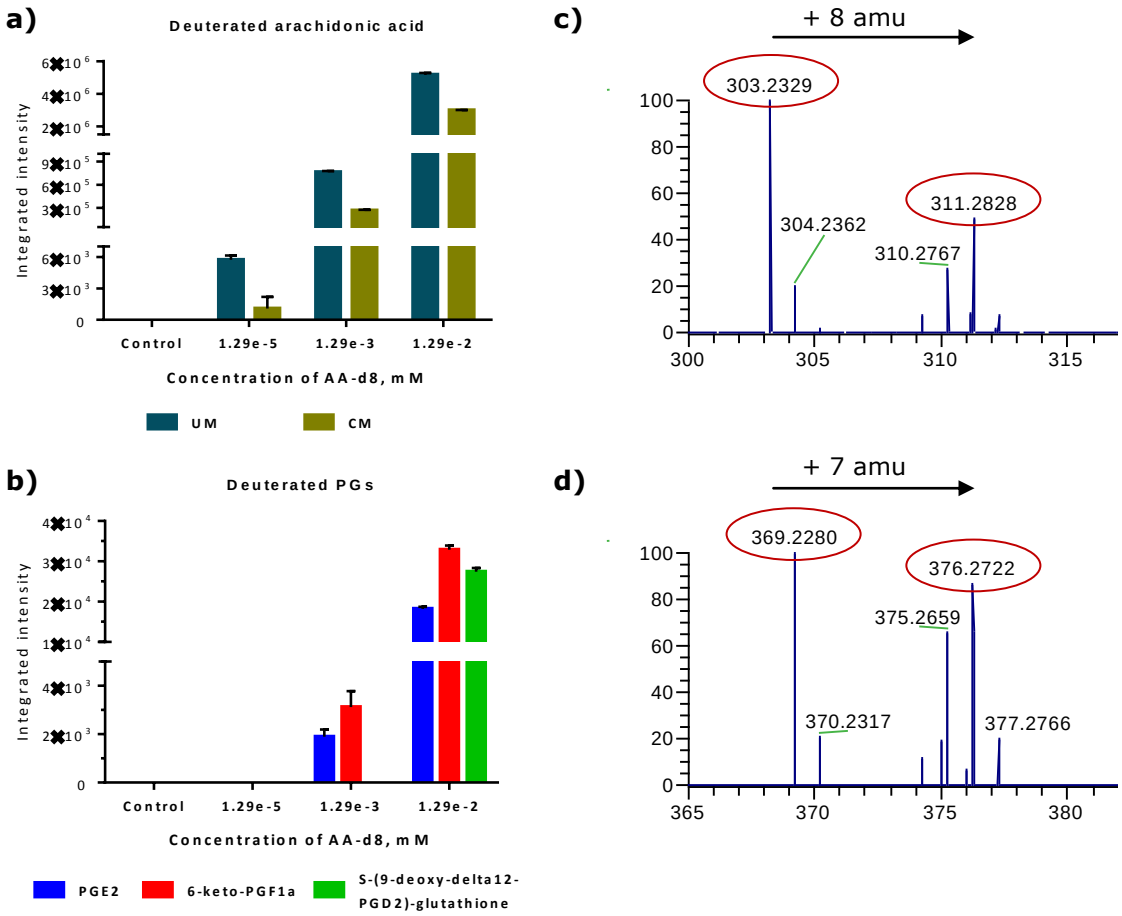

Figure 3-9 a) and b) peak areas of deuterated arachidonic acid (AA-d8) and deuterated prostaglandins, respectively. c) Starting AA-d8 (*m/z* 311.2828) 8 amu heavier than non-labelled (*m/z* 303.2329) and producing d) prostaglandins (6-keto-PGF1α, as an example) 7 amu different between deuterated (*m/z* 376.2722) and non-labelled (*m/z* 369.2280). Data represent mean ± SD (n=3).

3.3.3.2 Linoleic acid and α-linolenic acid metabolism

As shown in Figure 3-8, TriHOMEs are the result of linoleic acid oxidation, thus, it was expected that LA would be reduced in the CM; however, no significant reduction was observed (Figure 3-10). This suggests that either LA levels are being replenished by other metabolic reaction(s) or that TriHOMEs are formed from other sources. Since there have not been reported sources of TriHOMEs other than LA (Funk and Powell, 1983, Nording et al., 2010), it is more likely that hydrolysis of lysophosphatidylcholines (LPCs) release more LA.

Similarly, stearidonic acid is the main metabolite of α-linolenic acid (Guil-Guerrero, 2007) and no other sources of stearidonic acid have been identified. However, in this case, not only ALA concentrations were maintained or decreased but, surprisingly, they increased (Figure 3-10). Likewise the high content of LPCs (a source of fatty acids) in UM could explain such results.

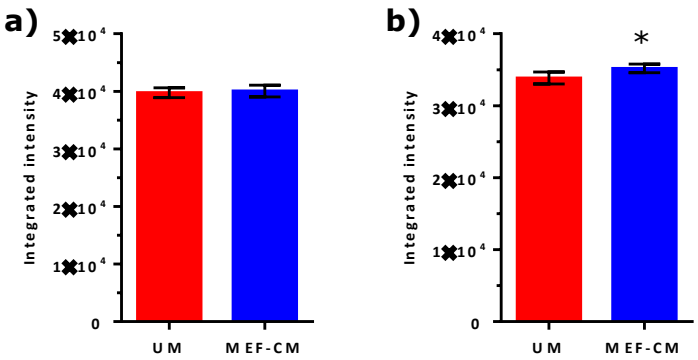

Figure 3-10 Peak areas of a) linoleic acid (LA) and b) α-linolenic acid (ALA) in unconditioned (UM) and conditioned medium (CM). No significant difference in LA levels was found in spite of being the only possible source of trihydroxyoctadecenoic acids (TriHOMEs) which are increased in CM. An unexpected significant increase of ALA was observed in CM when it would be expected to decrease as stearidonic acid (increased in CM) formation results mainly from ALA desaturation. The unexpected results could be explained by the lysophosphatidylcholines (source of fatty acids) present in UM. Data represent mean ± SD (n=18). Statistical analysis used was Student's *t*-test. Significance: *$p < 2.47x10^{-5}$.

3.3.4 Analysis of a series of batches of MEF-CM obtained from separate batches of MEFs

Initially, the analysis of conditioned media collected from different batches of MEFs was intended to investigate differences between supportive and non-supportive MEF-CM batches. It was expected that during isolation of MEFs some batches would fail to produce a suitable medium for hESC growth, hence, the difference between those batches that supported hESC proliferation from those that did not could be investigated. However, all the batches of MEF-CM were able to support hESC proliferation. Consequently, these batches were used to study the variability in small molecule composition of MEF-CM between batches.

PCA was applied in the first instance to obtain an overview of the samples. As seen in Figure 3-11a there is a clear separation between UM and the batches of CM. UM replicates clustered far on the right-hand side of the plot while the conditioned medium batches appeared more scattered in the middle showing metabolic differences even amongst them. This illustrates the considerable batch-to-batch variability in the small molecule components and hence the incubation conditions to which hESC are subjected during culture. To further investigate the differences between the two types of media, the corresponding PCA loadings plot was analysed (Figure 3-11b). Consistent with the first findings, UM samples presented higher levels of L-alanyl-L-glutamine, arachidonic acid, LPC(20:5) and LPC(20:4) while CM samples contained higher concentrations of lactic acid, 6-keto-PGF1a, PGE_2 (or PGD_2 or PGH_2), 9, 10, 13 TriHOME (or 9, 12, 13 TriHOME) and stearidonic acid (Figure 3-11b).

The metabolic differences observed amongst the batches in the PCA scores plot indicate that each batch of MEFs possesses different capabilities of transforming UM into a suitable medium for hESC culture; in other words, of secreting potential factors required for long term expansion of hESC. For example, MEF-CM batch 117 in Figure 3-12 is the one that produces the lowest levels of lactic acid and 6-keto-PGF1a, and also the one that consumes less arachidonic acid and LPC(20:4). This behaviour is also reflected in the PCA scores plot as MEF-CM-117 appears

closer to UM. On the contrary, MEF-CM-107 and MEF-CM-120 produced more lactic acid and prostaglandins and consumed more nutrients from the UM than the rest of batches. In this case, MEF-CM-107 and MEF-CM-120 appeared farther from UM.

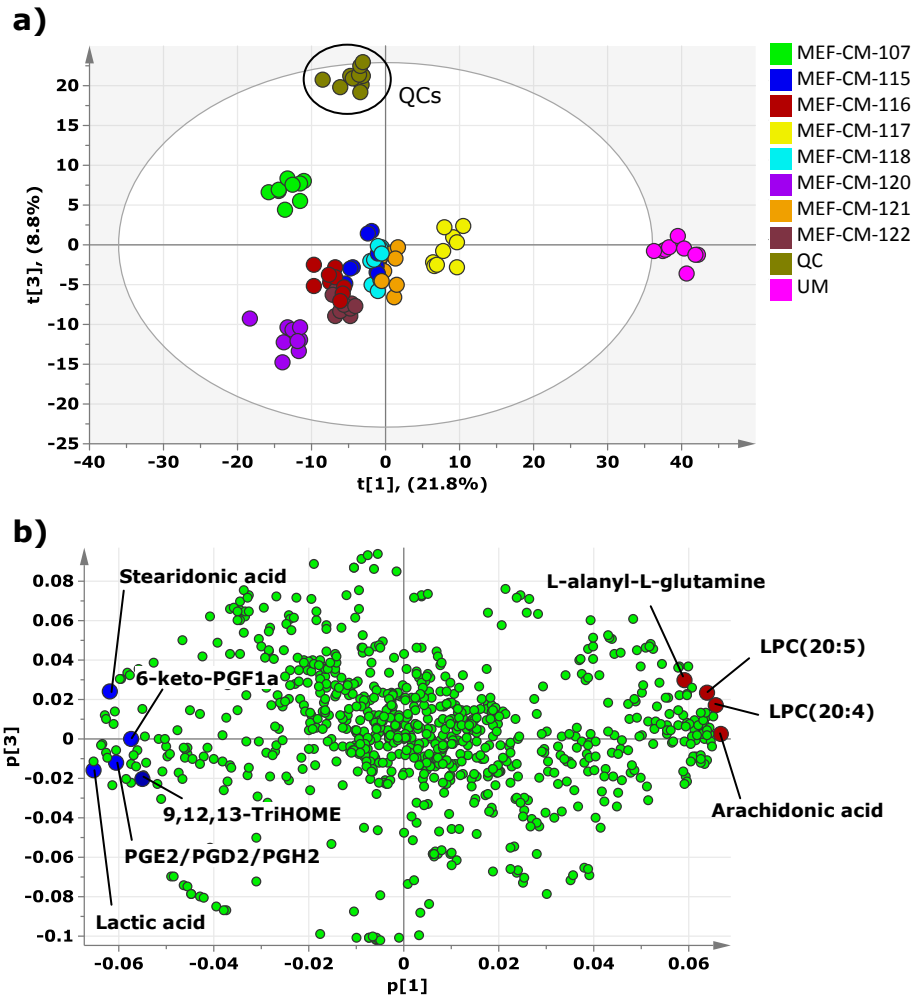

Figure 3-11 a) PCA scores plot and b) PCA loadings plot of MEF-CM obtained from different batches of MEFs. The position of an observation in a given direction in a scores plot is influenced by variables lying in the same direction in the loadings plot. Therefore, samples that appear on the right-hand side of the scores plot contain higher levels of the variables (metabolites) on the right-hand side of the loadings plot and vice versa. LPC, lysophosphatidylcholine.

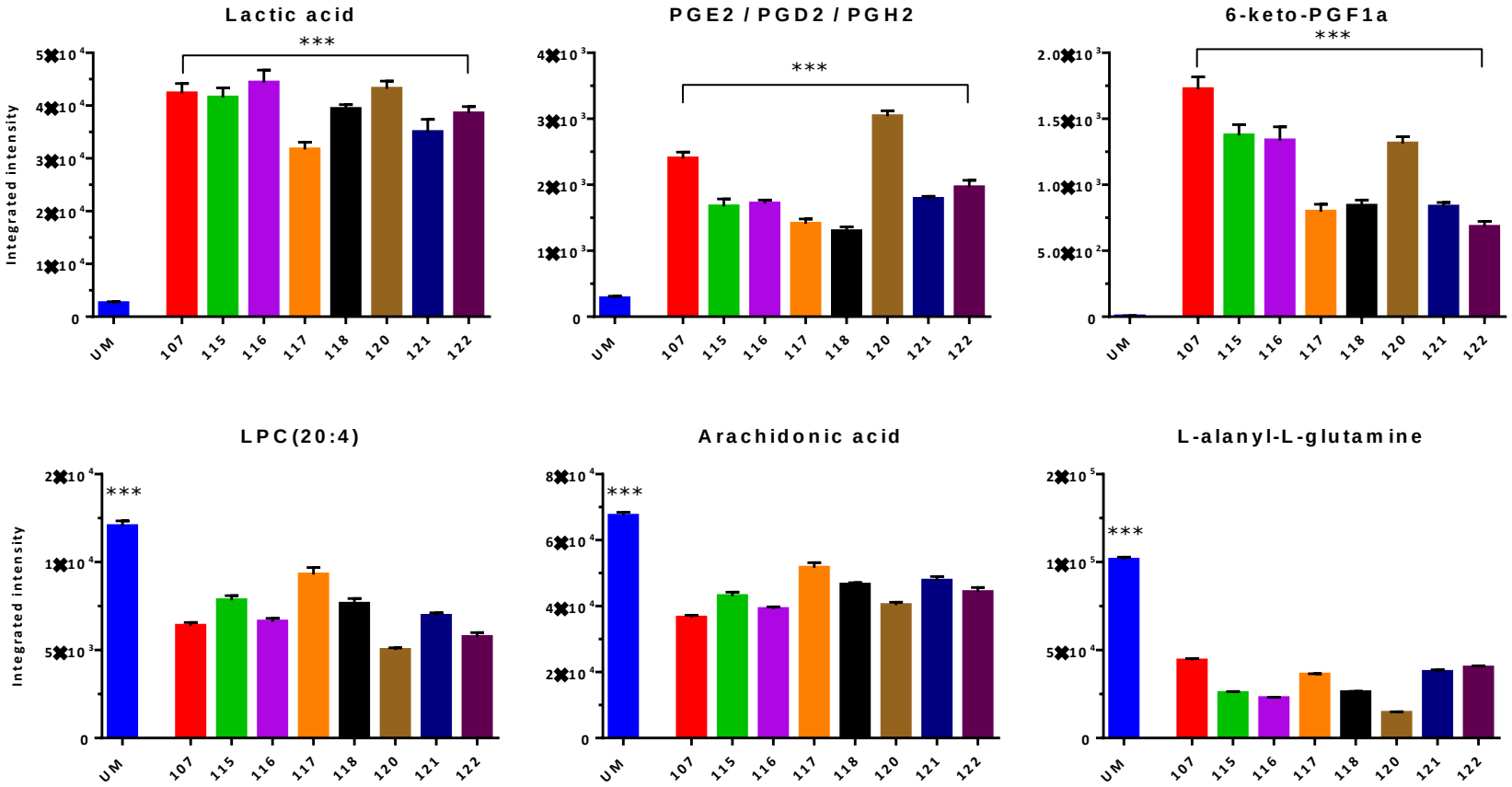

Figure 3-12 Batch to batch variability observed during the conditioning process. Different batches of MEFs (107, 115, 116, 117, 118, 120, 121 and 122) were used to condition the same batch of UM and the metabolic differences amongst batches are shown by selection of representative increased and decreased metabolites in CM. One-way ANOVA with Dunnett's post hoc test indicates significant differences between the CM batches and UM (control). Data represents mean ± SD (n=9). Significance: ***$p < 0.001$.

The small-molecule composition differences observed amongst the MEF-CM batches were also reflected in the efficacy in which each batch supported the expansion of hESC. Table 3-4 shows the hESC doubling times obtained with each batch of MEF-CM, doubling time is the period of time required by the hESC to double their population. According to this; the shorter the doubling time the greater the growth rate. In this case, batches 120, 121 and 122 showed the most efficient growth rates as they had the shortest doubling times. However, attributing this difference to solely observing changes in the small-molecule composition of the MEF-CM media would be difficult since when the MEF-CM batches were tested no protein had been removed from the media. Therefore, it is fair to say that a combination of protein factors and small-molecule factors may contribute to the observation of short doubling times. Nevertheless, evaluation of the increased metabolites in MEF-CM would determine if these small molecules can also affect the efficiency in which MEF-CM can support the proliferation of hESC. Biological evaluation of selected metabolites found increased in MEF-CM will be carried out in chapter 4 and will help to understand the effect of these small molecules on hESC proliferation.

Table 3-4. Population doubling times of hESC tested with several batches of MEF-CM.

	hESC doubling times (days)
MEF-CM-107	1.87
MEF-CM-115	1.99
MEF-CM-116	1.89
MEF-CM-117	1.79
MEF-CM-118	1.83
MEF-CM-120	1.73
MEF-CM-121	1.72
MEF-CM-122	1.74

Note: Data were kindly provided by Dr Maria Barbadillo-Munoz.

3.3.5 Investigating the effect of MEF age on CM small molecule composition

Routinely, batches of MEFs are used to prepare CM every 24 h for a period of seven days (Burridge et al., 2007, Mahlstedt et al., 2010), after which MEFs are disposed of as they get old and the CM is stored at -20ºC for future use. To investigate the effect of MEF age on the composition of MEF-CM, metabolite profiles of CM collected over a time course of ten days were analysed. PCA (Figure 3-13) revealed a time-effect trend in the collection of the media. The tendency observed from CM-day 2 to CM-day 8 could indicate two things: 1) that MEFs are producing more or less of certain metabolites every day or 2) that MEFs are consuming more or less nutrients from UM. In either case, this demonstrates that even with the same batch of MEFs, the CM produced and used in hESC culture varies greatly in its chemical composition, highlighting the need of a chemically defined medium for the reproducible expansion of hESC in order to realise their clinical use. Interestingly, CM-day 1, CM-day 9 and CM-day 10 appeared outside of the trend, suggesting that other metabolic changes are occurring when MEFs are used fresh (CM-day1) and when they get very old. A possible explanation is that MEFs coming from a different culture system (as the medium in which MEFs are derived is different from the medium used for conditioning) adjust to the new conditions (UM) to produce CM. To better understand these metabolic differences, peak areas from individual metabolites were examined. For illustration purposes, increased and decreased metabolites are presented as plots of metabolites present in low, medium and high concentration in MEF-CM (Figure 3-14 and Figure 3-15).

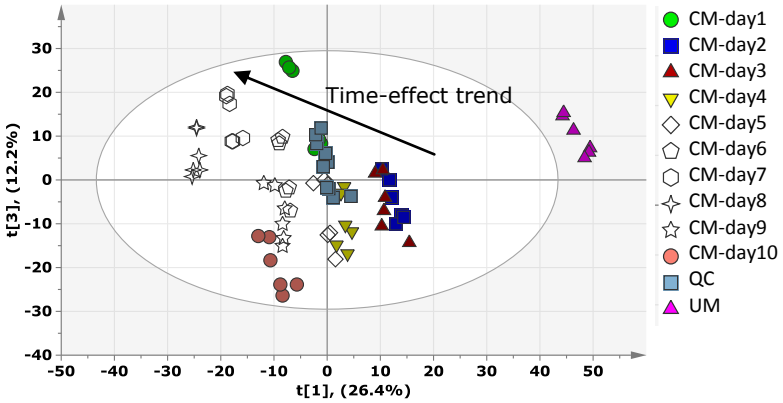

Figure 3-13 PCA scores plot of CM obtained every 24 h for 10 consecutive days (CM-day1 to CM-day10). A time-effect trend is observed during CM collection, indicating continuous increased or decreased metabolic changes.

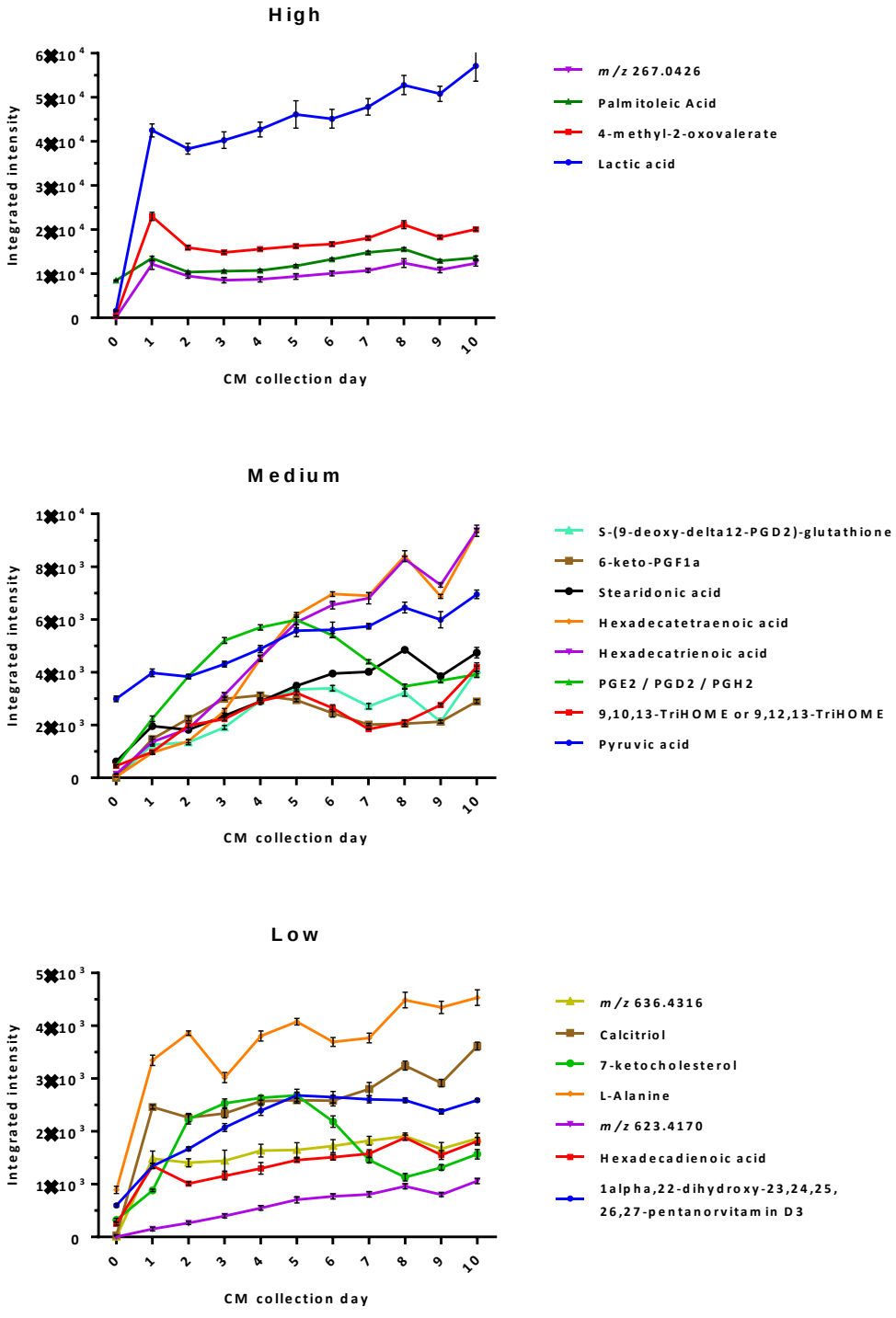

Figure 3-14 Low, medium and high concentration plots of metabolites with increasing trends in MEF-CM collected for ten consecutive days. Each point represents the average peak area ± SD (n=6) of the metabolites on each day. Day 0 means UM.

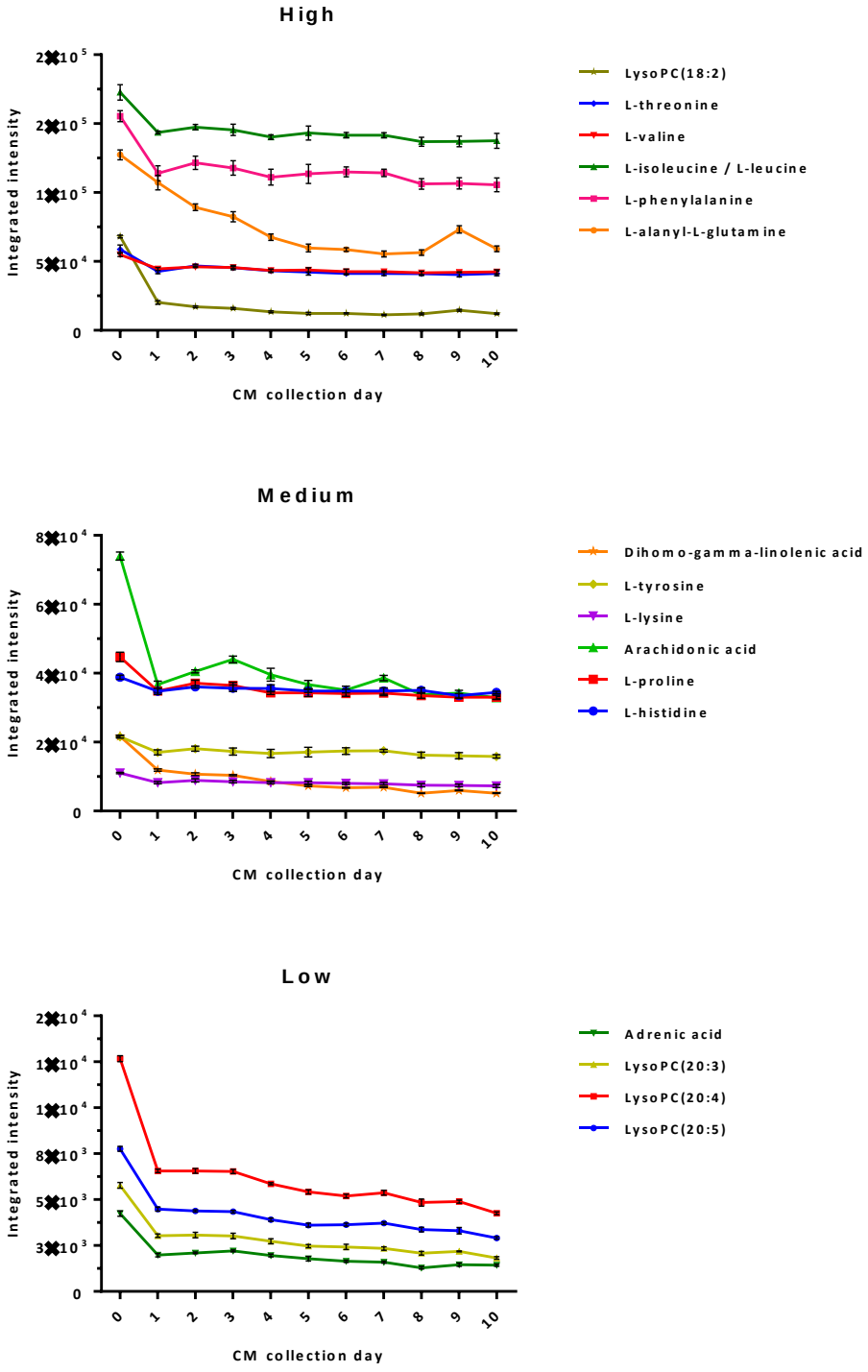

Figure 3-15 Low, medium and high concentration plots of metabolites with decreasing trends in MEF-CM collected over a 10-day period. Each point represents the average peak area ± SD (n=6) of the metabolites on each day. Day 0 means UM.

A more careful inspection of the metabolic differences revealed several trends. For example, metabolites that steadily increased or decreased over time (e.g. lactic acid and LPC(20:4), respectively); metabolites that had a day of maximum secretion (PGs); and metabolites that increased or decreased and then were maintained constant (e.g. L-histidine and 4-methyl-2-oxovalerate, respectively). This illustrates the metabolic changes caused by MEF ageing.

As demonstrated before, AA is the substrate for the production of PGs; therefore, it would be expected that at the day of maximum prostaglandin secretion (day 5), AA levels would show a minimum on the same day; however, the levels of AA were almost constant. This suggests that other sources of AA might be being activated to maintain steady concentrations of AA. These sources could be LPC(20:4) (Wenzel, 1997), adrenic acid (Mann et al., 1986) and dihomo-gamma-linolenic acid (Wang et al., 2012) (Figure 3-8) which were observed to be constantly reducing over time; however this requires further investigation.

The data also indicate that L-glutamine is highly needed when MEFs senesce as there is a large consumption of the dipeptide L-alanyl-L-glutamine which results in increased levels of L-alanine but not of L-glutamine. Other amino acids that seem to be essential in the diet of mice (MEFs in this case) (Bauer and Berg, 1943) were also reduced. These were L-valine, L-histidine, L-phenylalanine, L-threonine, L-lysine, L-leucine and L-isoleucine.

As MEFs get older they also present higher glycolytic activity as indicated by the increase over time of glycolysis endpoints such as pyruvate and lactate. These results are in agreement with the constant lactic acid increase reported elsewhere (Gupta et al., 2012) although the CM collection was for a shorter period of time (3 days). It has been shown however that above certain concentration (1.5 g/L), lactic acid becomes detrimental for the cells as demonstrated by inhibition of mouse embryonic stem cell growth (Ouyang et al., 2007). These observations may, in part, explain the low efficiencies observed when hESC are cultured with CM-day 7 when compared with those cultivated with CM from day 1 (Villa-Diaz et al., 2009). A lower percentage of

undifferentiated colonies were observed with CM-d7 (31.7%) whereas with CM-day 1 a higher proportion of hESC remained undifferentiated (78.6%) (Villa-Diaz et al., 2009). Together, these results indicate that MEFs' senescence affects the production of efficient CM that supports hESC growth.

In the same way as lactic acid, polyunsaturated fatty acids like hexadecatetraenoic acid, hexadecatrienoic acid, hexadecadienoic acid and stearidonic acid showed a continuous increase along the days of CM collection; however, there is lack of information about the possible beneficial or toxic effects on stem cells.

3.3.6 Biological significance of altered metabolites

Metabolites whose concentrations increased after the medium conditioning process include lactic acid, prostaglandins, polyunsaturated fatty acids (PUFAs), 7-ketocholesterol and vitamin D derivatives. On the other hand, metabolites that decreased or were used by MEFs during incubation were mainly lysophosphatidylcholines, some PUFAs (including arachidonic acid) and L-glutamine which was obtained directly from the medium or after *in situ* hydrolysis of the dipeptide L-alanyl-L-glutamine.

Amongst the increased metabolites, prostaglandins and vitamin D derivatives have been shown elsewhere to be involved in the proliferation and pluripotency maintenance of stem cells. For example, prostaglandin E_2 promotes cell proliferation (Kim and Han, 2008) and protects mouse embryonic stem cells from apoptosis (Liou et al., 2007). Additionally, PGE_2 stimulates proliferation of human mesenchymal stem cells (Arikawa et al., 2004) and enhances both mouse and human hematopoietic stem cell survival (Hoggatt et al., 2009). On the other hand, 6-keto-prostaglandin F1α (6-keto-PGF1α), a stable metabolite of prostaglandin I_2, has been reported to be involved in inducing hESC to form cardiomyocytes (Xu et al., 2008b), although a more recent report has associated both 6-keto-PGF1α and PGE_2 with hESC self-renewal (Jones et al., 2010). The biologically active form of vitamin D, 1, 25-

dihydroxyvitamin D3, on the other hand, has been reported to maintain the multipotent capacity of human mesenchymal stem cells (Klotz et al., 2012). To date, there is no direct evidence of their effect on hESC.

Even though there have not been reports associating the increased PUFAs in CM with stem cells, 9, 10, 13-TriHOME and 9, 12, 13-TriHOME are believed to regulate prostaglandin synthesis (Funk and Powell, 1983), which suggests that they could modulate the synthesis of more active compounds implicated in stem cell proliferation. Stearidonic acid, on the contrary, has been characterized as a potent inhibitor of cancer cell growth (Cantrill et al., 1993) and may have undesirable effects on hESC, but there is still not sufficient information to support this idea.

7-ketocholesterol (7-KC), another increased metabolite in the CM, has shown cytotoxic and pro-apoptotic effects on human adipose tissue mesenchymal stem cells (Levy et al., 2014). Nevertheless, oxysterols, the group of compounds to which 7-KC pertains, are known activators of the hedgehog signalling pathway (Dwyer et al., 2007) whose activation has stimulated the proliferation of mouse embryonic stem cells (Heo et al., 2007). Thus, in spite of the reported deleterious effects of 7-KC, it is likely that it can stimulate hESC growth by activation of the hedgehog pathway.

With regards to the decreasing metabolites, the importance of arachidonic acid has been shown in the production of prostaglandins; although some prostaglandins can also be produced from dihomo-gamma-linolenic acid (Wang et al., 2012) (Figure 3-8). Further, it has been pointed out previously that lysophosphatidylcholines, dihomo-gamma-linolenic acid and adrenic acid could act as alternative sources of arachidonic acid and so maintain AA levels.

Overall, whether or not the increased metabolites of MEF-CM have an effect on hESC proliferation and/or pluripotency maintenance they have to be tested in hESC culture. Such investigations will be described and discussed later in chapter 4.

3.4 Conclusions

In an attempt to identify the small-molecule factors secreted by MEFs during the medium conditioning process, the LC-MS metabolomics method, described in chapter 2, was applied and successfully identified metabolic differences between UM and CM samples. The LC-MS approach showed excellent advantages for the study of conditioned medium as it could detect changes in levels of low abundance bioactive molecules with potential roles in hESC growth, survival and maintenance of pluripotency.

Lactic acid, prostaglandins, polyunsaturated fatty acids, 7-ketocholesterol and vitamin D derivatives were found to be increased or were only detected in MEF-CM samples. However, their increased concentration in CM does not necessarily imply that the metabolites are involved in hESC growth or pluripotency as some of the increased metabolites have also been associated with deleterious effects (i.e. lactic acid, 7-KC) on other stem cell types. Therefore, to corroborate whether or not these metabolites exert a positive or negative effect on hESC proliferation, they need to be tested in *in vitro* hESC culture (investigated in chapter 4).

It was demonstrated that arachidonic acid metabolism by cyclooxygenase is an enzyme pathway highly active during MEF-conditioning which led to the formation of prostaglandins (PGE_2 and 6-keto-PGF1α) associated with stem cell proliferation. Nonetheless, this enzyme activity varies from batch to batch and even from day to day of collection as demonstrated by the analysis of CM obtained with different batches of MEFs and CM collected every 24 h from the same batch of MEFs. The chemical variability of these conditioned media points out the need of a culture medium with a more consistent composition for the reproducible expansion of pluripotent hESC required in clinical applications. The insights provided by the metabolic profiling results of these experiments may greatly contribute towards this end.

CHAPTER 4

The effect of small molecules found in MEF-CM on the maintenance of hESC cultures

4 The effect of small molecules found in MEF-CM on the maintenance of hESC cultures

4.1 Introduction

Following the successful identification of metabolites present in MEF-CM with potential implications in the proliferation of undifferentiated human embryonic stem cells, it was investigated whether or not these metabolites had a positive effect on hESC. For this, hESC were exposed to the compounds during *in vitro* hESC culture; however, prior to hESC culture testing, it was necessary to confirm the putative identity of the metabolites (assigned in chapter 3) so that only those successfully confirmed could then be tested. Additionally, the concentrations of the confirmed metabolites were measured in order to investigate their effects at levels similar to those at which they are normally found in MEF-CM.

Amongst the increased metabolites found in MEF-CM (Table 3-3, chapter 3), only those with potential biological activity in stem cell regulation were chosen for further identification/confirmation and subsequent test in hESC culture in this chapter. The selected metabolites were PGE_2 (or its possible isomers PGD_2 and PGH_2), 6-keto-PGF1α, stearidonic acid, 9, 10, 13-TriHOME (or its possible isomer 9, 12, 13-TriHOME), calcitriol and 7-ketocholesterol. Confirmation of these metabolites was achieved by chromatography and mass spectrometry methods with the use of authentic standards as a means of unambiguous identification (Gika et al., 2014).

4.1.1 Potential roles of selected metabolites in stem cell regulation

From the selected metabolites, PGE_2 is the compound that has been studied the most in stem cells. For example, it was found that when PGE_2 was added to the culture medium, it promoted the proliferation of both human mesenchymal stem cells (hMSC) and mouse embryonic stem cells (mESC) (Arikawa et al., 2004, Kim and Han, 2008). Furthermore, PGE_2 also showed the ability to protect mESC from apoptosis (Liou et al., 2007) and enhance homing, survival and proliferation of hematopoietic

stem cells (Hoggatt et al., 2009). Contrary to the aforementioned, in the case of hESC, it was reported that PGE_2 induced differentiation (Garcia-Gonzalo and Izpisua Belmonte, 2008); however, it is probable that such an effect might have been caused by the relatively high concentration at which PGE_2 was tested (20 μM). Therefore, for the benefits of PGE_2 to other stem cells, it is possible that PGE_2, at concentrations normally found in MEF-CM, may have survival and proliferation effects on hESC as it does with mESC and hMSC.

7-ketocholesterol, one of the oxidation products of cholesterol (known as oxysterols) has been shown to exhibit cytotoxicity in mesenchymal stem cells (Levy et al., 2014); nonetheless, oxysterols have also shown novel biological activities in cell signalling (Olkkonen et al., 2012). For instance, it has been found that oxysterols are activators of the Hedgehog signalling pathway (Dwyer et al., 2007) whose activation has been demonstrated to stimulate mESC proliferation (Heo et al., 2007). Additionally, oxysterols can bind to members of the cytoplasmic oxysterol-binding protein (OSBP) family, a group of intracellular lipid receptors. In particular, it was found that 7-ketocholesterol can form a complex with OSBP proteins which interacts with the tyrosin kinase JAK-2 which in turn leads to the activation of the signal transducers and activators of transcription 3 (STAT-3) (Romeo and Kazlauskas, 2008). Activation of STAT-3 pathway in mESC is known to maintain the cells in an undifferentiated state (Matsuda et al., 1999). Consequently, it seems likely that 7-ketocholesterol can mediate some biological functions in hESC by coupling to OSBP proteins or by activation of the Hedgehog signalling pathway.

In the literature, 9, 10, 13-TriHOME and 9, 12, 13-TriHOME, lipoxygenase metabolites of linoleic acid, have not shown any biological activity related with stem cells; nevertheless, it has been shown that these hydroxylated fatty acids possess PGE-like activity (Claeys et al., 1986). Thus, it is possible that these lipids could further enhance the activities of PGE_2 already mentioned.

6-keto-PGF1α and calcitriol have had relatively few reports associating their functions with stem cells. For example, when hESC were exposed as

embryoid bodies (EBs) to 6-keto-PGF1α in basic serum-free medium, a small percentage of cardiomyocytes were obtained (Xu et al., 2008b), demonstrating with this the cardiogenic activity of 6-keto-PGF1α. However, more recently, 6-keto-PGF1α has also been associated with the proliferation and pluripotency of hESC as its levels were found to be increased in MEF-conditioned medium supporting undifferentiated hESC (Jones et al., 2010). Calcitriol, has been shown to inhibit the proliferation rates of hMSC, but also inhibited apoptosis and maintained the multipotent capacity of the cells (Klotz et al., 2012). Apart from the above circumstantial evidence, to date, none of these metabolites have shown direct evidence of their functions in the maintenance of undifferentiated hESC.

Finally, with regard to stearidonic acid no relevant study has linked its biological activities with hESC or any other type of stem cells. Nevertheless, due to the action of omega-3 fatty acids (like stearidonic acid) on cellular mechanisms associated with inflammation (Weylandt et al., 2012) and cell signalling (Kim et al., 2008) it is perhaps possible that stearidonic acid modulates some signalling pathways in hESC.

4.1.2 Known functions of small molecules in hESC

Most of the identified mechanisms that control hESC self-renewal, pluripotency and differentiation are known to be regulated by proteins, more specifically, growth factors (e.g. basic fibroblast growth factor (bFGF), transforming growth factor-β (TGFβ)) and cytokines (i.e. activin A) (Avery et al., 2006). However, small molecules have also been shown to play an important role in the maintenance of pluripotent hESC. For example, when cultured in medium supplemented with sphingosine-1-phosphate (S1P), it was found that S1P enhanced survival and proliferation of hESC (Inniss and Moore, 2006). Furthermore, when S1P was used in combination with platelet-derived growth factor (PDGF), hESC also maintained an undifferentiated state (Pebay et al., 2005). More recently, evidence has emerged that synthetic small molecules may have relevance in modulating hESC self-renewal. Using high-throughput chemical screening approaches, Xu et al identified two small molecules,

thiazovivin (Tzv) and tyrintegin (Ptn), that promoted hESC survival and self-renewal (Xu et al., 2010). Interestingly, they discovered that the survival-promoting effect was due to the fact that Tzv and Ptn increased cell attachment following cell dissociation and seeding processes (Xu et al., 2010). A recent high-content screening also reported the identification of other synthetic small molecules, some of which were neurotransmitter antagonists (trimipramine and ethopropazine), that supported the long-term expansion of undifferentiated hESC without bFGF in the medium, however, the efficiency was lower than when cells were cultured in MEF-CM (Kumagai et al., 2013). All this highlights the notion that low-molecular weight factors can be of paramount importance during maintenance of pluripotent hESC.

Therefore, given the increasing evidence that small molecules have important roles in the maintenance of undifferentiated hESC, it is possible that the selected metabolites generated in MEF-CM (previously identified in chapter 3) play key roles in the proliferation and pluripotency maintenance of hESC as they do in other type of stem cells. Such a possibility will be explored in this chapter. To the best of the author's knowledge, this is the first time that metabolites identified in MEF-CM have been investigated for their effects on hESC.

4.1.3 Aims and objectives

- To confirm by liquid chromatography and mass spectrometry the identity of the selected metabolites found in MEF-CM that could potentially mediate some functions in hESC.

- To develop a quantification method and measure the concentrations of the confirmed metabolites in several batches of MEF-CM.

- To investigate the effects of selected and confirmed metabolites of MEF-CM on the proliferation of hESC in culture.

4.2 Materials and methods

4.2.1 Chemicals

Acetonitrile, methanol and chloroform were HPLC-grade and obtained from Fischer Scientific (Loughborough, UK). Deionized water (18.2MΩ) was prepared using an ELGA USF-Maxima water purification system (Marlow, UK). Mass spectrometry-grade formic acid, dimethylsulfoxide and 7-ketocholesterol (7-KC) were purchased from Sigma-Aldrich (Gillingham, UK). Prostaglandin D_2 (PGD_2), prostaglandin H_2 (PGH_2), 6-keto-prostaglandin F1α (6-keto-PGF1α) and stearidonic acid (SA) were all obtained from Cambridge Bioscience (Cambridge, UK). Prostaglandin E_2 (PGE_2) was purchased from BioVision (Bedfordshire, UK) whereas 1, 25-dihydroxyvitamin D3 (calcitriol) was obtained from Tocris Bioscience (Bristol, UK). 9(S), 10(S), 13(S)-trihydroxy-11(E)-octadecenoic acid (9, 10, 13-TriHOME) and 9(S), 12(S), 13(S)-trihydroxy-10(E)-octadecenoic acid (9, 12, 13-TriHOME) were both purchased from Larodan Fine Chemicals (Malmö, Sweden). All tissue culture reagents were obtained from Invitrogen.

4.2.2 Preparation of standards

Standards were prepared according to the purpose of the individual experiments as described in sections below. For identity confirmation of the increased metabolites of MEF-conditioned medium (previously reported in chapter 3), the standards were subjected to LC-MS and LC-MS/MS analyses. The successfully confirmed analytes were then tested in hESC culture.

4.2.2.1 Preparation of standards for LC-MS and LC-MS/MS analyses

All standards stock solutions for LC-MS and LC-MS/MS analyses were prepared with 75% MeOH with the exception of 7-KC which, due to its lower polarity, was diluted in a 50:50 chloroform/MeOH mixture. To reach a final working concentration solution, further dilutions were made for all the standards with 75% MeOH. The working concentration for all

the standards was 20 ng/mL except for calcitriol whose final concentration was 1 µg/mL. The stock solutions were stored at -80ºC.

4.2.2.2 Preparation of standards for hESC culture

Stock solutions of PGE_2, 6-keto-PGF1α, 7-KC, SA and 9, 12, 13-TriHOME were prepared with DMSO under sterile conditions for hESC culture. Further dilutions were also made with DMSO in order to achieve the tested concentrations which are detailed later in the results and discussion section of this chapter. Likewise, the stock solutions were stored at -80ºC.

4.2.3 Sample preparation

MEF-conditioned medium (MEF-CM) samples from batches 107, 115, 116, 117, 118, 120, 121 and 122 were prepared three times using the protein precipitation method described in chapter 2. The preparation of the MEF-CM batches has been described in section 3.2.3, chapter 3.

4.2.4 Liquid chromatography and mass spectrometry methods

The chromatographic conditions of all the experiments in this chapter were as described in section 3.2.6, chapter 3. Different mass spectrometry (MS) settings were employed for metabolite identification/confirmation and for metabolite quantification as described in sections 4.2.4.1 and 4.2.4.2.

4.2.4.1 LC-MS for identity confirmation

To compare exact masses and retention times, samples and standards were injected into the Exactive Orbitrap mass spectrometer via an Accela U-HPLC system (both from Thermo Fischer Scientific, USA) and were analysed maintaining the MS parameters detailed in section 3.2.7, chapter 3.

To obtain MS/MS spectra both samples and standards were injected into an Accela U-HPLC system hyphenated to an LTQ Velos mass spectrometer (Thermo Fischer Scientific, USA) operated in data

dependent mode. The collision energy used was 35 eV. The MS settings were the same as those described in section 2.2.5.

4.2.4.2 LC-MS for metabolite quantification

For metabolite quantification slight modifications to the original MS settings (section 3.2.6, chapter 3) were made in order to increase the number of data points to measure more accurately the analyte peak areas. First, instead of analysing the samples in +ESI and –ESI modes simultaneously, the number of scan events was restricted to only that ionisation mode (+ve or –ve) in which the analyte was detected. Second, in addition to the original 2 Hz (50000 FWHM) scan rate of the method, a 4 Hz (25000 FWHM) scan rate was also explored to compare the number of data points obtained with each scan rate. Metabolite quantification was performed using the Exactive Orbitrap mass spectrometer.

4.2.5 Human embryonic stem cell culture

The hESC line HUES7, between passages 26 and 30, was cultured on Matrigel with unconditioned medium (UM) as negative control, unconditioned medium supplemented with the small molecules (UM+sup) and with MEF-CM as positive control. Cells were passaged every three days by incubation with 0.05% accutase for 3 min at 37ºC. Population doublings (PDs) were calculated at each passage with the formula $[\log_{10}(\text{cells harvested/cells seeded})/\log_{10}(2)]$, where the number of seeded cells was $2x10^6$ cells/well. Proliferation rates were calculated by hours in test culture/cumulative PDs (Mahlstedt et al., 2010). The hESC culture was carried out by Dr James Smith, Wolfson Centre for Stem Cells, Tissue Engineering & Modelling, Centre for Biomolecular Sciences, University of Nottingham.

4.2.6 Data analysis

LC-MS data were quantified using QuanBrowser Xcalibur 2.2 software (Thermo Fischer Scientific, USA) and are expressed as mean ± SD.

4.3 Results and discussion

4.3.1 Confirmation of chemical identity of increased metabolites found in MEF-CM

The selected metabolites to be tested in hESC culture are shown in Table 4-1 along with their *m/z* values and their possible isomers. The putative identity of these metabolites was confirmed by means of liquid chromatography and mass spectrometry as detailed below.

Table 4-1. List of metabolites selected for hESC culture testing.

Accurate mass (m/z)	Ion	Formula	Putative identification
275.2016	$[M-H]^-$	$C_{18}H_{28}O_2$	Stearidonic acid
329.2333	$[M-H]^-$	$C_{18}H_{34}O_5$	9, 10, 13-TriHOME or 9, 12, 13-TriHOME
333.2071	$[M-H_2O-H]^-$	$C_{20}H_{32}O_5$	PGE_2 or PGD_2 or PGH_2
369.2282	$[M-H]^-$	$C_{20}H_{34}O_6$	6-keto-PGF1α
401.3414	$[M+H]^+$	$C_{27}H_{44}O_2$	7-Ketocholesterol
417.3363	$[M+H]^+$	$C_{27}H_{44}O_3$	Calcitriol

4.3.1.1 Chromatography and exact mass matching identification

Initial identity confirmation started with the comparison of retention times and exact masses of the metabolites in the samples with those of the standards (Figure 4-1). The extracted ion chromatograms (EICs) of 6-keto-PGF1α, stearidonic acid, and 7-KC in the samples matched perfectly the retention time and exact mass of their respective standards. Because the results of PGE_2 (or its isomers PGD_2 and PGH_2), 9, 10, 13-TriHOME (or its isomer 9, 12, 13-TriHOME) and calcitriol represented special cases, they will be discussed below in more detail.

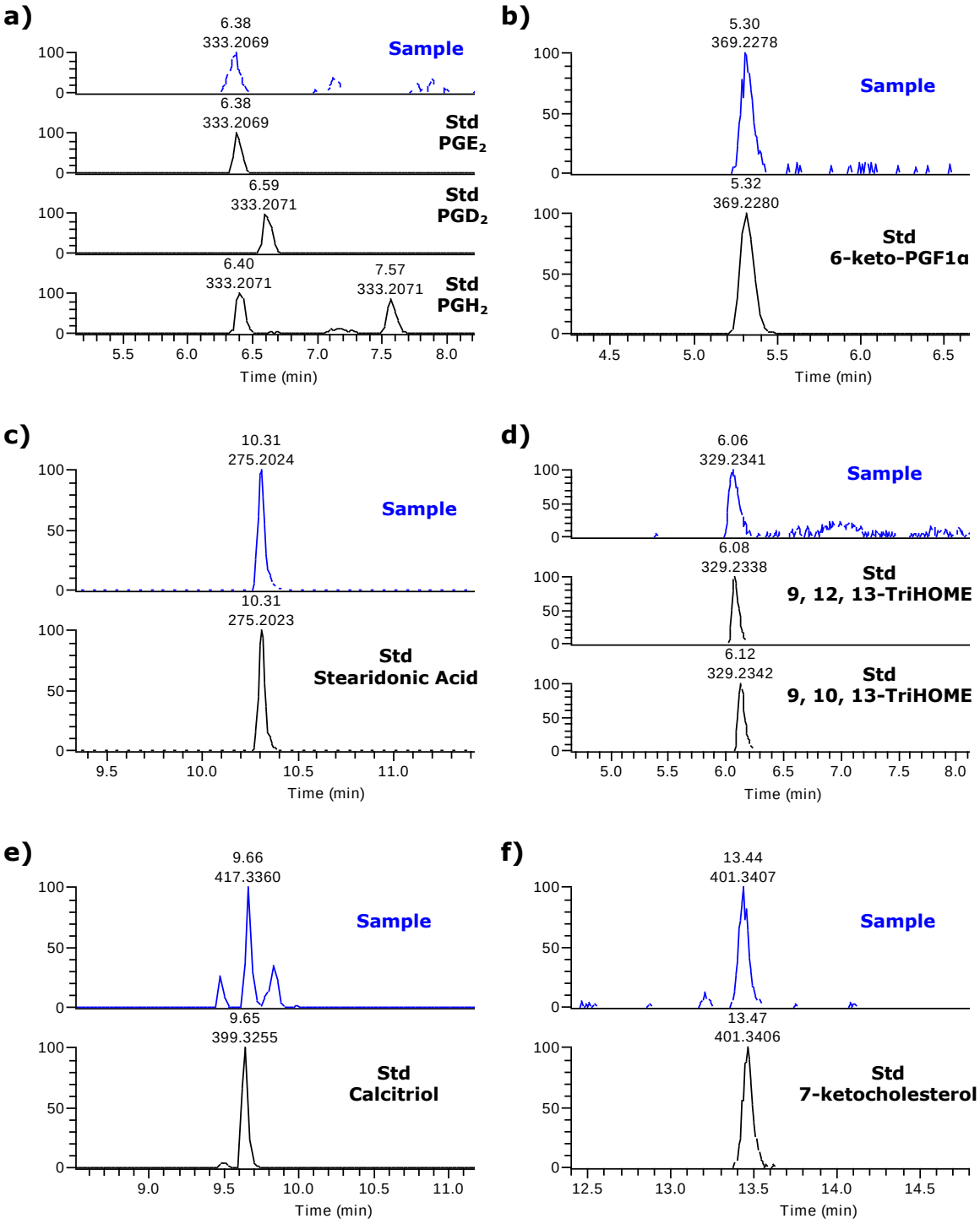

Figure 4-1 Comparison of retention times and exact masses using extracted ion chromatograms (EICs) of metabolites in the samples (blue) and standards (black). Chromatographic confirmation of a) PGE_2, b) 6-keto-PGF1α, c) stearidonic acid, d) 9, 12, 13-TriHOME and possibly 9, 10, 13-TriHOME and f) 7-ketocholesterol in MEF-CM. e) calcitriol standard matched the retention time of the sample but failed to show the $[M+H]^+$ ion.

PGE_2, PGD_2 or PGH_2

Since the ion at *m/z* 333.2071 matched the exact $[M–H_2O–H]^-$ ion mass of PGE_2, PGD_2 and PGH_2, the standards of the three prostaglandins were injected in order to find out which of the three isomers was present in MEF-CM. Chromatographically, PGE_2 standard was the only one that matched the retention time of the sample (Figure 4-1a). The peak at 6.40 min of PGH_2 standard is the result of its inherent instability that converts a proportion of PGH_2 to PGE_2 (Quraishi et al., 2002) and so likewise pairs up with the retention time of the sample and of PGE_2 standard; however, the actual retention time of PGH_2 standard is the second peak at 7.57 min. As PGD_2 standard clearly eluted at different retention time of the sample, then it can be concluded that PGE_2 is the compound that is present in MEF-CM.

9, 10, 13-TriHOME or 9, 12, 13-TriHOME

The ion at *m/z* 329.2336 matched the exact mass of 9, 10, 13-TriHOME and 9, 12, 13-TriHOME. Both standards were injected but due to their high chemical structure similarity (Figure 4-2a,b) they were separated only by a small fraction of time (Figure 4-1d). When the EICs of the sample and standards were superimposed (Figure 4-2c), it was observed that 9, 12, 13-TriHOME was the most likely compound present in MEF-CM as its retention time matched better that of the sample, nevertheless, it was not ruled out the possibility that a small proportion of 9, 10, 13-TriHOME was also present.

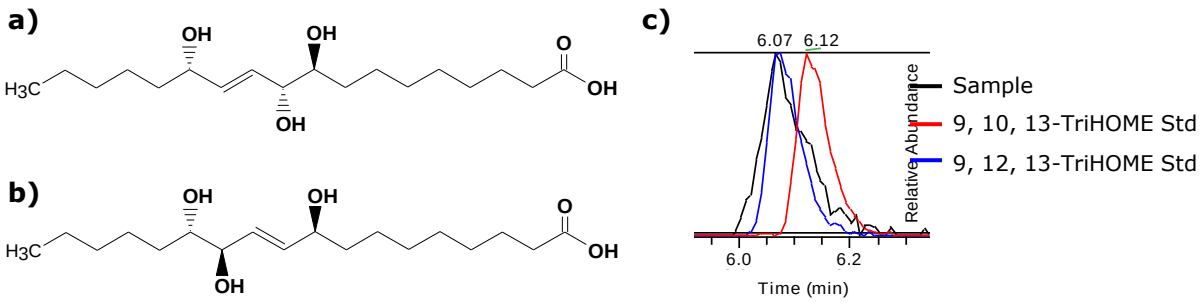

Figure 4-2 Chemical structure of a) 9, 10, 13-TriHOME and b) 9, 12, 13-TriHOME. c) superimposition of the extracted ion chromatograms of the two standards and of the sample.

Calcitriol

An interesting result was that obtained with calcitriol standard as it matched the retention time of the sample, but spectrometrically it behaved differently. As observed in Figure 4-1e, the most abundant ion of calcitriol standard was the $[M–H2O+H]^+$ ion at *m/z* 399.3255 whereas that of the sample was the $[M+H]^+$ ion at *m/z* 417.3360. When the *m/z* 417.3360 ion of calcitriol standard was extracted, the peak was almost undetectable as it produced a very low intensity peak (data not shown). Therefore, these results suggest that the compound detected in MEF-CM was not calcitriol but possibly a structural isomer whose $[M+H]^+$ ion is more stable. Further investigation was conducted with MS/MS experiments to confirm the false identity.

4.3.1.2 Tandem mass spectrometry (MS/MS) confirmation

Final metabolite confirmation was accomplished with tandem mass spectrometry by comparing the MS/MS spectra of both the metabolites in the samples and authentic standards (Figure 4-3 and Figure 4-4). With the exception of calcitriol, the rest of metabolites' MS/MS spectra matched those of their standards, thus, confirming their presence in MEF-CM. In the case of the ion at *m/z* 329.2336, the MS/MS spectrum of the sample presented characteristic fragment peaks of both standards (9, 10, 13-TriHOME and 9, 12, 13-TriHOME). The specific peak of 9, 10, 13-TriHOME was the fragment ion at *m/z* 171.1 whilst those of 9, 12, 13-TriHOME were *m/z* 211.2 and *m/z* 229.2 (Figure 4-4). The presence of the three fragment ions in the MS/MS spectrum of the sample strongly suggests that both compounds are present in MEF-CM. On the other hand, the MS/MS spectrum of calcitriol standard did not match that of the sample, therefore the presence of calcitriol in MEF-CM was ruled out. Nonetheless, the matching in retention time and exact mass of the unknown compound still suggests that possibly a very close structural isomer of 1, 25-dihydroxyvitamin D3 (calcitriol) might be the one present in the sample. The most likely compound seems to be 24, 25-dihydroxyvitamin D3 according to the human metabolome database (Wishart et al., 2009); however this requires further experimental

verification with the authentic standard which was beyond the scope of this thesis.

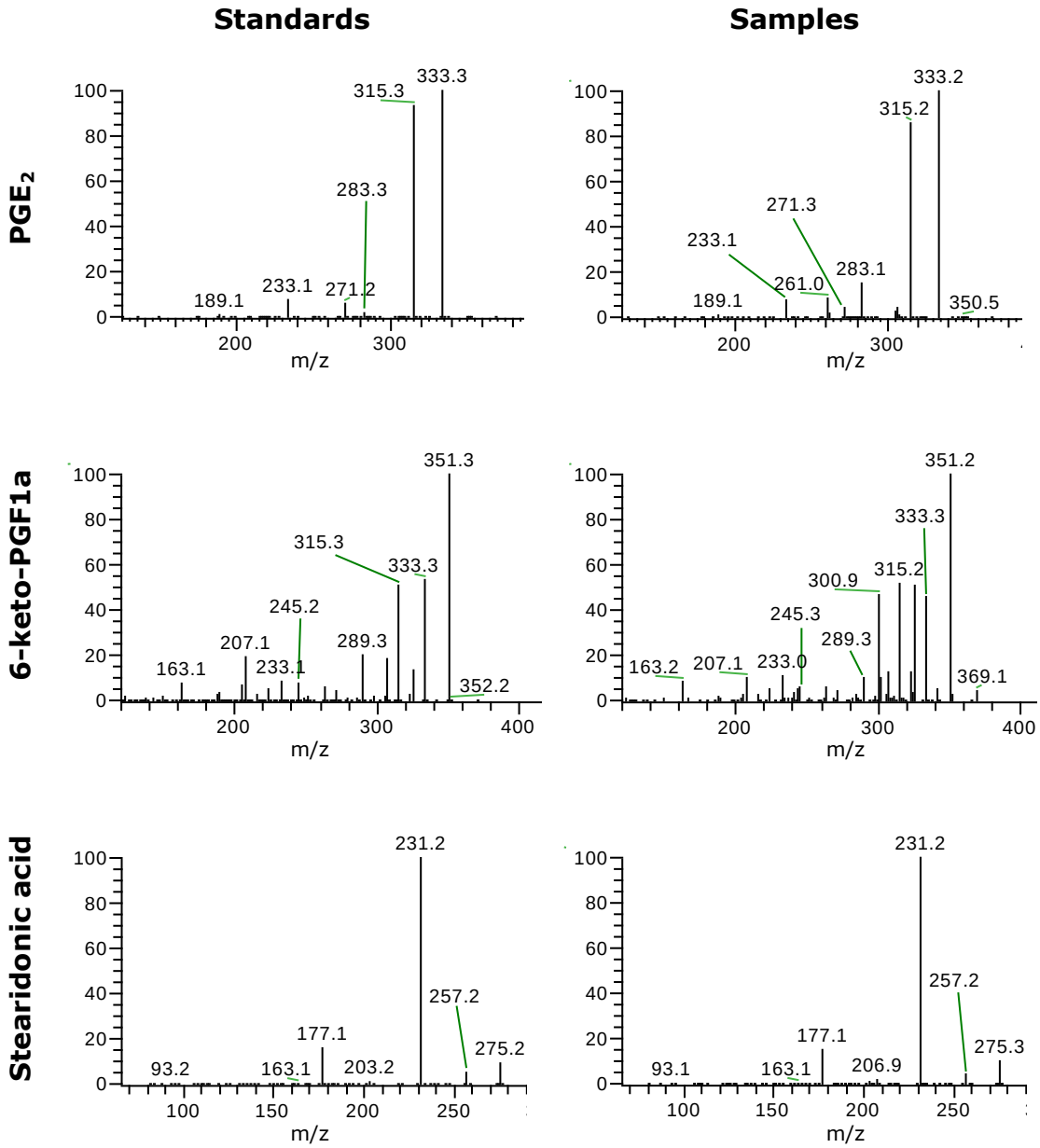

Figure 4-3 Comparison of MS/MS spectra of standards (left panel) and samples (right panel). Tandem MS finally confirmed the presence of these metabolites in MEF-CM.

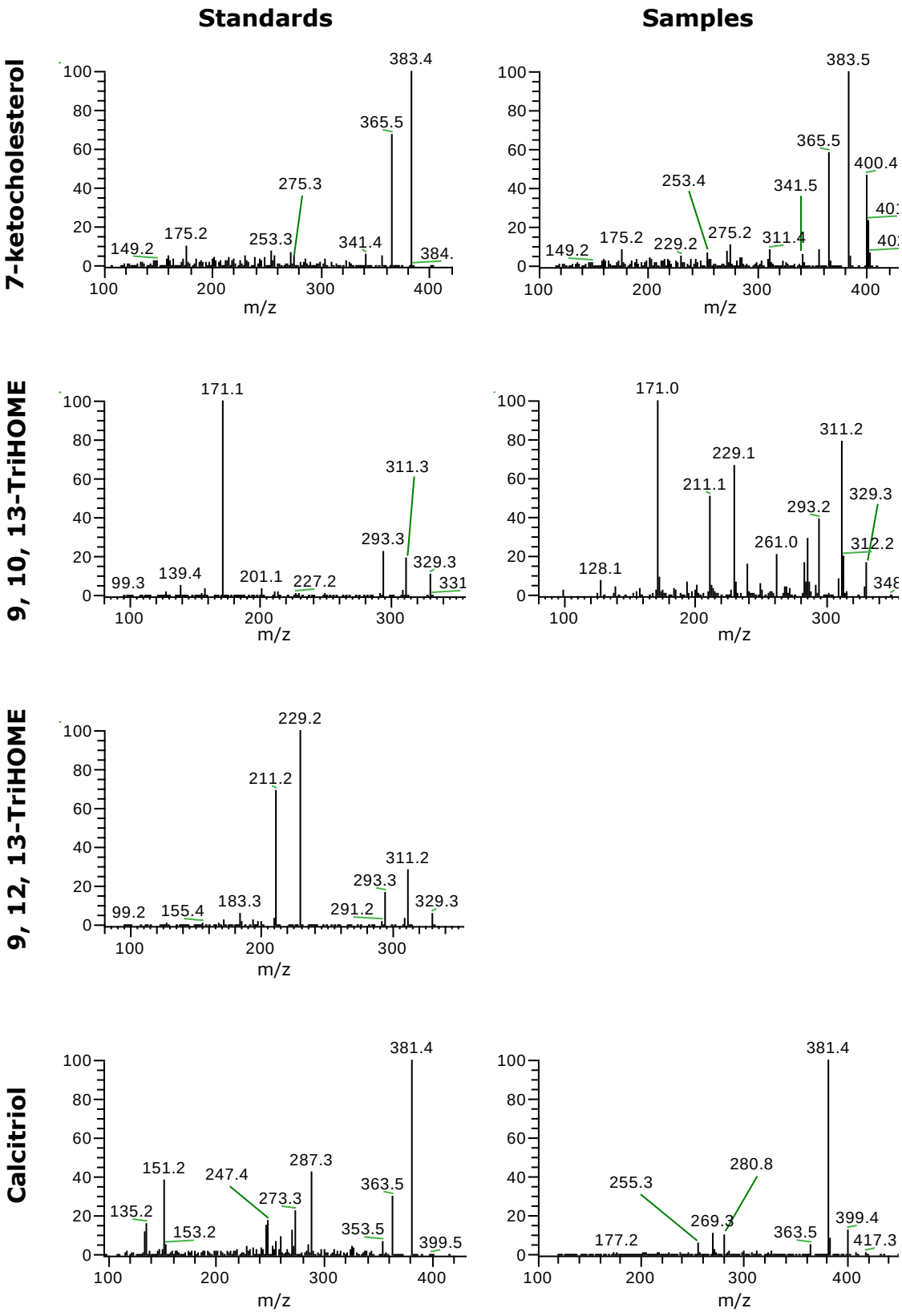

Figure 4-4 Comparison of MS/MS spectra of standards (left panel) and samples (right panel). The ion at *m/z* 329 in the sample showed the characteristic peaks of the standards 9, 10, 13-TriHOME and 9, 12, 13-TriHOME, suggesting that both compounds may be present in MEF-CM. MS/MS spectrum of calcitriol standard did not match that of the sample thus ruling out definitely that the *m/z* 417 ion in the sample is calcitriol.

4.3.2 Quantification of confirmed metabolites

Having confirmed which of the selected metabolites were truly present in MEF-CM, it was decided to estimate their concentrations in several batches of MEF-CM so that the tested concentrations used in hESC culture experiments (described in section 4.3.3) resembled the levels at which these metabolites are normally present in MEF-CM. For this purpose a quantification method was developed.

4.3.2.1 MS quantification method development

Metabolite quantification was carried out in the Exactive Orbitrap mass spectrometer. Two scan rates (2 and 4 Hz) were investigated during the quantification method development in order to find out the scan rate that produced the largest number of data points per peak while maintaining high mass accuracy. Figure 4-5 indicates the number of data points and mass errors obtained at 2 and 4 Hz for selected peaks (PGE_2 and 6-keto-PGF1α).

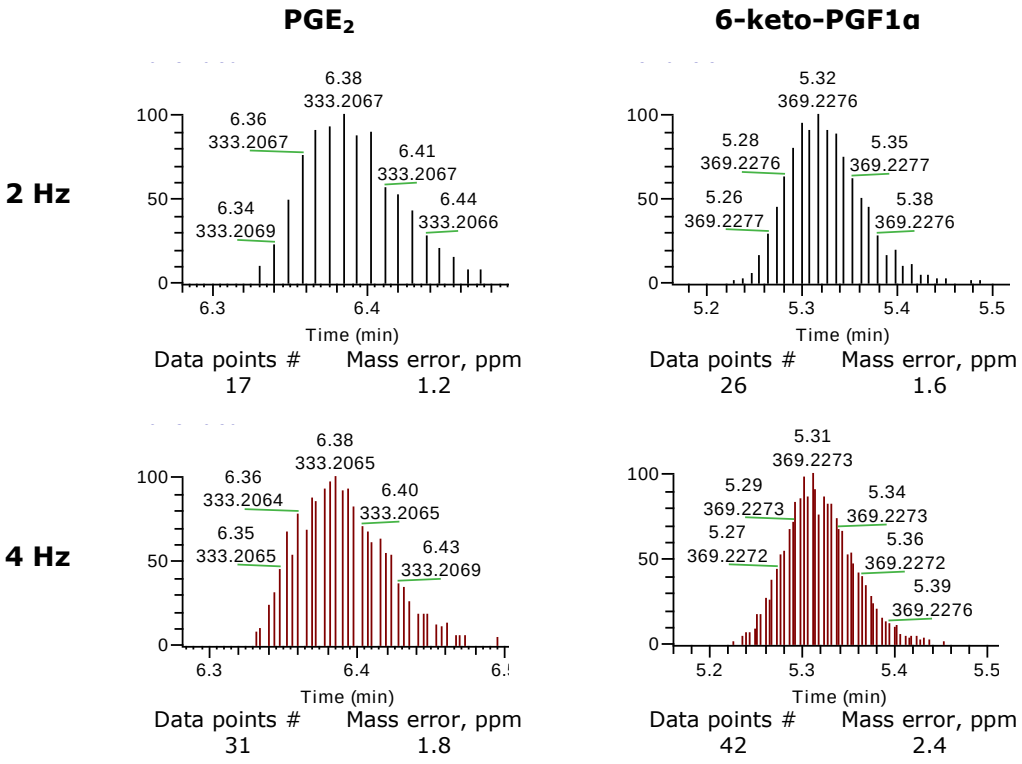

Figure 4-5 Extracted ion chromatograms of PGE_2 and 6-keto-PGF1α showing the number of data points obtained at 2 and 4 Hz scan rates as well as the mass accuracy across the peak. Each line represents one data point.

Because quantification selectivity with high resolution mass spectrometry (HRMS) is attained by the employment of EICs by centring a narrow mass window on the theoretical *m/z* value of the analyte (Xiao et al., 2012), the scan rate with the highest mass accuracy will produce the most reliable results. In this experiment, the 2 Hz scan rate produced better mass accuracy (smaller mass errors) than the 4 Hz scan rate although at the expense of reduced number of data points per peak; however, since the number of points was still enough for precise quantification (>10) (Frank and McIntyre, 2009), the 2 Hz scan rate was selected for quantification of all the confirmed metabolites.

The use of Orbitrap-based HRMS was preferred over the traditional triple quadrupole mass spectrometer (QqQ) (Lu et al., 2008) for quantification of the small molecules studied because the methodology was readily adapted from the untargeted metabolomics procedures already used. Using the Orbitrap Exactive method avoided the preoptimisation (collision energy, declustering voltage and collision cell exit potential) of target analytes which is a prerequisite for method development with QqQ. Furthermore, the quantitative capabilities of Orbitrap-based HRMS have been demonstrated to be similar to those of QqQ (Lu et al., 2010, Bateman et al., 2009); thus, offering a reliable and faster alternative to QqQ.

4.3.2.2 Measurement of metabolites in MEF-CM

Supportive MEF-CM batches 107, 115, 116, 117, 118, 120, 121 and 122 were analysed using the method described to give targetted, quantitative measurements of the concentrations of all the confirmed metabolites of interest. The concentrations obtained for each metabolite in each batch are presented in Table 4-2. In spite of the fact that 9, 10, 13-TriHOME and 9, 12, 13-TriHOME may be both present in the conditioned medium, it was decided to use 9, 12, 13-TriHOME for quantification and subsequent test in hESC culture since it matched better the retention time of the sample and seemed to be the molecule at higher proportion in the sample as it covered a larger area of the sample peak (Figure 4-2c).

Table 4-2. Quantification results of the metabolites that were confirmed to be present in MEF-CM.

Prostaglandin E_2

Range: 12.51 – 37.08 ng/mL

Batch #	Mean ± SD, ng/mL	RSD%
107	12.54 ± 0.14	1.09
115	21.94 ± 0.76	3.48
116	21.98 ± 0.51	2.34
117	14.16 ± 0.27	1.87
118	12.51 ± 0.17	1.39
120	37.08 ± 1.50	4.05
121	19.35 ± 0.44	2.30
122	13.64 ± 0.44	3.19

6-Keto-prostaglandin F1a

Range: 0.93 – 2.67 ng/mL

Batch #	Mean ± SD, ng/mL	RSD%
107	2.58 ± 0.19	7.33
115	2.20 ± 0.10	4.54
116	2.67 ± 0.10	3.62
117	1.02 ± 0.06	5.75
118	1.01 ± 0.07	6.69
120	2.14 ± 0.07	3.20
121	1.28 ± 0.05	4.18
122	0.93 ± 0.10	10.96

7-Ketocholesterol

Range: 38.47 – 48.65 ng/mL

Batch #	Mean ± SD, ng/mL	RSD%
107	46.94 ± 2.51	5.34
115	48.65 ± 1.25	2.57
116	43.96 ± 0.48	1.10
117	43.08 ± 2.36	5.49
118	46.35 ± 1.44	3.10
120	48.00 ± 1.60	3.34
121	41.28 ± 1.08	2.61
122	38.47 ± 0.56	1.46

Stearidonic acid

Range: 75.35 – 126.50 ng/mL

Batch #	Mean ± SD, ng/mL	RSD%
107	124.66 ± 3.97	3.18
115	97.08 ± 1.60	1.65
116	126.50 ± 5.68	4.49
117	75.35 ± 0.39	0.52
118	90.32 ± 1.36	1.51
120	92.19 ± 1.22	1.32
121	89.48 ± 2.42	2.71
122	95.13 ± 0.62	0.65

9, 12, 13-TriHOME

Range: 2.43 – 4.42 ng/mL

Batch #	Mean ± SD, ng/mL	RSD%
107	2.43 ± 0.10	4.26
115	4.42 ± 0.20	4.46
116	4.27 ± 0.11	2.66
117	3.27 ± 0.24	7.37
118	3.96 ± 0.07	1.65
120	4.24 ± 0.12	2.89
121	3.53 ± 0.26	7.34
122	3.45 ± 0.10	2.84

Results for each batch expressed as mean ± standard deviation (n=3)

High batch-to-batch variability was observed as judged by the wide range of concentrations found for each metabolite. Amongst all the metabolites quantified, PGE_2 and 6-keto-PGF1α showed the highest variability with maximum concentrations 3-fold greater than the minimum concentrations. Other metabolites showed more constant levels, but still with considerable variations. On the other hand, as to the method performance, high reproducible measurements were obtained with precision variability (RSD%) below 15%, an acceptable criterion for LC-MS methods (FDA, 2013). Furthermore, the calibration curves for all the analytes showed excellent linearity of response (R^2 > 0.99) over the entire concentration range tested for each analyte (Table 4-3). What is more, at all concentration levels, the variability in the precision (RSD%) was also less than 15%. Although it is recognised that full validation of the method would be required for a greater degree of confidence on the results; for the purpose of this experiment, the results obtained with this quantification method offered a good estimate of the concentrations of the selected metabolites in MEF-CM.

With the exception of PGE_2 and 6-keto-PGF1α, no study had previously confirmed and reported concentrations of 7-ketocholesterol, stearidonic acid and 9, 12, 13-TriHOME in MEF-CM. Jones et al, by means of DNA microarray analysis, had identified in MEF-CM increased mRNA levels of cyclooxygenase-2 (COX-2) and prostaglandin I_2 synthase (PGIS), two prostaglandin biosynthesis genes, whose downstream products are PGE_2 and 6-keto-PGF1α, respectively. Therefore, they quantified and reported levels of PGE_2 and 6-keto-PGF1α at 9.1 and 4.3 ng/mL, respectively (Jones et al., 2010). They measured the prostaglandins' levels using only one batch of MEFs (CF1 strain) to condition the medium and their quantification method was based on an enzyme-linked immunosorbent assay (ELISA). The differences in mouse strain and quantification methodology used by Jones et al and the ones employed here could explain the discrepancies between their results and those reported in this chapter. For example, it is known that antibody-based methods for quantification of prostaglandins suffer from cross-reactivity with related

Table 4-3. Linearity and precision of the calibration curves for metabolites measured in MEF-CM.

Analyte	Slope	R^2	Concentration, ng/mL	Peak area mean (n=3)	Precision RSD%
PGE_2	y = 12390x	0.9933	1.0	12028	1.64
			2.5	28430	3.56
			5.0	71674	2.07
			10.0	133095	0.40
			20.0	241097	0.91
6-keto-PGF1α	y = 50763x	0.9972	1.0	51665	0.86
			2.5	125245	0.77
			5.0	282409	1.58
			10.0	529747	1.79
			20.0	997211	0.69
7-Ketocholesterol	y = 5850.87x	0.9947	2.6	14847	14.80
			5.2	26619	2.32
			6.9	38723	7.57
			10.4	59366	2.07
			20.8	123978	2.14
Stearidonic acid	y = 5904.24x	0.9986	5.0	13527	14.64
			10.0	31000	1.74
			20.0	59254	1.38
			40.0	147126	0.39
			80.0	293176	2.68
9, 12, 13-TriHOME	y = 58741.5x	0.9988	0.16	26371	4.12
			0.50	55048	2.15
			1.00	112017	0.97
			2.50	235465	0.29
			5.00	474904	2.71

compounds which results in reduced selectivity, producing ambiguous and possibly misleading results (Il'yasova et al., 2004). In contrast, mass spectrometry-based approaches have demonstrated to be more selective and reliable (Cao et al., 2008, Il'yasova et al., 2004). Consequently, given the number of batches analysed in this chapter, the results reported in Table 4-2 represent, with high degree of confidence, the typically secreted concentrations of PGE_2, 6-keto-PGF1α, 7-ketocholesterol, stearidonic acid and 9, 12, 13-TriHOME in MEF-conditioned medium.

4.3.3 Effect of medium supplementation with confirmed metabolites on proliferation of cultured hESCs

Finally, to determine whether or not the small molecules found in MEF-CM had an effect on hESC, HUES7 cells were cultured on Matrigel with UM supplemented with the compounds listed in Table 4-4 (UM+sup). Because of the wide range of concentrations found for each metabolite in MEF-CM batches (Table 4-2), the concentration chosen to be tested was the grand mean (mean of means) of the batches' concentration means, also shown in Table 4-4.

Table 4-4. Compounds tested in hESC culture.

Compound name	Concentration tested, ng/mL
Stearidonic acid	98.84
9, 12, 13-TriHOME	3.70
PGE_2	19.15
6-keto-PGF1α	1.73
7-Ketocholesterol	44.59

Additionally, the cells were cultivated with UM and MEF-CM to be used as negative and positive control, respectively. Figure 4-6a shows the growth curves for each culture system.

a)

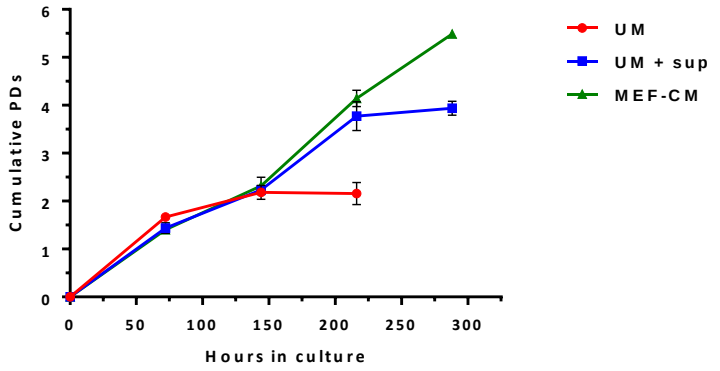

b)

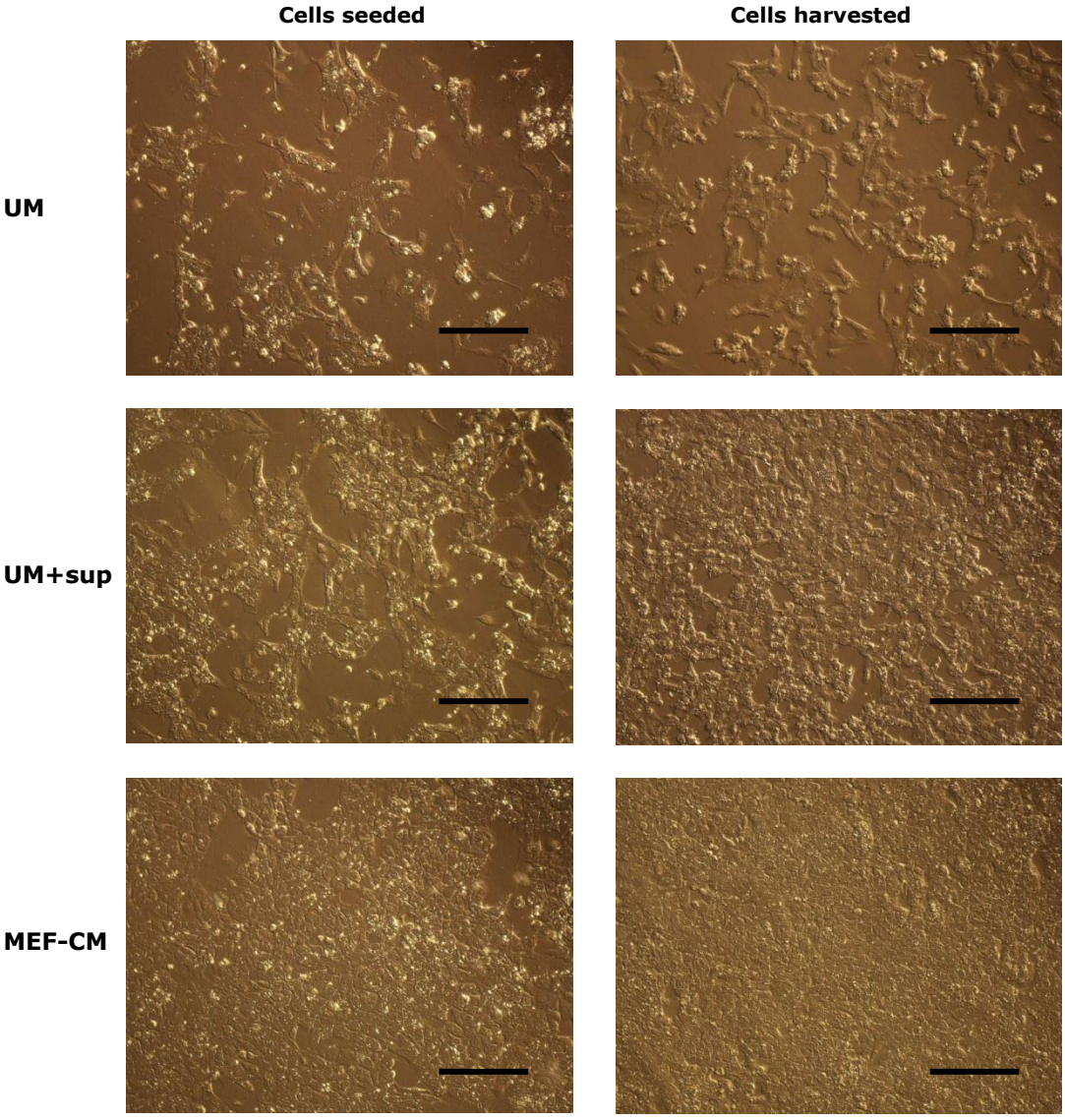

Figure 4-6 a) Growth curves of HUES7 cells when cultured with UM, UM+sup and MEF-CM. b) Proliferation of HUES7 cells at passage number 3. When cultured with UM alone, the cells could no longer be expanded; however, when the small molecules were added (UM+sup) an enhancement in proliferation was observed, indicating that the mix of molecules had a proliferative effect. As expected, with MEF-CM, cells had the best growth rate. Scale bars = 250 µm.

Whereas cells cultured with MEF-CM showed a continuous growth over the test period, cells cultivated with UM alone could no longer be expanded after passage 3. In contrast, when UM was supplemented with the small molecules (UM+sup), cells could still expand for one more passage. A significant increase in the cell number is observed at passage 3 when cells are incubated in the presence of the small molecules than when the small molecules are absent (Figure 4-6a). Figure 4-6b shows the proliferation observed at passage number 3 with UM+sup as compared with the loss of expansion using UM alone. Cells appear to be more confluent when exposed to the compounds than when they are not. These results imply that the mix of compounds exerted a proliferative effect; however, as the proliferation observed was only in the short term, it is not clear yet whether the proliferative effect was indeed of undifferentiated cells or if some differentiation occurred. If long-term culture had been achieved then examination of pluripotency markers (e.g. Oct4, Sox2) would have determined if the cells still preserved their undifferentiated state. Nonetheless, the proliferative effect is a great achievement taking into account that the molecules were tested in the absence of MEF-derived growth factors. Therefore, it is very likely that if supplemented with growth factors that promote hESC survival, the tested small molecules could be beneficial for the long-term expansion of hESC. Furthermore, as none of these compounds have been reported in the formulations of more defined culture media like StemPro (Wang et al., 2007) and mTeSR1 (Ludwig et al., 2006a), they represent potential candidates to enhance their efficiency.

Although further research is needed, these results represent one more step towards the development of more defined and efficient culture systems.

4.4 Conclusions

Based on retention time, exact mass and tandem mass spectrometry (MS/MS) it was possible to confirm the identity of PGE_2, 6-keto-PGF1α, 7-ketocholesterol, stearidonic acid, 9, 10, 13-TriHOME and 9, 12, 13-TriHOME. To the best of the thesis author's knowledge this was the first time that 7-ketocholesterol, stearidonic acid, 9, 10, 13-TriHOME and 9, 12, 13-TriHOME were reported to be present in MEF-CM.

The ion at *m/z* 417.3360 remained unidentified as it failed to match the MS/MS spectrum of calcitriol standard. Nevertheless, its exact mass and retention time matched those of calcitriol standard which suggested that a structural isomer of calcitriol (24, 25-dihydroxyvitamin D3) may be the one present in MEF-CM. However, because this was beyond the scope of this chapter the final identity of the ion at *m/z* 417.3360 could not be confirmed.

A quantification method was developed using the Exactive Orbitrap mass spectrometer and it showed excellent linearity of response for all the analytes measured. Quantification of the compounds using different batches of MEF-CM showed great variability between batches.

When PGE_2, 6-keto-PGF1α, 7-ketocholesterol, stearidonic acid and 9, 12, 13-TriHOME were finally tested in the *in vitro* culture of hESC they seemed to enhance the proliferation of hESC as compare to the negative control (UM alone). This demonstrated that metabolites secreted by MEFs are also important in the maintenance and proliferation of hESC. However, further research is required to identify more precisely which of the five molecules exerted the observed effect.

CHAPTER 5

Metabolomics analysis of the spent culture media of hESC when cultured with MEF-CM and StemPro

5 Metabolomics analysis of the spent culture media of hESC when cultured with MEF-CM and StemPro

5.1 Introduction

An alternative strategy to investigate the factors that allow hESC to proliferate and maintain an undifferentiated state is the study of their extracellular microenvironment; that is, the study of the culture medium that has been used to support their growth. It has been demonstrated that hESC can secrete a number of factors that also contribute to their own survival and proliferation (Dvorak et al., 2005, Przybyla and Voldman, 2012), in addition to the extrinsic growth factors added to the culture medium. The rich and complex set of small- and macro-molecules secreted from living cells is known as the secretome (Makridakis et al., 2013). Furthermore, some of the factors released in the secretome have the ability to activate signalling pathways in an autocrine and/or paracrine manner. An autocrine mediator is that which binds and activates the receptors present on the surface of the same cell that produced it, whereas a paracrine mediator is released by one cell and subsequently interacts with receptors on neighbouring cells (Figure 5-1). Several autocrine and paracrine factors have been identified in hESC and will be described next.

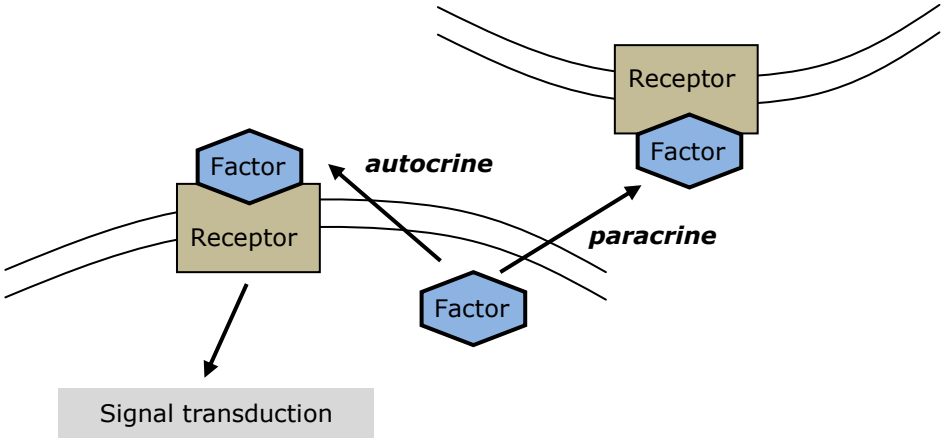

Figure 5-1 Schematic representing the autocrine and paracrine functions of a factor released into the extracellular microenvironment.

5.1.1 Known autocrine/paracrine signalling pathways in hESC

Fibroblast growth factor 2, also known as basic fibroblast growth factor (bFGF), has been extensively added exogenously to the medium in feeder-free culture systems to support the proliferation of undifferentiated hESC (Levenstein et al., 2006, Amit et al., 2004, Xu et al., 2001, Inzunza et al., 2005). However, it has also been demonstrated that hESC can release bFGF to the medium and that this can activate the bFGF-receptors in an autocrine and/or paracrine fashion (Dvorak et al., 2005), an activity which is thought to be reinforced by the exogenous bFGF (Greber et al., 2007). Members of the transforming growth factor β (TFG-β) superfamily have also been proposed as autocrine mediators (Xu et al., 2008a, Levine et al., 2009, Przybyla and Voldman, 2012). For example, when hESC were cultured at bFGF concentrations of 100 ng/mL but in the absence of exogenous TFG-β, only very minor effects on culture performance were observed; however, when additionally the TFG-β/activin signalling was inhibited, a significant reduction in pluripotent cells was observed which suggested that autocrine/paracrine TFG-β/activin signalling is important for the maintenance of hESC (Xu et al., 2008a). Growth differentiation factor 3 (GDF3), also in the TFG-β superfamily, has been found to be secreted from hESC and helps to maintain their pluripotent state by blocking the bone morphogenetic protein (BMP) signalling (Levine et al., 2009, Levine and Brivanlou, 2006). Finally, endogenous Wnts were also found to have an autocrine role in hESC by blocking neuronal differentiation; thus, maintaining the undifferentiated state (Wexler et al., 2009).

With regard to small molecules, sphingosine-1-phosphate (S1P) has been suggested as a proliferative and pro-stemness autocrine factor in glioblastoma stem cells (Marfia et al., 2014); however, nothing is known about whether such activity occurs in hESC. To date, no small molecule with autocrine function in hESC has been identified, most probably because research has focussed more on the discovery of higher molecular weight factors (i.e. proteins) rather than the small molecule components of the secretome.

5.1.2 Study of the hESC secretome

As with the search for the factors released from MEFs to maintain hESC in a pluripotent state (reviewed in chapter 3), most of the efforts into the investigation of the factors secreted by hESC have also focused on the protein components of the hESC secretome. For example, by employing an MS-based proteomics approach, Bendall et al reported the identification of 245 extracellular proteins in the culture medium obtained from hESC and amongst them 43 were growth factor-like proteins which represented potential hESC regulators (Bendall et al., 2009).

A different strategy for the analysis of the secretome was adopted by Sarkar and colleagues (Sarkar et al., 2012). Instead of the analysis of the culture supernatant, they developed protocols to obtain subcellular fractions from hESC that were enriched in secretory pathway organelles, while preserving the secretory protein cargo. The MS analysis of the fractions revealed 99 putatively secreted proteins from hESC cultured in MEF-CM (Sarkar et al., 2012). The advantage of this strategy was that it did not require the use of customised media (i.e. serum free) as it is usually employed in other secretome analyses (Lim and Bodnar, 2002, Chin et al., 2007). However, one of its drawbacks was the potential cross-contamination of the secretory pathway organelle fractions during the extraction procedures.

At present, the search for small molecule components of the hESC sectretome has been limited by the lack of application of suitable methods for comprehensive analysis. Some methods have been applied for the analysis of the extracellular metabolites (exo-metabolome) of pluripotent stem cells but these have targeted their measurements to a specific set of compounds (e.g. glucose, amino acids) (Rathjen et al., 2014) or have addressed specific metabolic pathways (e.g. glycolysis) (Folmes et al., 2011, Folmes et al., 2013); thus, neglecting the rest of metabolites secreted by hESC. In this context, as the untargeted metabolomics approach developed in chapter 2 met the requirements for the comprehensive analysis of the low-molecular weight factors released by hESC in culture, it was applied here for this purpose. Additionally, the methodology could also detect the compounds that were potentially

consumed by the cells; thus, it also provided a better understanding of the metabolic processes occurring during the *in vitro* culture of hESC.

The untargeted measurement of the exo-metabolome (known as *metabolomics footprinting*) was applied here for the investigation of the metabolites secreted and/or consumed by hESC cultured under feeder-free conditions (Matrigel) using MEF-CM or StemPro™. A chemically defined medium such as StemPro™ (Wang et al., 2007) was also included because its less complex composition, in theory, would allow a better appreciation of the metabolites secreted into the medium. As far as the thesis author is aware, this is the first untargeted and most comprehensive LC-MS-based metabolomics study of the hESC small molecule secretome.

5.1.3 Aims and objectives

- To apply the untargeted metabolomics method developed in chapter 2 for the comprehensive analysis of low-molecular weight components of the hESC secretome.

- To identify potential small-molecule autocrine/paracrine factors released by hESC during *in vitro* culture.

- To analyse and compare the hESC exo-metabolome obtained with MEF-CM and the chemically defined medium StemPro™, when cells are cultured on Matrigel.

5.2 Material and methods

5.2.1 Chemicals

HPLC-grade acetonitrile and methanol were obtained from Fischer Scientific (Loughborough, UK). Deionized water (18.2MΩ) was prepared using an ELGA USF-Maxima water purification system (Marlow, UK). Mass spectrometry-grade formic acid was purchased from Sigma-Aldrich (Gillingham, UK) and the tissue culture reagents were obtained from Invitrogen.

5.2.2 Human embryonic stem cell culture

The hESC line HUES7, between passages 28 and 29, was cultured on Matrigel with two different culture media; namely, MEF-CM and the chemically defined medium StemPro™ (Life Technologies). Cells were seeded at $1.5x10^6$ cells per flask and given 24 hours to adhere. Subsequently, cells were fed with fresh culture media that was collected 24 hours after exposure to hESC (spent culture media). MEF-CM was prepared as described in section 3.2.3, chapter 3. The hESC culture was carried out by Dr James Smith, Wolfson Centre for Stem Cells, Tissue Engineering & Modelling, Centre for Biomolecular Sciences, University of Nottingham.

5.2.3 Samples and sample preparation

MEF-CM and StemPro™ culture medium samples were obtained before and after incubation with HUES7 cells as previously described.

Samples were prepared by solvent protein precipitation using a 3:1 MeOH-sample ratio as described in chapter 2. Briefly, 250 µL of sample were mixed with 750 µL of cold MeOH (kept at -20^0C), vortexed for 1 min to precipitate the proteins and stored at -20^0C for 20 min. After the cold storage period, samples were vortexed again for 15 s and centrifuged at 17000 rpm for 10 min at 4^0C. The supernatants were transferred to clean LC vials for analysis. Each type of culture medium (MEF-CM or StemPro, before and after hESC culture) was prepared six times and injected in triplicate into the LC-MS system.

As part of the system conditioning and quality control process, a pooled "quality control" (QC) sample was prepared by mixing equal volumes of the samples involved in each experiment (Gika et al., 2007, Want et al., 2010). These QC samples were also prepared in exactly the same manner as the test samples.

5.2.4 Sample analysis

Ten QC samples were injected at the beginning of each experiment to condition the LC system and then intermittently once every 6 test samples to assess the stability of the analysis. All test samples were injected in a randomised order to eliminate any bias.

5.2.5 Liquid chromatography and mass spectrometry

The LC-MS methodology developed in chapter 2 was applied in the same manner here. Briefly, culture medium samples were injected into an Accela U-HPLC system hyphenated with an Exactive Orbitrap mass spectrometer (both from Thermo Fisher Scientific, USA) equipped with a heated electrospray interface (HESI-II) operating in positive and negative ion mode. Samples were separated using a ZORBAX Eclipse Plus C18 column 1.8 µm (i.d. 2.1x100 mm) attached to a guard column (2.1x5 mm) of the same chemistry and particle size (Agilent Technologies, Cheadle, UK). For a detailed description of the LC-MS parameters please refer to sections 2.2.5 and 2.2.6 in chapter 2.

To obtain MS/MS spectra, samples were injected into an Accela U-HPLC system coupled online to an LTQ Velos mass spectrometer (Thermo Fischer Scientific, USA) operating in data dependent mode. The collision energy used was 35 eV. The electrospray and LC parameters were the same as those described in section 2.2.5 and 2.2.6 in chapter 2.

5.2.6 Data processing and analysis

The detailed methodology for data processing and data analysis has been previously described in section 3.2.8 (chapter 3) and in the same manner was applied here. Briefly, the LC-MS raw data files obtained from the

metabolomics analyses were imported to SIEVE software version 2.0 (Thermo Fisher Scientific, USA) for data pre-processing. Positive and negative ion electrospray datasets were analysed separately with the following settings: ion intensity threshold, 10000; peak width, 10 ppm; frame time width, 2.50 min and normalised to the total ion current. Subsequently, the positive and negative ESI data sets obtained from SIEVE were merged in one file and exported to SIMCA version 13.0 (Umetrics AB, Umea, Sweden) for multivariate analysis (MVA). The variables (ions) causing the class separation were searched against web-based databases such as the Human Metabolome Database (www.hmdb.ca), Lipid Maps (www.lipidmaps.org) and METLIN Metabolomics Database (www.metlin.scripps.edu). For a greater degree of confidence in the identification of the ions, MS/MS analysis was carried out as previously described and the MS/MS spectra of the ions were compared with those registered in the databases aforementioned or with those published in the literature. For univariate statistics, data were exported to GraphPad Prism version 6.03 (GraphPad Software Inc., California, USA). Two-tailed Student's *t*-tests with Welch's correction were applied and differences were considered significant at *p*-values below those indicated in the text after correcting for multiple comparisons (Bonferroni's correction).

5.3 Results and discussion

5.3.1 Spent culture media chromatography

Typical negative ESI mode base peak chromatograms of media exposed to hESC (referred to from here on as spent culture media) are shown in Figure 5-2a. Obvious differences between serum replacement-containing (MEF-CM) (black) and serum-free (StemPro) (blue) media are observed. As I (in chapter 2) and others (Frankland et al., 2007, Garcia-Gonzalo and Izpisua Belmonte, 2008) have reported, AlbuMAX I constituent of the knock out serum replacement (KOSR), used in the preparation of MEF-CM, contains high levels of free fatty acids and lysophospholipids (including lysophosphatidylcholines (LPCs) and lysophosphatidyl-ethanolamines (LPEs)) which are the main compounds responsible for the chromatographic peaks detected after minute 6 in MEF-CM and MEF-CM spent medium. For a more intuitive comparison of the differences between MEF-CM and StemPro spent media, Figure 5-2b shows extracted ion chromatograms (EICs) of selected peaks found in both spent culture media. Surprisingly, for the chemically defined medium StemPro, traces of the lipids shown in the EICs were found even before exposure to hESC, despite of the fact that StemPro formulation does not mention any other lipids apart from linoleic and lipoic acids (Wang et al., 2007). Although Life Technologies (StemPro manufacturer) uses the fatty acid-free (Cohn's fraction V) bovine serum albumin (BSA) for medium manufacturing (Wang et al., 2007), BSA seems to be the most likely source for the presence of the not published fatty acids and LPCs of StemPro. In fact, free fatty acids have been reported to be present in albumin fraction V of several species, including bovine (Chen, 1967). Furthermore, at present, vendors like Sigma-Aldrich still report ≤ 0.02% fatty acid-impurities in fatty acid-free (Cohn's fraction V) BSA (www.sigmaaldrich.com). As it will be shown later in the discussion, the unpublished lipids of StemPro may have an influence on hESC as they appear to be used by the cells; thus, implying that the unknown components of the so-called "chemically defined" medium StemPro are also important for the maintenance of hESC although they are not specified in its formulation.

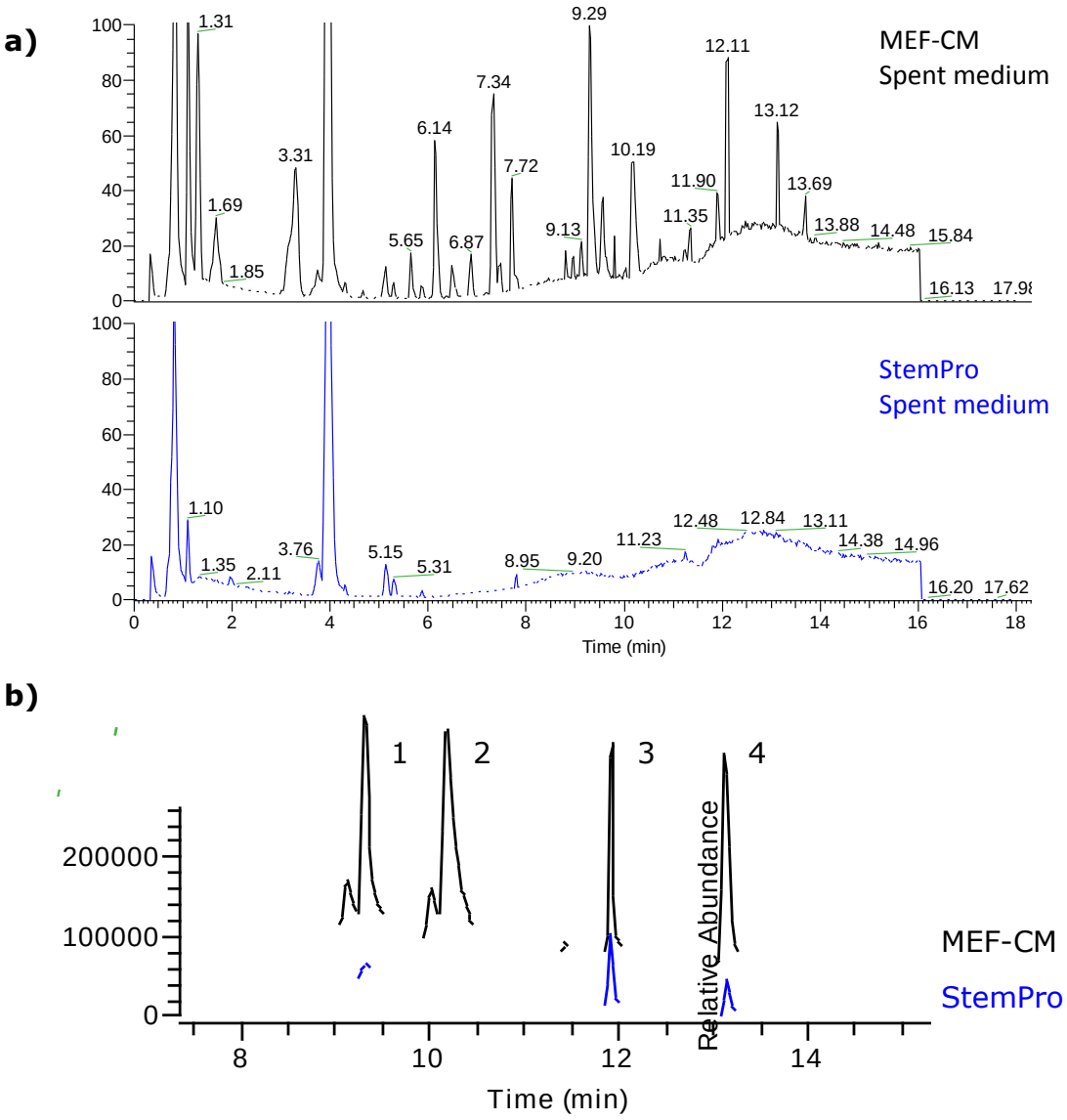

Figure 5-2 a) Negative ESI base peak chromatograms of MEF-CM (black) and StemPro (blue) spent culture media. b) Differences in signal intensity of metabolites found in both spent culture media are illustrated by the extracted ion chromatograms of 1) LPC(16:0), 2) LPC(18:0), 3) palmitic acid and 4) stearic acid.

5.3.2 Chromatography and mass spectrometry stability

As in chapter 3, quality control (QC) samples were used here to assess the data quality (Gika et al., 2007) of the metabolomics studies carried out in this chapter. Fresh versus cell-exposed medium experiments, using MEF-CM or StemPro (SP), are respectively referred to as MEF-CM vs. MEF-CM-HUES7 or SP vs. SP-HUES7. Data from both experiments were evaluated by examining the retention time (RT) and signal intensity repeatability of a small subset of peaks (5 in +ESI and 5 in –ESI),

covering a range of times and intensities, in the QC samples injected throughout the LC-MS analyses, discarding the first 10 QC samples that were used for system equilibration. Table 5-1 presents the percentages of coefficient of variation (%CV) of RT and intensity of the selected peaks in each experiment. Results showed high LC-MS reproducibility with variations below 2% for RT and below 15% for signal intensity, demonstrating with this the validity of the data and the excellent stability of the method. Furthermore, exact mass variations were found to be less than 5 mDa. Based on these evaluations it was concluded that the quality of the metabolomics analysis was acceptable and the data sets from each experiment were investigated further as described below.

5.3.3 Multivariate analysis

Positive and negative electrospray data from each culture system (MEF-CM or StemPro) were combined to perform multivariate analysis. In the first instance, PCA models were obtained to provide an overview of any patterns or groupings within the samples. Figure 5-3 shows the PCA scores plots of MEF-CM vs. MEF-CM-HUES7 and SP vs. SP-HUES7. In both cases clear differences in the metabolic profiles were observed between the cell-exposed and non-cell-exposed culture media. The class separation in the two PCA models was mainly depicted by the 1st principal component (t[1]) which accounted for approximately 30% of the explained variation of the data. The culture medium groups detected in the MEF-CM vs. MEF-CM-HUES7 model appeared more scattered than the culture medium groups of SP vs. SP-HUES7 which showed better clustering. Nevertheless, as described in the previous section and illustrated here with a tight cluster of QCs for each PCA model, both systems demonstrated sufficient stability throughout the LC-MS analyses. The datasets used to build the PCA models contained 2025 and 1223 variables (ions) detected in the MEF-CM and StemPro culture medium systems, respectively. Not surprisingly MEF-CM showed the highest number of variables since it is the medium with the most complex small-molecule composition as shown in Table 1-2, chapter 1 and demonstrated here with the base peak chromatograms presented in Figure 5-2.

Table 5-1. Variation in retention time and signal intensity of selected peaks in positive and negative ESI mode for MEF-CM vs. MEF-CM-HUES7 and SP vs. SP-HUES7 metabolomics experiments.

MEF-CM vs. MEF-CM-HUES7

Negative ESI mode

	Retention time, min		Intensity (arbitrary units)	
Peak (*m/z*)	mean ± SD	%CV	mean ± SD	%CV
218.1035	1.14 ± 0.01	**1.23**	898510 ± 64366	**7.16**
351.0336	4.31 ± 0.02	**0.48**	314342 ± 16707	**5.31**
313.0179	7.47 ± 0.03	**0.39**	36467 ± 4278	**11.73**
558.3338	10.17 ± 0.02	**0.15**	331804 ± 23973	**7.23**
309.2803	13.29 ± 0.01	**0.11**	79654 ± 5788	**7.27**

Positive ESI mode

	Retention time, min		Intensity (arbitrary units)	
Peak (*m/z*)	mean ± SD	%CV	mean ± SD	%CV
175.0341	1.67 ± 0.03	**1.62**	622764 ± 54790	**8.80**
226.1802	5.87 ± 0.01	**0.25**	88220 ± 4596	**5.21**
304.2998	8.29 ± 0.02	**0.18**	284966 ± 12904	**4.53**
270.2791	11.38 ± 0.01	**0.12**	1117404 ± 107040	**9.58**
338.3416	13.63 ± 0.02	**0.14**	1636368 ± 148094	**9.05**

SP vs. SP-HUES7

Negative ESI mode

	Retention time, min		Intensity (arbitrary units)	
Peak (*m/z*)	mean ± SD	%CV	mean ± SD	%CV
130.0874	1.10 ± 0.02	**1.86**	897892 ± 24159	**2.69**
371.0596	3.75 ± 0.01	**0.38**	1724432 ± 55433	**3.21**
429.0805	7.42 ± 0.01	**0.17**	42244 ± 2587	**6.12**
530.3021	9.30 ± 0.00	**0.00**	20632 ± 627	**3.04**
457.2267	12.45 ± 0.01	**0.10**	119031 ± 9769	**8.21**

Positive ESI mode

	Retention time, min		Intensity (arbitrary units)	
Peak (*m/z*)	mean ± SD	%CV	mean ± SD	%CV
240.0954	0.89 ± 0.01	**1.64**	2653292 ± 44479	**1.68**
377.1456	2.59 ± 0.03	**1.12**	309751 ± 11500	**3.71**
266.1722	5.86 ± 0.01	**0.17**	57789 ± 3136	**5.43**
455.3481	10.87 ± 0.00	**0.00**	28040 ± 1961	**6.99**
327.2280	12.08 ± 0.01	**0.08**	37284 ± 2312	**6.20**

Data expressed as mean ± standard deviation (n=8).

a) MEF-CM vs MEF-CM-HUES7

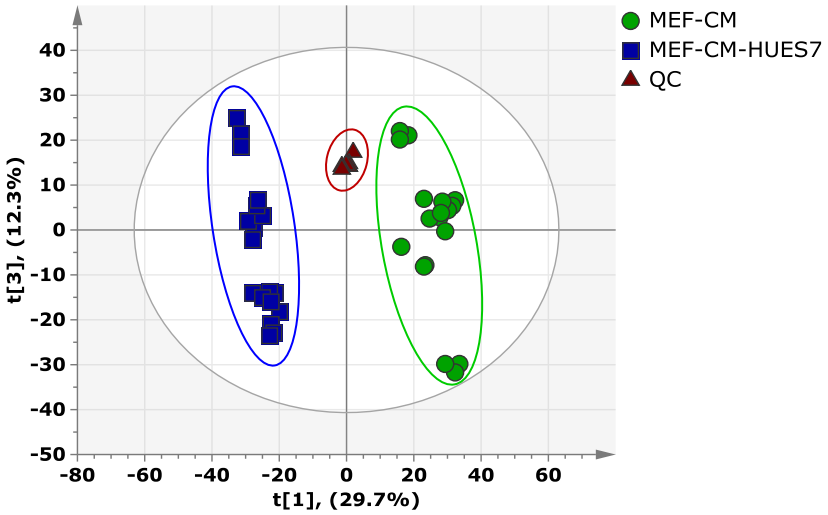

b) SP vs SP-HUES7

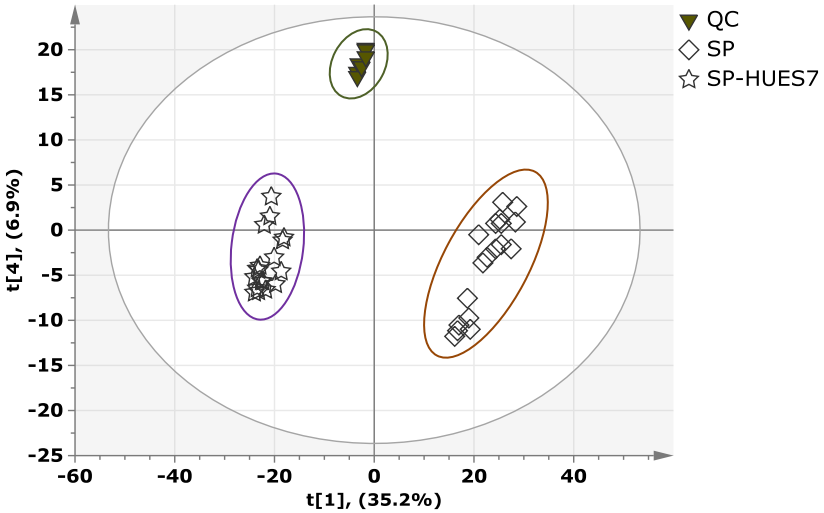

Figure 5-3 PCA scores plots of fresh vs. cell-exposed media using a) MEF-CM and b) StemPro (SP). In both cases, a clear separation between the culture medium classes was observed, indicating metabolic differences. The stability of the LC-MS system in each case is illustrated by the tight clusters of QC samples.

5.3.3.1 OPLS-DA model building and validation

In order to find out the variables (metabolites) responsible for the separation of the culture medium groups in each metabolomics experiment, orthogonal partial least squares-discriminant analysis (OPLS-DA) was applied. The inherent properties of OPLS-DA modelling to maximise the separation of the groups while minimising within class variation, in addition to its interpretational benefits (Bylesjo et al., 2006), allowed the extraction of the metabolites that contributed most significantly to the corresponding culture media separation. OPLS-DA models (Figure 5-4) were built independently for each metabolomics experiment with 75% of the samples (n=27) randomly selected from each data set. The remaining 25% (n=9) in each case was used for external model validation as explained later in this section. Initially, the OPLS-DA models were evaluated using the $R^2Y(cum)$ and $Q^2(cum)$ parameters (Table 5-2). As stated before in chapter 3, these parameters indicate respectively the fitness and prediction ability of the models; that is, how well the model fits the data and how well it predicts new data. For biological models, Q^2 values above 0.4 are empirically acceptable (Westerhuis et al., 2008), indicating good classification models. Overall, the results shown in Table 5-2 indicate that both OPLS-DA models showed good data fitness and good data predictivity with $R^2Y(cum)$ and $Q^2(cum)$ values superior to 0.4.

Table 5-2. OPLS-DA model evaluation parameters

Experiment	$R^2Y(cum)$	$Q^2(cum)$	CV-ANOVA, *p*-value
MEF-CM vs. MEF-CM-HUES7	0.996	0.990	$1.55x10^{-21}$
SP vs. SP-HUES7	0.998	0.995	$1.37x10^{-24}$

a) MEF-CM vs MEF-CM-HUES7

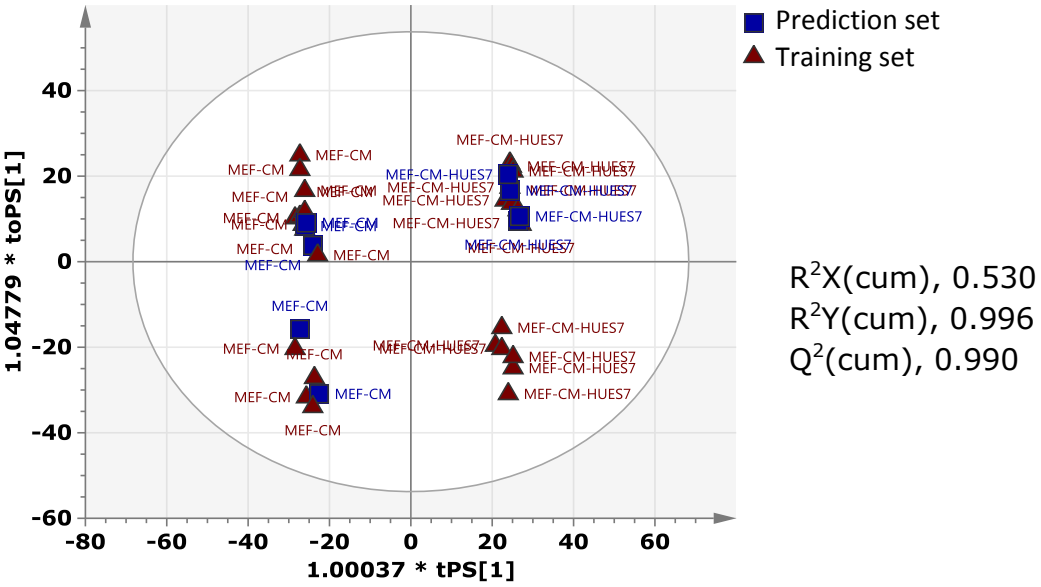

b) SP vs SP-HUES7

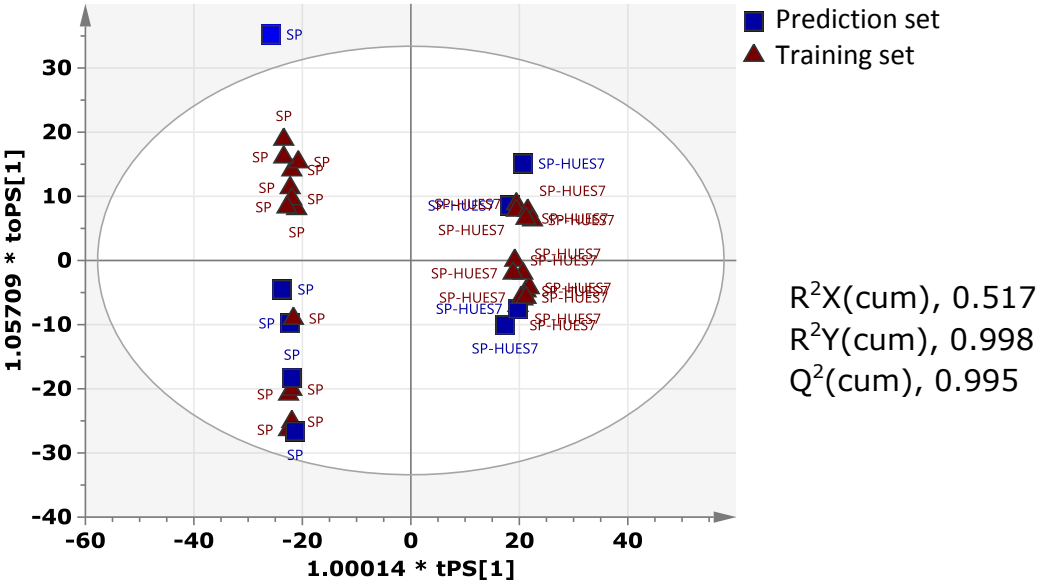

Figure 5-4 OPLS-DA models of fresh vs cell-exposed media using a) MEF-CM and b) StemPro. In red, samples used to build the OPLS-DA models (training set) and in blue, samples used for class prediction (prediction set) during the external model validation procedure.

Because supervised multivariate methods like OPLS-DA have a tendency to over-fit models to data, validation is critical in ensuring model reliability as well as in assessing their predictive ability (Westerhuis et al., 2008). Here, cross-validation and external validation were used to validate the models. To assess the significance of the models a cross-validation-analysis of variance (CV-ANOVA) test was performed on each OPLS-DA model. The results of the tests are displayed in Table 5-2. A model is considered significant when the resulting *p*-value is lower than 0.05 (Eriksson et al., 2008). Since the results showed *p*-values << 0.05, they indicate that the class separation observed in each culture system is not just the result of chance but of true experimental differences. Additionally, the two OPLS-DA models were further validated through external predictions. For this, the 25% of the samples that were initially excluded during model building were used to assess the predictivity of the models. Figure 5-4 shows in blue the 25% of the samples used in the prediction set. It is observed that in each case the OPLS-DA model was able to predict the class membership of the corresponding culture medium samples. Altogether, the results from the two diagnostics -CV-ANOVA and external validation- denoted highly significant and highly predictive OPLS-DA models for both metabolomics experiments.

5.3.3.2 Discovery and identification of discriminating metabolites in the MEF-CM and StemPro culture systems.

To select the metabolites (ions) that contributed most significantly to the separation of the culture medium groups (fresh vs. cell-exposed medium samples) in each culture system, the variable importance for the projection (VIP) value of each metabolite was taken into account. Ions with VIP values above 1.5 were selected and subjected to Student's *t*-tests to validate their significance. To correct for the multiple testing problem Bonferroni's correction was applied (Vinaixa et al., 2012), therefore, only those ions with *p*-values below 2.47×10^{-5} and 4.09×10^{-5} in the MEF-CM and StemPro culture system, respectively, were considered significant (for a detailed explanation of the Bonferroni's correction in metabolomics please refer to section 3.3.2.2 in chapter 3).

When a metabolite was found to be significantly different, then identification was carried out. The detailed method of compound identification has been described in section 2.3.6 and in the same way was applied here. Table 5-3 and Table 5-4 indicate respectively the compounds that increased or decreased significantly in the cell-exposed medium of each culture system. Whenever possible authentic standards were used to confirm the identity of the compounds; however, in many cases, metabolites remained without a definitive identification. Consequently, the metabolites will be discussed based on their putative identities assigned with a greater degree of confidence after comparing their MS/MS spectra with those registered in the databases' spectral libraries or with those reported in the literature. About 87% of the compounds were assigned a putative identity; however, the rest of ions remained unidentifiable due to insufficient intensity for MS/MS or limitations in the databases' repositories. MS/MS spectra of the identified compounds are provided in appendix C at the end of the thesis.

In electrospray ionisation, compounds are typically found in the form of their protonated $[M+H]^+$ or deprotonated $[M-H]^-$ ion depending on the ionization mode utilized. Nevertheless, the formation of anion (Cl^-) and cation (Na^+, K^+, NH_4^+) adducts of polar analytes that lack ionisable groups is also observed (Cech and Enke, 2001). For example, in the case of glucose which was found here as the sodium adduct $[M+Na^+]^+$, that is 22.9898 units more than its exact mass 180.0634 (

Figure 5-5). This observation is consistent with what has been reported in the literature (Koulman et al., 2009) and helps to confirm the identity assignment for the ion at *m/z* 203.0524 (Table 5-4).

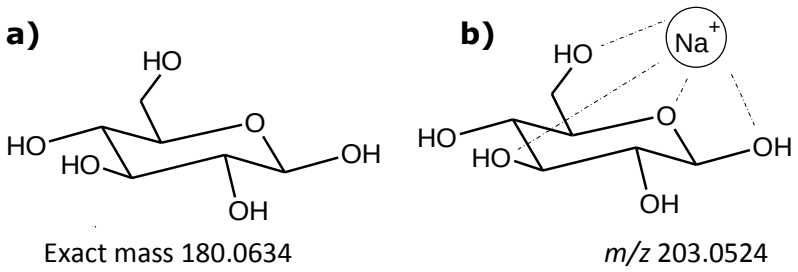

Figure 5-5 Under electrospray ionisation, polar compounds like glucose (a) which lack ionisable groups form sodium adducts (b); thus, they are detected as the $[M+Na^+]^+$ rather than the typical $[M+H^+]^+$.

Table 5-3 Tentative compounds significantly <u>increased</u> in spent culture media after 24 h exposure to hESC.

Putative identification	Formula	Ion	RT (min)	Accurate mass (*m/z*)	Δ ppm	Fold change		Database reference
						MEF-CM	StemPro	
L-Lactic acid	$C_3H_6O_3$	$[M-H]^-$	0.78	89.0245	-0.8	**2.57**	**31.75**	HMDB00190
Unknown		$[M+H]^+$	0.82	214.0060		**3.82**	**3.32**	
Pyruvic acid	$C_3H_4O_3$	$[M-H]^-$	1.09	87.0088	0.2	**1.57**		HMDB00243
L-Alanine	$C_3H_7NO_2$	$[M+H]^+$	1.12	90.0551	-0.7	**2.11**	**7.13**	HMDB00161
2-Hydroxy-3-methylbutyric acid	$C_5H_{10}O_3$	$[M-H]^-$	1.72	117.0558	-0.5	**N/A**		HMDB00407
Unknown		$[M-H]^-$	2.17	188.0927		**N/A**		
(R)-3-Hydroxyhexanoic acid	$C_6H_{12}O_3$	$[M-H]^-$	3.05	131.0714	0.3	**18.14**		HMDB10718
L-Acetylcarnitine	$C_9H_{17}NO_4$	$[M-H]^-$	3.37	202.1084	0.4	**144.87**	**N/A**	HMDB00201
Unknown		$[M-H]^-$	3.72	236.0928		**75.82**	**N/A**	
Unknown		$[M-H]^-$	3.84	204.0665		**2.02**		
Unknown		$[M-H]^-$	3.90	275.1041		**N/A**		
Unknown		$[M-H]^-$	4.30	327.0878		**1.40**		
9,12,13-TriHOME	$C_{18}H_{34}O_5$	$[M-H]^-$	6.05	329.2337	-1.3	**1.78**		HMDB04708
LPC(14:0)	$C_{22}H_{46}NO_7P$	$[M+HCOO^-]^-$	8.33	512.2996	-1.5		**N/A**	HMDB10379
LPC(16:1(9Z))	$C_{24}H_{48}NO_7P$	$[M+HCOO^-]^-$	8.60	538.3155	-1.8		**N/A**	HMDB10383
2-Hydroxymyristic acid	$C_{14}H_{28}O_3$	$[M-H]^-$	8.87	243.1965	0.2	**1.65**	**50.53**	HMDB02261
(9S,10S)-9,10-dihydroxyoctadecanoate	$C_{18}H_{36}O_4$	$[M-H]^-$	9.01	315.2545	-1.1	**1.50**		HMDB59633
17-Hydroxylinolenic acid	$C_{18}H_{30}O_3$	$[M-H]^-$	9.06	293.2124	-0.7	**2.60**		HMDB11108
LPE(16:0/0:0)	$C_{21}H_{44}NO_7P$	$[M-H]^-$	9.24	452.2784	-0.3		**N/A**	HMDB11503
Unknown LPC		$[M+HCOO^-]^-$	9.27	584.3577		**1.73**		
LPC(16:0/0:0)	$C_{24}H_{50}NO_7P$	$[M+HCOO^-]^-$	9.30	540.3307	-1.2		**12.73**	HMDB10382
Unknown		$[M+H]^+$	9.40	267.1716		**1.46**	**1.40**	

Table 5-3 *continued*

Putative identification	Formula	Ion	RT (min)	Accurate mass (*m/z*)	Δ ppm	Fold change		Database reference
						MEF-CM	StemPro	
24-Oxo-1alpha,25-dihydroxyvitamin D3	$C_{27}H_{42}O_4$	$[M-H]^-$	9.42	429.3011	-0.2	**1.99**		HMDB60128
LPE(18:1(9Z)/0:0)	$C_{23}H_{46}NO_7P$	$[M+H]^+$	9.46	480.3083	0.3	**2.49**	**N/A**	HMDB11506
PE(P-16:0e/0:0)	$C_{21}H_{44}NO_6P$	$[M+H]^+$	9.50	438.2980	-0.2	**2.51**	**N/A**	HMDB11152
LPC(18:1(9Z)/0:0)	$C_{26}H_{52}NO_7P$	$[M+HCOO^-]^-$	9.54	566.3463	-0.8		**27.64**	HMDB02815
Unknown		$[M+H]^+$	9.64	417.3364			**N/A**	
Unknown		$[M-H]^-$	9.71	462.2991		**1.56**	**N/A**	
Myristoylglycine	$C_{16}H_{31}NO_3$	$[M-H]^-$	9.80	284.2231	0.2	**3.17**	**N/A**	HMDB13250
2-hydroxy-heptadecanoic acid	$C_{17}H_{34}O_3$	$[M-H]^-$	9.86	285.2437	-0.6	**1.40**		LMFA01050052
20-HETE	$C_{20}H_{32}O_3$	$[M-H]^-$	9.97	319.2280	-0.4	**2.44**		HMDB05998
LPE(18:0/0:0)	$C_{23}H_{48}NO_7P$	$[M+H]^+$	10.06	482.3244	-0.6		**18.73**	HMDB11130
Monoacylglycerol (16:0/0:0/0:0)	$C_{19}H_{36}O_3$	$[M-H]^-$	10.16	311.2593	-0.3	**2.41**		HMDB11564
LPE(20:1(11Z)/0:0)	$C_{25}H_{50}NO_7P$	$[M+H]^+$	10.23	508.3399	-0.4		**N/A**	HMDB11512
1alpha,22-dihydroxy-23,24,25,26,27-pentanorvitamin D3	$C_{22}H_{34}O_3$	$[M-H]^-$	10.26	345.2437	-0.6	**2.66**		LMST03020011
PE(O-18:1(9Z)/0:0)	$C_{23}H_{48}NO_6P$	$[M+H]^+$	10.36	466.3295	-0.6		**N/A**	LMGP02060004
N-oleoyl ethanolamine	$C_{20}H_{39}NO_2$	$[M+H]^+$	10.80	326.3053	0.1	**2.34**		LMFA08040015
2-Hydroxypalmitic acid	$C_{16}H_{32}O_3$	$[M-H]^-$	10.90	271.2281	-0.9	**1.72**	**33.14**	HMDB31057
Myristic acid	$C_{14}H_{28}O_2$	$[M-H]^-$	10.85	227.2018	-0.9		**2.40**	HMDB00806
Linoleic acid	$C_{18}H_{32}O_2$	$[M-H]^-$	11.29	279.2329	0.1		**1.33**	HMDB00673
Docosapentaenoic acid	$C_{22}H_{34}O_2$	$[M-H]^-$	11.32	329.2488	-0.7		**N/A**	HMDB06528
Hexadecenal	$C_{16}H_{30}O$	$[M+H]^+$	11.34	239.2368	0.2	**1.45**	**1.28**	HMDB60482

Table 5-3 *continued*

Putative identification	Formula	Ion	RT (min)	Accurate mass (*m/z*)	Δ ppm	Fold change		Database reference
						MEF-CM	StemPro	
3-hydroxystearic acid	$C_{18}H_{36}O_3$	$[M-H]^-$	11.49	299.2594	-0.8	**2.06**	**6.64**	HMDB10737
14R-hydroxy-11Z-eicosenoic acid	$C_{20}H_{38}O_3$	$[M-H]^-$	11.62	325.2751	-1.0	**2.81**		LMFA01050257
Tetracosahexaenoic acid	$C_{24}H_{36}O_2$	$[M-H]^-$	11.64	355.2646	-0.7	**3.68**		LMFA01030822
Palmitic acid	$C_{16}H_{32}O_2$	$[M-H]^-$	11.91	255.2329	0.0		**3.95**	HMDB00220
Oleic acid	$C_{18}H_{34}O_2$	$[M-H]^-$	12.10	281.2487	-0.4		**18.77**	HMDB00207
Unknown		$[M+H]^+$	12.42	381.2971		**1.47**	**1.55**	
Eicosadienoic acid	$C_{20}H_{36}O_2$	$[M-H]^-$	12.45	307.2644	-0.6	**2.18**		HMDB05060
Eicosenoic acid	$C_{20}H_{38}O_2$	$[M-H]^-$	13.28	309.2802	-1.0	**2.79**	**N/A**	HMDB02231

Fold changes were calculated as the ratio of the average peak area (n=18) of the metabolites found in the cell-exposed medium and fresh culture medium either using MEF-CM or StemPro.

Lyosophospholipids are highlighted with grey-shaded rows.

LPC, lysophosphatidylcholine; LPE, lysophosphatidylethanolamines; PE, phosphoethanolamine; TriHOME, trihydroxyoctadecenoic acid.

N/A means that the metabolite was only found in the spent culture media.

Table 5-4. Tentative compounds significantly <u>decreased</u> in spent culture media after 24 h exposure to hESC.

Putative identification	Formula	Ion	RT (min)	Accurate mass (*m/z*)	Δ ppm	Fold change		Database reference
						MEF-CM	StemPro	
L-Arginine	$C_6H_{14}N_4O_2$	$[M+H]^+$	0.70	175.1190	-0.3	**-1.77**	**-2.34**	HMDB00517
L-Histidine	$C_6H_9N_3O_2$	$[M-H]^-$	0.73	154.0623	-0.4	**-1.32**	**-2.51**	HMDB00177
L-Lysine	$C_6H_{14}N_2O_2$	$[M-H]^-$	0.74	145.0983	-0.5	**-2.45**	**-5.21**	HMDB00182
L-Alanyl-L-glutamine	$C_8H_{15}N_3O_4$	$[M-H]^-$	0.78	216.0990	0.0	**-24.35**	**-33.30**	HMDB28685
D-Glucose	$C_6H_{12}O_6$	$[M+Na]^+$	0.79	203.0524	4.2	**-2.28**	**-2.62**	HMDB00122
Choline	$C_5H_{14}NO$	$[M]^+$	0.81	104.1069	5.4	**-1.86**	**-1.62**	HMDB00097
L-Glutamine	$C_5H_{10}N_2O_3$	$[M+H]^+$	0.88	147.0763	0.4	**-2.77**	**-7.23**	HMDB00641
L-Valine	$C_5H_{11}NO_2$	$[M-H]^-$	0.91	116.0718	-0.5	**-1.51**	**-7.04**	HMDB00883
L-Phenylalanine	$C_9H_{11}NO_2$	$[M-H]^-$	1.09	164.0718	-0.5	**-1.59**	**-4.37**	HMDB00159
L-Tyrosine	$C_9H_{11}NO_3$	$[M-H]^-$	1.09	180.0667	-0.4	**-2.05**	**-3.94**	HMDB00158
Pyridoxine	$C_8H_{11}NO_3$	$[M-H]^-$	1.10	168.0665	0.6	**-2.83**	**-3.64**	HMDB00239
L-Leucine/Isoleucine	$C_6H_{13}NO_2$	$[M+H]^+$	1.11	132.1019	0.0		**-1.72**	HMDB00687
L-Tryptophan	$C_{11}H_{12}N_2O_2$	$[M-H]^-$	1.30	203.0826	-0.2	**-1.16**	**-2.98**	HMDB00929
LPE(18:3(9Z,12Z,15Z)/0:0)	$C_{23}H_{42}NO_7P$	$[M-H]^-$	8.40	474.2631	-1.0	**-1.98**		HMDB11509
LPC(18:3(9Z,12Z,15Z))	$C_{26}H_{48}NO_7P$	$[M+HCOO^-]^-$	8.43	562.3155	-1.8	**-1.86**		HMDB10388
LPC(18:2(9Z,12Z))	$C_{26}H_{50}NO_7P$	$[M+HCOO^-]^-$	8.92	564.3310	-1.6	**-1.72**		HMDB10386
LPC(22:5(4Z,7Z,10Z,13Z,16Z))	$C_{30}H_{52}NO_7P$	$[M+HCOO^-]^-$	9.16	614.3469	-1.7	**-2.40**		HMDB10402
LPC(18:1(9Z)/0:0)	$C_{26}H_{52}NO_7P$	$[M+HCOO^-]^-$	9.54	566.3468	-1.8	**-1.51**		HMDB02815
LPC(P-16:0/0:0)	$C_{24}H_{50}NO_6P$	$[M+HCOO^-]^-$	9.58	524.3361	-1.8	**-1.55**		HMDB10407
Unknown		$[M+H]^+$	9.65	492.3447		**-1.59**		
LPC(17:0)	$C_{25}H_{52}NO_7P$	$[M+HCOO^-]^-$	9.73	554.3467	-1.6	**-1.60**		HMDB12108

Table 5-4 *continued*

Putative identification	Formula	Ion	RT (min)	Accurate mass (*m/z*)	Δ ppm	Fold change		Database reference
						MEF-CM	StemPro	
PS(O-20:0/0:0)	$C_{26}H_{54}NO_8P$	$[M-H]^-$	9.90	538.3520	-1.1	**-1.86**		LMGP03060001
PE(P-20:0/0:0)	$C_{25}H_{52}NO_6P$	$[M+H]^+$	9.92	494.3604	0.1	**-1.79**		LMGP02070004
LPC(18:0)	$C_{26}H_{54}NO_7P$	$[M+HCOO^-]^-$	10.14	568.3619	-1.0	**-1.71**	**-5.14**	HMDB10384
Stearidonic acid	$C_{18}H_{28}O_2$	$[M-H]^-$	10.29	275.2020	-1.4	**-3.06**		HMDB06547
LPC(20:0)	$C_{28}H_{58}NO_7P$	$[M+HCOO^-]^-$	10.45	596.3940	-2.2	**-1.51**		HMDB10390
Eicosapentaenoic acid	$C_{20}H_{30}O_2$	$[M-H]^-$	10.63	301.2173	0.1	**-7.71**		HMDB01999
Alpha-Linolenic acid	$C_{18}H_{30}O_2$	$[M-H]^-$	10.00	277.2175	-0.8	**-2.54**		HMDB01388
Docosahexaenoic acid	$C_{22}H_{32}O_2$	$[M-H]^-$	10.98	327.2332	-0.9	**-2.54**		HMDB02183
Palmitoleic acid	$C_{16}H_{30}O_2$	$[M-H]^-$	11.05	253.2175	-1.0	**-1.72**		HMDB03229
Arachidonic acid	$C_{20}H_{32}O_2$	$[M-H]^-$	11.17	303.2332	-1.0	**-4.93**		HMDB01043
Pentadecanoic acid	$C_{15}H_{30}O_2$	$[M-H]^-$	11.22	241.2175	-0.8	**-2.34**		HMDB00826
Docosapentaenoic acid	$C_{22}H_{34}O_2$	$[M-H]^-$	11.32	329.2484	0.5	**-3.30**		HMDB06528
Linoleic acid	$C_{18}H_{32}O_2$	$[M-H]^-$	11.33	279.2329	-0.0	**-1.73**		HMDB00673
(Z)-9-Heptadecenoic acid	$C_{17}H_{32}O_2$	$[M-H]^-$	11.58	267.2331	-0.8	**-1.65**		HMDB31046
Palmitic acid	$C_{16}H_{32}O_2$	$[M-H]^-$	11.90	255.2332	-1.1	**-1.95**		HMDB00220
Adrenic acid	$C_{22}H_{36}O_2$	$[M-H]^-$	11.91	331.2644	-0.5	**-2.89**		HMDB02226
Oleic acid	$C_{18}H_{34}O_2$	$[M-H]^-$	12.08	281.2488	-0.9	**-1.36**		HMDB00207
Heptadecanoic acid	$C_{17}H_{34}O_2$	$[M-H]^-$	12.44	269.2488	-0.9	**-1.97**		HMDB02259
Stearic acid	$C_{18}H_{36}O_2$	$[M-H]^-$	13.11	283.2645	-0.9	**-1.50**		HMDB00827

Fold changes were calculated as the ratio of the average peak area (n=18) of the metabolites found in the fresh culture medium and cell-exposed medium either using MEF-CM or StemPro. The sign was changed to indicate a decrease.

Another 'atypical' behaviour in electrospray ionisation is that of LPCs. Due to their zwitterionic molecular structure (Figure 5-6a), this group of phospholipids are commonly observed in the negative ESI mode as the demethylated ion $[M–CH3]^-$ or as the formate adduct $[M+HCOO^-]^-$ (Fang et al., 2003). As an example, the full scan MS spectrum of LPC(18:3) is shown in Figure 5-6b. Although the chlorine ($[M+Cl^-]^-$) and the formic acid-sodium formate ($[M+HCOONa+HCOO^-]^-$) adducts are also observed, their abundance are considerably inferior to the $[M–CH3]^-$ or $[M+HCOO^-]^-$ ions. Therefore, in Table 5-3 and Table 5-4, LPCs are reported as the $[M+HCOO^-]^-$ adduct since it was the ion that produced the most intense peak under the LC-MS conditions used in this study. It should be noted that LPCs can also be detected in the positive ESI mode as the protonated ion $[M+H^+]^+$ (as shown in Table 2-6, chapter 2); however, because in these metabolomics studies the positive ions of the LPCs provided less discriminatory power than their corresponding negative ones, they were not reported in Table 5-3 and Table 5-4.

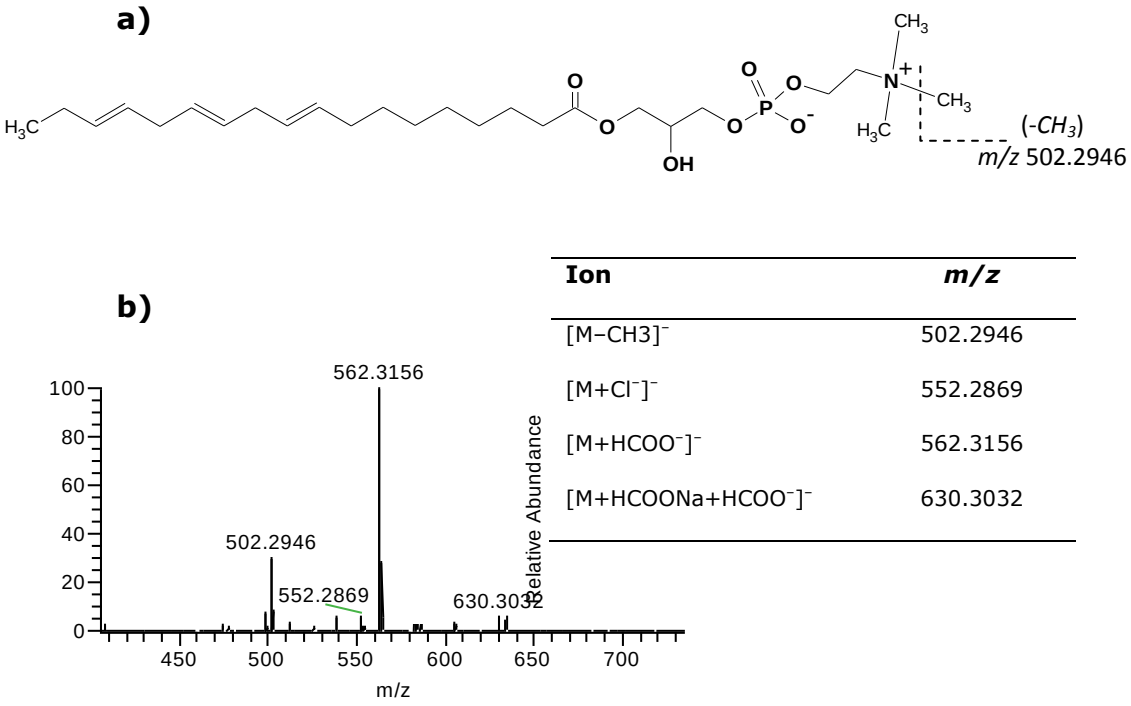

Ion	*m/z*
$[M–CH3]^-$	502.2946
$[M+Cl^-]^-$	552.2869
$[M+HCOO^-]^-$	562.3156
$[M+HCOONa+HCOO^-]^-$	630.3032

Figure 5-6 a) Chemical structure and b) full scan MS spectrum of lysophosphatidylcholine (18:3). The table insert shows the *m/z* values of the most commonly found adducts of this LPC.

5.3.4 Biological significance of increased metabolites in spent culture media

Fifty metabolites were found to be significantly increased in the culture media after exposure to hESC, ranging from very polar to non-polar compounds. Increased metabolites included glycolysis by-products such as lactate and pyruvate and some others like hydroxylated fatty acids, LPCs, LPEs, vitamin D_3 derivatives and free fatty acids. The two culture systems (MEF-CM and StemPro) had in common 16 increased metabolites (Figure 5-7a), while 20 and 14 were found to be uniquely secreted in MEF-CM and StemPro spent media, respectively. In general, StemPro spent medium rendered larger fold changes than MEF-CM spent medium, but this was due to the absence (or low concentration) of those compounds in StemPro fresh medium (medium before cell exposure). On the contrary, the small fold changes observed with MEF-CM were due to the fact that the compounds were already present in MEF-CM fresh medium which made the ratios (metabolite in spent medium/metabolite in fresh medium) smaller. Nevertheless, in both cases, the changes were statistically significant following correction for multiple comparisions (Bonferroni's correction), indicating that the increases were indeed the result of hESC metabolism. There were other metabolites however that showed more substantial changes in MEF-CM spent medium like the putatively identified 3-hydroxyhenanoic acid, L-acetylcarnitine, and the unknown ion at *m/z* 236.0928, the last two also found in StemPro spent medium, which could potentially be used as a metabolic signature of hESC in culture.

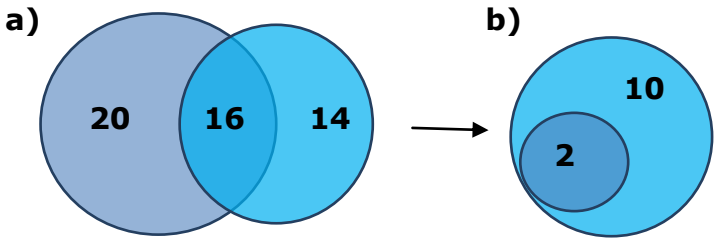

Figure 5-7 a) Venn diagram of significantly increased metabolites found in spent culture media using MEF-CM (dark blue) and StemPro (light blue). 16 metabolites were commonly identified in both spent culture media, while 20 and 14 were uniquely identified in MEF-CM and StemPro spent media, respectively. b) Venn diagram representing the amount of increased lysophospholipids (LPLs) found in each culture system, again MEF-CM (dark blue) and StemPro (light blue).

Of particular interest were the range and abundance of lysophospholipids (LPLs) secreted by human embryonic stem cells when StemPro was used as culture medium. In total, ten LPLs (4 LPCs and 6 LPEs) were found to be significantly increased in StemPro spent medium compared to 2 in MEF-CM spent medium (Figure 5-7b). The reason of why fewer LPLs were increased when MEF-CM was used might be because LPEs and LPCs were already present in the medium, provided by the knock out serum replacement (as shown in chapter 2) used for the preparation of MEF-CM. Therefore, in case the cells require the use of these types of compounds (as it will be shown later in section 5.3.5), cells can simply take them from the medium and it might not be necessary to secrete them. In support of the increased levels of LPLs, phospholipase A_2, the enzyme that hydrolyzes phosphatidylcholines to release fatty acids and LPCs, has been identified in H1 and H9 hESC cell lines (Sarkar et al., 2012), thus, providing evidence that LPLs can be produced and secreted by hESC.

It was interesting to observe that when hESC were grown in the absence of LPLs as in the case of StemPro, cells were able to synthesise them and release them to the extracellular microenvironment, while when they were cultured in a lysophospholipid-rich medium like MEF-CM, cells seemed to incorporate them (Table 5-3 and Table 5-4). It has been widely demonstrated that LPLs are not simply metabolites for membrane phospholipid synthesis but also bioactive compounds that act as extracellular signalling molecules activating specific G-protein coupled receptors (GPCRs) (Rivera and Chun, 2008, Hla et al., 2001). The most widely studied LPLs are lysophosphatidic acid (LPA) and sphingosine-1-phosphate (S1P) which have been shown to mediate a wide range of cellular processes such as proliferation, survival, adhesion, migration, morphogenesis and differentiation in a large number of cell types including T cells (Huang et al., 2002), neurons (Choi and Chun, 2013), vascular endothelial cells (Yatomi, 2006), lung cells (Brinkmann and Baumruker, 2006) and stem cells (Pebay et al., 2007, Avery et al., 2008).

In human embryonic stem cells, exogenous LPA does not appear to have any biological effect; however, S1P, in combination with platelet-derived

growth factor (PDGF), maintained hESC undifferentiated in the absence of serum (Pebay et al., 2005). Furthermore, in various mammalian cells (e.g. ovarian cancer cells, mast cells, glioblastoma stem cells) LPA and S1P have also been identified with autocrine and paracrine functions (Xie et al., 2002, Alvarez et al., 2007). Nonetheless, in the present study, neither LPA nor S1P were detected in the extracellular microenvironment of hESC with either culture medium.

It should be noted however that potential precursors for LPA were indeed identified. For example, as shown in Figure 5-8, LPA can be formed by hydrolysis of phosphatidic acid or LPCs or by the phosphorylation of monoacylglycerol (Pages et al., 2001). In the current study, LPCs and monoacylglycerol both with a 16-carbon moiety (as LPA) were identified. Therefore, it is possible that the LPCs and the monoacylgycerol secreted to the medium might be transformed to LPA by the action of lysophospholipase D (lysoPLD) or monoacylglycerol kinase, respectively (Figure 5-8). Although there is no evidence of the existence of these enzymes in the hESC secretome (Bendall et al., 2009, Sarkar et al., 2012), the possibility of extracellular LPA synthesis cannot be completely discarded, because as demonstrated by Bendall et al, in MS-based proteomics analyses, many low abundant proteins are masked by the most abundant ones thus suggesting that there may be many low abundant proteins that remain to be identified (Bendall et al., 2009). Even in the remote case that LPA could be synthesised extracellularly, it remains unknown whether obtained in this manner it would have an effect on hESC since when added exogenously LPA did not show any effect, in spite of the identification of LPA receptors on hESC (Pebay et al., 2005). Alternatively, the LPLs identified could mediate some biological activities by themselves as it will be described in section 5.3.5 where LPLs were found to be significantly decreased in MEF-CM.

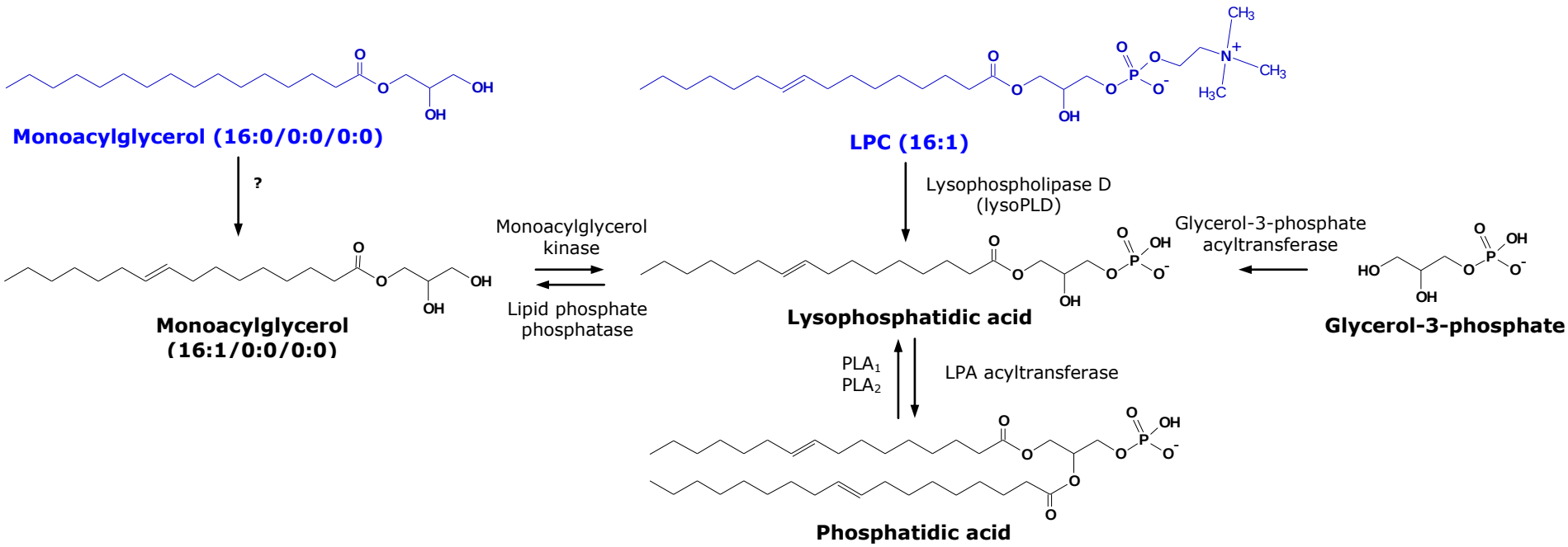

Figure 5-8 Biosynthetic routes of lysophosphatidic acid (LPA), a potent bioactive lysophospholipid. Different synthetic pathways for the formation of LPA have been identified (Pages et al., 2001) including the hydrolysis of LPCs by the action of lysophospholipase D and the phosphorylation of monoacylglycerol by monoacylglycerol kinase. In blue are depicted the potential precursors of LPA that were detected in hESC spent culture media. PLA, phospholipase.

Other compounds that were significantly increased in the media exposed to hESC were lactic acid, pyruvic acid, hydroxylated fatty acids (e.g. 3-hydroxyhexanoic acid, 3-hydroxystearic acid) and L-acetylcarnitine, implicated in glycolysis and fatty acid metabolism, respectively, but with no function directly associated with hESC maintenance. Nevertheless, these metabolites provided valuable insights of the metabolic events occurring during the *in vitro* cultivation of undifferentiated hESC. Their increased levels in the spent media could be explained as follows. Undifferentiated hESC are characterised by a low mitochondrial mass, reduced mitochondrial reactive oxygen species (ROS) production and by a small number of mitochondria when compared to their more mature differentiated-derivatives which are characterised by an increase in mitochondrial mass and number as well as higher ROS activity (Armstrong et al., 2010, Rehman, 2010) (Figure 5-9). As a result, undifferentiated hESC rely more on glycolysis (occurring in the cytosol) to meet their energy demands than on the Kreb's cycle and oxidative phosphorylation (OxPhos) metabolic pathways that take place in the mitochondria (Varum et al., 2011, Shyh-Chang et al., 2013). The end products of glycolysis are lactate and pyruvate which can exit the cell or be further metabolised. Particularly, pyruvate can be transformed in the mitochondria by pyruvate dehydrogenase (PDH) to acetyl-coenzyme A (Ac-CoA) and enter the Kreb's cycle to be further oxidised by OxPhos to produce adenosine triphosphate (ATP), although at the expense of generating ROS in the process (Zhang and Gutterman, 2007). However, because undifferentiated hESC have low mitochondrial mass and reduced mitochondrial number, only a small portion of Ac-CoA could enter the Kreb's cylce and the rest would start to accumulate. Therefore alternate routes may be required by the cells to dispose of the excess of Ac-CoA, otherwise, more Ac-CoA could be metabolised by the mitochondria and more ROS released to the cytosol which would increase the oxidation state of the cells and lead to differentiation (Yanes et al., 2010, Shyh-Chang et al., 2013, Tsatmali et al., 2005, Smith et al., 2000). One possible route is to use Ac-CoA for fatty acid biosynthesis or alternatively transform Ac-CoA to L-acetylcarnitine which can then be transported to the cytosol (Schroeder et al., 2012, Pettegrew et al., 2000) where it

could finally be secreted to the extracellular space. These alternative metabolic pathways could explain the increased concentrations observed of fatty acid intermediates and fatty acid metabolites (both with hydroxyl groups in the carbon backbone) as well as the increase of L-acetylcarnitine in the cell-exposed media. Nevertheless, metabolomics experiments targeting these metabolic routes and metabolites would be required to confirm these observations.

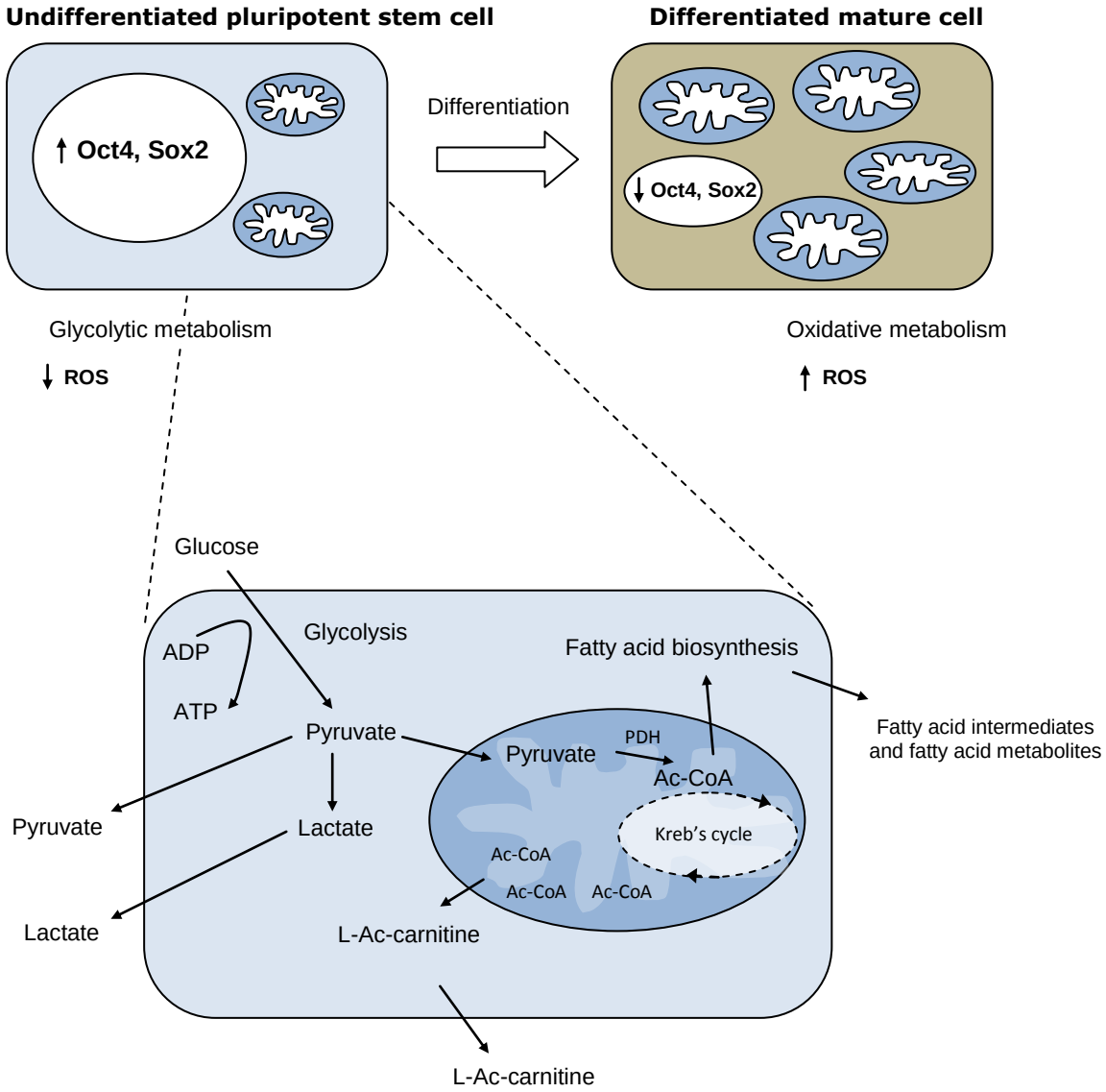

Figure 5-9 Upper panel: undifferentiated hESC and mature (differentiated) cell. Pluripotent stem cells show high expression of pluripotency markers such as Oct4 and Sox2 but low mitochondrial mass and number as well as reduced production of reactive oxygen species (ROS) (Rehman, 2010). They rely on glycolysis for their energy needs. On the contrary, differentiated cells show reduced expression of pluripotency markers and increased mitochondrial activity (oxidative metabolism) associated with high production of ROS. Lower panel: Metabolic events occurring in undifferentiated hESC during *in vitro* culture explaining increases in the concentration of metabolites like pyruvate, lactate, L-acetylcarnitine (L-Ac-carnitine) and hydroxylated fatty acids as well as the reduction of glucose in the spent culture media. PDH, pyruvate dehydrogenase; Ac-CoA, acetyl-coenzyme A.

Interestingly, some of the compounds identified previously in chapter 3 as significantly increased in MEF-CM, after the medium conditioning process, were further increased after exposure to hESC which suggests that they were not required by the cells; furthermore, that hESC also produced them. These compounds were 9, 12, 13-TriHOME and the ion at *m/z* 345.2437 putatively identified as 1alpha, 22-dihydroxy-23, 24, 25, 26, 27-pentanorvitamin D_3 (Table 5-3). The potential role of these metabolites in the maintenance of pluripotent hESC has been discussed in chapter 3 and 4, but since they seem not to be used by the cells, it is believed that these metabolites might be just excretion products of hESC metabolism. Furthermore, these metabolites were only observed when MEF-CM was used.

As mentioned in chapter 3, the main source of 9, 12, 13-TriHOME is linoleic acid (Funk and Powell, 1983, Nording et al., 2010) which consistently appeared here in the list of significantly decreased compounds of MEF-CM (Table 5-4). However, when cells were cultured in StemPro, linoleic acid appeared significantly increased and no 9, 12, 13-TriHOME was observed. A similar case occurred with docosapentaenoic acid (DPA). DPA decreased in MEF-CM but increased in StemPro spent medium. The reasons for these metabolic differences are not completely understood, but certainly indicate that hESC metabolism adjusts in response to the surrounding environment (i.e. culture medium).

Due to limitations in the available databases repositories many metabolites that were observed to increase significantly in the spent culture media remain unidentified. Consequently, their relevance in hESC culture could not be assessed. Whether some of the unknown metabolites exert a biological effect on hESC, it still remains to be determined.

5.3.5 Biological significance of decreased metabolites in spent culture media

Thirty nine compounds in MEF-CM and 14 in StemPro were significantly reduced after exposure to hESC (Table 5-4, Figure 5-10), suggesting that they were used by the cells; however, it is possible that they could have been adsorbed/absorbed by the culture substrate (Matrigel) too as it will be discussed later.

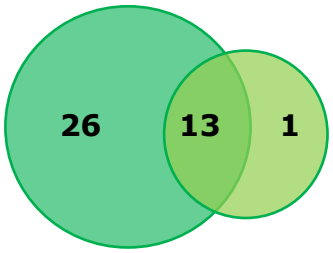

Figure 5-10 Venn diagram representing the compounds significantly decreased in MEF-CM (dark green) and StemPro (light green) after 24 h exposure to hESC.

Differences in the chemical composition between MEF-CM and StemPro (Table 1-2, chapter 1) are reflected here in the number of nutrients potentially consumed by hESC from each culture medium. Because StemPro is a serum-free medium, the cells are limited to a smaller number of nutrients; namely, amino acids and vitamins which are the major small-molecule components of StemPro (Wang et al., 2007). Therefore, it is not unexpected that most of the compounds that were significantly reduced in StemPro after culture with hESC were amino acids and vitamins (Table 5-4). Surprisingly, however, was the observation of a significant decrease of LPC(18:0), a compound not listed in the StemPro formulation and that most probably originated from the BSA used in StemPro manufacturing as it was discussed earlier in section 5.3.1. To confirm that the LPC(18:0) observed in StemPro fresh medium was not part of the LC-MS system or any other contamination during sample preparation, extracted ion chromatograms of a blank and StemPro before hESC culture were compared (Figure 5-11). The results indicated that StemPro indeed contained traces of LPC(18:0) since there

were no signs of carryover or contamination in the blank (Figure 5-11). In the same manner, arachidonic acid (*m/z* 303.2329) and LPC(16:0) (*m/z* 540.3312), not listed in StemPro recipe (Wang et al., 2007), were also confirmed to be present. As a consequence, it could be said that StemPro is not a complete chemically defined medium and that its 'known' composition is somewhat deceptive since there are compounds associated with BSA that are not published in its chemically defined formula. Furthermore, that some of these unpublished compounds may be relevant for hESC since, as demonstrated here, they appeared to be used by hESC in culture.

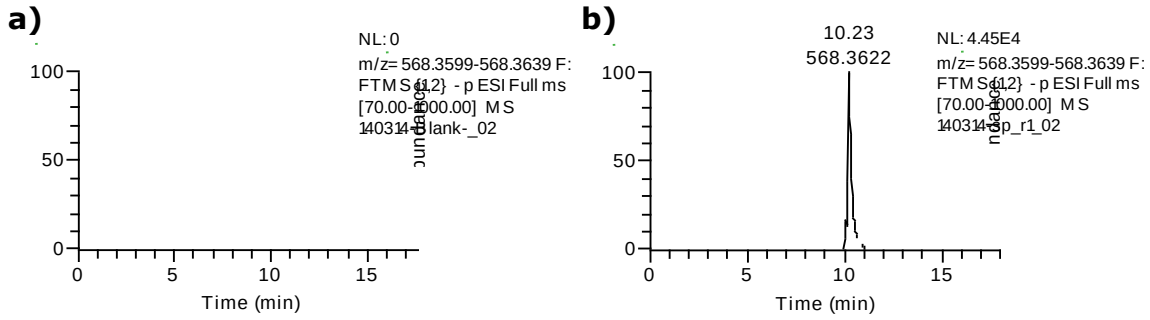

Figure 5-11 Extracted ion chromatograms of the ion *m/z* 568.3622 (LPC(18:0)) in a) blank and b) StemPro before hESC culture confirming the presence of this lysophospholipid in StemPro culture medium, even though it does not appear in StemPro published formulation (Wang et al., 2007).

As with StemPro, MEF-CM also showed reduced quantities of amino acids and vitamins. However, because MEF-CM is a complex, serum replacement-containing medium (which provides more nutrients to the cells), other MEF-CM components were also significantly reduced; amongst them, lysophospholipids and free fatty acids. Interestingly, most of the LPLs that were reduced contained 18-carbon length moieties, although entities of 16- and 20-carbon chains were also observed. It is still unclear however whether these LPLs were taken by the cells or if they were adsorbed to the substrate Matrigel. The most abundant constituents of Matrigel are laminin, type IV collagen, perlecan (a heparan sulfate proteoglycan) and entactin (Kleinman and Martin, 2005). As published by Roberts et al, these are a group of glycoproteins that

bind more specifically and with high affinity to sulphated glycolipids and show very low or null binding to phospholipids (Roberts et al., 1985); thus, strongly suggesting that the reduced LPLs were most likely used by the cells rather than being adsorbed to Matrigel, although there may be other unknown components of Matrigel that could have also sequestered the LPLs however this is unknown. Whether hESC used the LPLs, the next question would be, what could hESC have used LPLs for? It has been reported that LPLs, including LPCs, induce the expression of adhesion molecules such as vascular cell adhesion molecule-1 (VCAM-1) and intracellular adhesion molecule-1 (ICAM-1) in a wide variety of cells including prostate cells (YPEN-1 cell line), human embryonic kidney cells (293T cell line), leukocytes, human umbilical vein endothelial cells (HUVECs) and splenic B cells (Zou et al., 2007, Kume et al., 1992, Rieken et al., 2006, Lee et al., 2004). Therefore, it might be possible that hESC take the LPLs listed in Table 5-4 from the medium to enhance cell attachment and consequently their proliferation; however, no study has been published to support this notion.

With regard to the fatty acids that were decreased in spent culture medium, it was observed that amongst them, the most highly consumed were mono- and poly-unsaturated fatty acids as compared to relatively few saturated ones (Table 5-4, Figure 5-12).

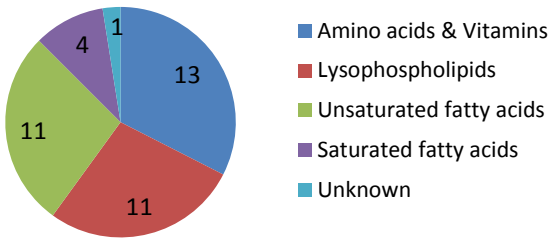

Figure 5-12 Compounds significantly decreased in MEF-CM after 24 h exposure to hESC. Note the large proportion of unsaturated fatty acids potentially consumed by hESC as compared to the small proportion of saturated fatty acids.

In total, eleven unsaturated- and 4 saturated- fatty acids were significantly decreased in MEF-CM after exposure to hESC. In agreement with these results, Yanes and colleagues, by studying the intracellular metabolites of hESC (also cultured with MEF-CM), reported that undifferentiated hESC were characterised by abundant unsaturated molecules (Yanes et al., 2010) and that such compounds were important in the regulation of the cellular redox status since they are reactive and susceptible to oxygenation and hydrogenation reactions which ultimately can mediate the balance between self-renewal and differentiation (Yanes et al., 2010, Rehman, 2010). Examples of polyunsaturated fatty acids that were reduced in MEF-CM after hESC exposure are linolenic, docosapentaenoic, arachidonic and eicosapentaenoic acids (Figure 5-13) which consistently were found in the metabolite profile of hESC performed by Yanes et al (Yanes et al., 2010).

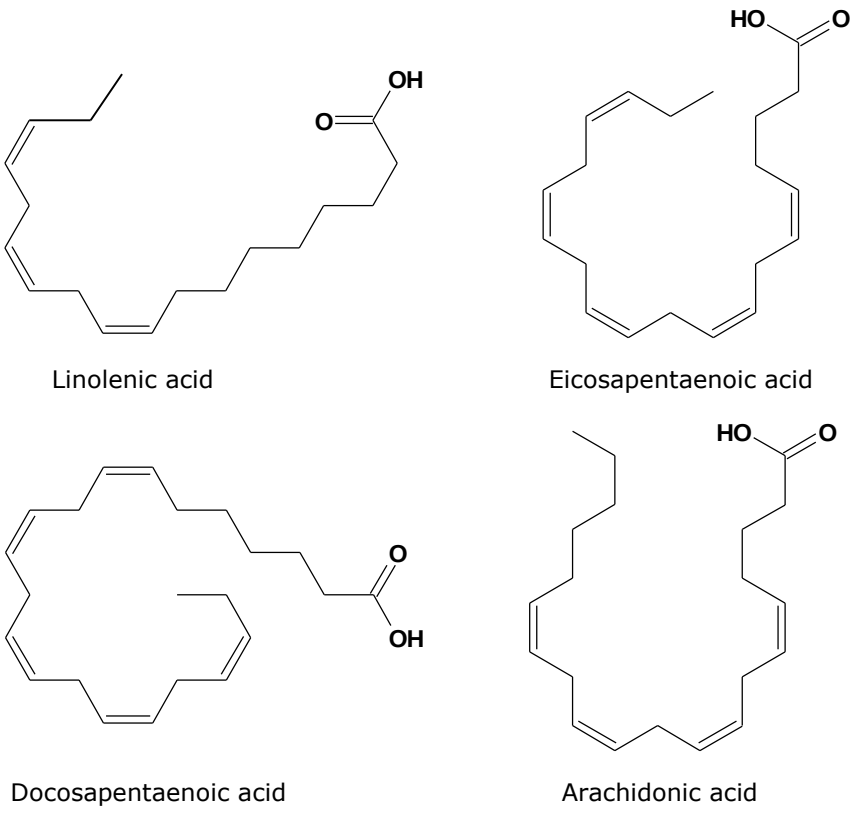

Figure 5-13 Examples of unsaturated fatty acids potentially incorporated by hESC when cultured with MEF-CM.

5.4 Conclusions

The chemical investigation of the hESC secretome has become of vital importance in the identification of the autrocrine and paracrine factors released by hESC. In this study, the untargeted LC-MS-based metabolomics method developed in chapter 2 was applied and proved to be successful in the identification of a number of low-molecular weight factors secreted by hESC in culture. To the best of the thesis author's knowledge, this is the most comprehensive metabolomics analysis of the hESC secretome which complements the discoveries of other research groups aiming at the identification of the protein components.

The use of a chemically defined medium such as StemPro, in addition to the traditional MEF-CM, allowed a better appreciation of the secreted metabolites. For example, increases in the lysophospholipids levels were more noticeable in StemPro than in MEF-CM. Furthermore, comparison of the increased and decreased metabolites in both spent culture media highlighted the importance of lysophospholipids in hESC since when cells were cultured in the absence (or low abundance) of lysophospholipids like StemPro, hESC were able to produce and secrete them to the extracellular space, whereas when they were cultured in a lysophospholipid-rich medium like MEF-CM, hESC seemed to incorporate/use them. What is more, amongst the increased metabolites in the spent culture media, lysophospholipids were the ones with known biological activity. These results suggest lysophospholipids as potential small-molecule autocrine/paracrine factors; however, their precise role in the maintenance of hESC still remains to be determined.

Overall, the use of an untargeted metabolomics method for the study of the hESC secretome has provided valuable and complementary information in our understanding of the molecular mechanism governing hESC which ultimately will aid in the development of more efficient protocols for the large-scale expansion of undifferentiated hESC *in vitro*.

CHAPTER 6

General conclusions

6 General conclusions

Through a series of metabolomics experiments this thesis aimed to identify small-molecule factors with potential biological activity in the proliferation and/or pluripotency of hESC. To accomplish this, an untargeted metabolomics method was developed and applied to the analysis of culture media used in *in vitro* growth of hESC.

The metabolomics method, based on the use of liquid chromatography and mass spectrometry, was developed aiming the comprehensive analysis of the small molecule components of the culture media. The initial application of the method was the identification of the unknown components of UM. The analysis revealed that AlbuMax I, the constituent of knock out serum replacement, was responsible for the peaks observed after minute 6 of the chromatographic run. Several classes of lipids were identified including lysophosphatidylcholines, lysophosphatidylethanol-amines, cholic-acid derivatives, fatty-acid amides and free fatty acids. The characterisation of the UM constituents represented one of the major achievements of the methodology as it was possible to enhance the chemical definition of a widely used hESC culture medium revealing not previously reported information that could help cell biologist to get a deeper understanding of hESC behaviour *in vitro*.

The ability of the LC-MS method to provide putative identities to the components of UM surpassed previous attempts (Frankland et al., 2007, Garcia-Gonzalo and Izpisua Belmonte, 2008) trying to characterise such components and that were only able to provide lipid classes rather than more defined identities. To date, the chemical characterisation achieved with the method developed in this thesis represents the most comprehensive chemical definition of UM.

The application of the methodology to the investigation of the metabolites secreted by MEFs into the conditioned medium successfully identified a number of compounds whose concentrations increased after the medium conditioning process. To the majority of these compounds a putative identity was assigned; however, due to limitations in the databases' repositories some remained unidentified. Amongst the increased small molecules were compounds with known biological activity such as the prostaglandins PGE_2 and 6-keto-PGF1α, 7-ketocholesterol and some polyunsaturated fatty acids like 9, 12, 13-TriHOME and stearidonic acid. The use of authentic standards finally confirmed their presence in MEF-CM. With the exception of PGE_2 and 6-keto-PGF1α, the rest of molecules were for the first time identified in MEF-CM.

In addition to the identification of increased metabolites in MEF-CM, the methodology was also able to detect those compounds whose concentrations declined after incubation with MEFs. Examination of the increasing and decreasing molecules led to the identification of some metabolic activities taking place during the conditioning of the medium. One of those metabolic activities identified was arachidonic acid metabolism. It was observed that while levels of arachidonic acid decreased, those of prostaglandins (PGE_2 and 6-keto-PGF1α) increased. With the use of isotope labelled arachidonic acid, it was confirmed that MEFs, and not any enzyme present in the serum replacement, were responsible for the conversion of arachidonic acid into prostaglandins.

The analysis of a series of MEF-CM obtained from different batches of MEFs or on different days employing the same batch of MEFs, showed chemical variability between MEF-CM batches and underscored the inconsistent and fluctuating conditions to which hESC are exposed to in routine culture. The information attained with these experiments might help understand the varying culture efficiencies reported in the literature (Villa-Diaz et al., 2009) when hESC are cultured with batches of MEF-CM obtained on different days.

Having successfully identified low-molecular weight factors in MEF-CM with potential biological activity, the compounds were investigated to test their effects on hESC. However, because it is unknown at what concentration they possibly exert their effects, it was decided to quantify the selected compounds in several batches of MEF-CM and use the grand mean in order to resemble the concentrations at which they are normally found in MEF-CM. PGE_2, 6-keto-PGF1α, 7-ketocholesterol, 9, 12, 13-TriHOME and stearidonic acid, previously confirmed with standards, were supplemented in combination to UM and tested for their effects. In spite of the stringent conditions (absence of growth factors) in which the compounds were investigated, it was observed that hESC cultivated in the presence of these chemicals could proliferate for at least one more passage compared to cells grown with UM alone (the negative control). For the first time it was demonstrated that small-molecule components identified in MEF-CM can mediate some proliferative effects. This represented another major achievement of the work undertaken in this thesis as the small molecules identified are potential candidates to the creation of more defined and efficient culture protocols or to the enhancement of others such as mTeSR1 or StemPro. Because of the lack of time, no further research could be done but some planned experiments derived from these results are proposed in the future work section.

Due to the increasing evidence of the importance of autocrine and paracrine factors in the regulation of pluripotency and self-renewal of hESC, it was decided to study the hESC secretome. Employing the same methodology, the spent culture medium of hESC using MEF-CM or StemPro was investigated. The use of a less complex medium such as StemPro facilitated the identification of metabolites secreted by hESC under normal culture with Matrigel. Although all the identified metabolites provided insights into the metabolic activities of hESC in *in vitro* culture, the most relevant ones in terms of factors with potential biological activity were lysophospholipids. The importance of this class of lipids was identified due to the fact that when cells were cultured with StemPro (a lysophospholipid-free medium), hESC were able to secrete

lysophospholipids to their extracellular space, whereas when they were cultured in a lysophospholipid-rich medium like MEF-CM, they seemed to use them. Nevertheless, the precise biological activity of these compounds still remains to be determined and some proposed experiments towards this are described in the future work section.

The work carried out with this thesis has demonstrated that the relatively unexplored small-molecule components of MEF-CM and hESC secretome can provide valuable information to understanding stem cell biology and the small-molecule requirements for their long-term expansion. At the same time, the information garnered with this metabolomics method complements the extensive work of other research groups aiming the identification of the protein components of MEF-CM and hESC secretome.

The contribution of this work to the identification of potential low-molecular weight factors that can mediate some biological activities in hESC may be important to the establishment of a more defined culture system for the full realization of hESC in clinic and other research areas.

FUTURE WORK

Some proposed experiments derived from the results obtained in this thesis are detailed:

Given that 9, 10, 13-TriHOME and 9, 12, 13-TriHOME are mainly produced by the oxidation of linoleic acid and that linoleic acid levels remain unchanged after medium conditioning in spite of the production of TriHOMEs, it is proposed to use deuterated LPC(18:2) to determine whether the levels of linoleic acid are being replenished by the hydrolysis of LPC(18:2). Similarly, the use of deuterated LPC (18:3) would confirm whether LPC(18:3) is used to replenish the levels of alpha-linolenic acid, the most likely substrate for the production of stearidonic acid, one of the PUFAs increased in MEF-CM. If the deuterated LPCs are indeed converted to the corresponding fatty acid, linoleic acid or alpha-linolenic acid, then it would be expected to observe the deuterated form of these fatty acids and possibly small quantities of deuterated TriHOMEs or stearidonic acid, respectively. These isotope labelling flux experiments would confirm some of the metabolic pathways occurring during the conditioning of UM and explain the unexpected high levels of linoleic and alpha-linolenic acids.

In order to investigate more in depth how the age of MEFs influence the hESC growth efficiency of the MEF-CM they produce, it is proposed to perform PLS analysis where the X variables are the metabolites measured with the LC-MS methodology described in this thesis and the Y variables the percentages of cell viability, cell proliferation and percentage of undifferentiated cells observed with each batch of MEF-CM obtained on different days. The PLS model would reveal which X variables (metabolites) are correlated with the performance of the MEF-CM media. Likewise, this experiment can be repeated employing separate batches of MEFs in order to find out, in a more systematic way, which metabolites have major influence on the efficiency of MEF-CM batches.

With regard to the confirmation of metabolites present in MEF-CM, it would be necessary to test whether the structural isomer of calcitriol, 24, 25-dihydroxyvitamin D3, matches the experimental data of the $[M+H]^+$ ion at *m/z* 417.3360 in terms of full scan MS and tandem mass spectrometry since calcitriol failed to match them. Another experiment would be to improve the liquid-chromatography conditions of the current method in order to separate more efficiently the peaks of the standards 9, 10, 13-TriHOME and 9, 12, 13-TriHOME and therefore verify with a greater degree of certainty which of the two TriHOMEs is present in the conditioned medium.

It is also suggested to assess the biological activity of PGE_2, 6-keto-PGF1α, 7-ketocholesterol, 9, 12, 13-TriHOME and stearidonic acid in multiple ways. The first one, investigating each compound individually at varying concentrations and measuring cell viability and pluripotency markers to determine which one(s) exert a positive effect on the expansion of undifferentiated hESC. Another proposed experiment is to examine the compounds in a pairwise manner, also at varying concentrations, to look for any possible synergism. Once it has been determined which compound or mix of compounds (and the concentrations at which they perform the best) enhances the culture conditions, then it would be possible to add the selected compounds to defined culture media such as StemPro or mTeSR1 and subsequently determine whether the extra compounds improve the efficiency of such kind of media. In the first instance, the improved culture medium recipes would be tested with Matrigel as substrate. If successful, other synthetic substrates such as PE-TCPS, PMEDSAH and APMAAm would also be evaluated.

For the analysis of the hESC secretome, it is recommended to repeat the experiment adding a second control which would consist in the incubation of StemPro and MEF-CM with Matrigel alone (without hESC) and consequently determine if the reduced concentrations of lysophospholipids observed with both media are due to their adsorption

or absorption to Matrigel or because they were indeed used by the cells. It would be expected that the levels of the lysophospholipids in the fresh media and in the media incubated with Matrigel alone would not differ significantly; therefore suggesting that hESC consume/use the lysophospholipids during their *in vitro* culture. In order to confirm this outcome, hESC would be cultured with isotope labelled lysophospholipids and then carry out a metabolomics fingerprinting experiment employing Yanes et al method (Yanes et al., 2010). It would be expected to find isotope labelled lysophospholipids or any related isotope labelled metabolites such as free fatty acids as result of lysophospholipids hydrolysis.

Finally, in the event that the lysophospholipids were absorbed or adsorbed to Matrigel, then the following experiment would be to test hESC growth efficiency under two conditions. Firstly, cultivating hESC over Matrigel using the standard protocol; and secondly, preconditioning Matrigel with non-labelled lysophospholipids to allow their adsorption or absorption and then continue with the standard culture protocol. By measuring the percentages of cell viability, cell proliferation and the number of undifferentiated cells, it would be determine whether or not the lysophospholipids have an impact on hESC growth.

Appendix A

MS/MS spectra of compounds identified in unconditioned medium.

-ESI 187.0065
4-Sulfobenzyl alcohol

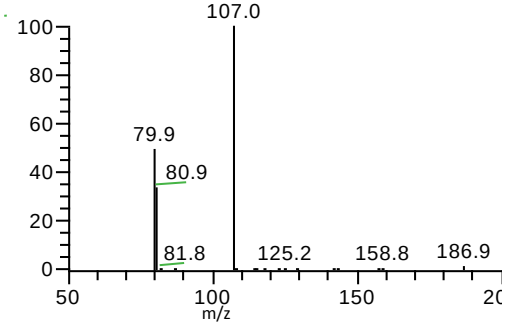

-ESI 375.1311
Riboflavin

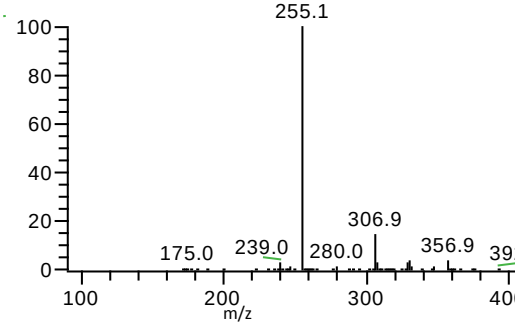

-ESI 353.0491
Phenol red

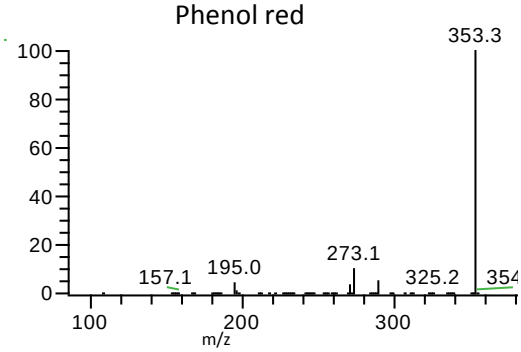

-ESI 371.0597
Unknown

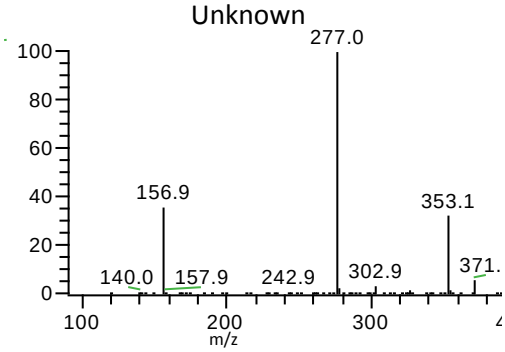

-ESI 351.0333
Unknown

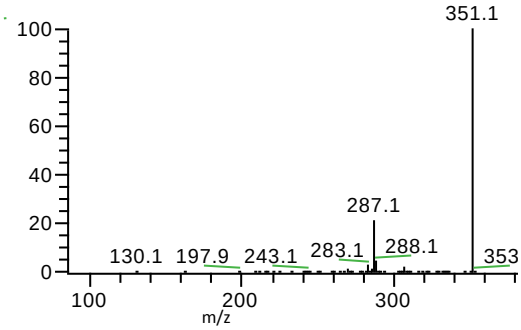

-ESI 514.2844
Taurocholic acid

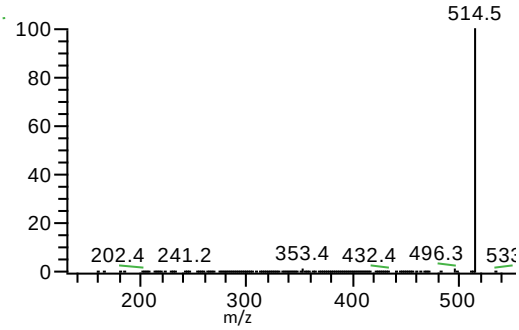

+ESI 516.2987
Taurocholic acid

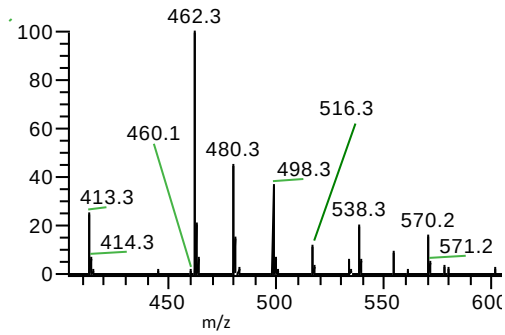

-ESI 498.29
Taurodeoxycholic acid

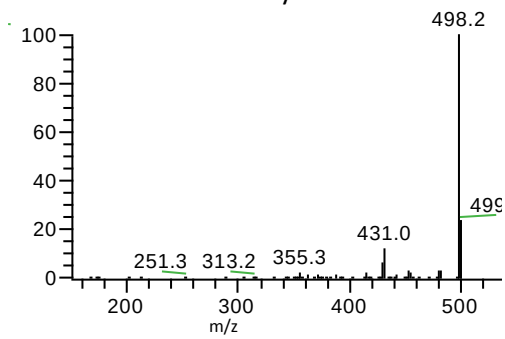

+ESI 500.3038
Taurodeoxycholic acid

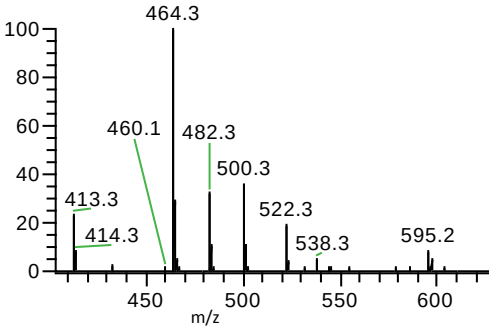

-ESI 464.3021
Glycocholic acid

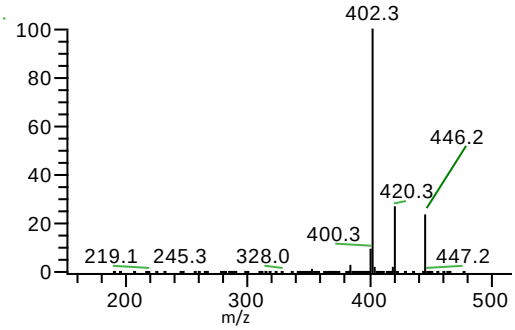

+ESI 466.3162
Glycocholic acid

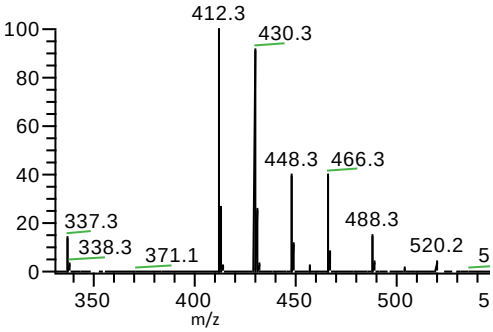

-ESI 482.2945
Lithocholyltaurine

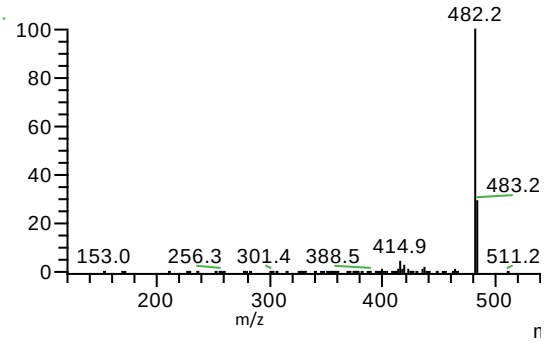

-ESI 407.2805
Cholic acid

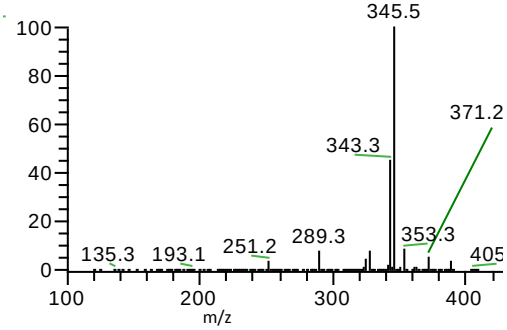

-ESI 448.3072
Glycodeoxycholic acid

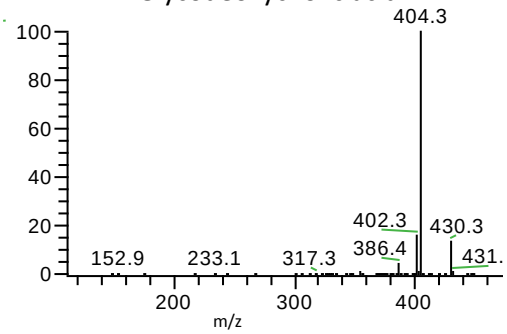

+ESI 450.3213
Glycodeoxycholic acid

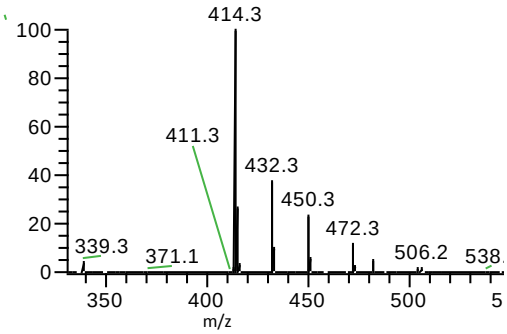

-ESI 293.1760
Unknown

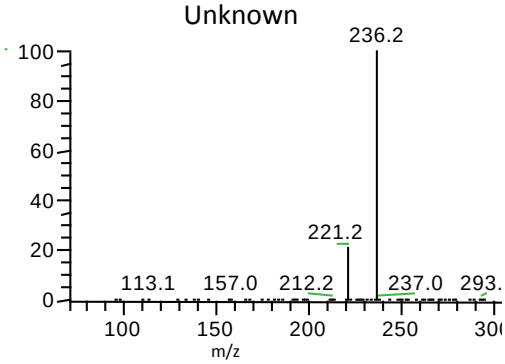

-ESI 452.2783
LysoPC(14:0)

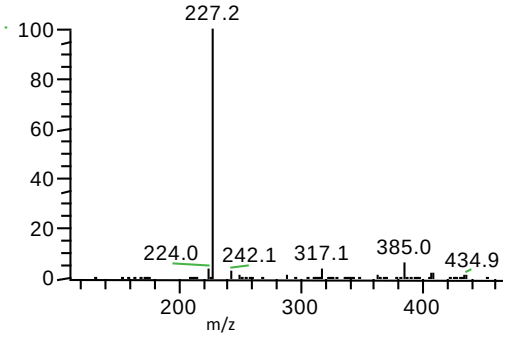

-ESI 452.2783
LysoPE(16:0/0:0)

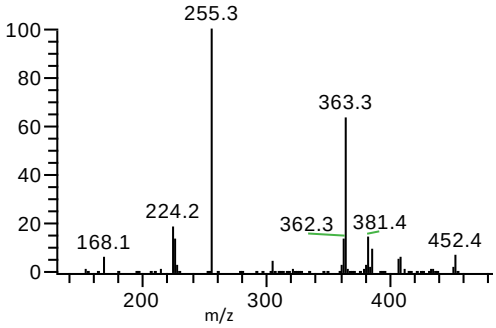

-ESI 502.2941
LysoPC(18:3)

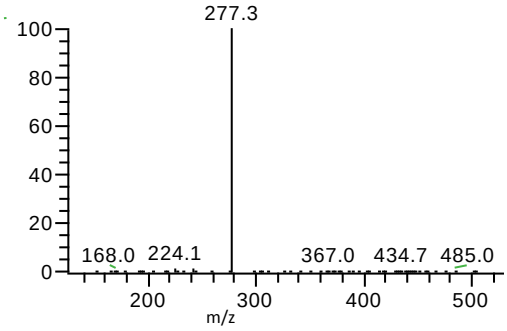

-ESI 474.2626
LysoPE(18:3)

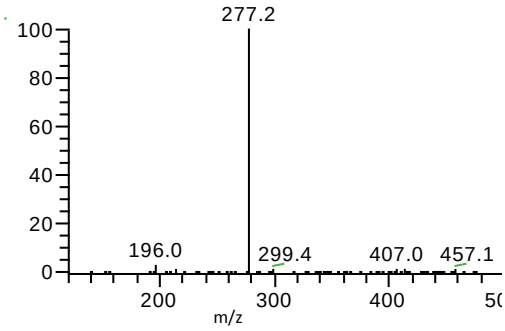

-ESI 526.2939
LysoPC(20:5)

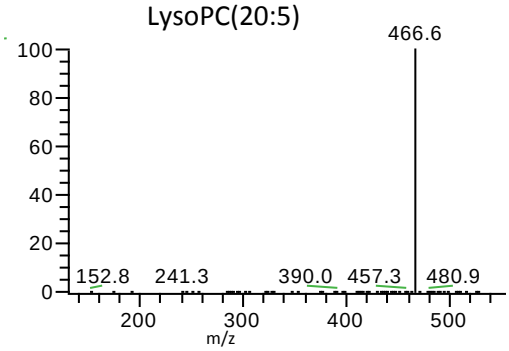

-ESI 526.2939
LysoPE(22:5)

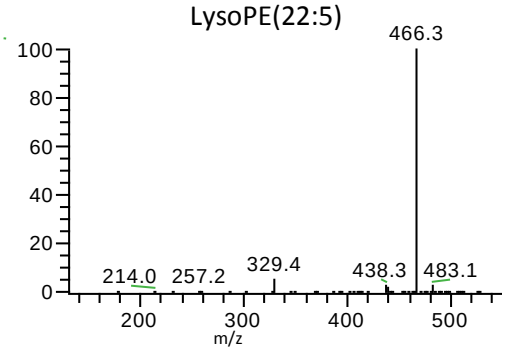

-ESI 436.2833
PC(O-14:1)

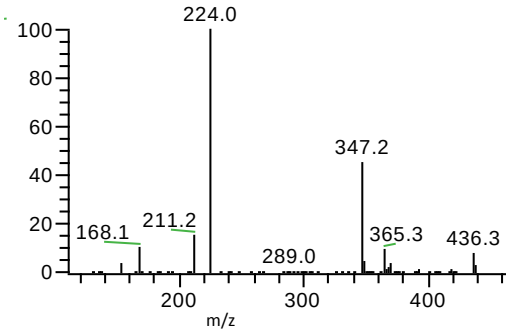

-ESI 436.2939
PE(P-16:0e/0:0)

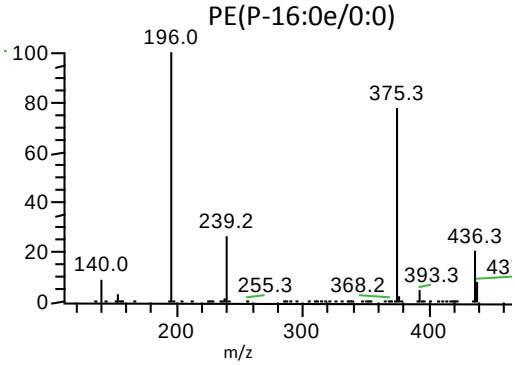

-ESI 478.2939
LysoPC(16:1)

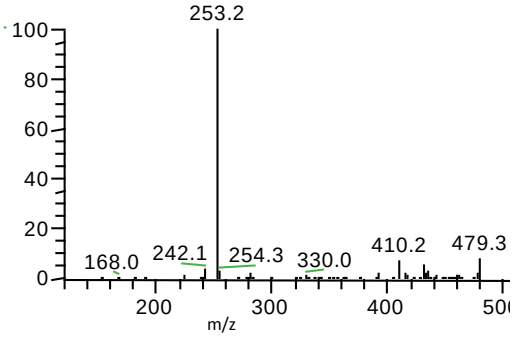

-ESI 478.2939
LysoPE(18:1)

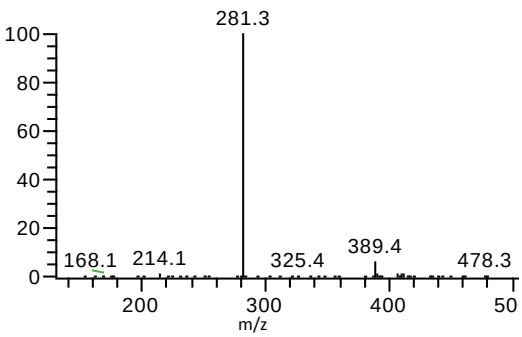

-ESI 466.2938
LysoPC(15:0/0:0)

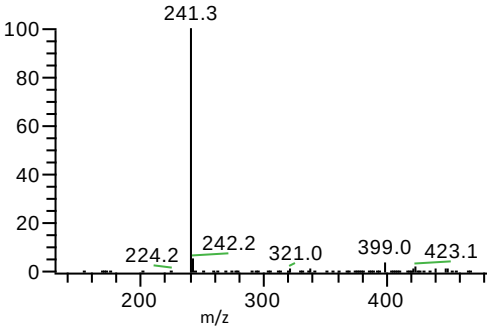

-ESI 391.2854
Deoxycholic acid

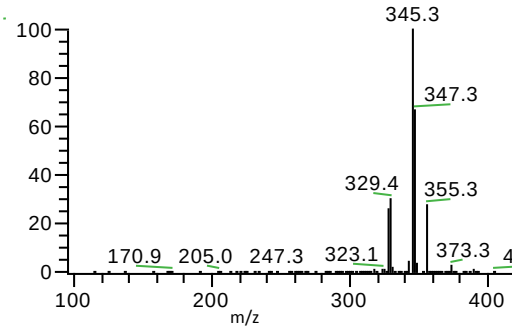

+ESI 375.2894
Deoxycholic acid

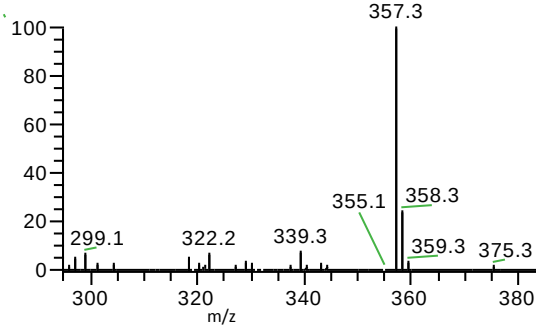

-ESI 476.2785
LysoPE(18:2)

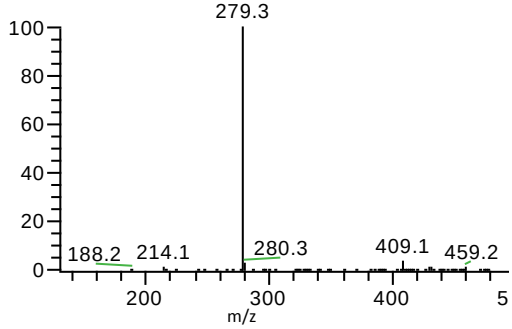

-ESI 500.2788
LysoPE(20:4)

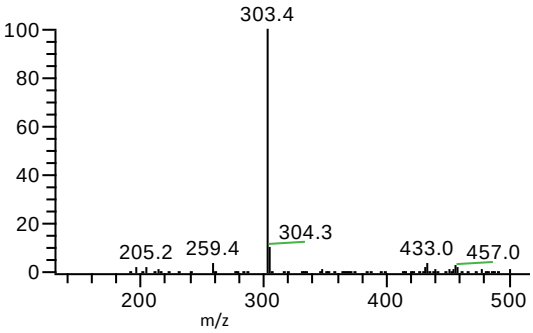

-ESI 504.3101
LysoPC(18:2)

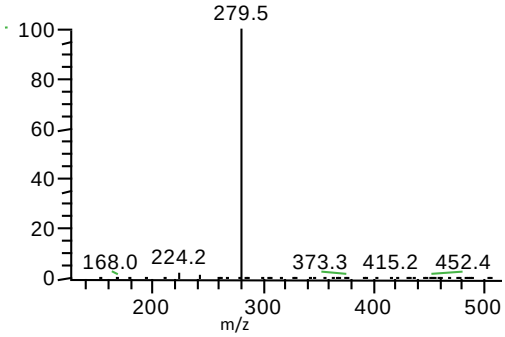

-ESI 450.2993
LysoPC(P-15:0/0:0)

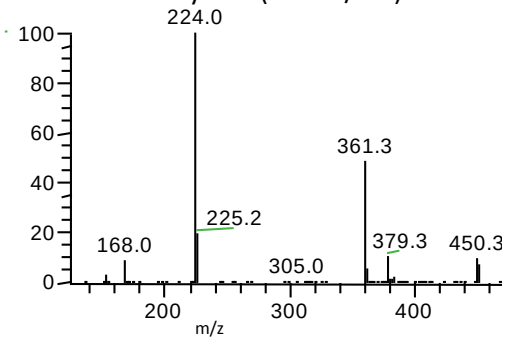

-ESI 480.3094
LysoPC(16:0/0:0)

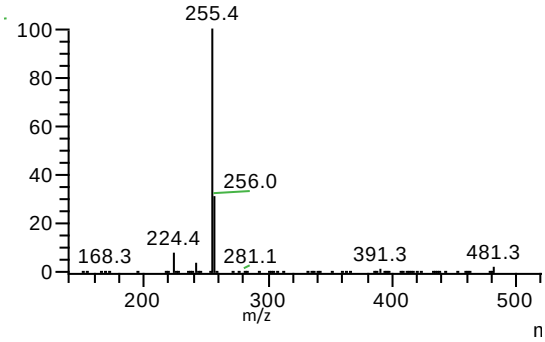

-ESI 480.3094
LysoPE(18:0/0:0)

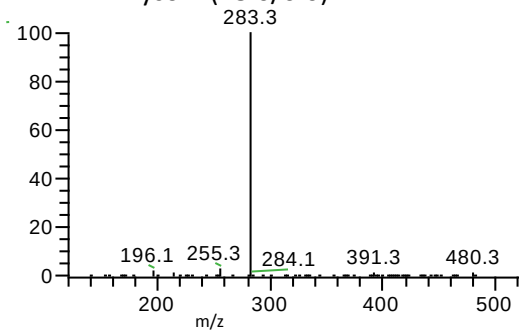

-ESI 554.3252
LysoPC(22:5)

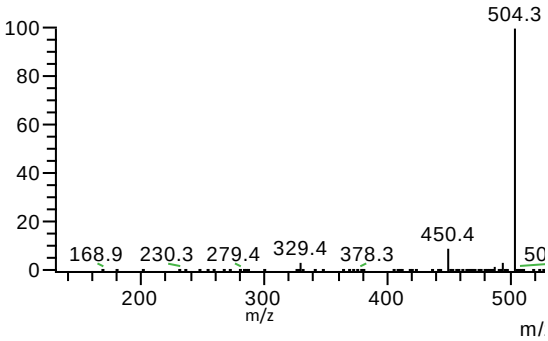

-ESI 506.3252
LysoPC(18:1)

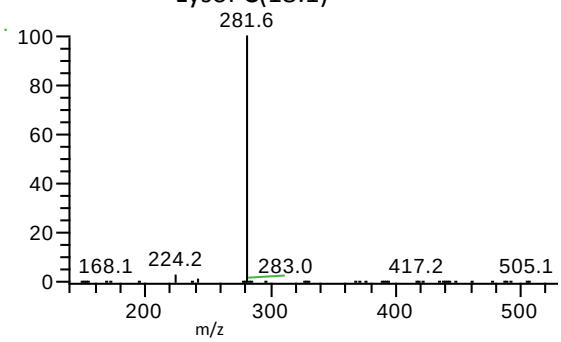

-ESI 464.3149
LysoPC(P-16:0/0:0)

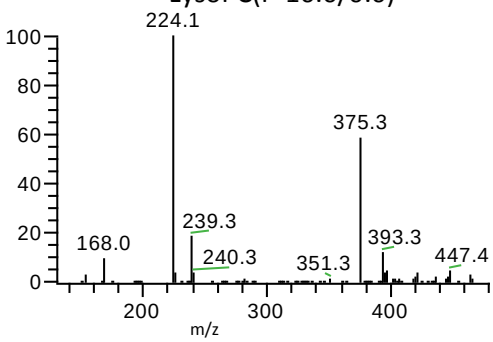

-ESI 528.3098
LysoPC(20:4)

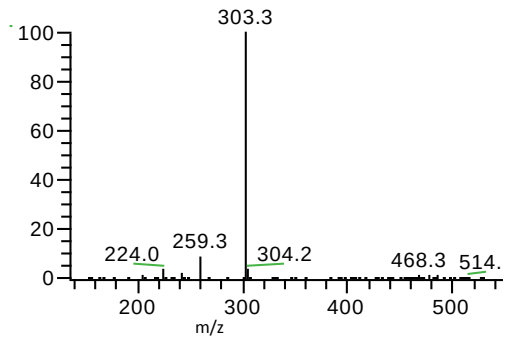

-ESI 530.3251
LysoPC(20:3)

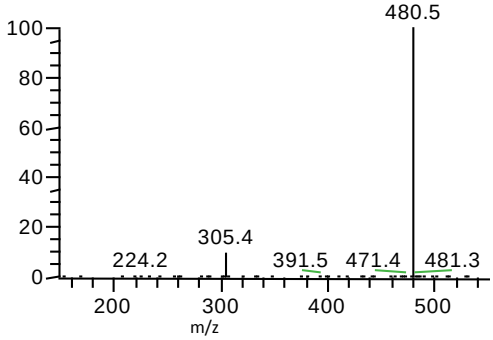

-ESI 536.3726
LysoPC(20:0)

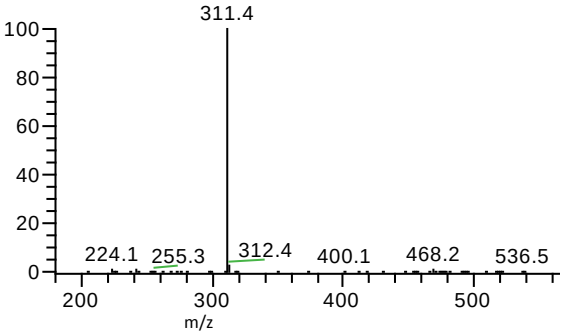

-ESI 494.3253
LysoPC(17:0)

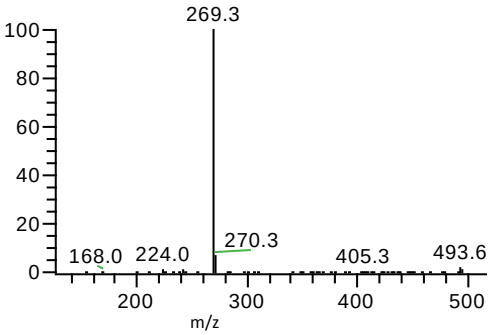

-ESI 508.3409
LysoPC(18:0)

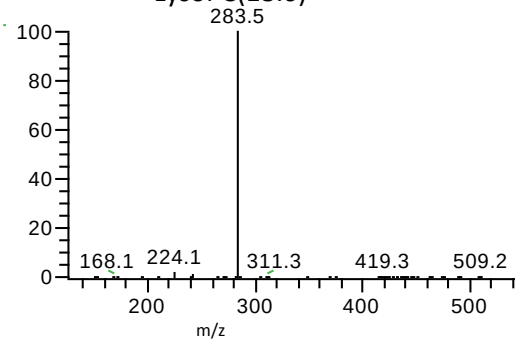

-ESI 313.2386
Octadecanedioic acid

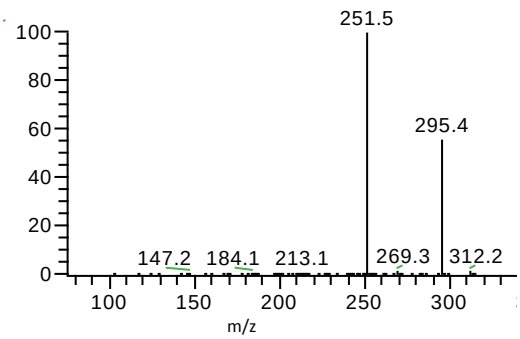

-ESI 337.2385
Unknown

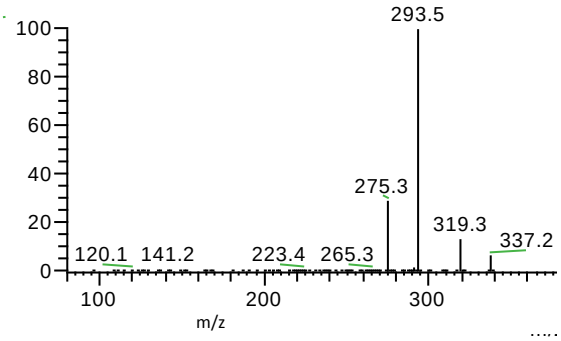

-ESI 299.2591
Hydroxystearic acid

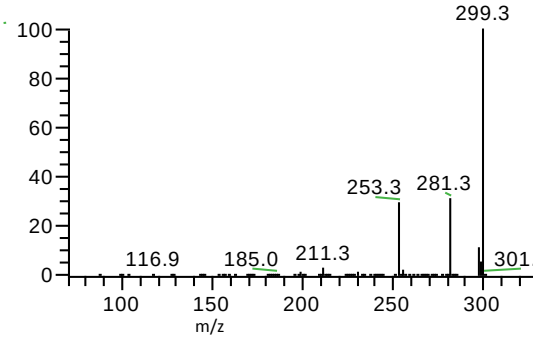

-ESI 313.2750
2-hydroxynonadecanoic acid

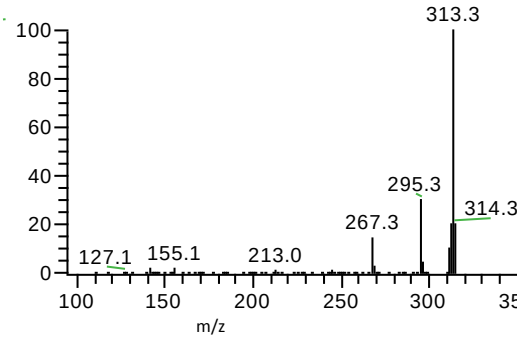

-ESI 301.2174
Eicosapentaenoic acid

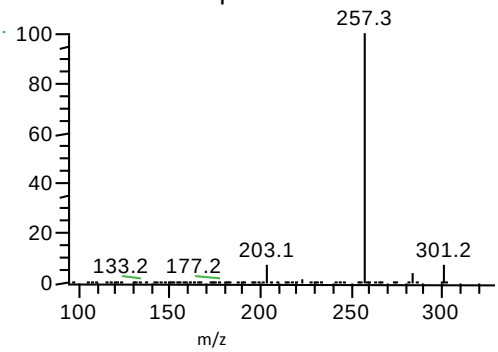

-ESI 277.2172

α-linolenic acid

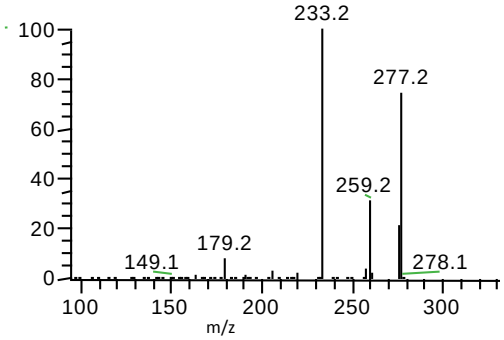

-ESI 227.2012

Myristic acid

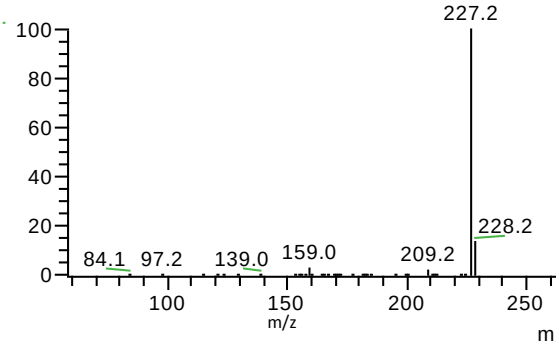

-ESI 327.2328

Docosahexaenoic acid

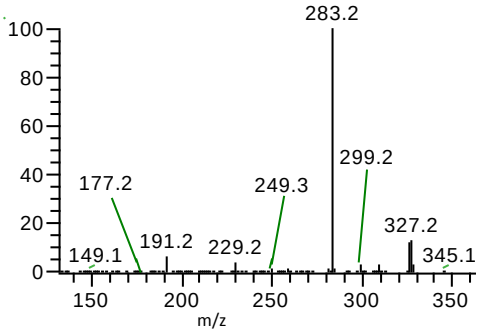

-ESI 253.2173

Palmitoleic acid

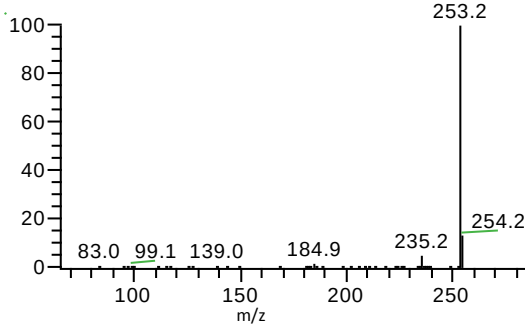

-ESI 303.2331

Arachidonic acid

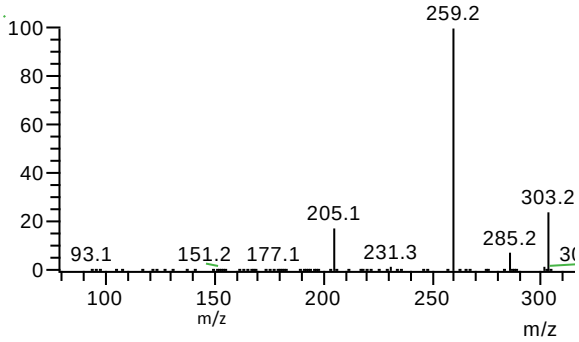

-ESI 241.2171

Pentadecanoic acid

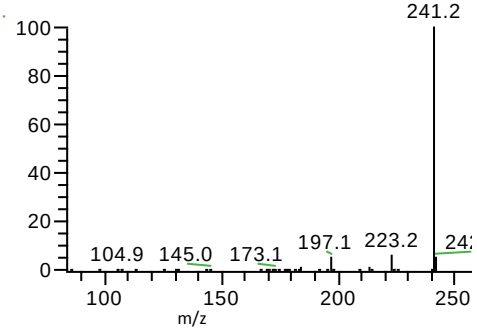

-ESI 329.2487

Docosapentaenoic acid

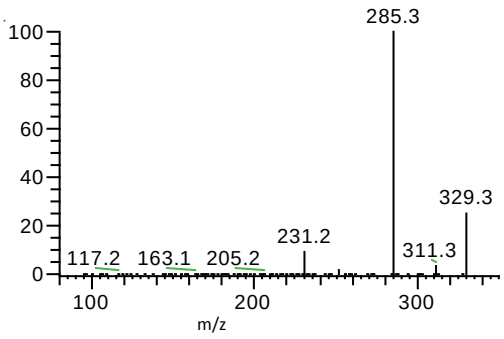

-ESI 279.2331

Linoleic acid

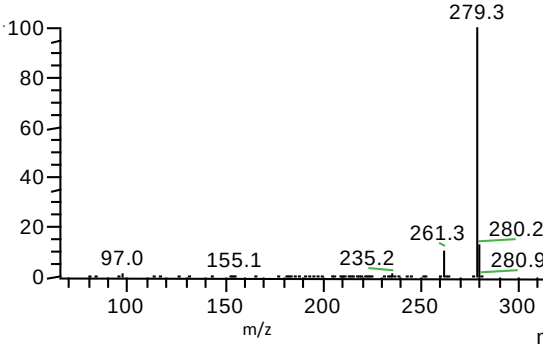

-ESI 267.2331
(Z)-9-Heptadecenoic acid

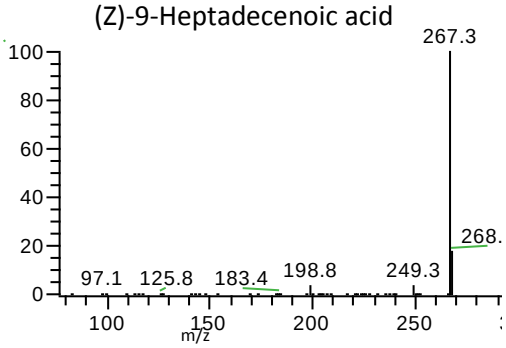

-ESI 305.2485
Dihomo-γ-linolenic acid

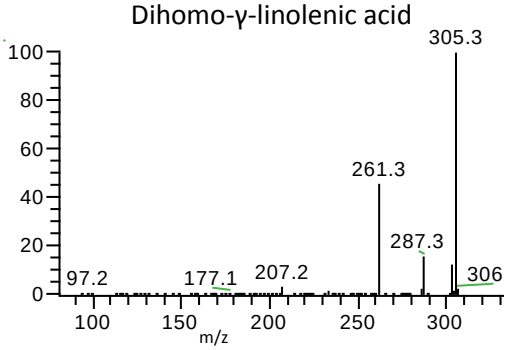

-ESI 255.2329
Palmitic acid

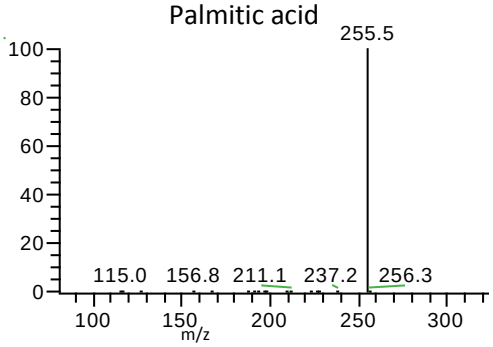

-ESI 281.2485
Oleic acid

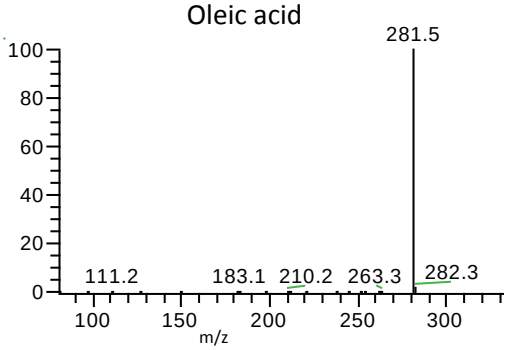

-ESI 269.2485
Heptadecanoic acid

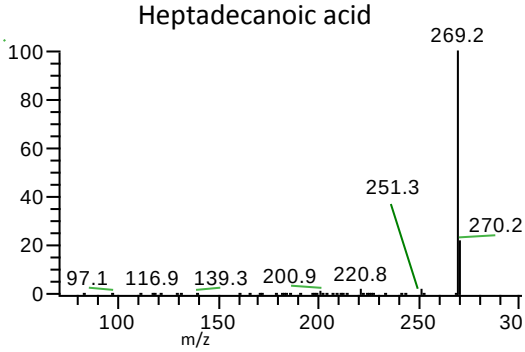

-ESI 283.2642
Stearic acid

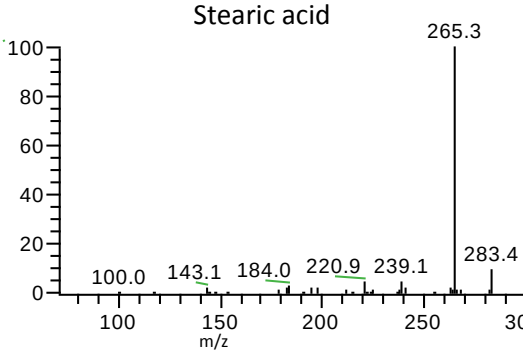

-ESI 311.2955
Arachidic acid

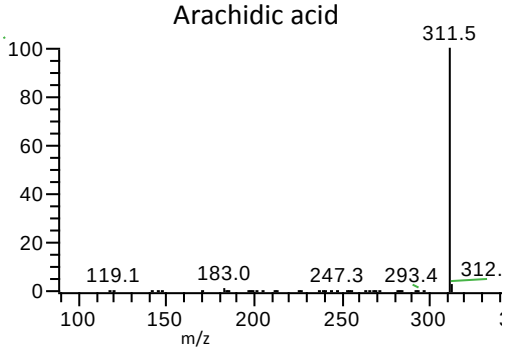

+ESI 288.2893
C17-Sphinganine

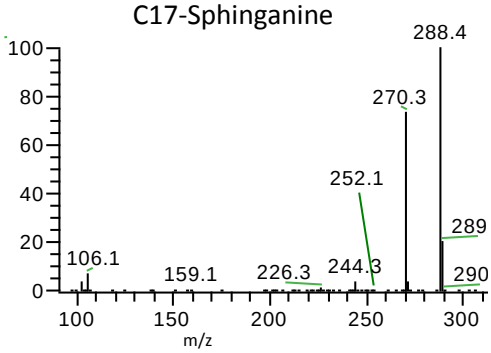

+ESI 254.2475
Palmitoleamide

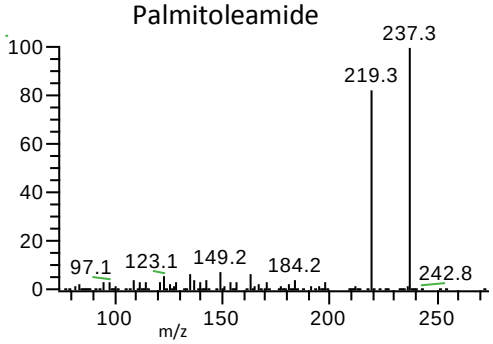

+ESI 280.2632
Linoleamide

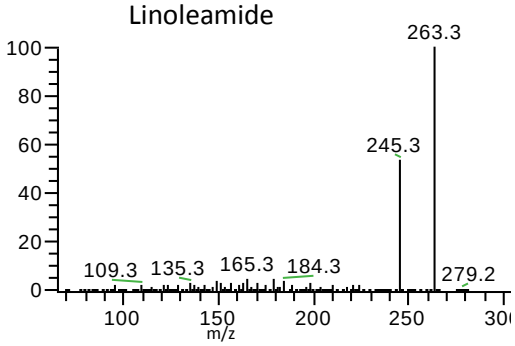

+ESI 256.2633
Palmitamide

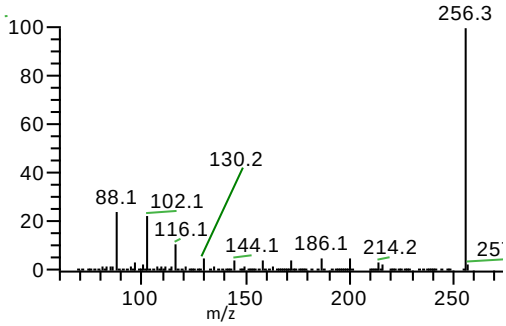

+ESI 282.2789
Oleamide

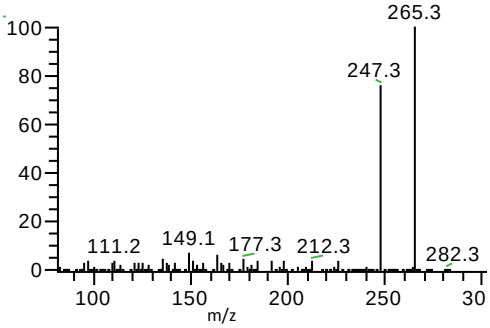

+ESI 284.2943
Stearamide

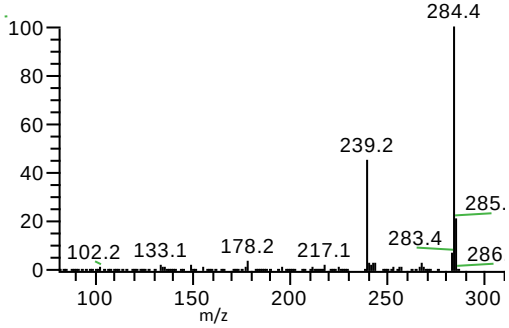

+ESI 310.3100
Oleoyl ethyl amide

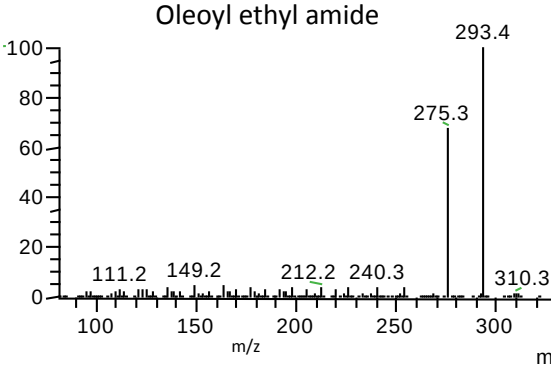

+ESI 338.3412
13Z-Docosenamide

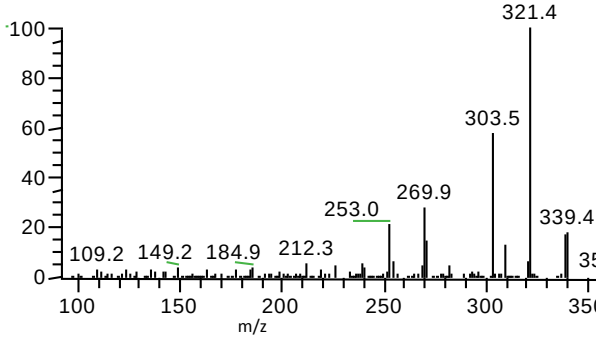

+ESI 296.2582
(4E,8E,10E-d18:3)sphingosine

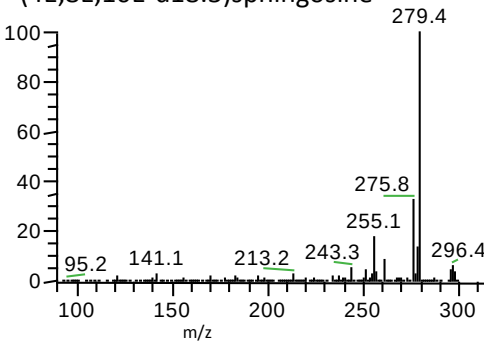

Appendix B

Experimental MS/MS spectra of significantly increased and decreased metabolites in MEF-CM.

-ESI 129.0548
4-methyl-2-oxovalerate

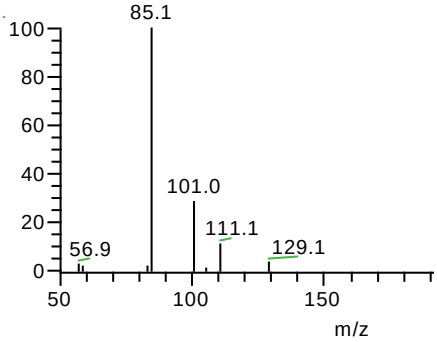

-ESI 89.0234
Lactic acid

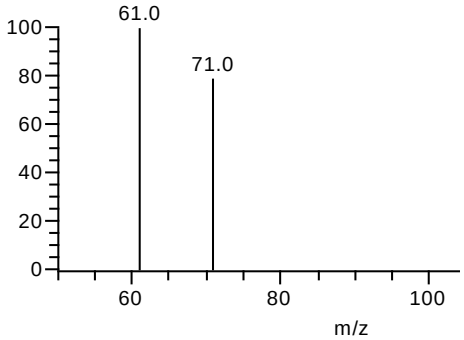

+ESI 147.0762
L-glutamine

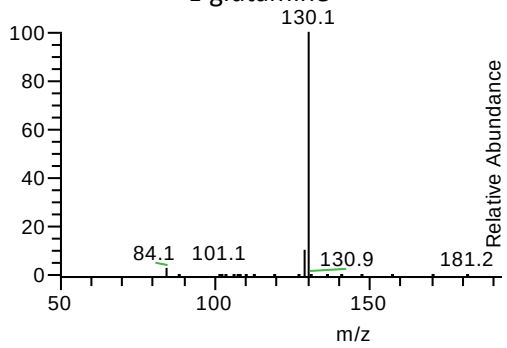

-ESI 369.2284
6-keto-PGF1a

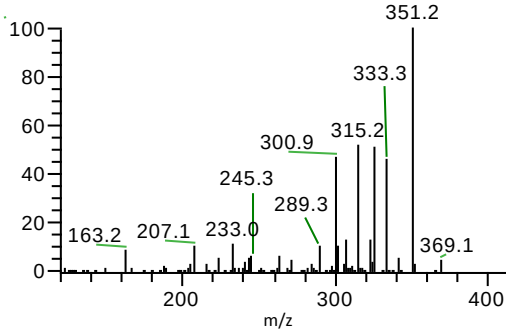

-ESI 329.2336
9, 12, 13-TriHOME

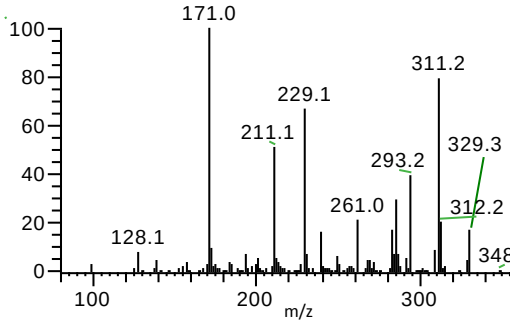

-ESI 333.2074
PGE_2

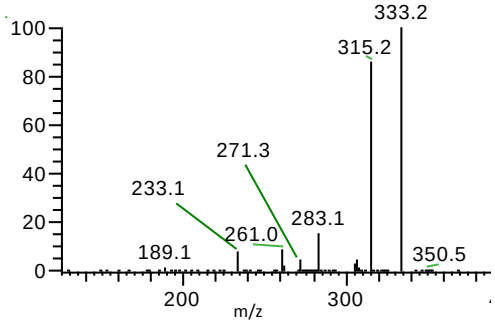

-ESI 586.3154
LPC(20:5(5Z,8Z,11Z,14Z,17Z))

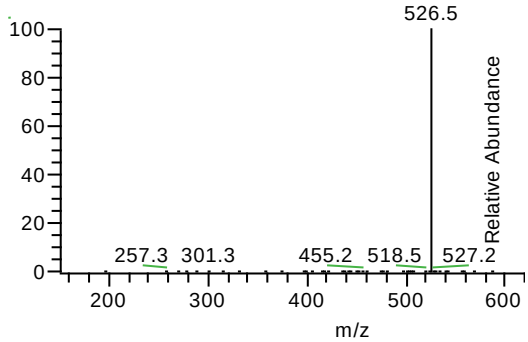

-ESI 588.3309
LPC(20:4(5Z,8Z,11Z,14Z))

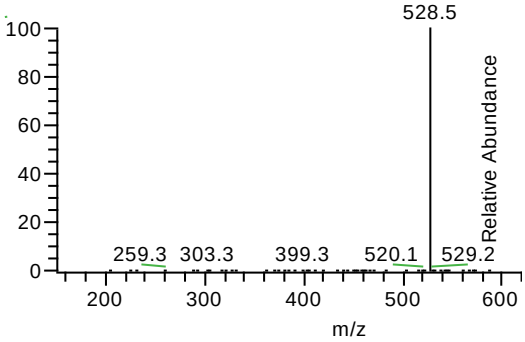

-ESI 590.3470
LPC(20:3(5Z,8Z,11Z))

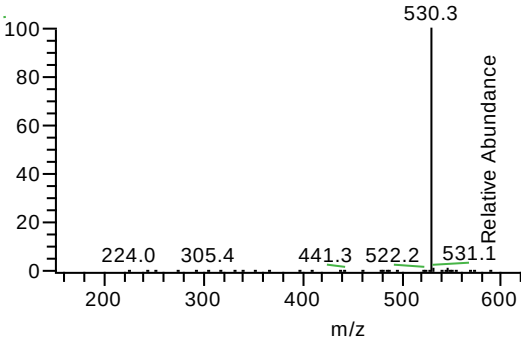

-ESI 614.3467
LPC(22:5(7Z,10Z,13Z,16Z,19Z))

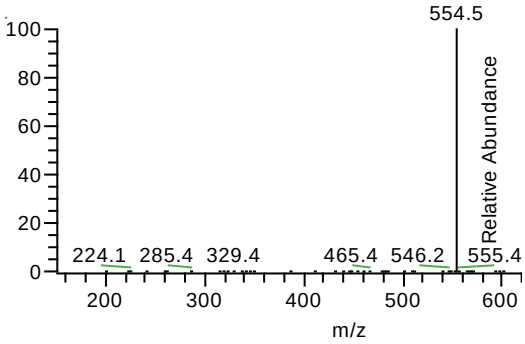

+ESI 417.3357
1, 25-Dihydroxyvitamin D3

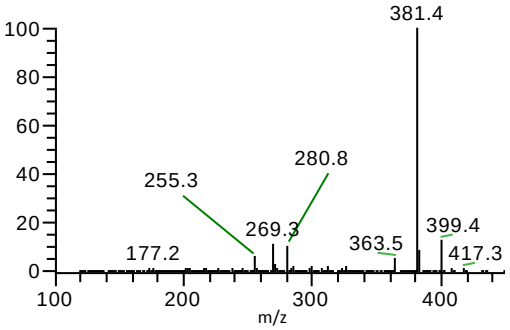

-ESI 247.1703
Hexadecatetraenoic acid

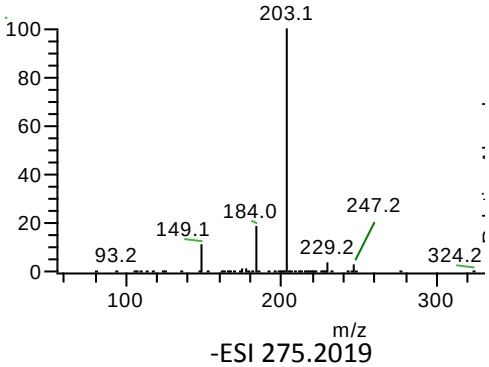

-ESI 249.1859
Hexadecatrienoic acid

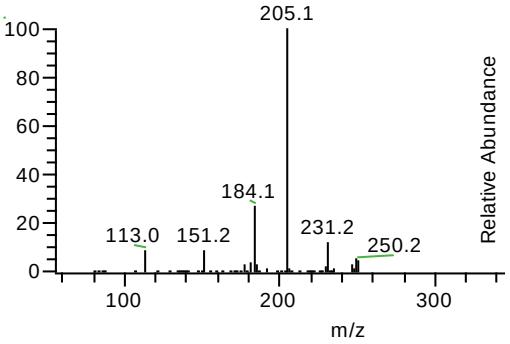

-ESI 275.2019
Stearidonic acid

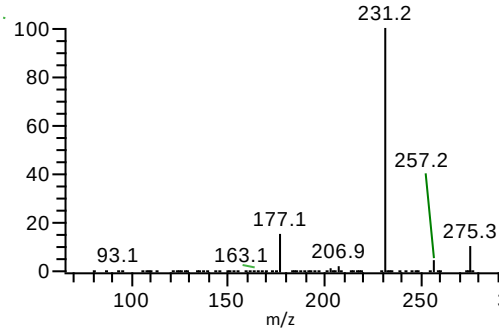

-ESI 303.2331
Arachidonic acid

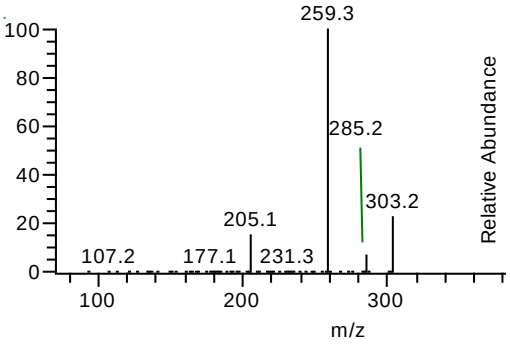

-ESI 305.2488
Dihomo-gamma-linolenic acid

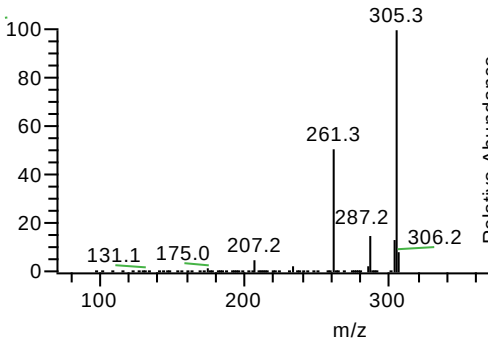

-ESI 331.2645
Adrenic acid

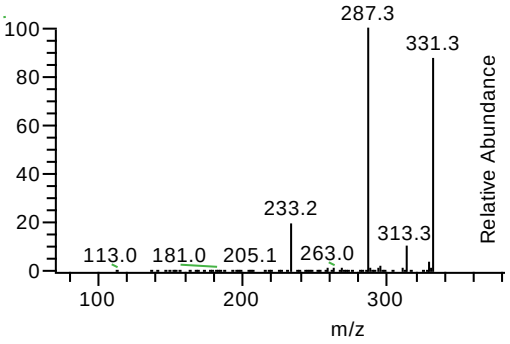

+ESI 401.3407
7-Ketocholesterol

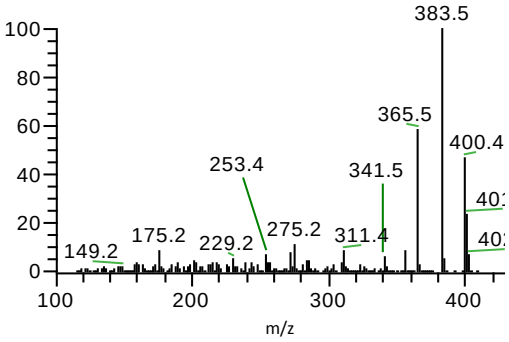

Appendix C

MS/MS spectra of putatively identified metabolites significantly increased in MEF-CM and StemPro spent culture media. MS/MS spectra of the significantly decreased metabolites have been previously provided in chapter 2 and are shown in appendix A.

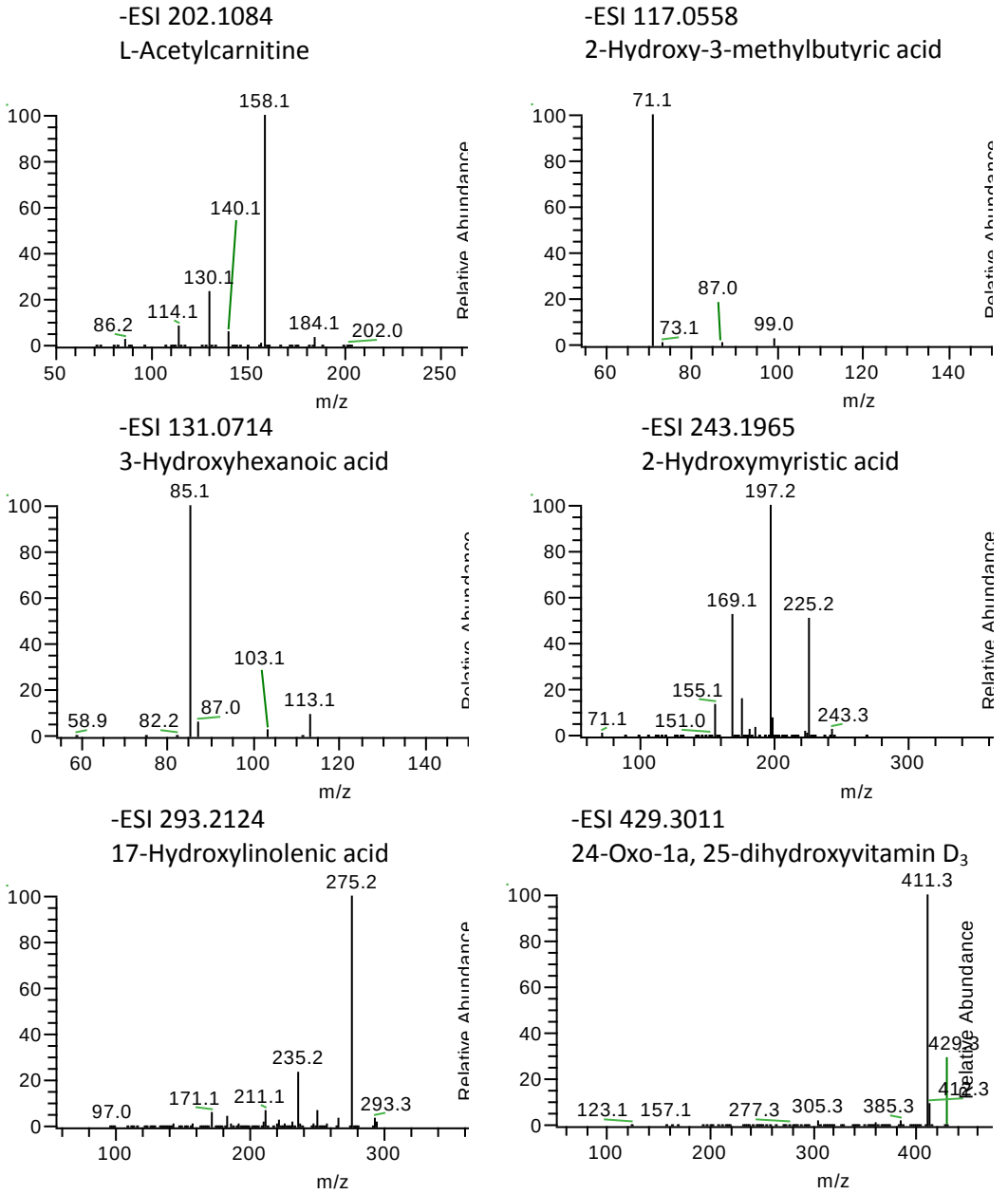

-ESI 284.2231
Myristoylglycine

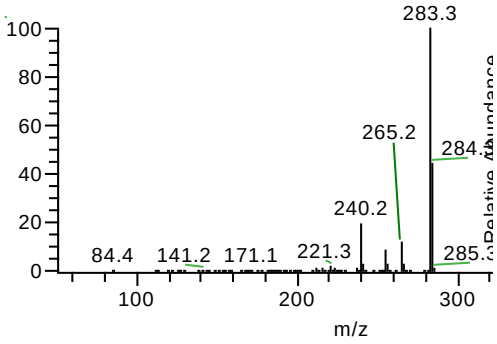

-ESI 319.2280
20-HETE

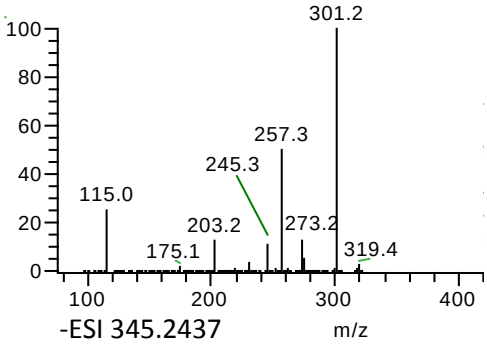

-ESI 311.26
Monoacylglycerol (16:0/0:0/0:0)

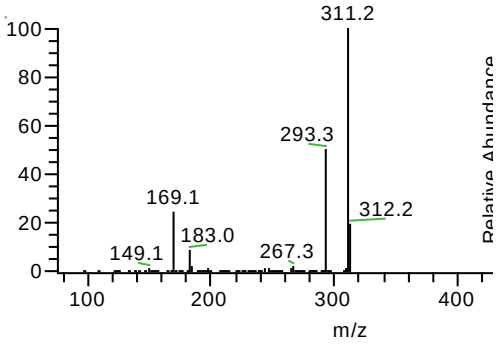

-ESI 345.2437
1a, 22-dihydroxy-23,24,25,26,27-pentarnorvitamin D_3

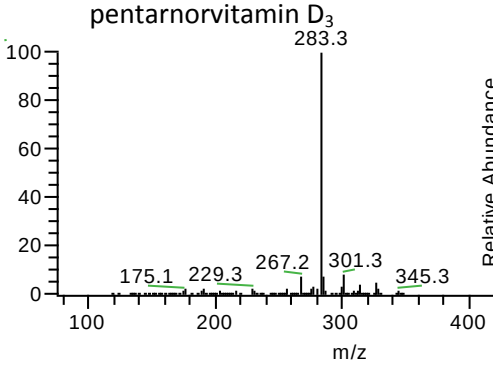

-ESI 271.22281
2-Hydroxypalmitic acid

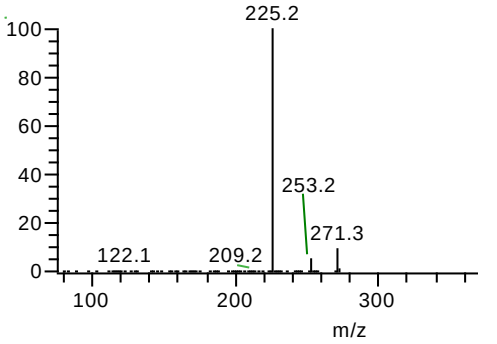

-ESI 325.2751
14-Hydroxy-11Z-eicosenoic acid

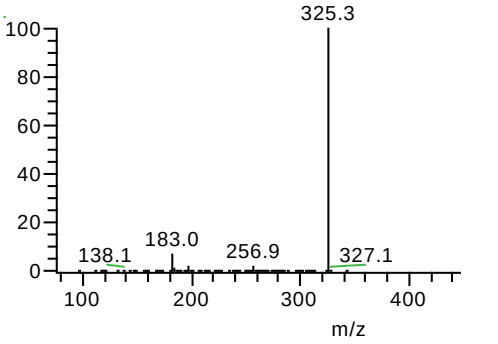

-ESI 355.2646
Tetracosahexaenoic acid

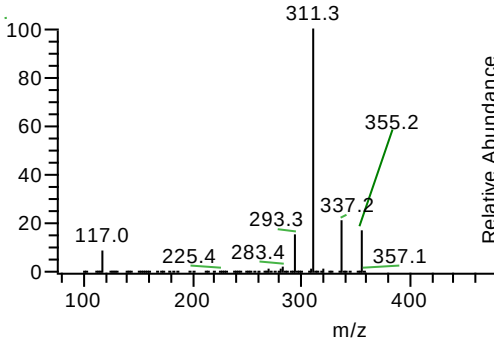

-ESI 307.2644
Eicosadienoic acid

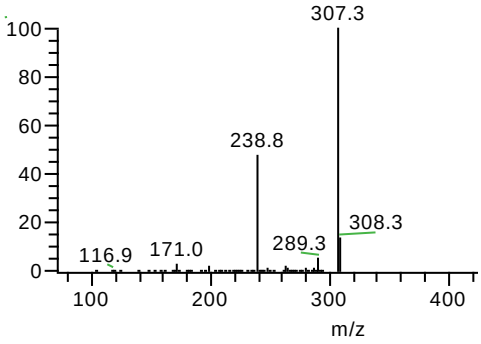

-ESI 309.2802
Eicosenoic acid

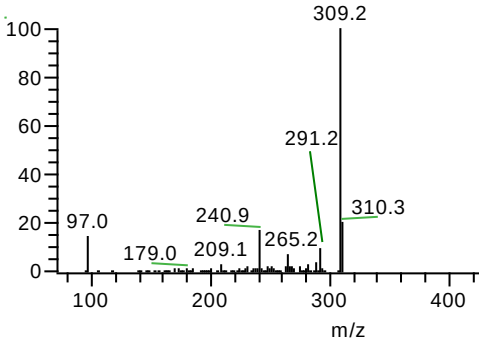

+ESI 438.2980
PE(P-16:0e/0:0)

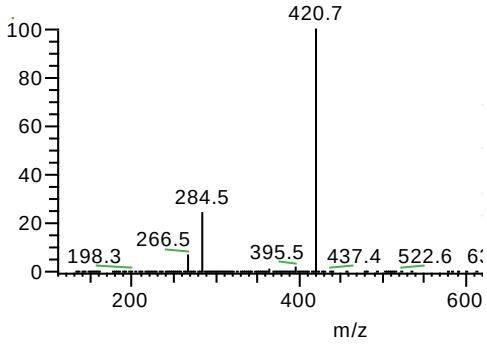

+ESI 326.3053
N-oleyl ethanolamine

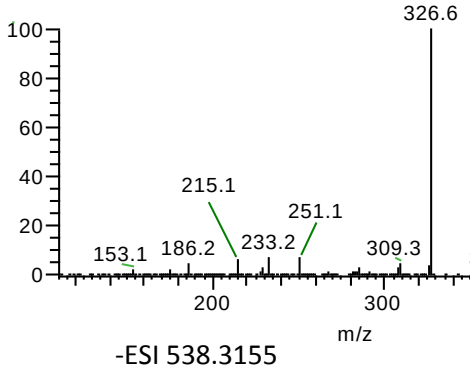

-ESI 512.2996
LPC(14:0)

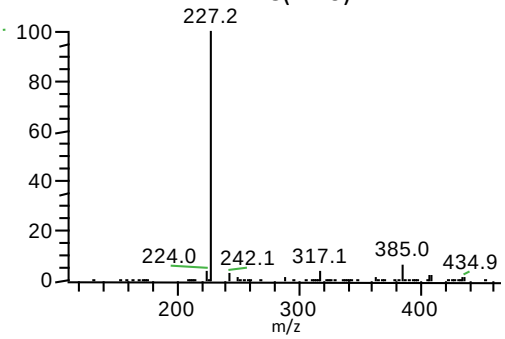

-ESI 538.3155
LPC(16:1)

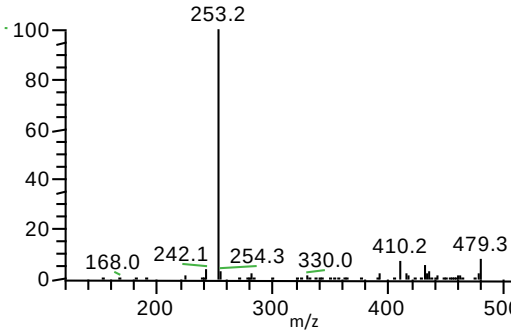

-ESI 452.2783
LPE(16:0/0:0)

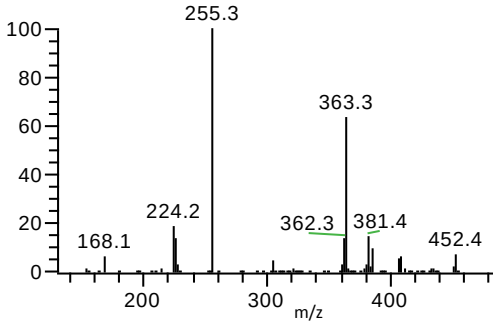

-ESI 540.3307
LPC(16:0/0:0)

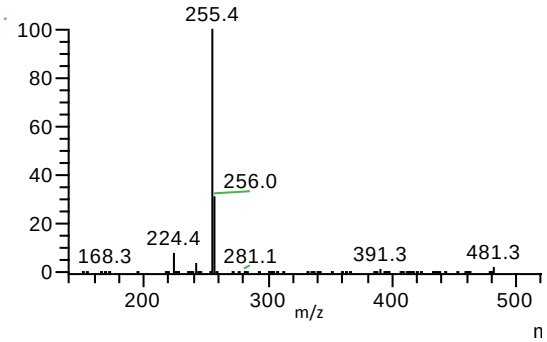

-ESI 478.2939
LPE(18:1)

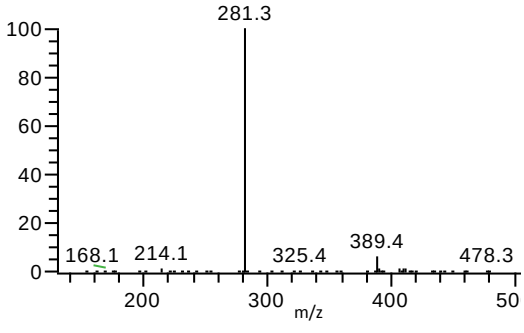

-ESI 436.2939
PE(P-16:0e/0:0)

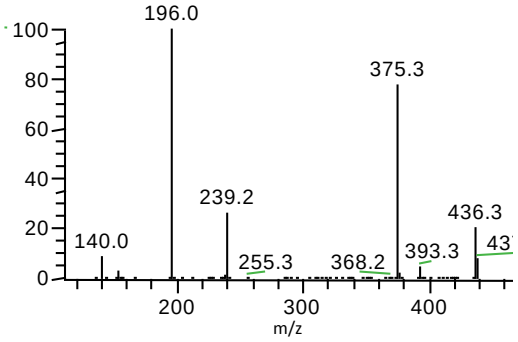

-ESI 566.3463
LPC(18:1)

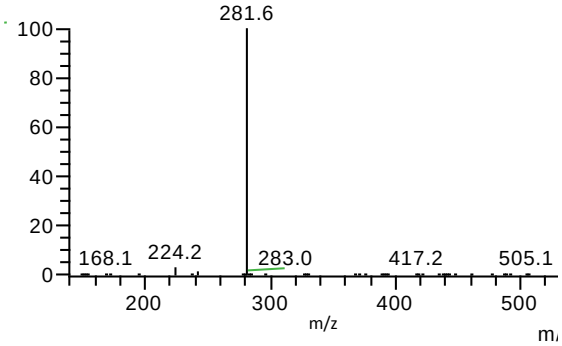

-ESI 480.3094
LPE(18:0/0:0)

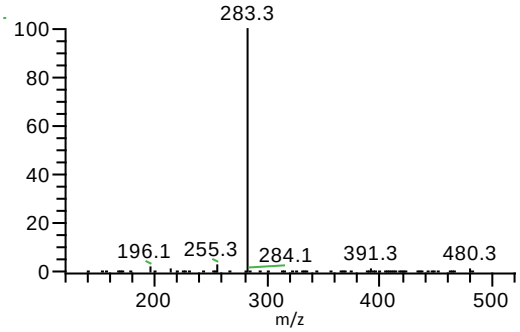

References

AKOPIAN, V., ANDREWS, P. W., BEIL, S., BENVENISTY, N., BREHM, J., CHRISTIE, M., FORD, A., FOX, V., GOKHALE, P. J., HEALY, L., HOLM, F., HOVATTA, O., KNOWLES, B. B., LUDWIG, T. E., MCKAY, R. D. G., MIYAZAKI, T., NAKATSUJI, N., OH, S. K. W., PERA, M. F., ROSSANT, J., STACEY, G. N., SUEMORI, H. & INT STEM CELL INITIATIVE, C. 2010. Comparison of defined culture systems for feeder cell free propagation of human embryonic stem cells. *In Vitro Cellular & Developmental Biology-Animal,* 46**,** 247-258.

ALLEN, J., DAVEY, H. M., BROADHURST, D., HEALD, J. K., ROWLAND, J. J., OLIVER, S. G. & KELL, D. B. 2003. High-throughput classification of yeast mutants for functional genomics using metabolic footprinting. *Nature Biotechnology,* 21**,** 692-696.

ALVAREZ, S. E., MILSTIEN, S. & SPIEGEL, S. 2007. Autocrine and paracrine roles of sphingosine-1-phosphate. *Trends in Endocrinology and Metabolism,* 18**,** 300-307.

AMIT, M., CARPENTER, M. K., INOKUMA, M. S., CHIU, C. P., HARRIS, C. P., WAKNITZ, M. A., ITSKOVITZ-ELDOR, J. & THOMSON, J. A. 2000. Clonally derived human embryonic stem cell lines maintain pluripotency and proliferative potential for prolonged periods of culture. *Developmental Biology,* 227**,** 271-278.

AMIT, M., MARGULETS, V., SEGEV, H., SHARIKI, K., LAEVSKY, I., COLEMAN, R. & ITSKOVITZ-ELDOR, J. 2003. Human feeder layers for human embryonic stem cells. *Biology of Reproduction,* 68**,** 2150-2156.

AMIT, M., SHARIKI, C., MARGULETS, V. & ITSKOVITZ-ELDOR, J. 2004. Feeder layer- and serum-free culture of human embryonic stem cells. *Biology of Reproduction,* 70**,** 837-845.

ANNESLEY, T. M. 2003. Ion suppression in mass spectrometry. *Clinical Chemistry,* 49**,** 1041-1044.

ANTONIO, C., LARSON, T., GILDAY, A., GRAHAM, I., BERGSTROEM, E. & THOMAS-OATES, J. 2008. Hydrophilic interaction chromatography/electrospray mass spectrometry analysis of carbohydrate-related metabolites from Arabidopsis thaliana leaf tissue. *Rapid Communications in Mass Spectrometry,* 22**,** 1399-1407.

ARIKAWA, T., OMURA, K. & MORITA, I. 2004. Regulation of bone morphogenetic protein-2 expression by endogenous prostaglandin E2 in human mesenchymal stem cells. *Journal of Cellular Physiology,* 200**,** 400-406.

ARMSTRONG, L., TILGNER, K., SARETZKI, G., ATKINSON, S. P., STOJKOVIC, M., MORENO, R., PRZYBORSKI, S. & LAKO, M. 2010. Human Induced Pluripotent Stem Cell Lines Show Stress Defense Mechanisms and Mitochondrial Regulation Similar to Those of Human Embryonic Stem Cells. *Stem Cells,* 28**,** 661-673.

AVERY, K., AVERY, S., SHEPHERD, J., HEATH, P. R. & MOORE, H. 2008. Sphingosine-1-Phosphate Mediates Transcriptional Regulation of Key Targets Associated with Survival, Proliferation, and Pluripotency in Human Embryonic Stem Cells. *Stem Cells and Development,* 17**,** 1195-1205.

AVERY, S., INNISS, K. & MOORE, H. 2006. The regulation of self-renewal in human embryonic stem cells. *Stem Cells and Development,* 15**,** 729-740.

BAJAD, S. U., LU, W., KIMBALL, E. H., YUAN, J., PETERSON, C. & RABINOWITZ, J. D. 2006. Separation and quantitation of water soluble cellular metabolites by hydrophilic interaction chromatography-tandem mass spectrometry. *Journal of Chromatography A,* 1125**,** 76-88.

BATEMAN, K. P., KELLMANN, M., MUENSTER, H., PAPP, R. & TAYLOR, L. 2009. Quantitative-Qualitative Data Acquisition Using a Benchtop Orbitrap Mass Spectrometer. *Journal of the American Society for Mass Spectrometry,* 20**,** 1441-1450.

BAUER, C. D. & BERG, C. P. 1943. The amino acids required for growth in mice and the availability of their optical isomers. *Journal of Nutrition,* 26**,** 51-63.

BEATTIE, G. M., LOPEZ, A. D., BUCAY, N., HINTON, A., FIRPO, M. T., KING, C. C. & HAYEK, A. 2005. Activin A maintains pluripotency of human embryonic stem cells in the absence of feeder layers. *Stem Cells,* 23**,** 489-495.

BENDALL, S. C., HUGHES, C., CAMPBELL, J. L., STEWART, M. H., PITTOCK, P., LIU, S., BONNEIL, E., THIBAULT, P., BHATIA, M. & LAJOIE, G. A. 2009. An Enhanced Mass Spectrometry Approach Reveals Human Embryonic Stem Cell Growth Factors in Culture. *Molecular & Cellular Proteomics,* 8**,** 421-432.

BIGDELI, N., ANDERSSON, M., STREHL, R., EMANUELSSON, K., KILMARE, E., HYLLNER, J. & LINDAHL, A. 2008. Adaptation of human embryonic stem cells to feeder-free and matrix-free culture conditions directly on plastic surfaces. *Journal of Biotechnology,* 133**,** 146-153.

BRINKMANN, V. & BAUMRUKER, T. 2006. Pulmonary and vascular pharmacology of sphingosine 1-phosphate. *Current Opinion in Pharmacology,* 6**,** 244-250.

BUHR, N., CARAPITO, C., SCHAEFFER, C., HOVASSE, A., VAN DORSSELAER, A. & VIVILLE, S. 2007. Proteome analysis of the culture environment supporting undifferentiated mouse embryonic stem and germ cell growth. *Electrophoresis,* 28**,** 1615-1623.

BURRIDGE, P. W., ANDERSON, D., PRIDDLE, H., MUNOZ, M. D. B., CHAMBERLAIN, S., ALLEGRUCCI, C., YOUNG, L. E. & DENNING, C. 2007. Improved human embryonic stem cell embryoid body homogeneity and cardiomyocyte differentiation from a novel V-96 plate aggregation system highlights interline variability. *Stem Cells,* 25**,** 929-938.

BYLESJO, M., RANTALAINEN, M., CLOAREC, O., NICHOLSON, J. K., HOLMES, E. & TRYGG, J. 2006. OPLS discriminant analysis: combining the strengths of PLS-DA and SIMCA classification. *Journal of Chemometrics,* 20**,** 341-351.

CANTRILL, R. C., HUANG, Y. S., ELLS, G. W. & HORROBIN, D. F. 1993. COMPARISON OF THE METABOLISM OF ALPHA-LINOLENIC ACID AND ITS DELTA-6 DESATURATION PRODUCT, STEARIDONIC ACID, IN CULTURED NIH-3T3 CELLS. *Lipids,* 28**,** 163-166.

CAO, H., XIAO, L., PARK, G., WANG, X., AZIM, A. C., CHRISTMAN, J. W. & VAN BREEMEN, R. B. 2008. An improved LC-MS/MS method for

the quantification of prostaglandins E-2 and D-2 production in biological fluids. *Analytical Biochemistry,* 372**,** 41-51.

CECH, N. B. & ENKE, C. G. 2001. Practical implications of some recent studies in electrospray ionization fundamentals. *Mass Spectrometry Reviews,* 20**,** 362-387.

CELIZ, A. D., SMITH, J. G. W., LANGER, R., ANDERSON, D. G., WINKLER, D. A., BARRETT, D. A., DAVIES, M. C., YOUNG, L. E., DENNING, C. & ALEXANDER, M. R. 2014. Materials for stem cell factories of the future. *Nature Materials,* 13**,** 570-579.

CEZAR, G. G., QUAM, J. A., SMITH, A. M., ROSA, G. J. M., PIEKARCZYK, M. S., BROWN, J. F., GAGE, F. H. & MUOTRI, A. R. 2007. Identification of small molecules from human embryonic stem cells using metabolomics. *Stem Cells and Development,* 16**,** 869-882.

CHAMBERS, E., WAGROWSKI-DIEHL, D. M., LU, Z. & MAZZEO, J. R. 2007. Systematic and comprehensive strategy for reducing matrix effects in LC/MS/MS analyses. *Journal of Chromatography B-Analytical Technologies in the Biomedical and Life Sciences,* 852**,** 22-34.

CHEN, G., GULBRANSON, D. R., HOU, Z., BOLIN, J. M., RUOTTI, V., PROBASCO, M. D., SMUGA-OTTO, K., HOWDEN, S. E., DIOL, N. R., PROPSON, N. E., WAGNER, R., LEE, G. O., ANTOSIEWICZ-BOURGET, J., TENG, J. M. C. & THOMSON, J. A. 2011. Chemically defined conditions for human iPSC derivation and culture. *Nature Methods,* 8**,** 424-U76.

CHEN, R. F. 1967. REMOVAL OF FATTY ACIDS FROM SERUM ALBUMIN BY CHARCOAL TREATMENT. *Journal of Biological Chemistry,* 242**,** 173-&.

CHIN, A. C. P., FONG, W. J., GOH, L.-T., PHILP, R., OH, S. K. W. & CHOO, A. B. H. 2007. Identification of proteins from feeder conditioned medium that support human embryonic stem cells. *Journal of Biotechnology,* 130**,** 320-328.

CHOI, J. W. & CHUN, J. 2013. Lysophospholipids and their receptors in the central nervous system. *Biochimica Et Biophysica Acta-Molecular and Cell Biology of Lipids,* 1831**,** 20-32.

CHONG, W. P. K., GOH, L. T., REDDY, S. G., YUSUFI, F. N. K., LEE, D. Y., WONG, N. S. C., HENG, C. K., YAP, M. G. S. & HO, Y. S. 2009. Metabolomics profiling of extracellular metabolites in recombinant Chinese Hamster Ovary fed-batch culture. *Rapid Communications in Mass Spectrometry,* 23**,** 3763-3771.

CHONG, W. P. K., REDDY, S. G., YUSUFI, F. N. K., LEE, D.-Y., WONG, N. S. C., HENG, C. K., YAP, M. G. S. & HO, Y. S. 2010. Metabolomics-driven approach for the improvement of Chinese hamster ovary cell growth: Overexpression of malate dehydrogenase II. *Journal of Biotechnology,* 147**,** 116-121.

CHRYSANTHOPOULOS, P. K., GOUDAR, C. T. & KLAPA, M. I. 2010. Metabolomics for high-resolution monitoring of the cellular physiological state in cell culture engineering. *Metabolic Engineering,* 12**,** 212-222.

CLAEYS, M., USTUNES, L., LAEKEMAN, G., HERMAN, A. G., VLIETINCK, A. J. & OZER, A. 1986. CHARACTERIZATION OF PROSTAGLANDIN-E-LIKE ACTIVITY ISOLATED FROM PLANT SOURCE (ALLIUM-CEPA). *Progress in Lipid Research,* 25**,** 53-58.

CROIXMARIE, V., UMBDENSTOCK, T., CLOAREC, O., MOREAU, A., PASCUSSI, J.-M., BOURSIER-NEYRET, C. & WALTHER, B. 2009. Integrated Comparison of Drug-Related and Drug-Induced Ultra Performance Liquid Chromatography/Mass Spectrometry Metabonomic Profiles Using Human Hepatocyte Cultures. *Analytical Chemistry,* 81**,** 6061-6069.

CUPERLOVIC-CULF, M., BARNETT, D. A., CULF, A. S. & CHUTE, I. 2010. Cell culture metabolomics: applications and future directions. *Drug Discovery Today,* 15**,** 610-621.

DENERY, J. R., NUNES, A. A. K., HIXON, M. S., DICKERSON, T. J. & JANDA, K. D. 2010. Metabolomics-Based Discovery of Diagnostic Biomarkers for Onchocerciasis. *Plos Neglected Tropical Diseases,* 4.

DERDA, R., LI, L., ORNER, B. P., LEWIS, R. L., THOMSON, J. A. & KIESSLING, L. L. 2007. Defined substrates for human embryonic stem cell growth identified from surface arrays. *Acs Chemical Biology,* 2**,** 347-355.

DETTMER, K., NUERNBERGER, N., KASPAR, H., GRUBER, M. A., ALMSTETTER, M. F. & OEFNER, P. J. 2011. Metabolite extraction from adherently growing mammalian cells for metabolomics studies: optimization of harvesting and extraction protocols. *Analytical and Bioanalytical Chemistry,* 399**,** 1127-1139.

DIETMAIR, S., HODSON, M. P., QUEK, L.-E., TIMMINS, N. E., CHRYSANTHOPOULOS, P., JACOB, S. S., GRAY, P. & NIELSEN, L. K. 2012. Metabolite profiling of CHO cells with different growth characteristics. *Biotechnology and Bioengineering,* 109**,** 1404-1414.

DUNN, W. B., BAILEY, N. J. C. & JOHNSON, H. E. 2005. Measuring the metabolome: current analytical technologies. *Analyst,* 130**,** 606-625.

DVORAK, P., DVORAKOVA, D., KOSKOVA, S., VODINSKA, M., NAJVIRTOVA, M., KREKAC, D. & HAMPL, A. 2005. Expression and potential role of fibroblast growth factor 2 and its receptors in human embryonic stem cells. *Stem Cells,* 23**,** 1200-1211.

DWYER, J. R., SEVER, N., CARLSON, M., NELSON, S. F., BEACHY, P. A. & PARHAMI, F. 2007. Oxysterols pathway in are novel activators of the hedgehog pluripotent mesenchymal cells. *Journal of Biological Chemistry,* 282**,** 8959-8968.

EISELLEOVA, L., PETERKOVA, I., NERADIL, J., SLANINOVA, I., HAMPL, A. & DVORAK, P. 2008. Comparative study of mouse and human feeder cells for human embryonic stem cells. *International Journal of Developmental Biology,* 52**,** 353-363.

ERIKSSON, L., TRYGG, J. & WOLD, S. 2008. CV-ANOVA for significance testing of PLS and OPLS (R) models. *Journal of Chemometrics,* 22**,** 594-600.

FAHY, E., SUD, M., COTTER, D. & SUBRAMANIAM, S. 2007. LIPID MAPS online tools for lipid research. *Nucleic Acids Research,* 35**,** W606-W612.

FANG, N. B., YU, S. G. & BADGER, T. M. 2003. LC-MS/MS analysis of lysophospholipids associated-with soy protein isolate. *Journal of Agricultural and Food Chemistry,* 51**,** 6676-6682.

FDA 2013. FDA Guidance for Industry, Bioanalytical Method Validation. Food and Drug Administration, Centre for Drug Evaluation and Research (CDER).

FERNANDEZ, C., FRANSSON, U., HALLGARD, E., SPEGEL, P., HOLM, C., KROGH, M., WARELL, K., JAMES, P. & MULDER, H. 2008. Metabolomic and proteomic analysis of a clonal insulin-producing beta-cell line (INS-1 832/13). *Journal of Proteome Research,* 7**,** 400-411.

FIEHN, O. 2001. Combining genomics, metabolome analysis, and biochemical modelling to understand metabolic networks. *Comparative and Functional Genomics,* 2**,** 155-168.

FIEHN, O. 2002. Metabolomics - the link between genotypes and phenotypes. *Plant Molecular Biology,* 48**,** 155-171.

FOLMES, C. D. L., ARRELL, D. K., ZLATKOVIC-LINDOR, J., MARTINEZ-FERNANDEZ, A., PEREZ-TERZIC, C., NELSON, T. J. & TERZIC, A. 2013. Metabolome and metaboproteome remodeling in nuclear reprogramming. *Cell Cycle,* 12**,** 2355-2365.

FOLMES, C. D. L., NELSON, T. J., MARTINEZ-FERNANDEZ, A., ARRELL, D. K., LINDOR, J. Z., DZEJA, P. P., IKEDA, Y., PEREZ-TERZIC, C. & TERZIC, A. 2011. Somatic Oxidative Bioenergetics Transitions into Pluripotency-Dependent Glycolysis to Facilitate Nuclear Reprogramming. *Cell Metabolism,* 14**,** 264-271.

FRANK, M. G. & MCINTYRE, D. E. 2009. Optimizing LC/MS Equipment to Increase Throughput in Pharmaceutical Analysis. *In:* WANG, P. G. (ed.) *High-throughput analysis in the pharmaceutical industry.* London, England: CRC Press.

FRANKLAND, S., ELLIOTT, S. R., YOSAATMADJA, F., BEESON, J. G., ROGERSON, S. J., ADISA, A. & TILLEY, L. 2007. Serum lipoproteins promote efficient presentation of the malaria virulence protein PfEMP1 at the erythrocyte surface. *Eukaryotic Cell,* 6**,** 1584-1594.

FUNK, C. D. & POWELL, W. S. 1983. METABOLISM OF LINOLEIC-ACID BY PROSTAGLANDIN ENDOPEROXIDE SYNTHASE FROM ADULT AND FETAL BLOOD-VESSELS. *Biochimica Et Biophysica Acta,* 754**,** 57-71.

GALLO, P. & CONDORELLI, G. 2006. Human embryonic stem cell-derived cardiomyocytes: inducing strategies. *Regenerative Medicine,* 1**,** 183-194.

GARCIA-GONZALO, F. R. & IZPISUA BELMONTE, J. C. 2008. Albumin-Associated Lipids Regulate Human Embryonic Stem Cell Self-Renewal. *Plos One,* 3.

GIKA, H. G., THEODORIDIS, G. A., PLUMB, R. S. & WILSON, I. D. 2014. Current practice of liquid chromatography-mass spectrometry in metabolomics and metabonomics. *Journal of Pharmaceutical and Biomedical Analysis,* 87**,** 12-25.

GIKA, H. G., THEODORIDIS, G. A., WINGATE, J. E. & WILSON, I. D. 2007. Within-day reproducibility of an HPLC-MS-Based method for metabonomic analysis: Application to human urine. *Journal of Proteome Research,* 6**,** 3291-3303.

GREBER, B., LEHRACH, H. & ADJAYE, J. 2007. Fibroblast growth factor 2 modulates transforming growth factor beta signaling in mouse embryonic fibroblasts and human ESCs (hESCs) to support hESC self-renewal. *Stem Cells,* 25**,** 455-464.

GUAN, K. M., CHANG, H., ROLLETSCHEK, A. & WOBUS, A. M. 2001. Embryonic stem cell-derived neurogenesis - Retinoic acid induction and lineage selection of neuronal cells. *Cell and Tissue Research,* 305**,** 171-176.

GUERRASIO, R., HABERHAUER-TROYER, C., MATTANOVICH, D., KOELLENSPERGER, G. & HANN, S. 2014. Metabolic profiling of amino acids in cellular samples via zwitterionic sub-2 mu m particle size HILIC-MS/MS and a uniformly C-13 labeled internal standard. *Analytical and Bioanalytical Chemistry,* 406**,** 915-922.

GUIL-GUERRERO, J. L. 2007. Stearidonic acid (18 : 4n-3): Metabolism, nutritional importance, medical uses and natural sources. *European Journal of Lipid Science and Technology,* 109**,** 1226-1236.

GUO, S., DUAN, J.-A., QIAN, D., WANG, H., TANG, Y., QIAN, Y., WU, D., SU, S. & SHANG, E. 2013. Hydrophilic interaction ultra-high performance liquid chromatography coupled with triple quadrupole mass spectrometry for determination of nucleotides, nucleosides and nucleobases in Ziziphus plants. *Journal of Chromatography A,* 1301**,** 147-155.

GUPTA, P., VERMA, P., HOURIGAN, K., BELLARE, J. & JADHAV, S. 2012. Metabolic Analysis of Fibroblast Conditioned Media and Comparison with Theoretical Modeling *World Academy of Science, Engineering and Technology,* 6**,** 260-264.

HENDRIKS, M. M. W. B., VAN EEUWIJK, F. A., JELLEMA, R. H., WESTERHUIS, J. A., REIJMERS, T. H., HOEFSLOOT, H. C. J. & SMILDE, A. K. 2011. Data-processing strategies for metabolomics studies. *Trac-Trends in Analytical Chemistry,* 30**,** 1685-1698.

HEO, J. S., LEE, M. Y. & HAN, H. J. 2007. Sonic hedgehog stimulates mouse embryonic stem cell proliferation by cooperation of Ca2+/Protein kinase c and epidermal growth factor receptor as well as Gli1 activation. *Stem Cells,* 25**,** 3069-3080.

HLA, T., LEE, M. J., ANCELLIN, N., PAIK, J. H. & KLUK, M. J. 2001. Lysophospholipids - Receptor revelations. *Science,* 294**,** 1875-1878.

HOGGATT, J., SINGH, P., SAMPATH, J. & PELUS, L. M. 2009. Prostaglandin E-2 enhances hematopoietic stem cell homing, survival, and proliferation. *Blood,* 113**,** 5444-5455.

HOVATTA, O., MIKKOLA, M., GERTOW, K., STROMBERG, A. M., INZUNZA, J., HREINSSON, J., ROZELL, B., BLENNOW, E., ANDANG, M. & AHRLUND-RICHTER, L. 2003. A culture system using human foreskin fibroblasts as feeder cells allows production of human embryonic stem cells. *Human Reproduction,* 18**,** 1404-1409.

HUANG, M. C., GRAELER, M., SHANKAR, G., SPENCER, J. & GOETZL, E. J. 2002. Lysophospholipid mediators of immunity and neoplasia. *Biochimica Et Biophysica Acta-Molecular and Cell Biology of Lipids,* 1582**,** 161-167.

IL'YASOVA, D., MORROW, J. D., IVANOVA, A. & WAGENKNECHT, L. E. 2004. Epidemiological marker for oxidant status: Comparison of the ELISA and the gas chromatography/mass spectrometry assay for urine 2,3 dinor-5,6-dihydro-15,F-2t-isoprostane. *Annals of Epidemiology,* 14**,** 793-797.

INNISS, K. & MOORE, H. 2006. Mediation of apoptosis and proliferation of human embryonic stem cells by sphingosine-1-phosphate. *Stem Cells and Development,* 15**,** 789-796.

INOUE, K., OBARA, R., HINO, T. & OKA, H. 2010. Development and Application of an HILIC-MS/MS Method for the Quantitation of Nucleotides in Infant Formula. *Journal of Agricultural and Food Chemistry,* 58**,** 9918-9924.

INZUNZA, J., GERTOW, K., STROMBERG, M. A., MATILAINEN, E., BLENNOW, E., SKOTTMAN, H., WOLBANK, S., AHRLUND-RICHTER, L. & HOVATTA, O. 2005. Derivation of human embryonic stem cell lines in serum replacement medium using postnatal human fibroblasts as feeder cells. *Stem Cells,* 23**,** 544-549.

IRWIN, E. E., GUPTA, R., DASHTI, D. C. & HEALY, K. E. 2011. Engineered polymer-media interfaces for the long-term self-renewal of human embryonic stem cells. *Biomaterials,* 32**,** 6912-6919.

JONES, M. B., CHU, C. H., PENDLETON, J. C., BETENBAUGH, M. J., SHILOACH, J., BALJINNYAM, B., RUBIN, J. S. & SHAMBLOTT, M. J. 2010. Proliferation and Pluripotency of Human Embryonic Stem Cells Maintained on Type I Collagen. *Stem Cells and Development,* 19**,** 1923-1935.

KATAJAMAA, M. & ORESIC, M. 2007. Data processing for mass spectrometry-based metabolomics. *Journal of Chromatography A,* 1158**,** 318-328.

KELLMANN, M., MUENSTER, H., ZOMER, P. & MOL, H. 2009. Full Scan MS in Comprehensive Qualitative and Quantitative Residue Analysis in Food and Feed Matrices: How Much Resolving Power is Required? *Journal of the American Society for Mass Spectrometry,* 20**,** 1464-1476.

KIM, J. Y., PARK, J. Y., KIM, O. Y., HAM, B. M., KIM, H.-J., KWON, D. Y., JANG, Y. & LEE, J. H. 2010. Metabolic Profiling of Plasma in Overweight/Obese and Lean Men using Ultra Performance Liquid Chromatography and Q-TOF Mass Spectrometry (UPLC-Q-TOF MS). *Journal of Proteome Research,* 9**,** 4368-4375.

KIM, W., FAN, Y.-Y., BARHOMNI, R., SMITH, R., MCMURRAY, D. N. & CHAPKIN, R. S. 2008. n-3 Polyunsaturated Fatty Acids Suppress the Localization and Activation of Signaling Proteins at the Immunological Synapse in Murine CD4(+) T Cells by Affecting Lipid Raft Formation. *Journal of Immunology,* 181**,** 6236-6243.

KIM, Y. H. & HAN, H. J. 2008. High-glucose-induced prostaglandin E-2 and peroxisome proliferator-activated receptor delta promote mouse embryonic stem cell proliferation. *Stem Cells,* 26**,** 745-755.

KLEINMAN, H. K. & MARTIN, G. R. 2005. Matrigel: Basement membrane matrix with biological activity. *Seminars in Cancer Biology,* 15**,** 378-386.

KLEINSTREUER, N. C., SMITH, A. M., WEST, P. R., CONARD, K. R., FONTAINE, B. R., WEIR-HAUPTMAN, A. M., PALMER, J. A., KNUDSEN, T. B., DIX, D. J., DONLEY, E. L. R. & CEZAR, G. G. 2011. Identifying developmental toxicity pathways for a subset of ToxCast chemicals using human embryonic stem cells and metabolomics. *Toxicology and Applied Pharmacology,* 257**,** 111-121.

KLIM, J. R., LI, L., WRIGHTON, P. J., PIEKARCZYK, M. S. & KIESSLING, L. L. 2010. A defined glycosaminoglycan-binding substratum for human pluripotent stem cells. *Nature Methods,* 7**,** 989-U72.

KLOTZ, B., MENTRUP, B., REGENSBURGER, M., ZECK, S., SCHNEIDEREIT, J., SCHUPP, N., LINDEN, C., MERZ, C., EBERT, R. & JAKOB, F. 2012. 1,25-Dihydroxyvitamin D3 Treatment Delays Cellular Aging in Human Mesenchymal Stem Cells while Maintaining Their Multipotent Capacity. *Plos One,* 7.

KOIVISTO, H., HYVARINEN, M., STROMBERG, A. M., INZUNZA, J., MATILAINEN, E., MIKKOLA, M., HOVATTA, O. & TEERIJOKI, H. 2004. Cultures of human embryonic stem cells: serum replacement medium or serum-containing media and the effect of basic fibroblast growth factor. *Reproductive Biomedicine Online,* 9**,** 330-337.

KOPKA, J., FERNIE, A., WECKWERTH, W., GIBON, Y. & STITT, M. 2004. Metabolite profiling in plant biology: platforms and destinations. *Genome Biology,* 5.

KOULMAN, A., WOFFENDIN, G., NARAYANA, V. K., WELCHMAN, H., CRONE, C. & VOLMER, D. A. 2009. High-resolution extracted ion chromatography, a new tool for metabolomics and lipidomics using a second-generation orbitrap mass spectrometer. *Rapid Communications in Mass Spectrometry,* 23**,** 1411-1418.

KUMAGAI, H., SUEMORI, H., UESUGI, M., NAKATSUJI, N. & KAWASE, E. 2013. Identification of small molecules that promote human embryonic stem cell self-renewal. *Biochemical and Biophysical Research Communications,* 434**,** 710-716.

KUME, N., CYBULSKY, M. I. & GIMBRONE, M. A. 1992. LYSOPHOSPHATIDYLCHOLINE, A COMPONENT OF ATHEROGENIC LIPOPROTEINS, INDUCES MONONUCLEAR LEUKOCYTE ADHESION MOLECULES IN CULTURED HUMAN AND RABBIT ARTERIAL ENDOTHELIAL-CELLS. *Journal of Clinical Investigation,* 90**,** 1138-1144.

LAI, L., MICHOPOULOS, F., GIKA, H., THEODORIDIS, G., WILKINSON, R. W., ODEDRA, R., WINGATE, J., BONNER, R., TATE, S. & WILSON, I. D. 2010. Methodological considerations in the development of HPLC-MS methods for the analysis of rodent plasma for metabonomic studies. *Molecular Biosystems,* 6**,** 108-120.

LEE, H. Y., LIN, C. I., LIAO, J. J., LEE, Y. W., YANG, H. Y., LEE, C. Y., HSU, H. Y. & WU, H. L. 2004. Lysophospholipids increase ICAM-1 expression in HUVEC through a G(i)- and NF-kappa B-dependent mechanism. *American Journal of Physiology-Cell Physiology,* 287**,** C1657-C1666.

LEON, Z., GARCIA-CANAVERAS, J. C., TERESA DONATO, M. & LAHOZ, A. 2013. Mammalian cell metabolomics: Experimental design and sample preparation. *Electrophoresis,* 34**,** 2762-2775.

LEVENBERG, S., GOLUB, J. S., AMIT, M., ITSKOVITZ-ELDOR, J. & LANGER, R. 2002. Endothelial cells derived from human embryonic stem cells. *Proceedings of the National Academy of Sciences of the United States of America,* 99**,** 4391-4396.

LEVENSTEIN, M. E., LUDWIG, T. E., XU, R.-H., LLANAS, R. A., VANDENHEUVEL-KRAMER, K., MANNING, D. & THOMSON, J. A.

2006. Basic fibroblast growth factor support of human embryonic stem cell self-renewal. *Stem Cells,* 24**,** 568-574.
LEVINE, A. J. & BRIVANLOU, A. H. 2006. GDF3, a BMP inhibitor, regulates cell fate in stem cells and early embryos. *Development,* 133**,** 209-216.
LEVINE, A. J., LEVINE, Z. J. & BRIVANLOU, A. H. 2009. GDF3 is a BMP inhibitor that can activate Nodal signaling only at very high doses. *Developmental Biology,* 325**,** 43-48.
LEVY, D., MARIA RUIZ, J. L., CELESTINO, A. T., SILVA, S. F., FERREIRA, A. K., ISAAC, C. & BYDLOWSKI, S. P. 2014. Short-term effects of 7-ketocholesterol on human adipose tissue mesenchymal stem cells in vitro. *Biochemical and Biophysical Research Communications,* 446**,** 720-725.
LI, N.-J., LIU, W.-T., LI, W., LI, S.-Q., CHEN, X.-H., BI, K.-S. & HE, P. 2010. Plasma metabolic profiling of Alzheimer's disease by liquid chromatography/mass spectrometry. *Clinical Biochemistry,* 43**,** 992-997.
LIM, J. W. E. & BODNAR, A. 2002. Proteome analysis of conditioned medium from mouse embryonic fibroblast feeder layers which support the growth of human embryonic stem cells. *Proteomics,* 2**,** 1187-1203.
LIN, L., HUANG, Z., GAO, Y., YAN, X., XING, J. & HANG, W. 2011. LC-MS based serum metabonomic analysis for renal cell carcinoma diagnosis, staging, and biomarker discovery. *Journal of Proteome Research,* 10**,** 1396-1405.
LIN, L., YU, Q., YAN, X., HANG, W., ZHENG, J., XING, J. & HUANG, B. 2010. Direct infusion mass spectrometry or liquid chromatography mass spectrometry for human metabonomics? A serum metabonomic study of kidney cancer. *Analyst,* 135**,** 2970-2978.
LIOU, J.-Y., ELLENT, D. P., LEE, S., GOLDSBY, J., KO, B.-S., MATIJEVIC, N., HUANG, J.-C. & WU, K. K. 2007. Cyclooxygenase-2-derived prostaglandin E-2 protects mouse embryonic stem cells from apoptosis. *Stem Cells,* 25**,** 1096-1103.
LIU, Y. X., SONG, Z. H., ZHAO, Y., QIN, H., CAI, J., ZHANG, H., YU, T. X., JIANG, S. M., WANG, G. W., DING, M. X. & DENG, H. K. 2006. A novel chemical-defined medium with bFGF and N2B27 supplements supports undifferentiated growth in human embryonic stem cells. *Biochemical and Biophysical Research Communications,* 346**,** 131-139.
LOFTUS, N., BARNES, A., ASHTON, S., MICHOPOULOS, F., THEODORIDIS, G., WILSON, I., JI, C. & KAPLOWITZ, N. 2011. Metabonomic Investigation of Liver Profiles of Nonpolar Metabolites Obtained from Alcohol-Dosed Rats and Mice Using High Mass Accuracy MSn Analysis. *Journal of Proteome Research,* 10**,** 705-713.
LOMMEN, A. 2009. MetAlign: Interface-Driven, Versatile Metabolomics Tool for Hyphenated Full-Scan Mass Spectrometry Data Preprocessing. *Analytical Chemistry,* 81**,** 3079-3086.
LU, J., HOU, R. H., BOOTH, C. J., YANG, S. H. & SNYDER, M. 2006. Defined culture conditions of human embryonic stem cells. *Proceedings of the National Academy of Sciences of the United States of America,* 103**,** 5688-5693.

LU, W., BENNETT, B. D. & RABINOWITZ, J. D. 2008. Analytical strategies for LC-MS-based targeted metabolomics. *Journal of Chromatography B-Analytical Technologies in the Biomedical and Life Sciences,* 871**,** 236-242.

LU, W., CLASQUIN, M. F., MELAMUD, E., AMADOR-NOGUEZ, D., CAUDY, A. A. & RABINOWITZ, J. D. 2010. Metabolomic Analysis via Reversed-Phase Ion-Pairing Liquid Chromatography Coupled to a Stand Alone Orbitrap Mass Spectrometer. *Analytical Chemistry,* 82**,** 3212-3221.

LUDWIG, T. E., BERGENDAHL, V., LEVENSTEIN, M. E., YU, J., PROBASCO, M. D. & THOMSON, J. A. 2006a. Feeder-independent culture of human embryonic stem cells. *Nature Methods,* 3**,** 637-646.

LUDWIG, T. E., LEVENSTEIN, M. E., JONES, J. M., BERGGREN, W. T., MITCHEN, E. R., FRANE, J. L., CRANDALL, L. J., DAIGH, C. A., CONARD, K. R., PIEKARCZYK, M. S., LLANAS, R. A. & THOMSON, J. A. 2006b. Derivation of human embryonic stem cells in defined conditions. *Nature Biotechnology,* 24**,** 185-187.

MACINTYRE, D. A., MELGUIZO SANCHIS, D., JIMENEZ, B., MORENO, R., STOJKOVIC, M. & PINEDA-LUCENA, A. 2011. Characterisation of Human Embryonic Stem Cells Conditioning Media by H-1-Nuclear Magnetic Resonance Spectroscopy. *Plos One,* 6.

MAHLSTEDT, M. M., ANDERSON, D., SHARP, J. S., MCGILVRAY, R., MUNOZ, M. D. B., BUTTERY, L. D., ALEXANDER, M. R., ROSE, F. R. A. J. & DENNING, C. 2010. Maintenance of Pluripotency in Human Embryonic Stem Cells Cultured on a Synthetic Substrate in Conditioned Medium. *Biotechnology and Bioengineering,* 105**,** 130-140.

MAKAROV, A., DENISOV, E., KHOLOMEEV, A., BAISCHUN, W., LANGE, O., STRUPAT, K. & HORNING, S. 2006. Performance evaluation of a hybrid linear ion trap/orbitrap mass spectrometer. *Analytical Chemistry,* 78**,** 2113-2120.

MAKRIDAKIS, M., ROUBELAKIS, M. G. & VLAHOU, A. 2013. Stem cells: Insights into the secretome. *Biochimica Et Biophysica Acta-Proteins and Proteomics,* 1834**,** 2380-2384.

MANN, C. J., KADUCE, T. L., FIGARD, P. H. & SPECTOR, A. A. 1986. DOCOSATETRAENOIC ACID IN ENDOTHELIAL-CELLS - FORMATION, RETROCONVERSION TO ARACHIDONIC-ACID, AND EFFECT ON PROSTACYCLIN PRODUCTION. *Archives of Biochemistry and Biophysics,* 244**,** 813-823.

MARFIA, G., CAMPANELLA, R., NAVONE, S. E., DI VITO, C., RICCITELLI, E., HADI, L. A., BORNATI, A., DE REZENDE, G., GIUSSANI, P., TRINGALI, C., VIANI, P., RAMPINI, P., ALESSANDRI, G., PARATI, E. & RIBONI, L. 2014. Autocrine/Paracrine Sphingosine-1-Phosphate Fuels Proliferative and Stemness Qualities of Glioblastoma Stem Cells *GLIA,* 00**,** 1-14.

MARTIN, M. J., MUOTRI, A., GAGE, F. & VARKI, A. 2005. Human embryonic stem cells express an immunogenic nonhuman sialic acid. *Nature Medicine,* 11**,** 228-232.

MATSUDA, T., NAKAMURA, T., NAKAO, K., ARAI, T., KATSUKI, M., HEIKE, T. & YOKOTA, T. 1999. STAT3 activation is sufficient to maintain an undifferentiated state of mouse embryonic stem cells. *Embo Journal,* 18**,** 4261-4269.

MCNAMARA, L. E., SJOESTROEM, T., MEEK, R. M. D., OREFFO, R. O. C., SU, B., DALBY, M. J. & BURGESS, K. E. V. 2012. Metabolomics: a valuable tool for stem cell monitoring in regenerative medicine. *Journal of the Royal Society Interface,* 9**,** 1713-1724.

MOHMAD-SABERI, S. E., HASHIM, Y. Z. H.-Y., MEL, M., AMID, A., AHMAD-RAUS, R. & PACKEER-MOHAMED, V. 2013. Metabolomics profiling of extracellular metabolites in CHO-K1 cells cultured in different types of growth media. *Cytotechnology,* 65**,** 577-586.

NICHOLSON, J. K., LINDON, J. C. & HOLMES, E. 1999. 'Metabonomics': understanding the metabolic responses of living systems to pathophysiological stimuli via multivariate statistical analysis of biological NMR spectroscopic data. *Xenobiotica,* 29**,** 1181-1189.

NORDING, M. L., YANG, J., HEGEDUS, C. M., BHUSHAN, A., KENYON, N. J., DAVIS, C. E. & HAMMOCK, B. D. 2010. Endogenous Levels of Five Fatty Acid Metabolites in Exhaled Breath Condensate to Monitor Asthma by High-Performance Liquid Chromatography: Electrospray Tandem Mass Spectrometry. *Ieee Sensors Journal,* 10**,** 123-130.

ODORICO, J. S., KAUFMAN, D. S. & THOMSON, J. A. 2001. Multilineage differentiation from human embryonic stem cell lines. *Stem Cells,* 19**,** 193-204.

OLIVER, S. G., WINSON, M. K., KELL, D. B. & BAGANZ, F. 1998. Systematic functional analysis of the yeast genome. *Trends in Biotechnology,* 16**,** 373-378.

OLKKONEN, V. M., BEASLAS, O. & NISSILA, E. 2012. Oxysterols and their cellular effectors. *Biomolecules,* 2**,** 76-103.

OUYANG, A., NG, R. & YANG, S.-T. 2007. Long-term culturing of undifferentiated embryonic stem cells in conditioned media and three-dimensional fibrous matrices without extracellular matrix coating. *Stem Cells,* 25**,** 447-454.

PAGES, C., SIMON, M. F., VALET, P. & SAULNIER-BLACHE, J. S. 2001. Lysophosphatidic acid synthesis and release. *Prostaglandins & Other Lipid Mediators,* 64**,** 1-10.

PALMER, J. A., SMITH, A. M., EGNASH, L. A., CONARD, K. R., WEST, P. R., BURRIER, R. E., DONLEY, E. L. R. & KIRCHNER, F. R. 2013. Establishment and assessment of a new human embryonic stem cell-based biomarker assay for developmental toxicity screening. *Birth defects research. Part B, Developmental and reproductive toxicology,* 98**,** 343-63.

PATTI, G. J. 2011. Separation strategies for untargeted metabolomics. *Journal of Separation Science,* 34**,** 3460-3469.

PEBAY, A., BONDER, C. S. & PITSON, S. M. 2007. Stem cell regulation by lysophospholipids. *Prostaglandins & Other Lipid Mediators,* 84**,** 83-97.

PEBAY, A., WONG, R. C. B., PITSON, S. M., WOLVETANG, E. J., PEH, G. S. L., FILIPCZYK, A., KOH, K. L. L., TELLIS, I., NGUYEN, L. T. V. & PERA, M. F. 2005. Essential roles of sphingosine-1-phosphate and platelet-derived growth factor in the maintenance of human embryonic stem cells. *Stem Cells,* 23**,** 1541-1548.

PEREIRA, H., MARTIN, J.-F., JOLY, C., SEBEDIO, J.-L. & PUJOS-GUILLOT, E. 2010. Development and validation of a UPLC/MS method for a

nutritional metabolomic study of human plasma. *Metabolomics,* 6**,** 207-218.
PETTEGREW, J. W., LEVINE, J. & MCCLURE, R. J. 2000. Acetyl-L-carnitine physical-chemical, metabolic, and therapeutic properties: relevance for its mode of action in Alzheimer's disease and geriatric depression. *Molecular Psychiatry,* 5**,** 616-632.
PIRAUD, M., VIANEY-SABAN, C., PETRITIS, K., ELFAKIR, C., STEGHENS, J. P. & BOUCHU, D. 2005. Ion-pairing reversed-phase liquid chromatography/electrospray ionization mass spectrometric analysis of 76 underivatized amino acids of biological interest: a new tool for the diagnosis of inherited disorders of amino acid metabolism. *Rapid Communications in Mass Spectrometry,* 19**,** 1587-1602.
PLUSKAL, T., CASTILLO, S., VILLAR-BRIONES, A. & ORESIC, M. 2010. MZmine 2: Modular framework for processing, visualizing, and analyzing mass spectrometry-based molecular profile data. *Bmc Bioinformatics,* 11.
PRICE, P. J., GOLDSBOROUGH, M. D. & TILKINS, M. L. (1998). *Embryonic stem cell serum replacement. International Patent Application WO 98/30679*. WO 98/30679.
PROWSE, A. B. J., MCQUADE, L. R., BRYANT, K. J., MARCAL, H. & GRAY, P. P. 2007. Identification of potential pluripotency determinants for human embryonic stem cells following proteomic analysis of human and mouse fibroblast conditioned media. *Journal of Proteome Research,* 6**,** 3796-3807.
PROWSE, A. B. J., MCQUADE, L. R., BRYANT, K. J., VAN DYK, D. D., TUCH, B. E. & GRAY, P. P. 2005. A proteome analysis of conditioned media from human neonatal fibroblasts used in the maintenance of human embryonic stem cells. *Proteomics,* 5**,** 978-989.
PRZYBYLA, L. & VOLDMAN, J. 2012. Probing Embryonic Stem Cell Autocrine and Paracrine Signaling Using Microfluidics. *Annual Review of Analytical Chemistry, Vol 5,* 5**,** 293-315.
QURAISHI, O., MANCINI, J. A. & RIENDEAU, D. 2002. Inhibition of inducible prostaglandin E-2 synthase by 15-deoxy-Delta(12,14)-prostaglandin J(2) and polyunsaturated fatty acids. *Biochemical Pharmacology,* 63**,** 1183-1189.
RATHJEN, J., YEO, C., YAP, C., TAN, B. S. N., RATHJEN, P. D. & GARDNER, D. K. 2014. Culture environment regulates amino acid turnover and glucose utilisation in human ES cells. *Reproduction Fertility and Development,* 26**,** 703-716.
REHMAN, J. 2010. Empowering self-renewal and differentiation: the role of mitochondria in stem cells. *Journal of Molecular Medicine-Jmm,* 88**,** 981-986.
RICHARDS, M., FONG, C. Y., CHAN, W. K., WONG, P. C. & BONGSO, A. 2002. Human feeders support prolonged undifferentiated growth of human inner cell masses and embryonic stem cells. *Nature Biotechnology,* 20**,** 933-936.
RIEKEN, S., HERROEDER, S., SASSMANN, A., WALLENWEIN, B., MOERS, A., OFFERMANNS, S. & WETTSCHURECK, N. 2006. Lysophospholipids control integrin-dependent adhesion in splenic B cells through G(i) and G(12)/G(13) family g-proteins but not

through G(q)/G(11). *Journal of Biological Chemistry,* 281**,** 36985-36992.
RITTER, J. B., GENZEL, Y. & REICHL, U. 2008. Simultaneous extraction of several metabolites of energy metabolism and related substances in mammalian cells: Optimization using experimental design. *Analytical Biochemistry,* 373**,** 349-369.
RIVERA, R. & CHUN, J. 2008. Biological effects of lysophospholipids. *Reviews of Physiology, Biochemistry and Pharmacology, Vol 160,* 160**,** 25-46.
ROBERTS, D. D., RAO, C. N., MAGNANI, J. L., SPITALNIK, S. L., LIOTTA, L. A. & GINSBURG, V. 1985. LAMININ BINDS SPECIFICALLY TO SULFATED GLYCOLIPIDS. *Proceedings of the National Academy of Sciences of the United States of America,* 82**,** 1306-1310.
ROBERTS, L. D., SOUZA, A. L., GERSZTEN, R. E. & CLISH, C. B. 2012. Targeted metabolomics. *Current protocols in molecular biology / edited by Frederick M. Ausubel ... [et al.],* Chapter 30**,** Unit 30.2.1-24.
ROMEO, G. R. & KAZLAUSKAS, A. 2008. Oxysterol and diabetes activate STAT3 and control endothelial expression of profilin-1 via OSBP1. *Journal of Biological Chemistry,* 283**,** 9595-9605.
SARKAR, P., RANDALL, S. M., MUDDIMAN, D. C. & RAO, B. M. 2012. Targeted Proteomics of the Secretory Pathway Reveals the Secretome of Mouse Embryonic Fibroblasts and Human Embryonic Stem Cells. *Molecular & Cellular Proteomics,* 11**,** 1829-1839.
SATO, N., MEIJER, L., SKALTSOUNIS, L., GREENGARD, P. & BRIVANLOU, A. H. 2004. Maintenance of pluripotency in human and mouse embryonic stem cells through activation of Wnt signaling by a pharmacological GSK-3-specific inhibitor. *Nature Medicine,* 10**,** 55-63.
SCHROEDER, M. A., ATHERTON, H. J., DODD, M. S., LEE, P., COCHLIN, L. E., RADDA, G. K., CLARKE, K. & TYLER, D. J. 2012. The Cycling of Acetyl-Coenzyme A Through Acetylcarnitine Buffers Cardiac Substrate Supply A Hyperpolarized C-13 Magnetic Resonance Study. *Circulation-Cardiovascular Imaging,* 5**,** 201-U82.
SELLICK, C. A., KNIGHT, D., CROXFORD, A. S., MAQSOOD, A. R., STEPHENS, G. M., GOODACRE, R. & DICKSON, A. J. 2010. Evaluation of extraction processes for intracellular metabolite profiling of mammalian cells: matching extraction approaches to cell type and metabolite targets. *Metabolomics,* 6**,** 427-438.
SELVARASU, S., KIM, D. Y., KARIMI, I. A. & LEE, D.-Y. 2010. Combined data preprocessing and multivariate statistical analysis characterizes fed-batch culture of mouse hybridoma cells for rational medium design. *Journal of Biotechnology,* 150**,** 94-100.
SHARMA, G., ATTRI, S. V., BEHRA, B., BHISIKAR, S., KUMAR, P., TAGEJA, M., SHARDA, S., SINGHI, P. & SINGHI, S. 2014. Analysis of 26 amino acids in human plasma by HPLC using AQC as derivatizing agent and its application in metabolic laboratory. *Amino Acids,* 46**,** 1253-1263.
SHYH-CHANG, N., DALEY, G. Q. & CANTLEY, L. C. 2013. Stem cell metabolism in tissue development and aging. *Development,* 140**,** 2535-2547.

SMITH, C. A., O'MAILLE, G., WANT, E. J., QIN, C., TRAUGER, S. A., BRANDON, T. R., CUSTODIO, D. E., ABAGYAN, R. & SIUZDAK, G. 2005. METLIN - A metabolite mass spectral database. *Therapeutic Drug Monitoring,* 27**,** 747-751.

SMITH, C. A., WANT, E. J., O'MAILLE, G., ABAGYAN, R. & SIUZDAK, G. 2006. XCMS: Processing mass spectrometry data for metabolite profiling using Nonlinear peak alignment, matching, and identification. *Analytical Chemistry,* 78**,** 779-787.

SMITH, J., LADI, E., MAYER-PROSCHEL, M. & NOBLE, M. 2000. Redox state is a central modulator of the balance between self-renewal and differentiation in a dividing glial precursor cell. *Proceedings of the National Academy of Sciences of the United States of America,* 97**,** 10032-10037.

SMOLINSKA, A., BLANCHET, L., BUYDENS, L. M. C. & WIJMENGA, S. S. 2012. NMR and pattern recognition methods in metabolomics: From data acquisition to biomarker discovery: A review. *Analytica Chimica Acta,* 750**,** 82-97.

SNYDER, L. R., KIRKLAND, J. J. & GLAJCH, J. L. 1997. *Practical HPLC Method Development,* United States of America, John Wiley & Sons, Inc.

SOTELO, J. & SLUPSKY, C. M. 2013. Metabolomics using nuclear magnetic resonance (NMR). *In:* WEIMER, B. C. & SLUPSKY, C. (eds.) *Metabolomics in Food and Nutrition.*

SUMNER, L. W., AMBERG, A., BARRETT, D., BEALE, M. H., BEGER, R., DAYKIN, C. A., FAN, T. W. M., FIEHN, O., GOODACRE, R., GRIFFIN, J. L., HANKEMEIER, T., HARDY, N., HARNLY, J., HIGASHI, R., KOPKA, J., LANE, A. N., LINDON, J. C., MARRIOTT, P., NICHOLLS, A. W., REILY, M. D., THADEN, J. J. & VIANT, M. R. 2007a. Proposed minimum reporting standards for chemical analysis. *Metabolomics,* 3**,** 211-221.

SUMNER, L. W., URBANCZYK-WOCHNIAK, E. & BROECKLING, C. D. 2007b. Metabolomics data analysis, visualization, and integration. *Methods in Molecular Biology,* 406**,** 409-436.

SWARTZ, M. E. 2005. UPLC (TM): An introduction and review. *Journal of Liquid Chromatography & Related Technologies,* 28**,** 1253-1263.

T'KINDT, R., DE VEYLDER, L., STORME, M., DEFORCE, D. & VAN BOCXLAER, J. 2008. LC-MS metabolic profiling of Arabidopsis thaliana plant leaves and cell cultures: Optimization of pre-LC-MS procedure parameters. *Journal of Chromatography B-Analytical Technologies in the Biomedical and Life Sciences,* 871**,** 37-43.

TALBOT, N. C., SPARKS, W. O., POWELL, A. M., KAHL, S. & CAPERNA, T. J. 2012. Quantitative and semiquantitative immunoassay of growth factors and cytokines in the conditioned medium of STO and CF-1 mouse feeder cells. *In Vitro Cellular & Developmental Biology-Animal,* 48**,** 1-11.

THEODORIDIS, G., GIKA, H. G. & WILSON, I. D. 2011. MASS SPECTROMETRY-BASED HOLISTIC ANALYTICAL APPROACHES FOR METABOLITE PROFILING IN SYSTEMS BIOLOGY STUDIES. *Mass Spectrometry Reviews,* 30**,** 884-906.

THEODORIDIS, G. A., GIKA, H. G., WANT, E. J. & WILSON, I. D. 2012. Liquid chromatography-mass spectrometry based global metabolite profiling: A review. *Analytica Chimica Acta,* 711**,** 7-16.

THOMSON, J. A., ITSKOVITZ-ELDOR, J., SHAPIRO, S. S., WAKNITZ, M. A., SWIERGIEL, J. J., MARSHALL, V. S. & JONES, J. M. 1998. Embryonic stem cell lines derived from human blastocysts. *Science,* 282**,** 1145-1147.

TRYGG, J., HOLMES, E. & LUNDSTEDT, T. 2007. Chemometrics in metabonomics. *Journal of Proteome Research,* 6**,** 469-479.

TSATMALI, M., WALCOTT, E. C. & CROSSIN, K. L. 2005. Newborn neurons acquire high levels of reactive oxygen species and increased mitochondrial proteins upon differentiation from progenitors. *Brain Research,* 1040**,** 137-150.

VALETTE, J. C., DEMESMAY, C., ROCCA, J. L. & VERDON, E. 2004. Separation of tetracycline antibiotics by hydrophilic interaction chromatography using an amino-propyl stationary phase. *Chromatographia,* 59**,** 55-60.

VALLIER, L., ALEXANDER, M. & PEDERSEN, R. A. 2005. Activin/Nodal and FGF pathways cooperate to maintain pluripotency of human embryonic stem cells. *Journal of Cell Science,* 118**,** 4495-4509.

VARUM, S., RODRIGUES, A. S., MOURA, M. B., MOMCILOVIC, O., EASLEY, C. A., RAMALHO-SANTOS, J., VAN HOUTEN, B. & SCHATTEN, G. 2011. Energy Metabolism in Human Pluripotent Stem Cells and Their Differentiated Counterparts. *Plos One,* 6.

VILLA-DIAZ, L. G., NANDIVADA, H., DING, J., NOGUEIRA-DE-SOUZA, N. C., KREBSBACH, P. H., O'SHEA, K. S., LAHANN, J. & SMITH, G. D. 2010. Synthetic polymer coatings for long-term growth of human embryonic stem cells. *Nature Biotechnology,* 28**,** 581-583.

VILLA-DIAZ, L. G., PACUT, C., SLAWNY, N. A., DING, J., O'SHEA, K. S. & SMITH, G. D. 2009. Analysis of the Factors that Limit the Ability of Feeder Cells to Maintain the Undifferentiated State of Human Embryonic Stem Cells. *Stem Cells and Development,* 18**,** 641-651.

VILLA-DIAZ, L. G., ROSS, A. M., LAHANN, J. & KREBSBACH, P. H. 2013. Concise Review: The Evolution of Human Pluripotent Stem Cell Culture: From Feeder Cells to Synthetic Coatings. *Stem Cells,* 31**,** 1-7.

VILLAS-BOAS, S. G., MAS, S., AKESSON, M., SMEDSGAARD, J. & NIELSEN, J. 2005. Mass spectrometry in metabolome analysis. *Mass Spectrometry Reviews,* 24**,** 613-646.

VINAIXA, M., SAMINO, S., SAEZ, I., DURAN, J., GUINOVART, J. J. & YANES, O. 2012. A Guideline to Univariate Statistical Analysis for LC/MS-Based Untargeted Metabolomics-Derived Data. *Metabolites,* 2**,** 775-95.

WANG, L., SCHUIZ, T. C., SHERRER, E. S., DAUPHIN, D. S., SHIN, S., NELSON, A. M., WARE, C. B., ZHAN, M., SONG, C.-Z., CHEN, X., BRIMBLE, S. N., MCLEAN, A., GALEANO, M. J., UHL, E. W., D'AMOUR, K. A., CHESNUT, J. D., RAO, M. S., BLAU, C. A. & ROBINS, A. J. 2007. Self-renewal of human embryonic stem cells requires insuhn-like growth factor-1 receptor and ERBB2 receptor signaling. *Blood,* 110**,** 4111-4119.

WANG, X., LIN, H. & GU, Y. 2012. Multiple roles of dihomo-gamma-linolenic acid against proliferation diseases. *Lipids in Health and Disease,* 11.

WANT, E. J., WILSON, I. D., GIKA, H., THEODORIDIS, G., PLUMB, R. S., SHOCKCOR, J., HOLMES, E. & NICHOLSON, J. K. 2010. Global

metabolic profiling procedures for urine using UPLC-MS. *Nature Protocols,* 5**,** 1005-1018.
WENZEL, S. E. 1997. Arachidonic acid metabolites: Mediators of inflammation in asthma. *Pharmacotherapy,* 17**,** S3-S12.
WEST, P. R., WEIR, A. M., SMITH, A. M., DONLEY, E. L. R. & CEZAR, G. G. 2010. Predicting human developmental toxicity of pharmaceuticals using human embryonic stem cells and metabolomics. *Toxicology and Applied Pharmacology,* 247**,** 18-27.
WESTERHUIS, J. A., HOEFSLOOT, H. C. J., SMIT, S., VIS, D. J., SMILDE, A. K., VAN VELZEN, E. J. J., VAN DUIJNHOVEN, J. P. M. & VAN DORSTEN, F. A. 2008. Assessment of PLSDA cross validation. *Metabolomics,* 4**,** 81-89.
WEXLER, E. M., PAUCER, A., KORNBLUM, H. I., PLAMER, T. D. & GESCHWIND, D. H. 2009. Endogenous Wnt Signaling Maintains Neural Progenitor Cell Potency. *Stem Cells,* 27**,** 1130-1141.
WEYLANDT, K. H., CHIU, C.-Y., GOMOLKA, B., WAECHTER, S. F. & WIEDENMANN, B. 2012. Omega-3 fatty acids and their lipid mediators: Towards an understanding of resolvin and protectin formation Omega-3 fatty acids and their resolvin/protectin mediators. *Prostaglandins & Other Lipid Mediators,* 97**,** 73-82.
WIKOFF, W. R., GANGOITI, J. A., BARSHOP, B. A. & SIUZDAK, G. 2007. Metabolomics identifies perturbations in human disorders of propionate metabolism. *Clinical Chemistry,* 53**,** 2169-2176.
WILSON, I. D., NICHOLSON, J. K., CASTRO-PEREZ, J., GRANGER, J. H., JOHNSON, K. A., SMITH, B. W. & PLUMB, R. S. 2005. High resolution "Ultra performance" liquid chromatography coupled to oa-TOF mass spectrometry as a tool for differential metabolic pathway profiling in functional genomic studies. *Journal of Proteome Research,* 4**,** 591-598.
WISHART, D. S., KNOX, C., GUO, A. C., EISNER, R., YOUNG, N., GAUTAM, B., HAU, D. D., PSYCHOGIOS, N., DONG, E., BOUATRA, S., MANDAL, R., SINELNIKOV, I., XIA, J., JIA, L., CRUZ, J. A., LIM, E., SOBSEY, C. A., SHRIVASTAVA, S., HUANG, P., LIU, P., FANG, L., PENG, J., FRADETTE, R., CHENG, D., TZUR, D., CLEMENTS, M., LEWIS, A., DE SOUZA, A., ZUNIGA, A., DAWE, M., XIONG, Y., CLIVE, D., GREINER, R., NAZYROVA, A., SHAYKHUTDINOV, R., LI, L., VOGEL, H. J. & FORSYTHE, I. 2009. HMDB: a knowledgebase for the human metabolome. *Nucleic Acids Research,* 37**,** D603-D610.
WONG, R. L., XIN, B. & OLAH, T. 2011. Optimization of Exactive Orbitrap (TM) acquisition parameters for quantitative bioanalysis. *Bioanalysis,* 3**,** 863-871.
XIAO, J. F., ZHOU, B. & RESSOM, H. W. 2012. Metabolite identification and quantitation in LC-MS/MS-based metabolomics. *Trac-Trends in Analytical Chemistry,* 32**,** 1-14.
XIE, C. Q., LIN, G., LUO, K. L., LUO, S. W. & LU, G. X. 2004. Newly expressed proteins of mouse embryonic fibroblasts irradiated to be inactive. *Biochemical and Biophysical Research Communications,* 315**,** 581-588.
XIE, G. X., CHEN, T. L., QIU, Y. P., SHI, P., ZHENG, X. J., SU, M. M., ZHAO, A. H., ZHOU, Z. T. & JIA, W. 2012. Urine metabolite

profiling offers potential early diagnosis of oral cancer. *Metabolomics,* 8**,** 220-231.

XIE, Y. H., GIBBS, T. C. & MEIER, K. E. 2002. Lysophosphatidic acid as an autocrine and paracrine mediator. *Biochimica Et Biophysica Acta-Molecular and Cell Biology of Lipids,* 1582**,** 270-281.

XU, C. H., INOKUMA, M. S., DENHAM, J., GOLDS, K., KUNDU, P., GOLD, J. D. & CARPENTER, M. K. 2001. Feeder-free growth of undifferentiated human embryonic stem cells. *Nature Biotechnology,* 19**,** 971-974.

XU, C. H., ROSLER, E., JIANG, J. J., LEBKOWSKI, J. S., GOLD, J. D., O'SULLIVAN, C., DELAVAN-BOORSMA, K., MOK, M., BRONSTEIN, A. & CARPENTER, M. K. 2005a. Basic fibroblast growth factor supports undifferentiated human embryonic stem cell growth without conditioned medium. *Stem Cells,* 23**,** 315-323.

XU, R.-H., SAMPSELL-BARRON, T. L., GU, F., ROOT, S., PECK, R. M., PAN, G., YU, J., ANTOSIEWICZ-BOURGET, J., TIAN, S., STEWART, R. & THOMSON, J. A. 2008a. NANOG is a direct target of TGF beta/Activin-mediated SMAD signaling in human ESCs. *Cell Stem Cell,* 3**,** 196-206.

XU, R. H., PECK, R. M., LI, D. S., FENG, X. Z., LUDWIG, T. & THOMSON, J. A. 2005b. Basic FGF and suppression of BMP signaling sustain undifferentiated proliferation of human ES cells. *Nature Methods,* 2**,** 185-190.

XU, X. Q., GRAICHEN, R., SOO, S. Y., BALAKRISHNAN, T., RAHMAT, S. N. B., SIEH, S., THAM, S. C., FREUND, C., MOORE, J., MUMMERY, C., COLMAN, A., ZWEIGERDT, R. & DAVIDSON, B. P. 2008b. Chemically defined medium supporting cardiomyocyte differentiation of human embryonic stem cells. *Differentiation,* 76**,** 958-970.

XU, Y., ZHU, X., HAHM, H. S., WEI, W., HAO, E., HAYEK, A. & DING, S. 2010. Revealing a core signaling regulatory mechanism for pluripotent stem cell survival and self-renewal by small molecules. *Proceedings of the National Academy of Sciences of the United States of America,* 107**,** 8129-8134.

YANES, O., CLARK, J., WONG, D. M., PATTI, G. J., SANCHEZ-RUIZ, A., BENTON, H. P., TRAUGER, S. A., DESPONTS, C., DING, S. & SIUZDAK, G. 2010. Metabolic oxidation regulates embryonic stem cell differentiation. *Nature Chemical Biology,* 6**,** 411-417.

YAO, S., CHEN, S., CLARK, J., HAO, E., BEATTIE, G. M., HAYEK, A. & DING, S. 2006. Long-term self-renewal and directed differentiation of human embryonic stem cells in chemically defined conditions. *Proceedings of the National Academy of Sciences of the United States of America,* 103**,** 6907-6912.

YATOMI, Y. 2006. Sphingosine 1-phosphate in vascular biology: Possible therapeutic strategies to control vascular diseases. *Current Pharmaceutical Design,* 12**,** 575-587.

ZELENA, E., DUNN, W. B., BROADHURST, D., FRANCIS-MCINTYRE, S., CARROLL, K. M., BEGLEY, P., O'HAGAN, S., KNOWLES, J. D., HALSALL, A., WILSON, I. D., KELLT, D. B. & CONSORTIUM, H. 2009. Development of a Robust and Repeatable UPLC-MS Method for the Long-Term Metabolomic Study of Human Serum. *Analytical Chemistry,* 81**,** 1357-1364.

ZHANG, D., JIANG, W., SHI, Y. & DENG, H. 2009a. Generation of pancreatic islet cells from human embryonic stem cells. *Science in China Series C-Life Sciences,* 52**,** 615-621.

ZHANG, D. X. & GUTTERMAN, D. D. 2007. Mitochondrial reactive oxygen species-mediated signaling in endothelial cells. *American Journal of Physiology-Heart and Circulatory Physiology,* 292**,** H2023-H2031.

ZHANG, J., YAN, L., CHEN, W., LIN, L., SONG, X., YAN, X., HANG, W. & HUANG, B. 2009b. Metabonomics research of diabetic nephropathy and type 2 diabetes mellitus based on UPLC-oaTOF-MS system. *Analytica Chimica Acta,* 650**,** 16-22.

ZHANG, R., MJOSENG, H. K., HOEVE, M. A., BAUER, N. G., PELLS, S., BESSELING, R., VELUGOTLA, S., TOURNIAIRE, G., KISHEN, R. E. B., TSENKINA, Y., ARMIT, C., DUFFY, C. R. E., HELFEN, M., EDENHOFER, F., DE SOUSA, P. A. & BRADLEY, M. 2013. A thermoresponsive and chemically defined hydrogel for long-term culture of human embryonic stem cells. *Nature Communications,* 4.

ZHOU, B., XIAO, J. F., TULI, L. & RESSOM, H. W. 2012. LC-MS-based metabolomics. *Molecular Biosystems,* 8**,** 470-481.

ZOU, Y., KIM, C. H., CHUNG, J. H., KIM, J. Y., CHUNG, S. W., KIM, M. K., IM, D. S., LEE, J., YU, B. P. & CHUNG, H. Y. 2007. Upregulation of endothelial adhesion molecules by lysophosphatidylcholine - Involvement of G protein-coupled receptor GPR4. *Febs Journal,* 274**,** 2573-2584.